



**UNIVERSITY OF  
BIRMINGHAM**

# **Continuous granulation of pharmaceutical powder using a twin screw granulator**

**By**

**Kai Teck Lee**

A thesis submitted to  
The University of Birmingham  
for the degree of  
**DOCTOR OF PHILOSOPHY**

School of Chemical Engineering  
The University of Birmingham  
July 2012

UNIVERSITY OF  
BIRMINGHAM

**University of Birmingham Research Archive**

**e-theses repository**

This unpublished thesis/dissertation is copyright of the author and/or third parties. The intellectual property rights of the author or third parties in respect of this work are as defined by The Copyright Designs and Patents Act 1988 or as modified by any successor legislation.

Any use made of information contained in this thesis/dissertation must be in accordance with that legislation and must be properly acknowledged. Further distribution or reproduction in any format is prohibited without the permission of the copyright holder.

## Abstract

Twin screw wet granulation is becoming popular in continuous granulation as the process brings significant advantages over the conventional processes. Twin screw extruders have been studied extensively as a continuous granulator since FDA implemented the concept of Quality by Design (QbD) in pharmaceutical industry which emphasizes the quality of a product should be built with the understanding of the product and process (FDA 2003). The concept should be executed together with the utilization of the Process Analytical Technology to ensure consistency of the product quality over time (Yu 2008). In QbD systems, the desired upfront product performance needs to be identified and the formulation and the process need to be designed to meet the product critical to quality attributes (CQAs). The understanding of the impact of materials and process parameters on the product quality is essential and the sources of variability in materials and process need to be identified. Finally the process requires continuous monitoring and updating to assure consistent quality.

A preliminary study was carried out and it was shown that the mechanisms of the twin screw wet granulation process involve wetting, nucleation, compaction, elongation and breakage with the absence of the consolidation stage that exists in the conventional granulation methods. PEPT was successfully utilised to study the material flow behaviour in the opaque system and it revealed that the flow stream of the material in the mixing zones is not only due to the conveying capacity but also the granulator fill, in particularly for the 90° mixing zone which is believed to be a dispersion type of mechanism driven by the granulator fill gradient.

Residence time distribution which is essential to characterise the mixing and flow in a process was measured and simulated by fitting the experimental data using a continuous stirred tank reactor model. The model describes the experimental curves well when a plug flow fraction was considered in the model. Generally the mean residence time of the system is proportional to the mixing zone angle and is inversely proportional to the screw speeds and flowrate. However, both the RTD shape and the model parameters (n and p) show similarity for different configurations and process conditions which suggest that the extent of the axial mixing in the granulator remains similar regardless of screw geometries, feedrate and screw speeds of the process.

Another approach being used to study the mixing performance in the granulator is Variance Reduction Ratio which measures the ability of a system to remove input stream instability. The convolution of the input stream signal and the RTD demonstrates that the twin screw granulator used in the present study is able to remove the feed instability given that the ratio of the frequency of the input stream fluctuation to the mean residence time is high.

Granulation of a common placebo formulation using a twin screw granulator shows that the granules are consistent and have acceptable quality. With appropriate formulation and process conditions, twin screw granulation could produce free flowing and mono-modal distribution granules with relatively high yield. Also, the tablets compacted using these granules have acceptable quality. The tablets are anticipated to have the strength to withstand external impact force during transportation. The dissolution rate of the tablets is considered fast (less than 1 hour) and the API distribution is expected to be homogenous as indicated by the observation of the well dispersed caffeine on the surface of the tablets using Raman Spectroscopy.

Twin screw extruder is proven to have the ability to run wet granulation process efficiently. The self-wiping feature that keeps the screws inherently clean and the flexibility of the screw geometries that gives different compounding actions are among the many advantages that consecutively drive the development of the tool to run wet granulation continuously.

## **ACKNOWLEDGEMENTS**

First of all I would like to express the deepest gratitude towards my academic supervisors, Dr. Neil Rowson and Dr. Andy Ingram for their excellent supervision, constant guidance as well as their encouragement and patience throughout the course of this research. Besides ensuring that the work I delivered is always at consistent high standard, Neil and Andy help with my personal and career development.

Thanks also go to Professor David Parker, Joseph Gargiuli and Tom Leadbeater from department of Physics for consistent help on PEPT experiment. A huge thank to Dr. James Bowen, the manager of Science City lab, for the training of the instruments involved in this research as well as his advice towards the completion of my thesis. Thanks are extended to Mr. Dave Boylin from the workshop for all the technical support and the excellent staff in The School of Chemical Engineering particularly those in General office for their administration support.

I would also like to acknowledge the Overseas Research Students Awards Scheme and The School of Chemical Engineering for the financial support for this research.

Finally I would like to express my deepest appreciation towards my family and Miss Yulan Zhang for their loves, continuous motivation, supports and encouragements throughout my study.

**CHAPTER 1 : THESIS INTRODUCTION**

1.1 BACKGROUND OF THE STUDY ..... 1  
1.2 CHALLENGES IN WET GRANULATION PROCESS..... 3  
1.3 MAIN OBJECTIVE AND WORK OF THE STUDY ..... 4

**CHAPTER 2 : AN INTRODUCTION TO GRANULATION PROCESS, TWIN SCREW EXTRUDER AND TWIN SCREW WET GRANULATION**

SUMMARY ..... 7  
2.1 OBJECTIVE..... 8  
2.2 INTRODUCTION TO GRANULATION PROCESS ..... 8  
2.3 DRY GRANULATION..... 9  
2.4 WET GRANULATION ..... 10  
    2.4.1 Wetting and nucleation..... 12  
    2.4.2 Granule growth and consolidation..... 17  
    2.4.3 Granules breakage and attrition..... 20  
2.5 TWIN SCREW EXTRUDER..... 21  
    2.5.1 Flow characteristic in twin screw extruder..... 21  
    2.5.2 Prediction of mixing in twin screw extruder ..... 23  
2.6 TWIN SCREW GRANULATION..... 27  
2.7 CONCLUSION ..... 32

**CHAPTER 3 : THE FORMULATION OF GRANULE AND CO-ROTATING TWIN SCREW EXTRUDER**

SUMMARY ..... 41  
3.1 OBJECTIVE..... 42  
3.2 PHARMACEUTICAL INGREDIENTS..... 42  
3.3 COMMONLY USED EXCIPIENTS IN THE GRANULATION PROCESS..... 43  
    3.3.1 Pharmaceutical filler..... 43  
    3.3.2 Pharmaceutical binder ..... 44  
    3.3.3 Pharmaceutical disintegrants ..... 44

---

3.3.4 Lubricants .....	45
3.3.5 Pharmaceutical Stabilisers .....	45
3.4 FORMULATION OF GRANULES USED IN THIS STUDY .....	45
3.4.1 Lactose .....	47
3.4.2 Microcrystalline Cellulose .....	47
3.4.3 Hydroxypropyl Cellulose .....	48
3.4.4 Croscarmellose sodium (Ac-Di-Sol) .....	48
3.5 CO-ROTATING TWIN SCREW .....	49
3.5.1 Basic screw types .....	49
3.5.2 Cross section view of twin screw .....	51
3.5.3 Extruder used in current study .....	53
3.6 KEY PROPERTIES OF GRANULES .....	55
3.6.1 Particle size distribution .....	55
3.6.2 Porosity .....	55
3.6.3 Flowability .....	56
<b>CHAPTER 4 : UNDERSTANDING THE MECHANISM OF CONTINUOUS WET GRANULATION OF PHARMACEUTICAL POWDER USING TWIN SCREW EXTRUDER</b>	
SUMMARY .....	58
4.1 INTRODUCTION .....	59
4.2 OBJECTIVES .....	59
4.3 MATERIALS AND EXPERIMENTAL METHOD .....	60
4.3.1 Formulation of granule .....	60
4.3.2 Twin screw granulation .....	60
4.3.3 High shear mixer granulation .....	61
4.3.4 Tablet compression .....	62
4.3.5 Granule Characterisations .....	63

4.3.5.1 Particle Size Distribution (PSD)-----	63
4.3.5.2 Shape and morphology-----	63
4.3.5.3 Internal structure and Porosity of granules-----	64
4.3.5.4 Estimation of granule strength using Uni-axial Bulk Confined Compression	65
4.3.6 Tablet Tensile Strength.....	67
4.4 RESULTS AND DISCUSSIONS .....	67
4.4.1 Particle size distribution (PSD) .....	71
4.4.2 Mean granule size.....	75
4.4.3 Shape and morphology .....	76
4.4.4 Internal structure of granules.....	78
4.4.5 Porosity of Granules .....	80
4.4.6 Estimated granule fracture strength.....	82
4.4.7 Mechanisms of twin screw wet granulation .....	84
4.4.8 Effect of granule properties on tablet tensile strength.....	86
4.5 CONCLUSION .....	88
<b>CHAPTER 5 : THE STUDY OF CONTINUOUS TWIN SCREW GRANULATOR USING POSITRON EMISSION PARTICLE TRACKING (PEPT) TECHNIQUE</b>	
SUMMARY .....	90
5.1 INTRODUCTION.....	91
5.2 OBJECTIVES.....	93
5.3 MATERIALS AND EXPERIMENTAL METHOD.....	93
5.3.1 Formulation of granules.....	93
5.3.2 Granulation Process.....	93
5.3.3 Positron Emission Particle Tracking (PEPT) .....	95
5.3.4 PEPT Data Processing.....	97
5.3.5 Residence Time Distribution.....	100
5.3.6 Granulator Fill .....	101

---

5.4 RESULTS AND DISCUSSION.....	102
5.4.1 Single particle Trajectory .....	102
5.4.2 Single particle 2-D trajectory .....	104
5.4.3 Overall Residence Time Distribution .....	107
5.4.4 Normalised Residence Time Distribution .....	112
5.4.5 Overall fill fraction of the TSE granulator .....	115
5.4.6 Fill fraction along the TSE granulator .....	116
5.4.7 Effect of fill level on granule properties.....	120
5.5 CONCLUSION .....	121
<b>CHAPTER 6 : MODELLING OF RESIDENCE TIME DISTRIBUTION TO INVESTIGATE SOLID MIXING</b>	
SUMMARY .....	123
6.1 1. INTRODUCTION .....	124
6.2 MATERIALS AND EXPERIMENTAL METHOD .....	125
6.3 RESULTS AND DISCUSSION.....	126
6.3.1 Modelling of residence time distribution .....	126
6.3.2 Parameters estimated using Tank-in-series (T-I-S) models .....	127
6.3.3 T-I-S with plug flow model .....	131
6.3.4 Residence time distribution of the granulator sections.....	133
6.3.5 Variance reduction ratio for axial mixing in continuous processing.....	140
6.3.6 Influences of input stream fluctuation frequency on variance reduction ratio .....	142
6.3.7 Variance Reduction Ratio achievable by the granulator .....	145



---

6.4 CONCLUSION .....	147
<b>CHAPTER 7 : THE EFFECT OF SCREW SPEED AND SCREW CONFIGURATION ON GRANULE AND TABLET QUALITY</b>	
SUMMARY .....	153
7.1 INTRODUCTION .....	154
7.2 OBJECTIVES.....	155
7.3 MATERIALS AND EXPERIMENTAL METHOD.....	155
7.3.1 Formulation of granules.....	155
7.3.2 Granulation Process.....	156
7.3.3 Tablet preparation.....	158
7.3.4 Granule characterisation .....	158
7.3.4.1 Particle size distribution (PSD)-----	158
7.3.4.2 Shape and morphology-----	159
7.3.4.3 Confined uni-axial bulk compression-----	159
7.3.4.4 Determination of packing coefficient-----	160
7.3.5 Tablet characterisation.....	162
7.3.5.1 Tensile strength-----	162
7.3.5.2 Dissolution rate-----	162
7.3.5.3 Active ingredient distribution-----	162
7.4 RESULTS AND DISCUSSIONS .....	164
7.4.1 Granule Particle Size Distribution (PSD).....	164
7.4.2 Granule Shape and Morphology.....	169
7.4.3 Granule Strength and Packing Coefficient .....	173
7.4.4 Tablet Tensile Strength.....	174
7.4.5 Caffeine Dissolution Rate.....	176
7.4.6 Caffeine Distribution in Tablet.....	179

CONCLUSION .....	182
<b>CHAPTER 8 : OVERALL CONCLUSION AND FUTURE WORK</b>	
8.1 OVERALL CONCLUSION.....	185
8.2 FUTURE WORK .....	189
<b>APPENDIX: PUBLISHED WORK</b>	
<b>REFERENCES</b>	

## List of Figures

Figure 1-1: Typical pharmaceutical tablet manufacturing process .....	2
Figure 2-1 Mechanism of wet granulation; (a) wetting and nucleation, (b) consolidation and coalescence, (c) breakage and attrition (Iveson, Beathe et al. 2002; Hapgood, Iveson et al. 2007).....	11
Figure 2-2: Nucleation when (a) liquid droplet is smaller than particle and (b) liquid droplet is larger than particle. Obtained from (Hapgood, Iveson et al. 2007).....	13
Figure 2-3: Nucleation process of wet granulation (Hapgood, Litster et al. 2002; Hapgood, Iveson et al. 2007) .....	13
Figure 2-4: Nucleation regime map (Hapgood, Litster et al. 2003) .....	16
Figure 2-5: Granule growth regime map proposed by (Iveson and Litster 1998; Iveson, Wauters et al. 2001).....	18
Figure 2-6: Overview of the experiments performed to evaluate: (a) the influence of water concentration during extrusion and PVP-concentration (◀screw▶ speed: 250 rpm; total input rate 5.6 kg h <sup>-1</sup> ); and (b) the influence of screw speed and total input rate (water concentration during extrusion: 7.5%, w/w) on the properties of α -lactose monohydrate granules. Method of binder addition: (○) without PVP; (◻) wet addition of PVP; (+) dry addition of PVP. Extract from original document (Keleb, Vermeire et al. 2002). .....	29
Figure 3-1: Composition of ingredients for current student .....	46
Figure 3-2: Classical co-rotating twin screw.....	49
Figure 3-3: Mass transfer region of co-rotating twin screw extruder.....	52
Figure 3-4: Overview of the twin screw extruder used in the present study .....	53
Figure 3-5: Twin screw granulator used for PEPT study provided by GEA Pharma System..	54
Figure 4-1: Plan view of the extruder barrel and co-rotating twin screw with two mixing zones with kneading discs arranged in 90° .....	61
Figure 4-2: Schematic diagram of High Shear Mixer and 3-bladed impeller (Tu, Ingram et al. 2009).....	62
Figure 4-3: Granules produced by TSE at 500 rpm using various liquid to solid ratio (dimension in cm).....	68
Figure 4-4: Granules produced by HSM at 600 rpm using various liquid to solid ratio (dimension in cm).....	69

---

Figure 4-5: Unwanted fines and oversized granules produced by TSE and HSM at 500 rpm using different L/S ratio.....	70
Figure 4-6: Particle size distribution of granules produced using L/S of 0.6 at different speed.....	71
Figure 4-7: Particle size distribution of granules produced using L/S of 0.8 at different speed.....	72
Figure 4-8: Particle size distribution of granules produced using L/S of 1.0 at different speed.....	72
Figure 4-9: Particle size distribution of granules produced using L/S of 1.2 at different speed.....	73
Figure 4-10: Particle size distribution of granules produced using L/S of 1.2 at different speed.....	73
Figure 4-11: Mean diameter ( $d_{50}$ ) of granules produced using TSE.....	76
Figure 4-12: Image obtained from scanning electron microscopy High shear mixer (left), Twin screw extruder (right).....	76
Figure 4-13: Aspect ratio of granules produced by TSE and HSM using various speed and L/S ratio.....	77
Figure 4-14: Sphericity of granules produced by TSE and HSM using various speed and L/S ratio.....	77
Figure 4-15: Raw Images and Binary Images of granules (centre slice) obtained from Micro X-Ray Tomography produced with liquid to solid ratio of 1.0: (a) High Shear Mixer 450 rpm; (b) Twin Screw Extruder 400 rpm. The numbers in last figure show the smaller individual granules that can be distinguished within the HSM granule. ....	78
Figure 4-16: Porosity of granules measured by mercury porosimeter.....	80
Figure 4-17: Porosity of granules measured by Micro X-Ray Tomography.....	80
Figure 4-18: Experimental uniaxial confined compression test and Adam's model plotted in form of natural log of applied pressure against natural strain.....	66
Figure 4-19: Estimated strength of granules produced using TSE and HSM at liquid to solid ratio of 1.0 for various impeller or screw speed.....	82
Figure 4-20: Estimated strength of granules produced using TSE and HSM at liquid to solid ratio of 1.0 for various impeller or screw speed.....	83
Figure 4-21: Relation between granule porosity and strength.....	84
Figure 4-22: SEM images of fracture surface of the tablets.....	86

---

Figure 4-23: Tablet tensile strength produced using TSE and HSM granules produced at L/S = 1.0 (based on 5 tablets) .....	87
Figure 4-24: Tablet tensile strength produced using TSE and HSM granules produced at L/S = 1.2 .....	87
Figure 5-1. Schematic diagram of the granulator barrel and screw (dimensions are in mm) ..	94
Figure 5-2: Experimental Matrix of PEPT for this study .....	95
Figure 5-3: Experiment set up and location by triangulation of a particle in the granulator....	97
Figure 5-4: Trajectory with optimum and high number of events per slice of a weak tracer particle, E300F20 = 300 events per slice and $F_{opt}$ of 20% .....	99
Figure 5-5: Trajectory with optimum and low number of events per slice of a weak tracer particle, E50F20 = 50 events per slice and $F_{opt}$ of 20% .....	99
Figure 5-6: Single Particle Trajectory in X, Y and Z direction for (a) 30°; (b) 60° and (c) 90° mixing zones.....	103
Figure 5-7: Track of a single particle tracer in Y-Z (cross section view) direction .....	104
Figure 5-8: Example of particle tracer moving in shape of '∞' .....	104
Figure 5-9: Example of particle tracer moving in a circle.....	104
Figure 5-10: Track of single particle tracer in Z-X (plan view) direction.....	105
Figure 5-11: Track of single particle tracer in Y-X (side view) direction.....	106
Figure 5-12: Mean Residence Time (MRT) for various screw configuration at different process conditions .....	108
Figure 5-13: Residence Time Distribution curves at various process parameter (a) 30°, (b) 60° and (c) 90° mixing zones.....	110
Figure 5-14: Situation when particle tracer gets stuck on the screw .....	111
Figure 5-15: Situation when particle tracer gets stuck on the wall of granulator.....	111
Figure 5-16. 30° mixing zones normalised RTD .....	112
Figure 5-17. 60° mixing zones normalised RTD .....	113
Figure 5-18. 90° mixing zones normalised RTD.....	113
Figure 5-19: Overall occupancy of the granulator for various screw geometry at different process parameters.....	115

---

Figure 5-20. Calculated experiment data showing material occupancy of the granulator in different sections.....	117
Figure 5-21: Occupancy of granulator with 30 degree mixing zones .....	117
Figure 5-22: Occupancy of granulator with 60 degree mixing zones .....	118
Figure 5-23: Occupancy of granulator with 90 degree mixing zones .....	118
Figure 6-1: schematic diagram of plug flow fraction in a series of continuous stirred tank reactors having a dead volume fraction.....	131
Figure 6-2: Model residence time distribution using 21 Tank-In-Series.....	142
Figure 6-3: Variance reduction ratio achieved by system with RTD in Figure 6-2 with low frequency noise.....	143
Figure 6-4: Variance reduction ratio achieved by system with RTD in Figure 6-2 with high frequency noise.....	144
Figure 6-5: Variance reduction ratio achieved by system with RTD in Figure 6-2 with both low and high frequency noise.....	144
Figure 6-6: Effects of input signal frequency on VRR for different N .....	145
Figure 6-7: Mass flowrate fluctuation along the granulator. (30° mixing zone; 10 g/min; 300 rpm) .....	149
Figure 6-8: Predicted RTD by Tank-In-Series and Complete model; (30-10-150 means geometry = 30°; feedrate = 10 g/min; screw speed = 150 rpm) .....	130
Figure 6-9: T-I-S model and complete model for section RTD for 30° mixing zone .....	137
Figure 6-10: T-I-S model and complete model for section RTD for 60° mixing zone .....	138
Figure 6-11: T-I-S model and complete model for section RTD for 90° mixing zone .....	139
Figure 6-12: Mass flow rate fluctuation of input stream and along the granulator with screw geometry 30°.....	150
Figure 6-13: Mass flow rate fluctuation of input stream and along the granulator with screw geometry 60°.....	151
Figure 6-14: Mass flow rate fluctuation of input stream and along the granulator with screw geometry 90°.....	152
Figure 7-1: Experiments matrix.....	157
Figure 7-2: Evolution of incremental packing coefficient value correspond to the applied pressure.....	161

---

Figure 7-3: Raman spectra of lactose, MCC, HPC and caffeine .....	163
Figure 7-4: PSD of granules produced using 30 degree mixing zones .....	164
Figure 7-5: PSD of granules produced using 60 degree mixing zones .....	165
Figure 7-6: PSD of granules produced using 90 degree mixing zones .....	165
Figure 7-7: Fines (<125 $\mu\text{m}$ ), yield (125 – 1400 $\mu\text{m}$ ) and oversize (> 1400 $\mu\text{m}$ ) of granules produced using various screw speed and screw configuration (30-200 = 30 degree mixing zones with 200 rpm screw speed).....	166
Figure 7-8: Mean diameter ( $d_{50}$ ) of granules produced with different screw speed and screw configuration.....	167
Figure 7-9: SEM images of granules at different magnification .....	169
Figure 7-10: Sphericity for various size classifications of granules produced using different screw configuration .....	171
Figure 7-11: Sphericity for various size classifications of granules produced using different screw speed.....	171
Figure 7-12: Estimated fracture strength of granules produced using various screw speed and screw configuration .....	173
Figure 7-13: Tablet tensile strength for various screw speeds and configurations .....	175
Figure 7-14: Mean dissolution time of caffeine tablets for various screw speed and screw configuration.....	178
Figure 7-15: Dissolution curves of tablets made using granules produced using different types of process conditions .....	177
7-16: Plot of $\tau_d$ against mean granule size .....	179
Figure 7-17: Raman mapping of caffeine (a & c) and excipients (b & d) of tablet made using granules produced by 30° mixing configuration.....	181
Figure 7-18: Raman mapping of caffeine (a & c) and excipients (b & d) of tablet made using granules produced by 60° mixing configuration.....	181
Figure 7-19: Raman mapping of caffeine (a & c) and excipients (b & d) of tablet made using granules produced by 90° mixing configuration.....	182

## List of Tables

Table 2-1: Summary of previous studies on residence time distribution to characterise mixing.....	26
Table 2-2: Work done by previous researchers on characterisation of granule produced using twin screw extruder .....	37
Table 2-3: Work done from previous researchers on tablets characterisation .....	39
Table 2-4: Other published work on twin screw wet granulation .....	40
Table 3-1: Basic types of screw elements .....	50
Table 5-1: Fraction of $\theta > 1.5$ by assuming that particle is considered stuck either on screw or wall at this value .....	110
Table 5-2: Peclet number for various process parameters and screw configuration .....	112
Table 6-1: Parameters estimated using T-I-S Model.....	128
Table 6-2: Parameters estimated using complete model .....	132
Table 6-3: Prediction of the parameters of T-I-S model of the conveying and mixing zones (Z1 = zone 1; C = conveying zone) .....	133
Table 6-4: Prediction of the parameters of complete model of the conveying and mixing zones (S1 = section 1; C = conveying zone; M = mixing zone).....	136
Table 6-5: Variance reduction ratio achievable by the granulator for various conditions .....	146
Table 6: Formulation of granules (J. Cartwright 2009).....	156
Table 7: Behaviour of particles for different $C_t$ classification.....	161
Table 8: Packing coefficient of granules .....	174



# Nomenclature

<b>A</b>	Area or projected area ( $\text{m}^2$ )
<b>AR</b>	Aspect ratio (-)
<b>a(t)</b>	Number of passes with residence time between $t$ and $t + \delta t$ (-)
<b>B</b>	Denoted width of granule (m)
<b>b</b>	Diameter of tablet (m)
<b>C<sub>t</sub></b>	Packing coefficient (-)
<b>C%</b>	Compressibility index (%)
<b>c(t)</b>	Concentration at time $t$ ( $\text{mol dm}^{-3}$ )
<b>c<sub>in</sub>(t)</b>	Concentration of input stream at time $t$ ( $\text{mol dm}^{-3}$ )
<b>c<sub>out</sub>(t)</b>	Concentration of output stream at time $t$ ( $\text{mol dm}^{-3}$ )
<b>cos <math>\theta</math></b>	Adhesion tension (-)
<b>D<sub>diff</sub></b>	Diffusion coefficient ( $\text{m}^2 \text{s}^{-1}$ )
<b>D<sub>eq</sub></b>	Equivalent diameter (m)
<b>d</b>	Dead volume fraction (-)
<b>d<sub>d</sub></b>	Droplet diameter (m)
<b>d<sub>v</sub></b>	Volume diameter (m)

---

<b>e(t)</b>	Residence time function (-)
<b>F</b>	Compaction force (N)
<b>h<sub>0</sub></b>	Initial bed height (mm)
<b>h<sub>i</sub></b>	Bed height at corresponding pressure (mm)
<b>h<sub>0.5</sub></b>	Bed height at pressure 0.5 MPa (mm)
<b>L</b>	Characteristic length (m)
<b>L<sub>1</sub></b>	Denoted length of granule (m)
<b>M</b>	Weight (N)
<b>N</b>	Screw speed (rpm)
<b>n</b>	Number of tank (-)
<b>P</b>	Pressure (Pa)
<b>P<sub>equivalent</sub></b>	Equivalent perimeter (m)
<b>Pe</b>	Peclet number (-)
<b>Po</b>	Porosity (-)
<b>P<sub>real</sub></b>	Actual perimeter (m)
<b>p</b>	Plug flow fraction (-)
<b>Q</b>	Volumetric flowrate (m <sup>3</sup> s <sup>-1</sup> )

---

<b>R</b>	Coefficient of determination (-)
<b>R<sub>eff</sub></b>	Effective pore radius (m)
<b>S</b>	Sphericity (-)
<b>SS<sub>error</sub></b>	Sum square error (-)
<b>SS<sub>total</sub></b>	Total sum square error (-)
<b>S<sub>max</sub></b>	Maximum granule pore saturation (-)
<b>St<sub>def</sub></b>	Stokes deformation number (-)
<b>T</b>	Tensile strength (Pa)
<b>t</b>	Time (s)
<b>t<sub>m</sub></b>	Mean residence time (s)
<b>t<sub>0</sub></b>	Lag time of dissolution (s)
<b>t<sub>p</sub></b>	Drop penetration time (s)
<b>t<sub>t</sub></b>	Thickness of tablet (m)
<b>U</b>	Velocity (ms <sup>-1</sup> )
<b>U<sub>c</sub></b>	Collision velocity (ms <sup>-1</sup> )
<b>V<sub>d</sub></b>	Drop size (m)
<b>V<sub>0</sub></b>	Bulk volume (m <sup>3</sup> )

<b>w</b>	Mass ratio of solid to liquid (-)
<b>Y</b>	Fraction of active ingredient dissolves at time t (-)
<b>Y<sub>d</sub></b>	Granule dynamic yield stress (Nm <sup>-2</sup> )

## Greek Symbol

$\dot{A}$	Constant of geometric term (-)
$\dot{A}$	Flux of powder surface traverses to the spray zone ( $\text{m}^2$ )
$\dot{B}$	Constant of geometric and rheological terms (-)
$\dot{V}$	Volumetric spray rate ( $\text{m}^3\text{s}^{-1}$ )
$\alpha$	Material constant related to Mohr-Column failure criterion (-)
$\Delta P$	Pressure gradient ( $\text{Nm}^{-2}$ )
$\varepsilon$	Natural strain ( $\ln h_o/h_i$ ) (-)
$\varepsilon_{\text{eff}}$	Effective bed porosity (-)
$\varepsilon_{\text{min}}$	Minimum porosity (-)
$\sigma^2$	Variance (-)
$\sigma_{\text{in}}^2$	Input stream variance (-)
$\sigma_{\text{out}}^2$	Output stream variance (-)
$\beta$	Dissolution curve shape factor (-)
$\theta$	Normalised time ( $t/t_m$ ) (-)
$\rho_{\text{bulk}}$	Bulk density ( $\text{kgm}^{-3}$ )
$\rho_g$	Granule density ( $\text{kgm}^{-3}$ )

$\rho_l$	Density of liquid ( $\text{kgm}^{-3}$ )
$\rho_s$	Density of solid particle ( $\text{kgm}^{-3}$ )
$\rho_{\text{tapped}}$	Tapped density ( $\text{kgm}^{-3}$ )
$\rho_{\text{true}}$	True density ( $\text{kgm}^{-3}$ )
$\tau$	Material constant related to granule fracture strength (-)
$\tau_d$	Mean dissolution time when 63.2 % of active ingredient has been dissolved (s)
$\tau_p$	Dimensionless penetration time (-)
$\mu$	Binder viscosity (Pa s)
$\Psi_a$	Dimensionless spray flux (-)

## **Abbreviations**

HSM	High shear mixer
PEPT	Positron emission particle tracking
PET	Positron emission tomography
PSD	Particle size distribution
RTD	Residence time distribution
SEM	Scanning electron microscopy
TSE	Twin screw extruder
TSG	Twin screw granulator
VRR	Variances reduction ratio

# CHAPTER 1 : THESIS INTRODUCTION

---

## 1.1 BACKGROUND OF THE STUDY

Material that is in granular form is one of the products that commonly exist in our daily lives and are the second-most manipulated material in industry after water (Richard, Nicodemi et al. 2005). Some examples of granular materials that can be found in daily lives are sand, coffee, rice and fertilizer. Granular form is popular because it is convenient, easy to store, safe and eases the material handling process. In many industries, the existence of materials in granular form is important particularly in pharmaceutical processing. In the pharmaceutical industry, granular form can be found as an intermediate product or final product in granule or tablet form.

The tablet is the most common solid dosage form for administering drugs via an oral route. This is generally because the tablet is simple to take and it is convenient in terms of storage, handling and administration. The tablet is also popular due to its accurate dose and the ease of controlling drug release. Also, tablets have a long shelf life where they can be made to be chemical and physical stable. Direct compression is usually used for tablet production as it is fast and simple and the technique minimises the operations needed during the manufacturing process. However, not all ingredients are suitable for direct compression. For example, cohesive material that does not flow freely will cause problems during the die filling process (Wu, Ruddy et al. 2005; Wu, Best et al. 2006; Wu, Hancock et al. 2008); materials that are low in compactibility will easily produce tablets with low tensile strength; and material segregation could lead to inaccurate dosage as a homogenous mixture of the components cannot be obtained with a simple blending processes. Due to these reasons, an extra granulation process is needed prior to compression to assure uniform distribution of the



active ingredients in the final tablet. A typical pharmaceutical tablet manufacturing process that involves granulation is shown in Figure 1-1.

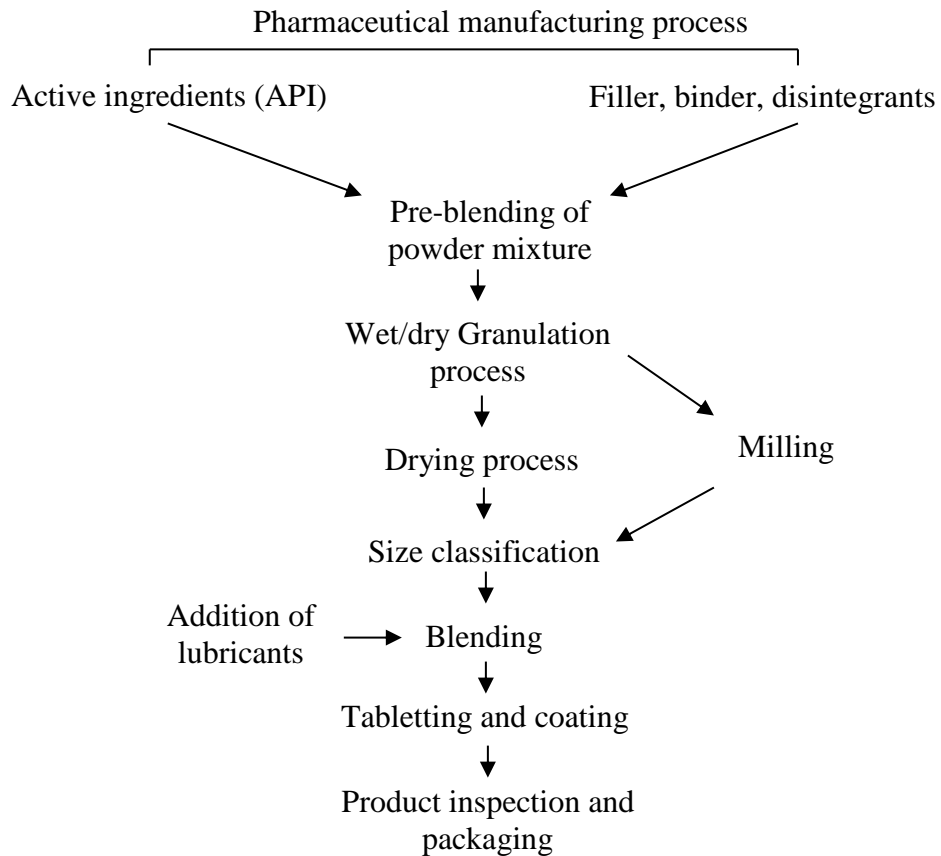


Figure 1-1: Typical pharmaceutical tablet manufacturing process

The granulation process can be performed wet or dry depending on the materials selection. Dry granulation is normally followed by milling and sieving before blending with lubricant and being compacted. Wet granulation on the other hand involves the addition of a liquid binder during granulation followed by a drying process before being lubricated and compacted. The amount of liquid added needs to be very well controlled in wet granulation process as over-wetting will cause over granulation producing large and hard granules that are not compressible whilst under-wetting will lead to soft and fragile granules. Many types of

equipment can be used to perform the wet granulation process, for example, high shear mixer, fluidised bed and rotating drum. These techniques are generally well established and the predictable process allows the production of quality tablets.

## **1.2 CHALLENGES IN WET GRANULATION PROCESS**

In the past few decades, there has been a huge step forward in understanding the mechanisms of wet granulation process. Among those, the wetting and nucleation stage where nuclei are formed and liquid being distributed in the powder bed is one of the most important aspects. Distribution and immersion are the types of nucleation mechanism being distinguished and is strongly controlled by the liquid binder droplet size, surface tension and concentration. Redistribution of liquid binder is possible as the particles coalesce and break during the process and therefore the size enlargement process which includes particle-particle interaction is also well understood. Saturation level, kinetic energy, for example, impeller tip speed of high shear mixer, and binder viscosity were very well evaluated and a regime map was also created to predict the behaviour of granulation process. Nevertheless, wet granulation process remains challenging and there is much to be done. Among those, one of the main challenges in wet granulation is to run the process continuously.

In industry at present, the wet granulation process is mostly run in batch mode. Batch processing brings certain advantages in the pharmaceutical industry, for example, various products can be produced from the same production line and it is also very useful for small production scale. However, there is a major downside to batch processing as it is inefficient as the equipment must be stopped for cleaning and reconfiguration in between the batches. Besides this, the quality of the products needs to be determined after the process before the next batch can be started. Although the granulation process is well understood and

predictable, there is a still a huge potential for inconsistency in the product quality as a slight variation may still appear from batch to batch during the operation. Besides this, more labour work is also needed to operate batch processes and there are a numerous testing stages during the manufacturing. If the quality of the product at the end of a batch does not meet the required specification, it will be discarded as Out of Specification, resulting in a waste of resources and money.

With the implementation of Quality by Design (QbD) concepts by the FDA in the pharmaceutical industry, the wet granulation process becomes more challenging as the systematic, scientific, risk-based concepts emphasize that the quality should be built into a product with the understanding of the product and the process from which it is developed and manufactured (FDA 2003). Also, process control of manufacturing processes, for example using Process Analytical Technology (PAT), is necessary to ensure consistency of product quality over time (Yu 2008).

In recent years, twin screw granulation has been considered as a potential alternative technique for traditional batch wet granulation processes. The process can be run in controlled continuous mode with the potential application of PAT and it is highly complementary to QbD. Unlike batch processing, there is no batch to batch variation in twin screw wet granulation and the risk of powder exposure and contamination is small as material handling during the process is minimized. In term of process scale up, twin screw process is considered to be straight forward as it can be done by running the process for a longer period.

### **1.3 MAIN OBJECTIVE AND WORK OF THE STUDY**

The main focus of the present study is to attempt to understand the mechanism of twin screw wet granulation process as well as assessing the mixing performance of the twin screw

granulator. As continuous granulation using a twin screw granulator is relatively new in wet granulation processing; only limited information is available from literature. Therefore, high shear mixer granulation which is well studied in terms of its mechanism is used as the process comparison. The comparison of the two processes as well as the granules is considered as a step to fundamentally understanding the mechanism of twin screw wet granulation.

Positron Emission Particle Tracking, which is ideal to study an opaque system, is also used to study the twin screw wet granulation process. A particle is first labelled with radioactive isotope and is tracked to reveal the quantitative detail of the motion of a particle that then reflects the material flow in the twin screw extruder. Besides this, the residence time distribution of system is measured to get an insight into the mixing performance of the extruder. Fill level along the extruder is also estimated to predict the flow mechanism and the compaction force of the extruder.

Homogeneity of the products is essential in the pharmaceutical industry as it determines the accuracy of a solid dosage form. The performance of the mixing of the twin screw extruder is therefore studied by verifying the ability of the system to remove feed variability. Variance Reduction Ratio which can be calculated from residence time distribution is used as a parameter to represent the mixing performance of the extruder.

Finally, a well-studied model drug formulation is used to produce granules and tablets to study the validity and robustness of twin screw wet granulation. The properties of the granules (including particle size distribution, morphology, packing coefficient and strength evaluated) and tablets (dissolution and tensile strength) are evaluated as well as the homogeneity of model drug distribution in a tablet.

Chapter 2 reviews the mechanism of wet granulation together with the previous studies on continuous granulation using a twin screw extruder. A brief description of a twin screw granulator and the formulation of the granules are discussed in chapter 3 followed by experimental results and discussion with a final conclusion of this study.

# **CHAPTER 2 : AN INTRODUCTION TO GRANULATION PROCESS, TWIN SCREW EXTRUDER AND TWIN SCREW WET GRANULATION**

---

## **SUMMARY**

A conventional wet granulation process consists of three main stages which are, wetting and nucleation, consolidation and coalescence and breakage and attrition. Wetting is the first stage of the process where granulation liquid is sprayed or poured into the powder bed which is followed by the formation of nuclei. The nuclei will consolidate within the equipment and the neighbouring particles to force the liquid towards the surface which then allows the granules to grow when the surface wetted particles coalesce. Breakage of the granules will only occur when the granule is not sufficiently strong to withstand the force that exists from agitation or collision during the process. Those three stages occur simultaneously and will decide the final properties of the granules produced.

Twin screw extruders are commonly used in polymer industry for compounding and mixing purposes and to generate paste in the food industry. Extensive work has been carried out to study the residence time distribution and the mixing of the extruder but there is a lack of a general consensus regarding the effect of the operating conditions and the geometry on mixing.

Twin screw wet granulation, which is becoming popular in pharmaceutical wet granulation, has also been studied by many research groups (see Table 2-2). The research focuses on the characterisation of the granules and tablets properties produced using different

formulations and process conditions. There is limited published work on these studies and limited understanding of the mechanisms of the twin screw wet granulation process.

## **2.1 OBJECTIVE**

The aim of this chapter is to describe the theoretical basis of the wet granulation process. Besides this, the background of flow mechanism and mixing efficiency in a twin screw extruder is also described by summarizing the work published in recent years. Finally, previous studies on twin screw wet granulation process are also summarized in this chapter.

## **2.2 INTRODUCTION TO GRANULATION PROCESS**

The term “Granulation” is defined by Perry’s Chemical Engineering (Perry, Green et al. 1998) as the process where small particles are agglomerated, compacted or otherwise brought together into larger relatively permanent masses in which the original particles can still be distinguished. Granulation is one of the most important unit operations in today’s chemical industry. It is widely used in industries such as pharmaceutical formulation, food manufacture, agriculture product manufacture, and the plastics industry.

The general objectives of granulation are,

- To minimize waste by producing larger particles that are easier to be handled. Dust explosions can also be reduced by incorporating dust into larger particles through granulation processes.
- To improve materials properties that facilitate controlled metering for example flowability. Small particles are cohesive because of their strong inter-particles forces and stagnant flowing zones are common. This can be avoided by granulation

by modifying the shape, size and density of materials by combining the ingredients into particles.

- To design materials with desirable targets including a controlled dissolution and disintegration rate of the drugs. These properties can be achieved by assigning the products with a specific area and porosity during the granulation processes.

In order to produce granules, several primary particles are required to be bound together to form agglomerates. This can be achieved by the solid bond created from materials interlocking through dry granulation or liquid bridges, and the viscous force by the addition of liquid binder through wet granulation.

### **2.3 DRY GRANULATION**

The dry granulation is a process to make granules without using any liquid solution as the materials being granulated are sensitive to moisture and heat. Without the liquid content, the particulate materials can be aggregated when compressed at high pressure because of the bonding forces developed by direct contact between the solid surfaces (Miller and Parikh 2005). Tablet pressing is a type of dry granulation conducted by using a slugging tool or roller compactor. This technique is externally influenced by primary materials properties such as powder cohesiveness, density, flowability, compressibility and particle size distribution. If the powder does not possess enough natural flow to be fed uniformly into a die, the degrees of the densification will be varied within the product.

In addition to the tablet press, powder can be delivered consistently using an auger-feed system between two pressure rolls. The powder will be compacted into ribbons or pellets between these pressured rolls which rotate in opposite direction. The ribbons or pellets



produced were then milled using a low shear mill to form smaller aggregates for a final blend before tablet compression. This technique has been popular in the past decades as the equipment can offer a wide range of pressure that allows various densifications in final products. However, the compressibility of the material will be reduced in the end which result in a decrease in the tablet tensile strength (Freitag and Kleinebudde 2003). Moreover, screening of a large amount of fines is common to roller compaction depending on the nature of primary materials. Further analysis of the removed fines is necessary to examine the materials being removed.

## **2.4 WET GRANULATION**

Wet granulation is another popular type of granulation method that can be performed using a wide range of equipment. A high shear mixer is the most general type of granulator that produces dense and uniform granules. A fluidized bed is an option for granulation with a more porous granule. A tumbling drum is another example of low shear granulation that produces porous granules. Wet mass extrusion which is normally followed by spheronisation is also commonly used to produce spherical granules.

Wet granulation which involves the use of a liquid binder for particle enlargement will require a more complex process. The liquid binder is firstly added into the pre-mixed powder bed by pouring or spraying directly into the bed. It can also be added as a solid constituent to be melted by heating the vessel to the melting point of the solid binder. The liquid binder is distributed in the agitated powder bed and the wetted particle will form nuclei that are deformed and densified when colliding with the vessel wall, the blade and the neighbouring particles. The densification process will force the liquid to migrate to the nucleus surface that allows coalescence and binding with other particles to form a larger aggregate. Breakage also

occurs during the process when the collision force exceeds the critical value a granule can withstand. Generally the process of wet granulation can be classified into three steps as shown in Figure 2-1.

In this chapter, the underlying physics of each rate process is briefly discussed. Besides this, the process parameters for each rate process are defined. The use of a regime map to establish the operating regime of wet granulation is also discussed:

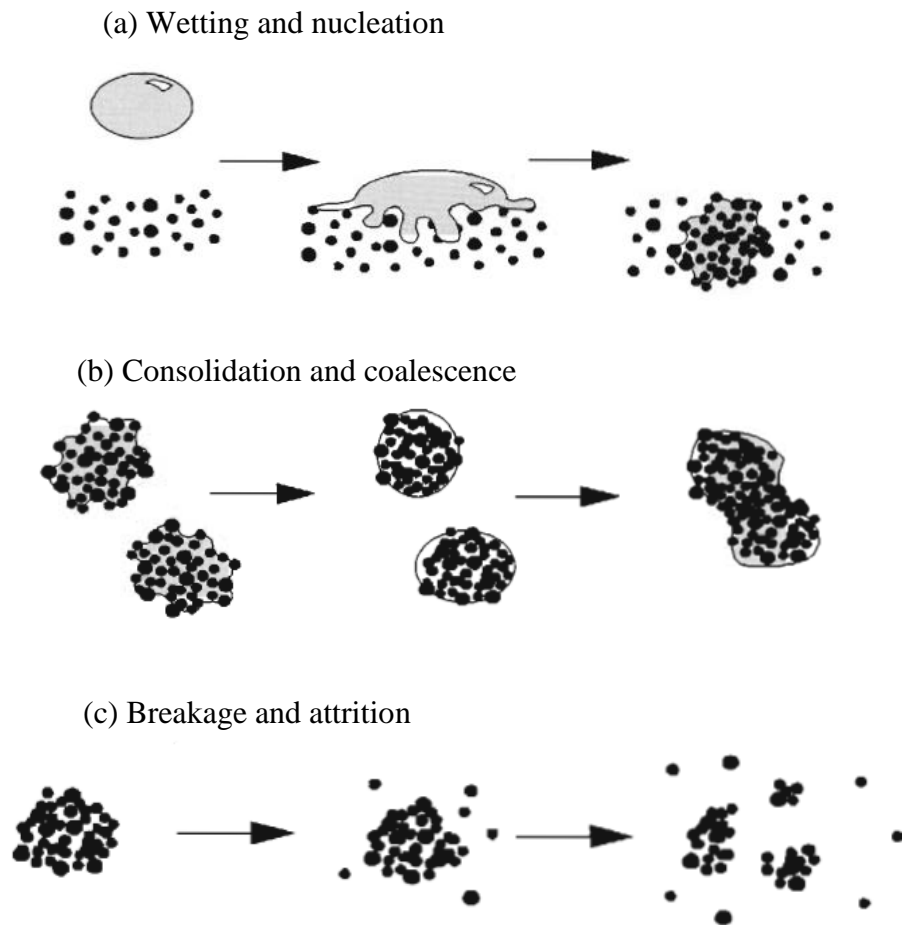


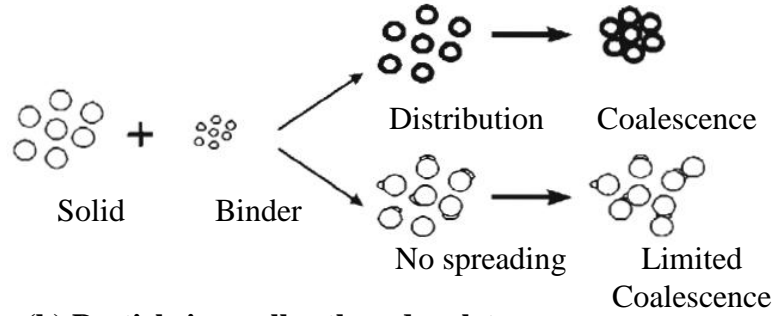
Figure 2-1 Mechanism of wet granulation; (a) wetting and nucleation, (b) consolidation and coalescence, (c) breakage and attrition (Iveson, Beathe et al. 2002; Hapgood, Iveson et al. 2007)

### **2.4.1 Wetting and nucleation**

Wetting is the very first stage of wet granulation where the liquid is added into the powder bed and being distributed through the powder to form nuclei or wet particle. Wetting and liquid distribution is important as poor wetting will give a very broad size of nuclei distribution leading to a broad granule size distribution. Component segregation may also occur if there is a preferential distribution between each ingredient.

Generally, there are two types of nucleation mechanism based on the relative primary particle size and the liquid droplet size. If the droplet size is smaller than the primary particle, nucleation will occur by distributing the drops on the surface of the particle which will allow the wet particle to coalesce with other dry particles. This type of nucleation may produce nuclei and granules with air trapped inside (Hapgood, Iveson et al. 2007) and more open agglomerate structure (Abberger, Seo et al. 2002). On the other hand when the liquid droplet is larger than the primary particle, immersion type of nucleation occurs and the nuclei with saturated pores are produced. Immersion type of nucleation will lead to a more compact structure. Figure 2-2 summaries the possible nucleation mechanisms as a function of primary particle size and liquid droplet size. These nucleation mechanisms also depend on parameters such as contact angle and spreading coefficients which was discussed in details by (Litster, Ennis et al. 2004).

**(a) Particle is larger than droplet**



**(b) Particle is smaller than droplet**

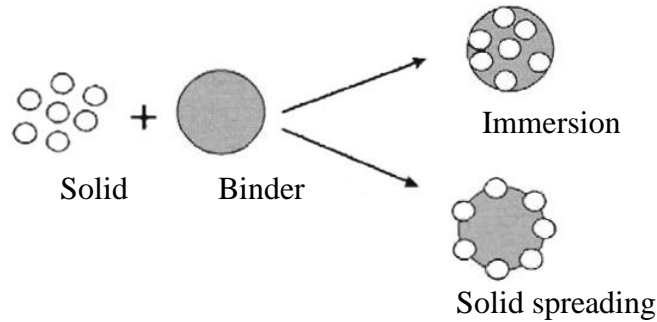


Figure 2-2: Nucleation when (a) liquid droplet is smaller than particle and (b) liquid droplet is larger than particle. Obtained from (Hapgood, Iveson et al. 2007)

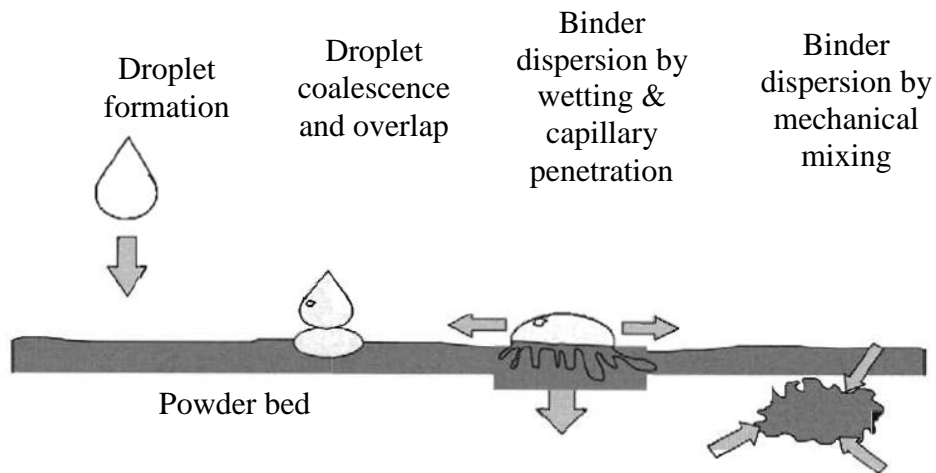


Figure 2-3: Nucleation process of wet granulation (Hapgood, Litster et al. 2002; Hapgood, Iveson et al. 2007)

Figure 2-3 shown is the nucleation process during wet granulation process. The nucleation process can be classified into four stages, which are (Hapgood, Litster et al. 2002; Hapgood, Iveson et al. 2007),

- i. The formation of the liquid droplets from a spray with a certain size distribution.
- ii. The liquid droplets formed will impact on the powder bed, coalescence and overlap with the surface of the powder bed.
- iii. The liquid droplet will then spread on the surface to wet the primary particles and penetrates into the powder bed by capillary action to form nuclei.
- iv. These nuclei will break up to form small entities due to the shear forces existing in the process. In other words, the liquid binder is distributed thoroughly within the bed.

The nucleation process is regarded as an important stage in wet granulation process as granulation often retains a "memory" of the nucleation stage (Hapgood, Iveson et al. 2007). If a wide nuclei size distribution is obtained during the nucleation stage, it will normally lead to a wide granule size distribution for the end product. Therefore, (Hapgood, Litster et al. 2002; Hapgood, Litster et al. 2003; Litster 2003) proposed the importance of the drop penetration time,  $t_p$ , and the drop overlap in the nucleation process.

The kinetics of drop penetration time,  $t_p$ , was previously studied by filming single drops of several different fluids as they penetrated into a loosely packed powder bed (Hapgood, Litster et al. 2002). Drop penetration time can either be measured directly or estimated in advance from the material properties using the equation proposed by (Hapgood, Litster et al. 2002),

$$t_p = 1.35 \frac{V_d^{2/3}}{\varepsilon_{\text{eff}}^2} \left[ \frac{\mu}{R_{\text{eff}} \cos \theta} \right] \quad \dots \text{Eq. 2-1}$$

$R_{\text{eff}}$  is pore radius;  $\mu$  is binder viscosity;  $\cos \theta$  is adhesion tension;  $V_d$  is drop size and  $R_{\text{eff}}$  is bed porosity. By including a circulation time,  $t_c$  the time taken for a packet of powder to return to the spray zone, the dimensionless penetration time is given by

$$\tau_p = \frac{t_p}{t_c} \quad \dots \text{Eq. 2-2}$$

The drop overlap is controlled by the dimensionless spray flux,  $\psi_a$ , which is the ratio of the projected area of drops from the spray nozzle to the area flux of powder surface through the spray zone and is expressed as (Litster 2003)

$$\psi_a = \frac{3 \cdot \dot{V}}{2 \cdot \dot{A} \cdot d_d} \quad \dots \text{Eq. 2-3}$$

The powder surface traverses the spray zone with a flux  $\dot{A}$  ( $\text{m}^2/\text{s}$ ),  $\dot{V}$  is the volumetric spray rate and  $d_d$  is the droplet diameter. At low dimensionless spray flux, the system is not wet enough and the droplets will not overlap as the wetted powder is quickly replaced by a not wetted particle due to the mixing action to form an individual separated nucleus. When the dimensionless spray flux is high, there is significant droplet overlapping or the powder bed becomes locally wetted leading to the formation of larger nuclei.

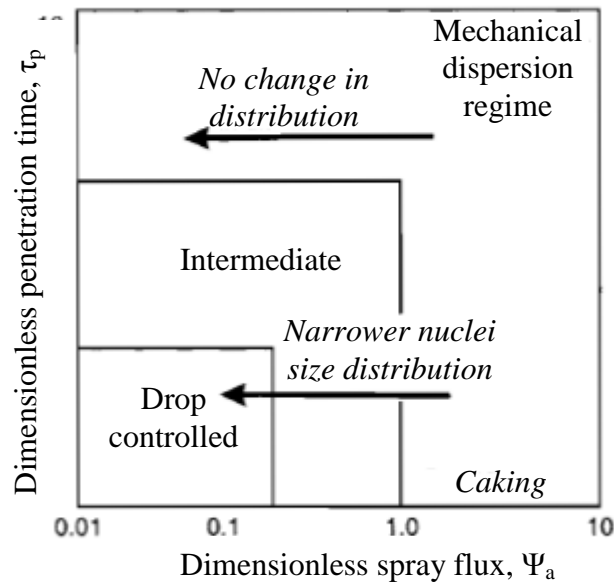


Figure 2-4: Nucleation regime map (Hapgood, Litster et al. 2003)

Figure 2-4 shows the nucleation regime map proposed by (Hapgood, Litster et al. 2003). Drop controlled nucleation occurs when there is a low dimensionless spray flux (no droplets overlapping) and a fast drop penetration time. Since each droplet produces a nucleus, the control of this regime is the droplet size. When this criterion is not met, the nucleation falls into mechanical dispersion regime where powder mixing dominates and the liquid dispersion depends on the mechanical mixing and agitations. If the mechanical dispersion is poor, at slow penetration time and high spray flux conditions, a broad nuclei size distribution will be produced. The intermediate regime is the zone where the nucleation process is extremely sensitive to small variations in nucleation zone conditions (Hapgood, Litster et al. 2003).

The nucleation regime map is a useful tool for in particle design, for example if the drop penetration time is large, an adjustment of the spray flux may lead to a narrower size distribution. During process scale up, the dimensionless spray flux should be kept constant (Litster 2003).

## **2.4.2 Granule growth and consolidation**

After the wetting and nucleation process, the particles will either exist as individual particles coated with a layer of liquid or loosely packed, partially or fully saturated nuclei granules. The granules will densify when they collide with neighbouring particles or the vessel wall. This is also the stage where granules start to grow larger. Granule consolidation and growth is important as the final granule properties (size and density) will be decided at this stage. Two major types of granule growth that normally occur are steady growth and induction growth. Steady growth is described as when the rate of growth is approximately constant and is normally seen in relatively coarser particle with non-viscous binder and high agitation intensity. Induction type of growth is described as when there is an induction time with no growth followed by a rapid growth which normally occurs in the system with fine power and viscous binder with low agitation intensity.

The two basic parameters that determine the behaviour of the granule growth are the pore saturation and the amount of granule deformation during the process (Iveson and Litster 1998; Iveson, Wauters et al. 2001). A granule growth regime (see Figure 2-5) was also proposed by (Iveson and Litster 1998; Iveson, Wauters et al. 2001) to predict the granule growth based on the pore saturation and the granule deformation.



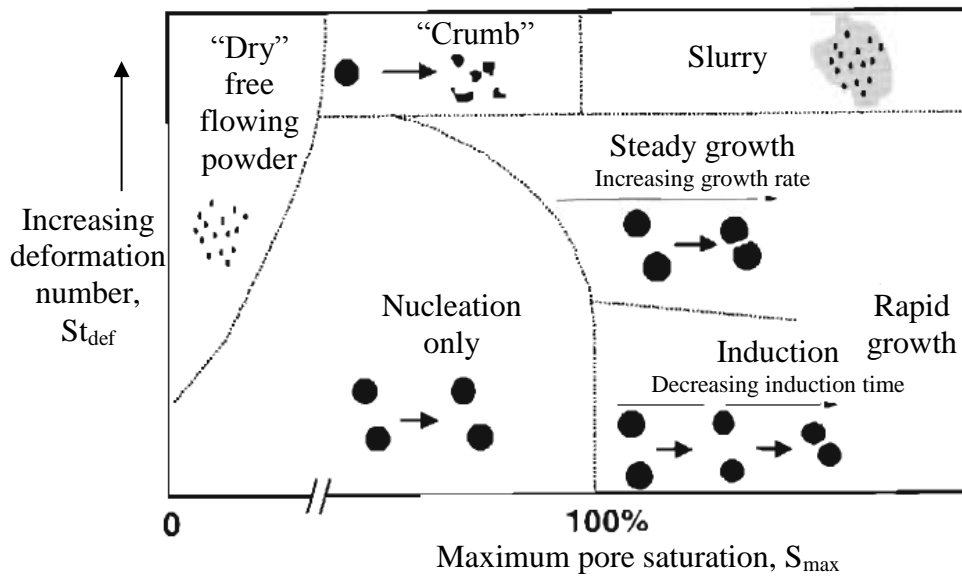


Figure 2-5: Granule growth regime map proposed by (Iveson and Litster 1998; Iveson, Wauters et al. 2001)

The maximum granule pore saturation,  $S_{max}$ , is used as a measure of the amount of liquid available in a granule using the following equation (Iveson and Litster 1998),

$$S_{max} = \frac{w\rho_s(1-\varepsilon_{min})}{\rho_l\varepsilon_{min}} \quad \dots \text{Eq. 2-4}$$

Where  $w$  is the mass ratio of liquid to solid,  $\rho_s$  is the density of the solid particles,  $\rho_l$  is the liquid density and  $\varepsilon_{min}$  is the minimum porosity the formulation reaches for that particular set of operating conditions.

Stokes deformation number,  $St_{def}$ , (Tardos, Khan et al. 1997) is a measure of the ratio of the impact kinetic energy to the plastic energy absorbed per unit strain. It takes into account of both the process agitation intensity and the granule mechanical properties and is described as the following equation (Tardos, Khan et al. 1997)

$$St_{\text{def}} = \frac{\rho_g U_c^2}{2 \cdot Y_d} \quad \dots \text{Eq. 2-5}$$

Where  $U_c$  is collision velocity in the granulator  $\rho_g$  is granule density  $Y_d$  granule dynamic yield stress.

When the liquid content is very low, the primary particle is dry and free flowing. An increase in the maximum pore saturation will lead to the formation of nuclei. However, there is insufficient amount of liquid for further growth in this regime. The coarser particle tends to form crumb with a few granules that continually break and reform due to the formation of weaker granules (Iveson and Litster 1998). For very wet conditions, a very weak system (high mechanical agitation and low granule strength) will form slurry. At high pore saturation, steady state growth occurs when the system has an intermediate strength and the growth rate increases with increasing  $S_{\text{max}}$ . When the  $St_{\text{def}}$  is low (strong system), induction type of growth occurs.

Consolidation occurs when there is collision between two granules, a granule and a powder particle or a granule and the equipment. It causes the granule compaction or densification due to the deformation of the granules (Darelius 2007) and as a result the inner liquid and the air from the interior are being squeezed to the surface and then form a liquid film. This may be followed by a rapid growth and thus an induction growth as described previously. Consolidation of granules determines the granule porosity and density. Granules may consolidate over extended times and achieve high density if there is no simultaneous drying to stop consolidation process (Parikh 2005). Hence, the consolidation stage is also important as it affects the final granule properties and the granule growth mechanism.

### 2.4.3 Granules breakage and attrition

Granules breakage and attrition is the last stage of the three stages in the wet granulation process. Granules breakage refers to the phenomena where wet granules break due to high shear forces exhibited in granulators (normally refers to high shear granulation). Breakage of wet granules can control the maximum and final granules sizes as well as to disperse highly viscous liquid binder within the powder bed. Vonk observed that breakage occurs in high shear mixer as coloured tracer was fragmented to form smaller fraction of fines (Vonk, Guillaume et al. 1997).

To predict wet granule breakage, (Tardos, Khan et al. 1997) considered that a granule will break if the applied kinetic energy during an impact exceeds the energy required for the breakage. This analysis leads to a Stokes deformation number criteria for breakage,  $St_{def} > St_{def}^*$  where  $St_{def}^*$  is the critical value of Stokes number that must be exceeded for breakage to occur (Tardos, Khan et al. 1997). This suggests that breakage will increase with increasing tip speed or in the other words the collision velocity between particles or with the wall of granulators (Tardos, Khan et al. 1997). Controlling the wet granule breakage gives the opportunity of a narrow granule size distribution by growing granules up to a breakage limit. It is important to note that the size distribution control will also depend on the impact velocity distribution and turnover of granules through the high impact region (impeller or chopper) (Salman, Hounslow et al. 2007).

Understanding of the wet granulation processes is important as the granulation behaviour of a formulation can be predicted directly. The granulation process can also be scaled up directly if the mechanism of wet granulation is well established, for example the nucleation condition could be maintained by keeping the dimensionless spray flux constant. Therefore,

the present study also focuses on the understanding of the twin screw wet granulation process and the comparison with the other established granulation processes.

## **2.5 TWIN SCREW EXTRUDER**

Extruders were originally used in the polymer processing industry for mixing, compounding or reacting of the polymeric materials. They are also popular in food processing, for example, in the production of various products such as snacks, cereals and pet food. The popularity of twin screw extruders is attributed to its versatility and applicability to a remarkably wide range of materials. Besides this, extruders allow continuous processing and are capable of delivering high value, high quality products in large quantities. The growing number of industrial applications of extrusion technology in the last few decades has led to an increasing interest in understanding the extrusion process. However, the complexity of the extrusion process such as the shear, mixing, flow performance and the material interaction make the study very challenging and empirical approaches have made little contribution to the fundamental understanding of the process.

### **2.5.1 Flow characteristic in twin screw extruder**

Mathematical modelling has been used widely for the quantitative understanding of transport phenomena in a twin screw extruder. Booy derived a mathematical model for the analysis of isothermal flow of a Newtonian liquid through a co-rotating twin screw extruder (Booy 1980). The study included the analysis of the flow in the nip region and it was reported that the volumetric flow rate through the nip region is proportional to the screw speed and that this flow is independent of the pressure gradient. The equation used for this study has a similar form as in Eq 2-6

For a Newtonian fluid, the flow behaviour in a screw or kneading disc element can be expressed as (Booy 1980; White 1991),

$$Q = \ddot{A}N + \dot{B}\Delta P \quad \dots \text{Eq. 2-6}$$

Where Q is the volumetric flowrate,  $\dot{A}N$  represents the contribution of drag flow,  $\ddot{A}$  is a constant composed solely of geometric terms and N is the screw speed.  $\dot{B}\Delta P$  represents the contribution to flow from the pressure flow,  $\dot{B}$  is a constant containing both the geometric and rheological terms and  $\Delta P$  is the pressure gradient.

Eq. 2.6 specifies the characteristics of a modular twin screw extruder when the screw and kneading disc elements are fully filled. However, in practice, some sections in twin screw extruders are in starved conditions where the screws are not fully filled by material. Hypothetically, starvation occurs when there is no pressure gradient and this region can be determined by back calculation from the die towards the hopper element by element. In general, a kneading disc element can reduce the pressure slowly and a screw element is able to reduce the pressure rapidly.

Research has been carried out using modified models based on Eq 2.6 to model the flow in the nip region of conveying zone and kneading zone of various types of fluid. However, a major drawback of the majority of modelling work is that the published experimental verification of the models is insufficient and the assumptions made regarding the flow, particularly in the nip and kneading sections are not well justified. Bakalis et. al started to study the flow of a co-rotating intermeshing twin screw extruders by measuring the volumetric flow-rate through the nip region using Doppler anemometry (Bakalis and Karwe 1999; Bakalis and Karwe 2002; Yerramilli and Karwe 2004). The experimentally measured velocity distribution in the nip region showed a positive displacement characteristic. It was

also reported that kneading blocks have a substantial leakage flow. These studies show that the experimental results are in a good agreement with theoretical predictions.

### **2.5.2 Prediction of mixing in twin screw extruder**

Residence time distribution, which arises from the fact that all particles of a material do not follow the same path through a vessel is widely used to characterise mixing in a twin screw extruder. Although there are many research papers on the axial and the transverse mixing in a twin screw extruder using the residence time distribution approach, there is no consistent outcome from those studies. Table 2-1 shows a few studies regarding residence time distribution of twin screw extruder previously carried out by different authors. The residence time distribution is reported to be obtained by injecting a pulse tracer into the system and samples were collected at the output stream at certain time interval for measurement of tracer concentration. A few authors reported that the mixing efficiency of a twin screw extruder varies with screw geometries and operating conditions but some reported that it is affected only by the screw geometries. There are other approaches to measure the residence time distribution in a single and twin screw extruder which is not reviewed in this section. Yet, there is still a lack of a general consensus regarding the effect of operating conditions and the geometry on mixing.

Authors	Method	Outcomes
(Oberlehner, Cassagnau et al. 1994)	<ul style="list-style-type: none"> <li>- Anthracenemethanol was used as a UV tracer and was injected as a pulse into the melt stream after steady state</li> <li>- Samples were collected every 10 s for determination of the intensity of the UV absorption peak</li> <li>- Dispersion axial, Tank in Series and Spectrum time models were used to fit the experimental data</li> </ul>	<ul style="list-style-type: none"> <li>- It was reported that the performance of mixing can be predicted using residence time distribution</li> <li>- Based on the calculated values of the model parameters, the mixing efficiency increases with the following order conveying element &lt; kneading section &lt; reverse element</li> </ul>
(Vainio, Harlin et al. 1995)	<ul style="list-style-type: none"> <li>- potassium thiocyanate tracer in an immiscible polymer blend</li> </ul>	<ul style="list-style-type: none"> <li>- It was reported that residence time distribution is a poor indicator of mixing efficiency in a twin screw extruder</li> <li>- High shear stress, sufficient residence time, and high fill ratio were the most important factors in achieving good dispersion</li> </ul>
(Gasner, Bigio et al. 1999)	<ul style="list-style-type: none"> <li>- introduced a new approach by normalising the residence time data with respect to screw speed to yield a residence revolution distribution (RRV)</li> <li>- reused data from previous studies and own studies</li> <li>- plot mean residence revolution against screw speed/volumetric (N/Q) flow rate</li> </ul>	<ul style="list-style-type: none"> <li>- filled volume of the extruder calculated from residence time data show that percent drag flow is linearly related to extruder filled volume</li> <li>- the average path taken by the tracer is closely related to the degree of fill</li> </ul>
(Gao, Walsh et al. 1999)	<ul style="list-style-type: none"> <li>- Transformation of the RTD to give both the residence-volume distribution (RVD) and the residence-revolution distribution (RRD) yields new physical insights into the extrusion process</li> </ul>	<ul style="list-style-type: none"> <li>- It was reported that for a given screw configuration the axial mixing of extrusion material as measured by a tracer is essentially the same for all operating conditions</li> <li>- These new tools motivate the development of a simple residence model that characterizes the partially filled and fully filled screw sections and is capable of distinguishing between screw configurations and operating conditions</li> </ul>

Authors	Method	Outcomes
(Carneiro, Caldeira et al. 1999)	<ul style="list-style-type: none"> <li>- Flow visualisation through a long transparent acrylic barrel by recording images with a conventional video camera</li> </ul>	<ul style="list-style-type: none"> <li>- The residence time distribution was independent of screw geometries and operating parameters</li> <li>- However, the flow patterns were highly dependent on the screw geometries but</li> <li>- Were insensitive to the process conditions</li> <li>- With the inclusion of a reverse element immediately downstream of the kneading section resulting in a greater generation of eddie currents within the kneading section</li> </ul>
(van Zuilichem, Kuiper et al. 1999)	<ul style="list-style-type: none"> <li>- Flow visualisation</li> </ul>	<ul style="list-style-type: none"> <li>- Axial mixing is not affected by operating conditions but screw geometries</li> <li>- Eddie currents were reported occurred mainly at the first kneading disc</li> <li>- Short kneading sections may provide more efficient axial mixing than a single long mixing section of an equivalent length</li> <li>- Reverse pumping sections have a significant effect on axial mixing</li> <li>- Only certain geometries have an effect on mixing for particular operating conditions</li> <li>-</li> </ul>
(Puaux, Bozga et al. 2000)	<ul style="list-style-type: none"> <li>- Small quantity of iron powder was injected in pulse mode</li> <li>- The tracer concentration was measured based on the change of the magnetic susceptibility of the polymer melt</li> <li>- Experiment data was fitted with one, two and three parameters flow models</li> </ul>	<ul style="list-style-type: none"> <li>- The axial dispersion, backflow cell and double backflow cell models fitted the experimental data accurately to the experimental data</li> <li>- No reports about the influences of screw geometries and operating conditions on residence time distribution</li> </ul>



Authors	Method	Outcomes
(Shearer and Tzoganakis 2000; Shearer and Tzoganakis 2001)	<ul style="list-style-type: none"> <li>- Carbon black as the tracer and an infrared temperature probe to detect the temperature decrease caused by the changing surface emissivity</li> <li>- mixing limited interfacial reaction between polymer tracers was used to directly measure the distributive mixing</li> <li>- Axial mixing and distributive mixing</li> </ul>	<ul style="list-style-type: none"> <li>- Similar outcomes to (van Zuilichem, Kuiper et al. 1999)</li> <li>- The axial mixing is not affected by the operating conditions</li> <li>- the screw speed has little effect on local residence time distribution for reverse pumping elements</li> <li>- the distributive mixing is most effective with kneading discs staggered at 30° which is opposite to previous studies which reported best mixing is under condition with backflow</li> </ul>
(Kumar, Ganjyal et al. 2008)	<ul style="list-style-type: none"> <li>- pulse injection of erythrosin (red) dye and samples were collected every 10 s</li> <li>- concentration of tracer was determined by colour measurement</li> <li>- experimental data fitting using Tank in series and complete model</li> </ul>	<ul style="list-style-type: none"> <li>- plug flow fraction, dead volume fraction and number of tanks can be calculated by fitting the empirical data using the proposed models</li> <li>- parameter n which describe the degree of mixing is affected by the operating conditions and the screw geometries</li> </ul>

Table 2-1: Summary of previous studies on residence time distribution to characterise mixing

## **2.6 TWIN SCREW GRANULATION**

The Twin Screw Extruder (TSE) is widely used in polymer and food processing. It is becoming popular in wet granulation operations as it allows for continuous processing. Since the granulator has a small hold up volume, it can also minimise material losses during start up and shut down due to maintenance purposes. The twin screw extruder is also popular because of its flexibility, for example, the option where to locate the feed ports, flexibility in screw configurations that give different mixing and compounding effects and heating and cooling by introducing a jacket around the barrel. Besides this, the screws are self-wiping which minimise the accumulation and possible degradation of materials that keeps the surface of the screws inherently clean. Moreover, twin screw granulations can lead to a more economic process (saving labour costs and time) and allow a 24 hour production line with automated control. Therefore, extrusion for granulation is currently one of the most studied technique for continuous wet granulation (Vervaet and Remon 2005).

Twin screw extruder was first applied in pharmaceutical research by Gamlen and Eardley in 1986 to produce extrudates (Gamlen and Eardley 1986). A Raker Perkins MP50 (Multipurpose) Extruder was used to produce paracetamol/avicel/lactose extrudates with high drug loading in the study. The quality of the paracetamol extrudates was evaluated to investigate the influences of formulation and moisture content. It was reported that the quality of paracetamol extrudates was not as good as predicted and they had a shark skin or very rough surface. The addition of hydroxypropyl methyl cellulose could improve the extrudability but it was very limited on the improvement of the quality of extrudates.

Lindberg then carried out a few studies using similar extruder set up in 1987 (Lindberg, Tufvesson et al. 1987) to characterize the process for an effervescent granulation formulation

as well as to investigate the suitability and the advantages of Twin Screw Extruder as an instant granulator. The mean residence time of the extrusion granulation process was determined by injection of a small amount of colour tracer in the inlet port and measuring the time to reach the outlet of the extruder. The mean residence time was significantly influenced by the screw speed and powder feedrate as reported in Linberg's study (Lindberg, Myrenas et al. 1988). A second objective of the studies was to investigate the effect of the process conditions on the granule intragranular porosity and liquid saturation. Granules were produced with anhydrous citric acid, sodium bicarbonate and ethanol as granulation liquid using the same extruder. It was reported that the porosity of granules produced was significantly influenced by the screw configuration and the ethanol concentration as well as the decomposition of sodium bicarbonate. Higher operating temperature (due to intense mixing) will enhance the formation of carbon dioxide and consequently producing a more porous granule. Nevertheless, the porosity of the granules decreased when larger amount of ethanol was used and this is as expected as the liquid phase occupied the granules.

Keleb, Vermeire et al. (2001) started studying twin screw granulation using a co-rotating twin screw extruder (Model MP 19 TC 25, APV Baker, Newcastle-under-Lyme, UK). Initially the potential of a cold extrusion as a continuous granulation/tabletting technique was investigated. Extrudates were made with a formulation containing  $\alpha$ -Lactose monohydrate as an excipient, polyvinylpyrrolidone (PVP) as binders, hydrochlorothiazide as the model drug and water as granulation liquid and were manually cut into tablets at room temperature. It was reported that the formulation (water and binder content) and the process conditions (screw speed and powder feedrate) had only a minor effect on the tablet properties. It was also reported that the technique produces porous tablets with acceptable quality at optimum extrusion conditions. Keleb, Vermeire et al. (2002) then studies the suitability of the twin

screw extruder to produce granules continuously. A map of possible operating conditions was produced as shown in Figure 2-6 and it was shown that variation in formulation and process conditions had a major impact on process feasibility. The properties of the granules produced were neither affected by the screw speed and input rate nor the formulation used. However, addition of PVP as binder in the formulation had a major impact on the tablet tensile strength.

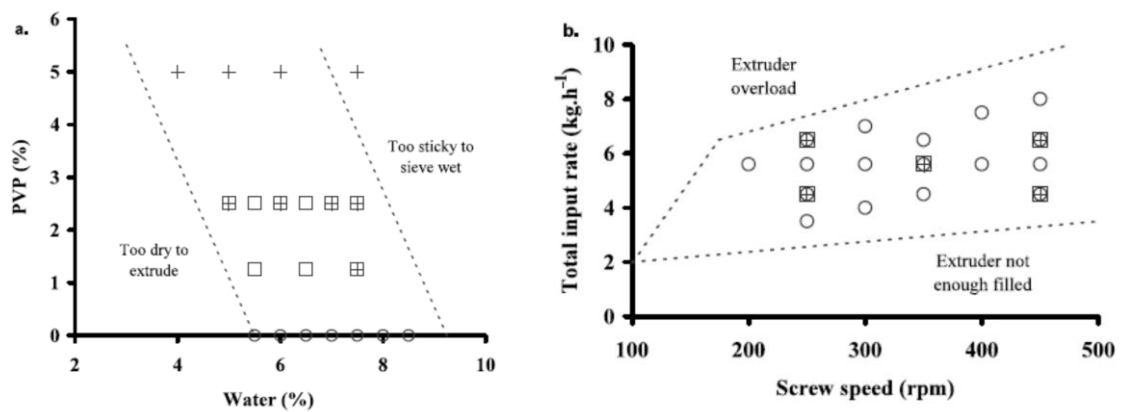


Figure 2-6: Overview of the experiments performed to evaluate: (a) the influence of water concentration during extrusion and PVP-concentration (screw speed: 250 rpm; total input rate 5.6 kg h<sup>-1</sup>); and (b) the influence of screw speed and total input rate (water concentration during extrusion: 7.5%, w/w) on the properties of  $\alpha$ -lactose monohydrate granules. Method of binder addition: (○) without PVP; (□) wet addition of PVP; (+) dry addition of PVP. Extract from original document (Keleb, Vermeire et al. 2002).

Keleb furthered the investigation of the twin screw granulation process by replacing the discharge zone with a conveying zone as well as using a smaller die for screening purposes (Keleb, Vermeire et al. 2004). The continuity of the process was assessed by continuously running the process at reference conditions for 8 h with an hourly evaluation of the granules and tablet properties. The granulation process fails when smaller die was used due to a high power consumption, high barrel temperature, screen distortion and screw blocking. Without a die the granules gave higher yield and the wet sieving stage can be neglected. For a period of 8 hours, the quality of the granules and tablets produced showed consistency and were reproducible throughout the process. In the same year, the authors repeated the study of single

step granulation/tabletting experiments but using different grades of  $\alpha$ -Lactose monohydrate. The study showed that different grade of primary powder will have a significant impact on materials feeding that will then affect the process performance and process capacity. Moreover, the disintegration time of the tablets produced was also strongly affected by the primary powder used and the duration of storage. Finally, the authors concluded that all the findings obtained were indication of the possibility of using twin screw extruder as an efficient tool for continuous granulation.

Besides wet granulation, melt granulation was also studied using a similar twin screw extruder with Polyethylene Glycol (PEG 400 and 4000) as the binders for the development of a drinking water formulation with an immediate drug release (Van Melkebeke, Vermeulen et al. 2006). It was found that the granulation temperature was the key factor that affects the process yield. A temperature near the melting point of PEG will lead to higher yield. However, the drug (BCS class II) was not immediately released from the tablets produced using this technique and the addition of a small fraction of surfactant (polysorbate 80 or Cremophor<sup>®</sup> RH40) was required. Moreover, the molten PEG allows the drug to be finely dispersed creating a micro-environment around the drug particles that enhances the dissolution rate. A second attempt was carried out by Van Melkebeke, Vervaet et al. (2008) to validate the twin screw granulation process using the same extruder under the same process conditions and process formulation used by Keleb, Vermeire et al. (2004). More screw geometry types were considered in this study and the mixing efficiency was also studied for the first time. It was reported that the conveying zone after the final mixing zone has the ability to break up larger granules. 90° mixing zone produced granules with lower friability but lower yield. Other than that, the properties of the granules and tablets were not significantly affected by the screw configurations. The mixing efficiency was determined by

means of adding different tracers (0.05% of aqueous riboflavin and 2.5% of solid hydrochlorothiazide) in the feeding zone and by measuring the concentration of the tracers in the product stream as a function of time. It was concluded that the kneading block of the extruder managed to ensure a homogeneous drug distribution during the granulation. The mixing efficiency was also independent of the tracer addition method used.

In recent years, there is increasing number of research groups investigating the continuous twin screw granulation process. Generally the properties of the granules and tablets are evaluated and there are also several studies focusing on the process and formulation optimisation (Dhenge, Fyles et al. 2010; El Hagrasy and Lister 2011). Djuric and Kleinebudde (2008); Thompson and Sun (2010) did similar experiments investigating the influences of screw geometries on granule properties using an extruder model (Leistritz Micro 27GL/28D Leistritz Extrusions technik GmbH, Nuremberg, Germany). A combing mixer (see Table 3-1) was considered in the study and the results were similar to Van Melkebeke, Vervaet et al. (2008) study. The authors also studied the impact of the powder feedrate on granule properties two years later using a similar experiment setup (Djuric and Kleinebudde 2010). It was reported that a higher material throughput will lead to the production of larger granules with lower porosity and lower friability due to higher fill levels in the barrel. Djuric, Van Melkebeke et al. (2009) carried out another study on twin screw granulation by comparing Di-calcium phosphate and  $\alpha$ -lactose monohydrate granules produced by two type of twin screw extruder (Leistritz Micro 27GL/28D and APV Baker Model MP 19 TC 25). For both types of extruder, granules could be easily produced by using any excipients but there was a huge impact on the granule mean diameter and friability. The study then showed that the two types of extruders were not interchangeable to produce similar granules for certain formulation. Dhenge, Cartwright et al. (2011) also investigated the influences of powder

feedrate on granule properties using a co-rotating twin screw granulator for pharmaceutical granulation (Euro lab 16 TSG, Thermo Fisher Scientific, Stone, United Kingdom) and similar outcomes were obtained.

## **2.7 CONCLUSION**

The mechanism of conventional wet granulation was briefly discussed in this chapter. It is clear that the wet granulation process consists of three main stages which are wetting and nucleation, consolidation and coalescence and breakage and attrition. Wetting and nucleation is one of the key processes as the granule size distribution will depend on the nuclei size distribution formed at this stage. The process is strongly controlled by the drop penetration time and dimensionless spray flux. The nuclei will also be densified and the liquid will be forced towards the surface which allows coalescence with neighbouring particles. This is the stage where granules start to grow into a larger size. The granule growth is affected by the maximum pore saturation and the Stoke's deformation number. The final stage of wet granulation is breakage which is least studied by researchers. Breakage only occurs when a granule is not sufficiently strong to withstand the force that exists from agitation or collision during the process. Critical Stokes deformation number,  $St_{def}^*$  is used to characterise the condition when breakage occur.

Twin screw extruders have been used widely in the polymer processing and food industry. There has been a great deal of work undertaken to study the residence time distribution and the mixing efficiency in a twin screw extruder as well as in the modelling of the flow performance in the nip region. However, there is a major drawback to the majority of modelling studies as there is insufficient of published empirical verification of the model and the limit of the assumptions made regarding the flow especially in the nip region and

kneading elements. The residence time and mixing studies also face the same drawback as there is still a lack of a general consensus regarding the effect of operating conditions and geometry on mixing.

There has been an extensive amount of research on the twin screw wet granulation process. However, the focus has been on the characteristic of the granules and tablets produced using a twin screw extruder with various process conditions and formulations. The work carried out by different research groups was summarised in Table 2-2, Table 2-3 and Table 2-4 for the past decade. The particle size distribution, porosity, density, yield, morphology, strength and friability have been studied for the granules produced using different types of formulation (different grades of primary powder and various binder contents) and process conditions (screw geometries, powder feedrate, screw speed). Moreover, tablets were made from the granules and the tensile strength, the friability, the dissolution rate and the stability of these tablets were also studied. Generally, it was concluded that by many researchers, the twin screw wet granulation process was robust enough to produce granules continuously. The process was also reproducible and able to produce granule consistently.

Yet, to date there has been only a little work published on the mechanism of twin screw wet granulation and therefore, the possibility to describe the process using conventional wet granulation remains unknown. The research scope of the current work involves the comparison of twin screw granulation and the high shear mixer granulation process as a fundamental step to get some insight of the differences in these processes mechanisms. Positron Emission Particle Technique is applied in order to visualise the particle in the opaque system that can be used to observe the flow performance of a twin screw granulator. A residence time distribution is also obtained using this technique to study the axial mixing in



the twin screw granulator. The ability of the process to remove feeding noise is also studied and the feasibility of the granulator to make granules is also examined.

**Granules Evaluation:**

<b>Test</b>	<b>Method/Equipment</b>	<b>Comment</b>
<b>Granule Size Distribution</b> (Keleb, Vermeire et al. 2002; Keleb, Vermeire et al. 2004; Van Melkebeke, Vermeulen et al. 2006; Djuric and Kleinebudde 2008; Van Melkebeke, Vervaet et al. 2008; Djuric, Van Melkebeke et al. 2009; Dhenge, Fyles et al. 2010; Djuric and Kleinebudde 2010; Dhenge, Cartwright et al. 2011)	Laser diffraction (Rodos, Sympatec.)  Image analysis (QICPIC, Sympatec.)  Sieve (Retsch VE 1000, Haan, Germany)	The volume diameter ( $d_v$ ) was used to determine the fraction of $F < 250\mu\text{m}$ , $250\text{--}1000\mu\text{m}$ and $F > 1000\mu\text{m}$ . Minimum air pressure is used during the measurement to avoid de-agglomeration and/or disintegration of the granules.  The projected area of particles is captured using high speed cameras. The size is then determined using software analysis for example by determining diameter of a Circle of Equal Projection Area  Separate at amplitude of 2mm in a series of sieve for 10 minutes.
<b>Granule Porosity (<math>\epsilon</math>)</b> (Keleb, Vermeire et al. 2004; Djuric and Kleinebudde 2008; Van Melkebeke, Vervaet et al. 2008; Djuric, Van Melkebeke et al. 2009; Djuric and Kleinebudde 2010)	Mercury Porosimeter (Autopore III, Micromeritics, Norcross, Georgia, USA)	Granule porosity and median pore diameter of granules (500–1000 $\mu\text{m}$ ) were using mercury porosimetry. Intragranular porosity was determined using the cumulative intrusion curve.
<b>Granule bulk density (<math>\rho_{bulk}</math>)</b> (Keleb, Vermeire et al. 2002; Keleb, Vermeire et al. 2004; Van Melkebeke, Vervaet et al. 2008)	Measuring cylinder	Bulk volume ( $V_o$ ) of granules (250 – 1000 $\mu\text{m}$ ) weight $M$ was recorded in measuring cylinder. Bulk density is calculated as $M/V_o$ .

<b>Granule Tapped Density</b> $(\rho_{tapped})$ (Keleb, Vermeire et al. 2002; Keleb, Vermeire et al. 2004; Van Melkebeke, Vervaet et al. 2008)	Tapping machine (J. Englesman, Ludwigshafen, Germany)	Volume of granules weight $M$ after 1500 taps ( $V_{1500}$ ) in tapping machine is measured Tapped density is then calculated as $M/V_{1500}$ .
<b>Granule Strength</b> (Bouwman 2005; Dhenge, Fyles et al. 2010; Dhenge, Cartwright et al. 2011)	Micromanipulation rig	
<b>Granule Friability</b> (Keleb, Vermeire et al. 2002; Keleb, Vermeire et al. 2004; Van Melkebeke, Vermeulen et al. 2006; Van Melkebeke, Vervaet et al. 2008)	Friabilator, PTF E Pharma Test Hainburg, Germany	Run at speed of 25 rpm for 10 min by subjecting 10 g ( $I_{wt}$ ) of granules ( $F_{250-1000 \mu m}$ ) together with 200 (4mm) glass beads. Fraction of 250 $\mu m$ ( $F_{wt}$ ) was sieved at amplitude of 2 mm. The friability was calculated as $(I_{wt} - F_{wt}/I_{wt}) \times 100$ .
<b>Yield</b> (Keleb, Vermeire et al. 2002; Keleb, Vermeire et al. 2004; Djuric and Kleinebudde 2008; Van Melkebeke, Vervaet et al. 2008; Djuric, Van Melkebeke et al. 2009; Djuric and Kleinebudde 2010)		The yield is determined as $F_{<1400 \mu m} (\%) \times F_{250-1000 \mu m} (\%) / 100$ Where $F_{<1400 \mu m}$ is fraction of dried granules smaller than 1400 $\mu m$ and $F_{250-1000 \mu m}$ is granules fraction between 250 and 1000 $\mu m$ .
<b>Compressibility index (C%)</b> (Keleb, Vermeire et al. 2002; Keleb, Vermeire et al. 2004)		$C\% = \left( \frac{\rho_{tapped} - \rho_{bulk}}{\rho_{tapped}} \right) \times 100$

<p><b>Morphology</b> (Schmidt, Lindner et al. 1997; Schmidt and Kleinebudde 1998; Dhenge, Fyles et al. 2010; Dhenge, Cartwright et al. 2011)</p>	<p>Optical microscope (Leica,)  Image Analysis (QICPIC, Sympatec)</p>	<p>Aspect ratio, <math>AR = \frac{L_1}{B}</math> where <math>L_1</math> and <math>B</math> were denoted as the length and width of granules.  Equivalent diameter, <math>D_{eq} = \sqrt{\frac{4 \times A}{\pi}}</math> where <math>A</math> represented as the projected area (can be considered as <math>\pi r^2</math> if the projected area is a round shape) of the extrudate/granule.</p>
<p><b>Granule surface/internal structure</b> (Keleb, Vermeire et al. 2002; Dhenge, Fyles et al. 2010; Dhenge, Cartwright et al. 2011)</p>	<p>Scanning electron microscopy (SEM)  Micro X-Ray CT scanner (SkyScan, )</p>	

Table 2-2: Work carried out by previous researchers on characterisation of granule produced using twin screw extruder

**Tablet evaluation:**

<p><b>Tablet Porosity, <math>\epsilon_{\text{tablet}}</math></b> (Keleb, Vermeire et al. 2001; Keleb, Vermeire et al. 2004; Djuric and Kleinebudde 2008; Djuric, Van Melkebeke et al. 2009; Djuric and Kleinebudde 2010)</p>	<p>He-pycnometry (Micromeritics, Norcross, GA)</p> <p>Mercury porosimetry (Autopore III, Micromeritics)</p>	<p>Skeletal volume was determined using He-pycnometry. Bulk volume is determined by measuring the tablet dimensions. Tablet porosity is calculated as <math>\epsilon_{\text{tablet}} = (\text{bulk volume} - \text{skeletal volume}) / \text{bulk volume} \times 100</math></p>
<p><b>Tablet tensile Strength</b> (Keleb, Vermeire et al. 2001; Keleb, Vermeire et al. 2002; Keleb, Vermeire et al. 2004; Keleb, Vermeire et al. 2004; Djuric and Kleinebudde 2008; Van Melkebeke, Vervaet et al. 2008; Djuric, Van Melkebeke et al. 2009; Djuric and Kleinebudde 2010)</p>	<p>PTB 311, Pharma Test, Hainburg, Germany</p> <p>Diametrical Compression (Zwick, )</p>	<p>Tablet tensile strength is determined using the following equation describe by Fell and Newton (1968) as</p> $T = \frac{2F}{\pi dt}$ <p>Where <math>F</math>, <math>d</math> and <math>t</math> were denoted as the crushing force, product diameter and thickness respectively.</p>
<p><b>Tablet Friability</b> (Keleb, Vermeire et al. 2001; Keleb, Vermeire et al. 2002; Keleb, Vermeire et al. 2004; Keleb, Vermeire et al. 2004; Van Melkebeke, Vervaet et al. 2008)</p>	<p>Friabilator, PTF E Pharma Test Hainburg, Germany</p>	<p>Test at speed 25 rpm for 4 min. Friability is express as percentage of tablet weight lost.</p>

<p><b>Disintegration Time</b> (Keleb, Vermeire et al. 2001; Keleb, Vermeire et al. 2002; Keleb, Vermeire et al. 2004; Keleb, Vermeire et al. 2004; Van Melkebeke, Vervaet et al. 2008)</p>	<p>Apparatus describe in Eur. Ph. III (PTZ-E, Pharma Test, Hainburg, Germany)  VK 7010 (Vankel, Cary, NC, USA)</p>	<p>Refer to Eur. Ph. III</p>
<p><b>Dissolution Test</b> (Keleb, Vermeire et al. 2001; Keleb, Vermeire et al. 2002; Keleb, Vermeire et al. 2004; Keleb, Vermeire et al. 2004; Van Melkebeke, Vermeulen et al. 2006; Van Melkebeke, Vervaet et al. 2008)</p>	<p>Paddle method (Vankel, Cary, NC, USA) Spectrophotometer (Lambda 12 Perkin Elmer, Norwalk, US)</p>	<p>Tablet is placed in a dissolution medium at rotational speed of 100 rpm, constant temperature of 37±0.5 °C (USP XXIII). Sample is withdrawn every 5 minutes for first 30 minutes, 45 and 60 minutes. Concentration will then be determined using spectrometer at 245 nm.</p>
<p><b>Microscopic Image</b> (Keleb, Vermeire et al. 2002; Keleb, Vermeire et al. 2004)</p>	<p>Scanning electron microscopy (SEM) Micro CT scanner</p>	

Table 2-3: Work carried out by previous researchers on tablet characterisation

## Other

<p><b>Residence Time distribution</b> (Fogler 2006)</p>	<p>Scanner, Image J software Dye as tracer</p>	<p>Dye was injected to extruder in 1 second after the extruder reached steady state. Granules were then collected every 5 seconds for a period of 1 minute. Each time interval granules were scanned and the colour was analysed using image software. The residence time is calculated as</p> $e(t) = \frac{c(t)}{\int_0^{\infty} c(t)dt}$ <p>Where <math>a(t)</math> is the concentration at time <math>t</math>. Mean residence time, <math>t_m = \int_0^{\infty} t \cdot e(t)dt</math> Variance, <math>\sigma^2 = \int_0^{\infty} (t - t_m)^2 \cdot e(t)dt</math></p> $\frac{\sigma^2}{t_m^2} = \frac{2}{Pe} - \frac{2}{Pe^2} (1 - e^{-Pe})$ <p>Where <math>Pe</math> is Peclet number which is measure of the colour spread.</p>
<p><b>Mixing efficiency</b> (Van Melkebeke, Vermeulen et al. 2006; Van Melkebeke, Vervaet et al. 2008)</p>	<p>Riboflavin (wet addition, suspended in liquid) Hydrochlorothiazide (dry addition, added separately using secondary feeder)</p>	<p>Mixing efficiency as function of time Tracer was added either ways into the extruder. Granule was produced and collected in an interval time of 1 – 5 minutes for a period of 1 hour without start up. Granule was then dried and concentration of tracer was measured using spectrometer.</p> <p>Mixing efficiency as a function of granule size The process is similar to previous experiment. The differences are there was a start up period of 5 minutes and the granule was separated into fractions according to size.</p>

Table 2-4: Other published work on twin screw wet granulation

## **CHAPTER 3 : THE FORMULATION OF GRANULE AND CO-ROTATING TWIN SCREW EXTRUDER**

---

### **SUMMARY**

General pharmaceutical ingredients normally used to produce granules and tablets are introduced in this chapter. Common excipients for example fillers, binders, lubricants, disintegrants and stabilisers and their functions are described.

The formulations to produce granules in the current study are discussed in this chapter. Two types of formulations are considered: (a) pure MCC and (b) lactose, MCC, HPC and croscarmellose sodium. Pure MCC is used to produce granules in order to keep the system simple so that the evaluation of granule structure becomes straight forward. The second type of formulation is well studied by other researchers and is used so that the experiments performed are close to actual pharmaceutical processing. The functions of each ingredient are discussed later in this chapter.

The basic design of co-rotating twin screw extruder is explained. The functionality of the screw elements, including conveying element, mixing disc element and combing elements are described briefly. Various arrangements of the kneading discs have different features and will give different compounding actions which are discussed. Two types of co-rotating twin screw extruders are used to produce granules in the current study. An extruder model type PTW16/25PC obtained from Haake, Germany (previously used for ceramic and polymer extrusion) is used to obtain a fundamental understanding of the twin screw wet granulation process. The second type of extruder is built in house by GEA Pharma System for the purpose of the PEPT study.



Finally some key properties of the granules, including particle size distribution, porosity, flowability and the mechanical strength are introduced.

### **3.1 OBJECTIVE**

The aim of this chapter is to introduce some of the general ingredients used in pharmaceutical formulation and their function in granules and tablet manufacturing. Besides this, some important design criteria of the twin screw extruder are also described in this chapter.

### **3.2 PHARMACEUTICAL INGREDIENTS**

A medical dosage form regardless of composition or mode of use must meet the following requirements (Swarbrick 2007),

- Contain an accurate dose.
- Be convenient to take or administer.
- Provide the drug in a form for absorption or other delivery to the target.
- Retain quality throughout the shelf life and usage period.
- Be manufactured by a process that does not compromise performance and that is reproducible and economical.

On most occasions, direct process of active pharmaceutical ingredients (API) will not give products that meet the above criteria and therefore, it is necessary to add other materials to overcome any shortfalls. Generally, a pharmaceutical dosage form is comprised of the active

ingredients and excipients. By definition from the FDA<sup>1</sup> an active ingredient is any component that provides pharmacological activity or other direct effect in the diagnosis, cure, mitigation, treatment, or prevention of disease, or to affect the structure or any function of the body of man or animals. Excipients on the other hand are the substances that allow a dosage form to meet the requirements stated above as they are related directly to the product performances.

### **3.3 COMMONLY USED EXCIPIENTS IN THE GRANULATION PROCESS**

For pharmaceutical wet granulation, the excipients can be classified into two major categories which are bulking agents and functional additives. Bulking agents are also called fillers and are different from the functional additives in that they are normally inert materials and are relatively inexpensive. The functional additives are normally added to give a particular function in the dosage form such as binders, disintegrants, lubricants, colorants and stabilizers. The selection of the excipients depends on the drugs, the process as well as the cost of the materials. For example, for fluidized bed granulation, the excipients selected must not have a huge difference in materials density so that segregation can be prevented.

#### **3.3.1 Pharmaceutical filler**

Lactose, dicalcium phosphate, starch and microcrystalline cellulose are fillers that are commonly used in pharmaceutical granulation. Fillers can also be considered serving another function, as they form the structure or matrix of a dosage form. Fillers are normally inactive substances that are used as the active ingredient carrier and they are relatively inexpensive. Besides this, fillers and glidants are also used as a process aid to improve the flow of the

---

<sup>1</sup> <http://www.fda.gov/default.htm>

powder from the hopper to the die during tablet compaction and therefore giving an enhanced accuracy and consistency of the produced tablets (Aulton 2007).

### **3.3.2 Pharmaceutical binder**

Binders are added wet or dry in dosage formulation as adhesives during wet granulation. The function of binders is mainly to provide the cohesiveness for the bonding between solid particles. Binders are also used to facilitate the granule size enlargement as the granulation liquid with higher viscosity creates a condition that allows efficient coalescence. The inclusion of a binder also results in production tablets with improved hardness by enhancing the intra-granular and inter-granular forces (Hamed, Moe et al. 2005). Binders can be classified into two groups which are natural polymers (e.g. starch and gelatine) or synthetic polymers (e.g. Polyvinylpyrrolidone, methyl cellulose). Sugars (e.g. Glucose, Sucrose, and Sorbitol) can also be considered as binders as they exhibit good bonding properties and produce hard and brittle tablets. The selection of binder depends on the requirements of the granule properties. However, excessive of binder might cause very slow dissolution of tablet.

### **3.3.3 Pharmaceutical disintegrants**

Disintegrants are the substances added to dosage (normally tablets or capsules) formulations to promote the breakup of the tablet into smaller fragments in an aqueous environment thereby increasing the available surface area and promoting a more rapid release of the drug substance. Examples of disintegrants are microcrystalline cellulose, croscamellulose sodium, and modified (chemically treated) starches. The mechanism of disintegration for the tablet involves swelling of the materials in contact with water, wick and effervescence to overcome the adhesiveness of other ingredients causing the tablet matrix to

fall apart. Some elastics materials are believed to be deformed, and under “energy rich” conditions under pressure and this energy will be released upon exposure to water.

### **3.3.4 Lubricants**

Lubricants are used to aid the manufacturing process. They are added in a dosage formulation to reduce friction between moving parts during compression or compaction; this also helps prevent materials sticking to the process equipment. The most widely used type of lubricant used in the pharmaceutical industry is magnesium stearate (Weiner and Kotkoskie 2000). The dosage level of this lubricant in tablets is relatively small as the substance is hydrophobic and will retard the release time of the active ingredients in tablets (Hussain, York et al. 1992).

### **3.3.5 Pharmaceutical Stabilisers**

Some drug substances are unstable and undergo chemical transformation or physical changes that alter their performance. The degradation of these substances may be due to environment component (such as vapour, sunlight and temperature) or the interactions between adjacent molecules of drugs. The degradation of the substances could be retarded by adding a stabiliser, for example, formulation with substances whose light absorption spectrum overlaps that of the photolabile drug or using an antioxidant in formulations that are susceptible to degradation by oxidation (Hussain, York et al. 1992).

## **3.4 FORMULATION OF GRANULES USED IN THIS STUDY**

There are two types of formulation used in this study. Initially, granules were made using 100 % microcrystalline cellulose in Chapter 4 in order to study the understanding of the fundamental mechanisms of twin screw wet granulation. The reason for using a wet

granulation process using 100 % microcrystalline cellulose is to simplify the system so that the structure of the granules can be examined easily. As microcrystalline cellulose is a widely used material in extrusion and spheronization processes, it would be expected that it can be granulated efficiently using a twin screw extruder.

Another formulation used in this study to make granules is a published and well studied recipe used by a number of researchers (Dhenge, Fyles et al. 2010; Dhenge, Cartwright et al. 2011). This formulation consists of lactose and microcrystalline cellulose as the filler, hydroxylpropyl cellulose as the binder and croscamellulose sodium (Ac-Di-Sol) as the disintegrant. The composition the ingredients are shown in Figure 3-1 and the characteristic of each ingredient is discussed as follows.

**Powder Mixture Compositions (%)**

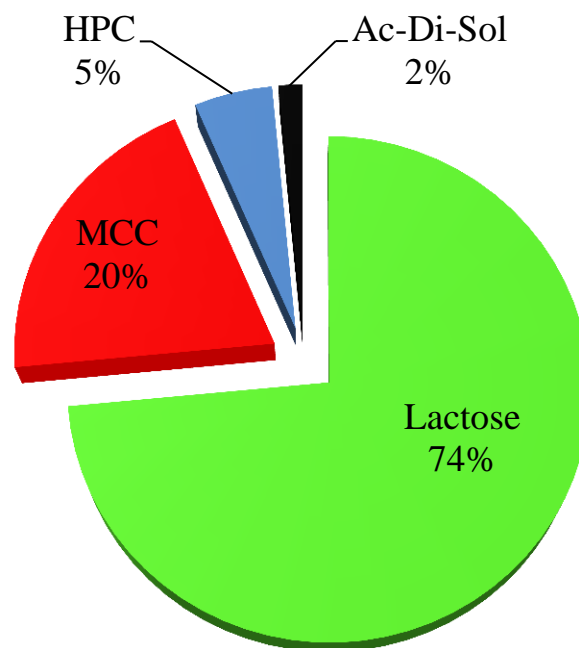


Figure 3-1: Composition of tablet ingredients for current study

### 3.4.1 Lactose

Lactose is the most common type of filler used in pharmaceutical manufacturing. It is a natural disaccharide consisting of galactose and glucose, and is present in the milk of most mammals (Rowe, Sheskey et al. 2009).  $\alpha$ -Lactose Monohydrate (Pharmatose 200 M, DMV-Fonterra, Netherlands) is the grade of lactose used in this study. The material has a mean particle diameter (d50) of 50  $\mu\text{m}$  and is supplied in a stable crystalline form.  $\alpha$ -Lactose Monohydrate appears as white to off-white crystalline particles or powder and is odourless and slightly sweet-tasting. This fine grade of lactose is suitable for the preparation of tablets and wet granulation processes due to the ability for better mixing with other formulation ingredients and utilizes the binder more efficiently.

### 3.4.2 Microcrystalline Cellulose

Microcrystalline cellulose is another type of filler widely used in the pharmaceutical industry. It is manufactured by controlled hydrolysis with dilute mineral acid solutions of  $\alpha$ -cellulose, obtained as a pulp from fibrous plant materials (Rowe, Sheskey et al. 2009). Avicel PH 101 supplied from FMC Biopolymer, Ireland was chosen for this study. The needle shape particles have a mean particle (d50) diameter of 50  $\mu\text{m}$  and the purified, partially depolymerised cellulose occurs as a white, odourless, tasteless, crystalline powder composed of porous particles (Rowe, Sheskey et al. 2009). The addition of this material in wet granulation will lead to rapid and homogenous wetting due to the wicking action of microcrystalline cellulose. Besides this, microcrystalline cellulose can improve the flow of the powder and the high compressibility of the material allows the production of harder tablets. The ability to swell of the material in contact with water also allows faster disintegration of the tablets.

### **3.4.3 Hydroxypropyl Cellulose**

Hydroxypropyl cellulose is used in this study as a binder to create cohesiveness for bonding for the solid particles. It is produced by reacting a purified form of cellulose with sodium hydroxide. The swollen alkali cellulose is then reacted with propylene oxide that can be substituted on the cellulose group through an ether linkage (Rowe, Sheskey et al. 2009). Hydroxypropyl Cellulose with a molecular weight 100,000 was purchased from Alfa Aesar, UK for this project. The material has a mean particle diameter of 150 µm and occurs in white to slightly yellow-coloured, odourless and tasteless flaky powder. Storage conditions can severely alter the properties of tablets through their effect on the physical characteristic of binder (Kiekens, Zelko et al. 2000; Hamed, Moe et al. 2005). It was reported that Hydroxypropyl cellulose has no glass transition temperature and thereby the tablets prepared using hydroxypropyl cellulose maintain their hardness and dissolution profile after storage for 24 weeks under various conditions (Fitzpatrick, McCabe et al. 2002).

### **3.4.4 Croscarmellose sodium (Ac-Di-Sol)**

Croscarmellose sodium is an internally cross-linked sodium carboxymethyl cellulose commonly use as a disintegrant in pharmaceutical formulations. It is made by steeping cellulose in sodium hydroxide and then reacting it with sodium monochloroacetate to obtain carboxymethylcellulose sodium. The glycolic acid, which forms by hydrolysis of excess sodium monochloroacetate and catalyzes the formation of crosslinks to produce croscarmellose sodium (Rowe, Sheskey et al. 2009). Croscarmellose sodium (Ac-Di-Sol SD-711 NF) was obtained from FMC Biopolymer, USA for this study. It appears as an odourless, white or greyish white powder. The cross linked structure creates an insoluble, hydrophilic, and highly absorbent excipient that results in exceptional swelling properties that results in

superior functionality in wet granulation. Ac-Di-Sol can also assure the long term stability of dissolution and disintegration.

### 3.5 CO-ROTATING TWIN SCREW

In this section, some basic design criteria of a co-rotating twin screw extruder will be described. The functionality of each screw type is also discussed. Some of the important regions in the extruder will be shown and the extruder types used in current study are briefly described.

#### 3.5.1 Basic screw types

The screws of an extruder generally consist of conveying zones for transporting materials and mixing zones for compounding actions. The screw elements will be mainly one of the basic types shown on Table 3-1. A schematic of classical type of co-rotating twin screw is shown in Figure 3-2.

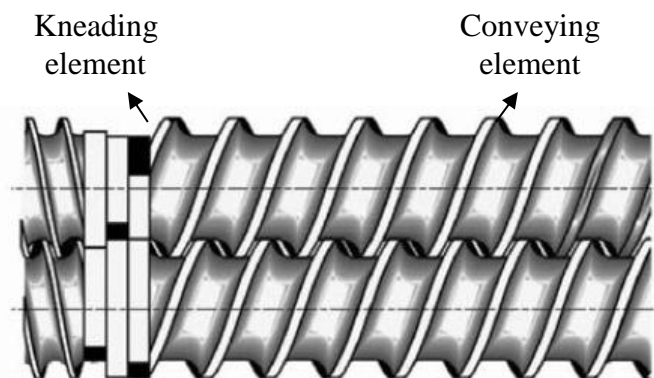


Figure 3-2: Classical co-rotating twin screw (Thiele, Ghebre-Selassie et al. 2003)






Screw type	Descriptions
 <p data-bbox="277 472 531 506">Conveying element</p>	<ul data-bbox="730 293 1394 539" style="list-style-type: none"> <li>• Always used for transporting, feeding and pumping materials</li> <li>• There are types of screws: right (forward) and left (backward) flight</li> <li>• Right handed flight was used in present for the purpose transporting materials in the barrel</li> </ul>
 <p data-bbox="277 770 576 804">Kneading disc element</p>	<ul data-bbox="730 589 1394 824" style="list-style-type: none"> <li>• Can arranged in a great variety of geometries to give different distributive and dispersive action as well as compounding actions</li> <li>• 30°, 60° and 90° mixing configurations were considered in current study (See Chapter 5, 6 and 7)</li> </ul>
 <p data-bbox="277 1070 512 1104">Combing element</p>	<ul data-bbox="730 869 1394 1048" style="list-style-type: none"> <li>• This elements consist of restrictive mixers and flighted elements</li> <li>• It can be used to assist mixers to function</li> <li>• This element is not used in current study</li> </ul>

Table 3-1: Basic types of screw elements (Thiele, Ghebre-Selassie et al. 2003)

Conveying elements or forwarding elements are used whenever there is an opening in the extruder for example the feed ports and the extruder discharge zone. Conveying elements serve as drivers to provide forwarding pressure to supply material into mixers (Thiele, Ghebre-Selassie et al. 2003). Conveying elements are almost always flighted and close meshing and self-wiping. They are also always used to perform the centring task as kneading elements are not self-centering in the extruder barrels.

Kneading elements can be arranged in wide varieties of geometries to give different compounding actions. The kneading elements can be dispersive or distributive. Dispersive mixers tend to break down the morphological units such as agglomerates. The materials are captured in pressure traps and thereby causing the material to become squeezed, sheared, and elongated. Wide kneading discs are the example of the dispersive type screw elements. On the

other hand, distributive types of elements tend to form easy paths for the materials dividing and recombining process. Narrow kneading discs and combing mixers are examples of distributive type screws. Kneading elements can also be arranged to give mixers with forwarding (that capable for transporting materials), neutrals (tends to push materials forward and backward) or reversing (create a huge pressure drop) actions. The angle of the kneading blocks arrangement will also determine the type of mixer, low angle will give a more dispersive mixer and large angle arrangements are more distributive.

### **3.5.2 Cross section view of twin screw**

The cross section of a twin screw extruder generally consists of five basic screw regions that are the channels, lobes, tips, apexes, and intermesh. Figure 3-3 shows the five mass transfer regions of a twin screw extruder.

The screw channel of an extruder is the region that has relatively low extensional mixing and shear mixing and generally associates with conveying elements. The fill of the channel is mainly dependent on the flow rate and screw speed and is normally not fully filled and therefore resulting zero pressure regions.

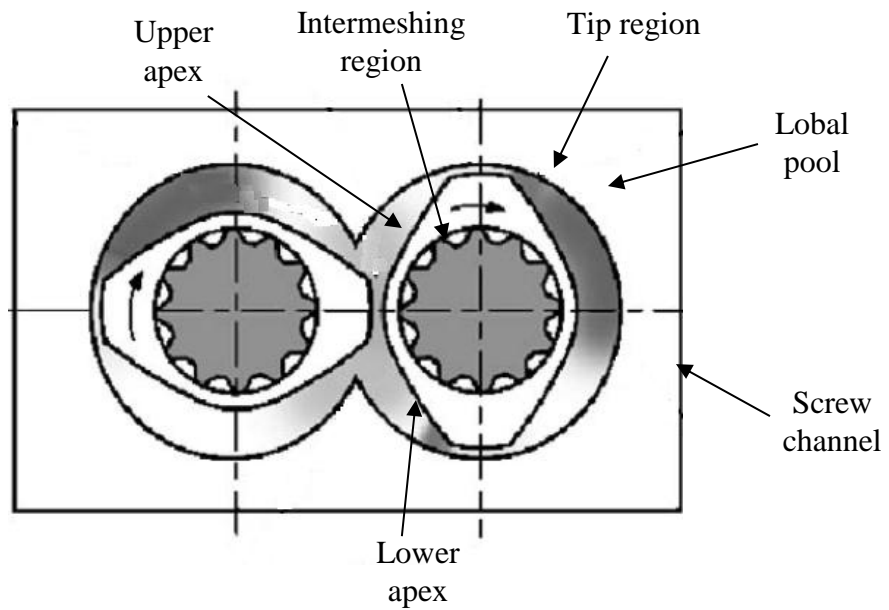


Figure 3-3: Mass transfer region of co-rotating twin screw extruder (Thiele, Ghebre-Selassie et al. 2003)

The lobal regions capture and pressurise material which are relieved up and over the screw tips to facilitate extensional and shear strain rate components. Two lobal pools might be captured in kneading disc elements. This region is generally very dispersive and the distributive process should avoid lobal regions.

The tip region is generally located in between the intermeshing region and the lobal region. It normally has the minimum distance between the screw elements and the barrel wall. The tip region exhibits very high shear and low extensional mixing. The shearing force of this region can be decreased by using narrower shear length, for example, by adjusting the kneading disc width.

The twin screw apexes are the region where barrels join in the lower and upper peninsulas of metal. This region gives a productive change in material direction when the materials transfer from one screw to the other. Apexes are the screw regions that provide moderate extensional and shear mixing as well as supporting the distributive and dispersive mixing.

The intermeshing region is the region when both screws come together. This region can have a moderate to high stress rate. The material in this region is always being squeezed to give axial movement either in positive or negative direction.

### 3.5.3 Extruder used in current study

In this study, two models of co-rotating twin screw extruder are used to produce granules. The first type of extruder was previously used for the study of polymer and ceramic paste extrusion was a model type PTW16/ 25PC unit obtained from Haake, Germany. The extruder has a stainless steel barrel and a pair of metal made screws. The diameter and length of the screws are 16 mm and 380 mm respectively. The screws are not manufactured to meet the pharmaceutical standard but it is useful for the fundamental study of twin screw wet granulation. The granulation process was run only with a 90° mixing configuration. An overview of the extruder is shown in Figure 3-4.

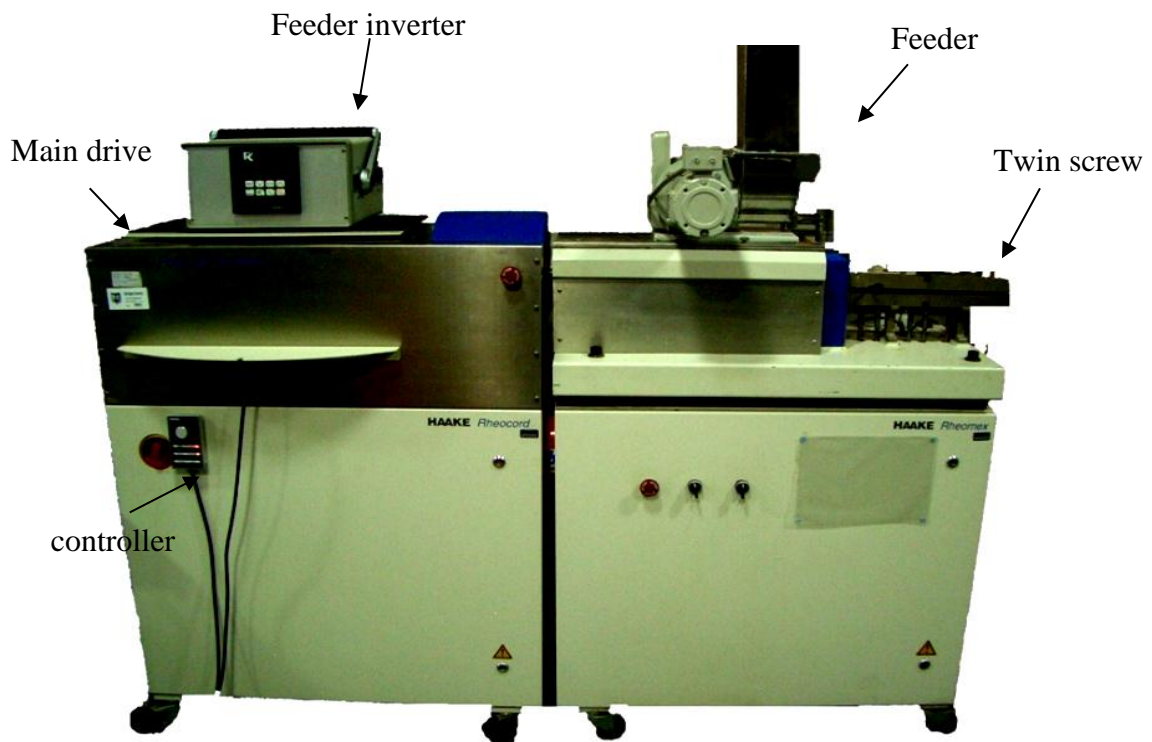


Figure 3-4: Overview of the twin screw extruder used in this study

The second model of twin screw extruder was built in house by GEA Pharma System. This type of extruder was used mainly for the purpose of Positron Emission Particle Tracking study and therefore the barrel wall is relatively thin so that the gamma rays can penetrate the construction material. Both the barrel and screws are made of stainless steel. The diameter of the screws is 19 mm and with a length of 160 m. There were various types of screw configurations considered in this study and they are discussed in Chapter 5.



Figure 3-5: Twin screw granulator used for PEPT study provided by GEA Pharma System

## **3.6 KEY PROPERTIES OF GRANULES**

### **3.6.1 Particle size distribution**

In many industries, a single number (for example) the mean size is required to characterize the particle size of a material. However, this can only be accurately and easily done for a narrow and mono-modal distribution of spherical particles. Practically, for multi-modal distribution particles in pharmaceutical formulation, it is too straight forward to describe the size population. Particle size distribution on other hand is normally used as one of the keys parameters in determining the bulk properties of powder and granular material and therefore it is important in characterising a material. In the granulation process, the granule particle size distribution is important to determine the granules resistance to segregation and also the homogeneity of drug distribution in both granules and tablets. Fine and coarse materials tend to separate from each other and will lead to process difficulties and affect the quality of downstream products, for example, the dissimilarity in composition result in the production of inhomogeneous tablets due to segregation. Besides this, the granule particle size distribution can also extend the understanding of twin screw wet granulation process, for example, a bi-modal granule distribution may be due to insufficient granulation liquid and poor liquid distribution during the process. Therefore by controlling the particle size distribution of the granules during the process, the quality of the products can easily be controlled. There are many types of measurement techniques used to determine the diameter of the granules and the one used in current study was described and summarised in Table 2-2.

### **3.6.2 Porosity**

Porosity is another important property as it is directly related to a few other important properties of the granules. Granule strength, which measures the resistance to attrition, is one

of the properties that are strongly influenced by porosity. Porous granules tend to be weaker whilst dense granules are stronger. Granule strength is very important in wet granulation process. The granules produced normally require a high strength to prevent attrition so that the possibility of materials (especially API) lost during the materials handling process is minimised.

Besides this, porosity also determines the compactibility of the granules. Porous and weak granules tend to have larger compactibility as high porosity offers a larger area of bonding which will facilitate and enhance compactibility (Bacher, Olsen et al. 2008). Therefore larger compactibility granules allow the production of porous tablets because a low compaction force is sufficient to give acceptable tablets mechanical strength (Bacher, Olsen et al. 2008).

The dissolution rate of granules and tablets is dependent on the porosity, pore structure and the pore size distribution. It was reported by (Mehta, Kislalioglu et al. 2000; Tunón, Gråsjö et al. 2003) that the dissolution rate increases with higher porosity and the total pore structure in pellets. The increases in porosity will effectively increase the contact area of the dissolution medium with the pellet surface resulting in a faster hydration and consequently leading to a higher erosion rates. Besides this, the pore size distribution is also an important parameter affecting dissolution rate. The penetration of the liquid into the porous matrix become more rapid when the pore size is large compare to small pores (Selkirk and Ganderton 1970). Thus the porosity parameter is important in characterizing and predicting the performance of drug release.

### **3.6.3 Flowability**

As pharmaceutical industry emphasises the important of drug uniformity, uniform feed from the hoppers into the tableting equipment is essential. Uniform tablet weight and drug

content can be maintained by using free flowing powder as they can ensure uniform feed from hoppers into the tableting machine (Kato, Ohkuma et al. 2005). The propensity of material flow is normally called flowability and it is an important parameter to describe the uniformity of materials flow during a process. The free flowing powders are usually sought because they are easier to handle and hence do not frequently cause difficulties on production plants (Santomaso, Lazzaro et al. 2003). However, free flowing particles will be segregated by size when the size distribution is wide (Santomaso, Lazzaro et al. 2003). On the other hand, the poor flowability material always causes uneven powder flow that could lead to excess entrapped air within the powders and may promote capping or lamination (Staniforth and Aulton 2002). The particle flowability is affected by the process or the equipment design as well as the properties of the particles. Mean particle size, particle size distribution, particle shape, surface roughness and moisture content are the most common properties that will affect the material flowability (Liu, Marziano et al. 2008). Therefore it is important being able to determine the flowing properties of a granular material in order to prevent serious problems during a granulation processes.

The materials and the equipment described in this chapter represent a platform for research and development of continuous twin screw wet granulation process. The following chapters describe in more details regarding the twin screw granulation process and the investigations of some important aspects of these materials and methods for the understanding of the process during the study.



# **CHAPTER 4 : UNDERSTANDING THE MECHANISM OF CONTINUOUS WET GRANULATION OF PHARMACEUTICAL POWDER USING TWIN SCREW EXTRUDER**

---

## **SUMMARY**

The wet granulation process plays an important role in the pharmaceutical industry. With the introduction of a Twin Screw Extruder (TSE), it allows the possibility of wet granulation to be operated continuously in contrast to a conventional batch process using a High Shear Mixer (HSM). However, the mechanism of Twin Screw Extruder wet granulation is not well understood and the aim of this study is to investigate this process and compare it with the High Shear Mixer with regards to wetting and nucleation, coalescence and consolidation and breakage and attrition.

Granules were produced using a Twin Screw Extruder and a High Shear Mixer with water as a liquid binder under different operating speeds and solid to liquid ratios. The physical properties (particle size distribution, shape, surface morphology, internal structure, internal porosity and strength) of the granules were then compared. It was found that the granules produced by the two methods have different physical properties. Granules produced by the High Shear Mixer are spherical in shape and dense whilst Twin Screw Extruder granules have irregular shapes and are porous with tiny pores spread uniformly throughout the granules. Moreover, Twin Screw Extruder granules have a lower fracture strength compared to HSM granules. However TSE granules are consistent in quality and relatively independent of process conditions. Due to over-granulation in high shear mixer, the granules produced are

too strong to be fragmented and therefore the tablets produced are weak. On the other hand, the granules produced by twin screw extruder are highly compressible due to porous structure and the tablets made by these granules have high tensile strength.

Finally, it can be concluded that the formulation mechanism of these two types of granulation is different with the consolidation stage apparently absent in the Twin Screw Extruder granulation. Although TSE granules show different properties from HSM, the tablets produced have an acceptable quality.

#### **4.1 INTRODUCTION**

Twin screw extruder (TSE) is currently one of the most studied techniques for continuous wet granulation (Vervaet and Remon 2005). As highlighted in Chapter 2, most research been carried out by several study groups regarding the influences of process and formulation parameters on the granules and tablets properties produced by TSE in the past decade. Yet, only a little work has been done to understand the granulation mechanisms in a TSE due to the complexity of the equipment. As the design of a twin screw extruder involves parameters like tip clearance, shear rate, screw configuration, fill level etc. it makes the process complicated and many assumptions are made in order to study this technique. For example in polymer processing, the extruder was assumed to be in fully filled condition when the volumetric flow of material through the nip region was measured (Bakalis and Karwe 1999; Bakalis and Karwe 2002).

#### **4.2 OBJECTIVES**

The aim of this study is to obtain a fundamental understanding of the process mechanisms of the twin screw wet granulation operation. The effect of twin screw speed and liquid to solid

ratio on granule properties, including particle size distribution, shape and morphology, internal structure and strength were investigated. In addition to this, twin screw wet granulation was compared with conventional high shear mixer granulation. Granules were produced using a high shear mixer at different impeller speeds and liquid to solid ratios and the properties of granules were then compared to the twin screw granules in order to get some insight into the process mechanisms of both techniques. The granules produced using both techniques were compacted in a die to make tablets with a diameter of 13 mm. The tensile strength of the tablets was then measured to examine the feasibility of twin screw extruder as a granulation technique to make tablets. Finally, the mechanism of both twin screw granulation and high shear mixer granulation was discussed and compared.

### **4.3 MATERIALS AND EXPERIMENTAL METHOD**

#### **4.3.1 Formulation of granule**

In order to have a better understanding of the fundamental mechanisms of both techniques, the chemical and physical formulation of the granules was initially simplistic in approach. The granules were produced using Avicel PH 101 Microcrystalline Cellulose (FMC Biopolymer, Ireland) with a mean particle size of 50  $\mu\text{m}$  in the absence of a binder. Distilled water was used as the granulation liquid for both techniques.

#### **4.3.2 Twin screw granulation**

The twin screw wet granulation process was carried out using a laboratory intermeshing co-rotating Twin Screw Extruder (Haake, Thermo Scientific, Germany) with a diameter 16 mm and length to diameter ratio of 25:1. In this initial study, the screws consist of conveying elements and two mixing zones each of five kneading elements oriented at 90° (Figure 4-1).

20 g/min of Avicel PH 101 Microcrystalline Cellulose (MCC) was fed continuously into the extruder barrel using a screw feeder (K-Tron T20) whilst distilled water was injected using a plunger metering pump (ProCam, Bran+Luebbe, SPX, Germany) at the desired rate. The temperature of the barrel was kept at 20 °C by circulating cool silicone oil using a refrigerated circulator through a jacket in the granulator.

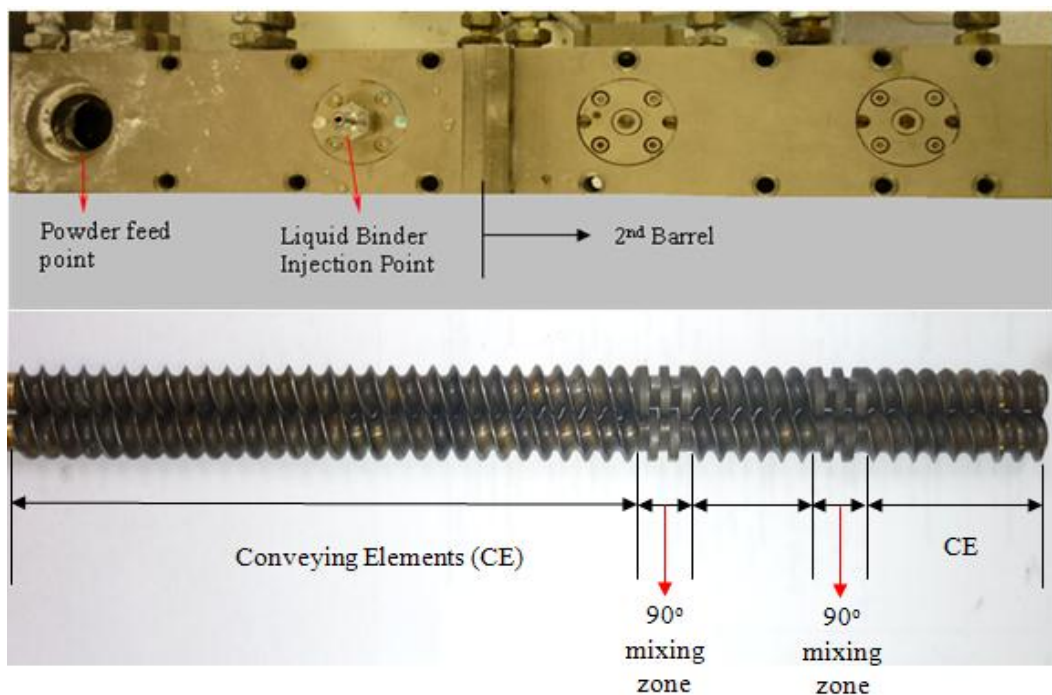


Figure 4-1: Plan view of the extruder barrel and co-rotating twin screw with two mixing zones with kneading discs arranged in 90°

### 4.3.3 High shear mixer granulation

For the batch process, 200g of Microcrystalline Cellulose was blended using the in house built High Shear Mixer (University of Birmingham, UK) (Knight, Seville et al. 2001; Bouwman, Henstra et al. 2005; Tu, Ingram et al. 2009) with a stainless steel bowl. The dimension of the bowl is 160 mm in diameter and 200 mm in height with a three bladed

impeller (leading edges inclined at  $13^\circ$ ) fitted at the bottom of the bowl and no side chopper (Figure 4-2). MCC was first pre-mixed at 100 rpm for 30 seconds and the required quantity of liquid binder was added slowly within 30 seconds at the centre of the powder bed. The powder bed was then blended at the desired speed for 30 minutes. Granules were collected and allowed to dry overnight at ambient condition before further analysis.

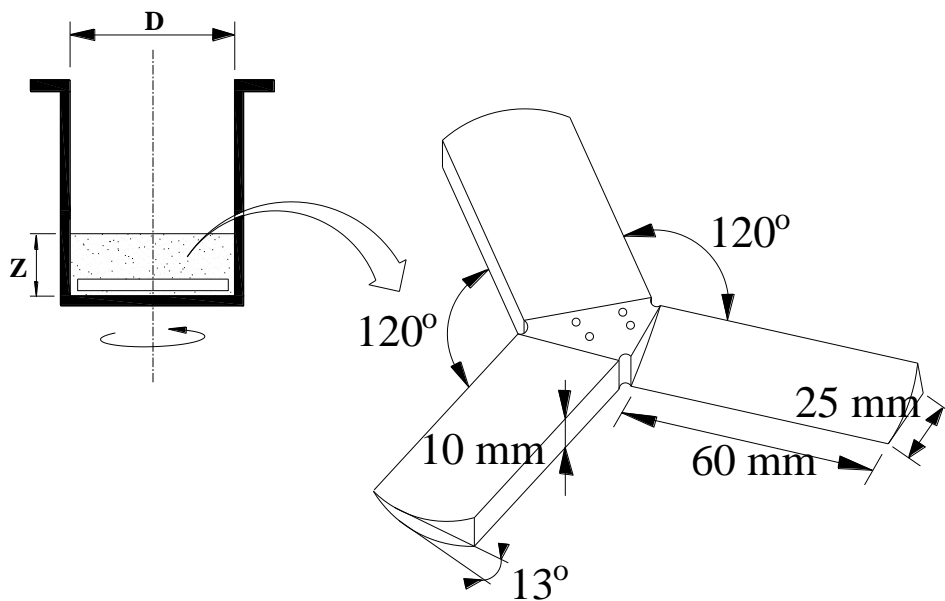


Figure 4-2: Schematic diagram of High Shear Mixer and 3-bladed impeller (Tu, Ingram et al. 2009)

#### 4.3.4 Tablet compression

Tablets were fabricated from granules produced by both TSE and HSM in order to investigate the influence of granule properties on the final products. The tablets were produced by compressing granules with a moving top piston in a confined cylindrical die. 700 mg of dry granules were manually fed into a 13 mm die (Specac, Kent, UK) and the powder bed was then compressed using a Universal Testing Machine (Zwick, Germany) to a maximum pressure between 50 MPa and 200 MPa. The load cell speed of the tester was set

constant at 1 mm/s and the compaction process was carried out without addition of any lubricant to the granules. However, the die was pre-lubricated by pressing magnesium stearate before each compaction.

### 4.3.5 Granule Characterisations

#### 4.3.5.1 Particle Size Distribution (PSD)

The granule size distribution was determined by sieving through 63, 90, 125, 180, 250, 355, 500, 710, 1000 and 1400  $\mu\text{m}$  sieves series (ISO standard, every third number of fortieth root of ten series). Approximately 100 - 200g of the granules produced by the High Shear Mixer (HSM) and the TSE were sieved at 1mm amplitude for 10 minutes (Retsch, AS 200, Germany). The weight of granules retained on each sieve was measured and particle size distribution curves were plotted. In this study, the fraction of granules smaller than 125  $\mu\text{m}$  were defined as fines

#### 4.3.5.2 Shape and morphology

The shape of the granule was measured in terms of aspect ratio and sphericity. Both aspect ratio and sphericity was determined using high speed image analysis sensor (QICPIC, VIBRI/L, WINDOX 5, Sympatec GmbH, Germany) by dispersing the granules under gravity through high speed cameras. The aspect ratio and the sphericity were calculated simultaneously by the software where aspect ratio is defined as the ratio of the maximal Feret Diameter to the minimal diameter orthogonal to it and Sphericity,  $S$ , is the ratio of the perimeter of the equivalent circle,  $P_{\text{equivalent}}$ , to the real perimeter,  $P_{\text{real}}$ .

$$\text{Sphericity, } S = \frac{P_{\text{equivalent}}}{P_{\text{real}}} = \frac{2\sqrt{\pi \cdot A}}{P_{\text{real}}} \quad \dots \text{ Eq. 4-1}$$

Where  $P_{\text{equivalent}}$  is the equivalent perimeter (m),  $P_{\text{real}}$  is the actual perimeter (m) and  $A$  is the area ( $\text{m}^2$ ). Sphericity has values between 0 and 1, with low values of  $S$  indicating deviation of particle shape from spheres, for example needles and fibres (Litster, Ennis et al. 2004) or crenulated surface morphology. The distinction between the two can then be ascertained with the aspect ratio. A Scanning Electron Microscopy, (SEM, JOEL 6060, Oxford Instrument, UK) was also used to observe the surface morphology of the granules.

#### **4.3.5.3 Internal structure and Porosity of granules**

##### *Observation of Internal Structure using Micro X-Ray Tomography (XRCT)*

The internal structure of granules was observed by using micro X-Ray Tomography (SkyScan, Belgium) which has a resolution down to 2  $\mu\text{m}$ . Granules with a size classification 500 – 710  $\mu\text{m}$  were selected randomly and scanned through 0-180° at 100 kV, 50 mA (without filter) with 0.9° rotation between images (Farber, Tardos et al. 2003). The raw images were then reconstructed into layers of 2D cross sectional images. The threshold of the image was selected visually, by decreasing the values slowly until the signal noise was at minimum, before 3D analysis was carried out to measure the internal porosity. All the image reconstructions and analyses were carried out using the SkyScan Software.

##### *Measurement of Porosity using Micro X-Ray Tomography and Mercury Porosimeter*

Besides X Ray Tomography, the porosity was measured using a Mercury Porosimeter (AutoPore IV 9500 series, Micromeritics, USA). Approximately 0.5 g of granules with size classification 500–710  $\mu\text{m}$  was placed in a 3cc penetrometer and degassed to 50 mmHg before the analysis. During the analysis, mercury will first fill the penetrometer and the capillary stem that give the granule bulk/envelope density. As the pressure increases, mercury

intrudes the granule pores beginning with those pores with larger diameter. The volume of the mercury was recorded with real time data logging by detecting the capacitance change between the mercury column inside the stem and the metal cladding on the outer surface of the stem. The mercury was intruded incrementally into the granules up until 200 Mpa (30,000 psia)

The porosity of the granules was obtained using Eq 4.2 (Farber, Tardos et al. 2003; Rahmanian, Ghadiri et al. 2009).

$$\text{Porosity, } \mathbf{Po} = 1 - \frac{\rho_{\text{bulk}}}{\rho_{\text{true}}} \quad \dots \text{ Eq. 4-2}$$

Where  $\rho_{\text{bulk}}$  is the bulk/envelope density of granule and  $\rho_{\text{true}}$  is the true density of granule. The bulk/envelope density of the granules was obtained from the mercury porosimeter as described previously when the mercury filled the penetrometer at 0.0034 MPa. The true density of the granules was measured using a Helium Pycnometer (AccuPyc II 1340, Micromeritics, USA). The granules were placed and sealed in the instrument compartment of known volume and helium gas was admitted and then expanded into another precision internal volume. The pressure before and after the expansion were measured and used to calculate the sample volume using ideal gas law. The absolute density of the granules was then calculated by dividing the known sample weight with the measured sample volume.

#### ***4.3.5.4 Estimation of granule strength using Uni-axial Bulk Confined Compression***

The granule strength was measured by compressing granules using a piston in a rigid cylinder (uniaxial bulk confined compression) (Adams, Mullier et al. 1994). 500 mg of dry granules were filled into a 13 mm stainless steel die (Specac, UK) and tapped to remove any



large packing irregularities (Adams, Mullier et al. 1994). The powder bed was then compressed using a Universal Testing Machine (Zwick, Germany) with real time data logging and analysis at a speed of 3.5 mm/min to an upper pressure limit of 100 MPa. The test was repeated 5 times in order to obtain reliable results. The fracture strength was then calculated using Adam's equation (Adams, Mullier et al. 1994; Adams and McKeown 1996) as shown below which is based on the parallel friction-element model.

$$\ln P = \ln\left(\frac{\tau}{\alpha}\right) + \alpha\varepsilon + \ln[1 - \exp(-\alpha\varepsilon)] \quad \dots \text{Eq. 4-3}$$

Where  $P$  is applied pressure (Pa),  $\tau$  the material constant related to granule fracture strength (Pa),  $\alpha$  is a material constant related to Mohr-Coulomb failure criterion,  $\varepsilon$  is the natural strain ( $\ln h_o/h_i$ ),  $h_o$  is the initial bed height (mm) and  $h_i$  is bed height at corresponding pressure (mm). The  $\tau$  and  $\alpha$  were calculated by non-linear regression of the data to Eq 4.3.

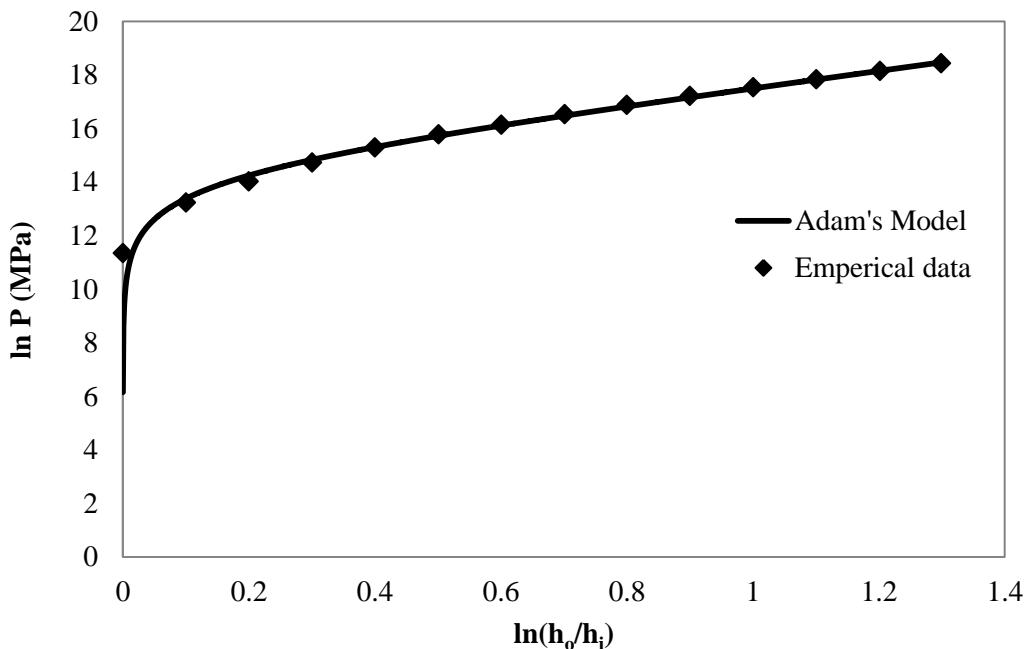


Figure 4-3: Experimental uniaxial confined compression test and Adam's model plotted in form of natural log of applied pressure against natural strain

Figure 4-3 shows a typical uniaxial confined compression test with a fit of Adam's model according to Eq. 4-3. The plot is linear when natural strain is large as the third expression in the equation is small and becomes negligible. The values of  $\tau$  and  $\alpha$  can be obtained from the intercept and the gradient of the straight line fitted to the linear part of the curve at large strain. The final estimated fracture strength of granules,  $\tau$ , is obtained by adjusting the values of  $\alpha$  and  $\tau$  to give the best fit to the whole curve using non-linear regression.

#### 4.3.6 Tablet Tensile Strength

The tensile strength of tablets produced by both TSE and HSM were determined from diametrical compression experiments. The experiments were carried out using the universal testing machine with a 5kN load cell to measure the maximum diametrical crushing force. The tablet tensile strength is related to the load at fracture as follows (Fell and Newton 1970),

$$\sigma = \frac{2F}{\pi Dt_t} \quad \dots \text{Eq. 4-4}$$

Where  $\sigma$  is the tablet tensile strength (Pa),  $F$  is the maximum diametrical fracture force (N),  $D$  is the tablet diameter (m) and  $t_t$  is the tablet thickness (m). The tablet's fracture surface was examined using a Scanning Electron Microscope, (SEM, JOEL 6060) to observe the fracture pattern and the arrangement of the granules within the tablets.

### 4.4 RESULTS AND DISCUSSIONS

Figure 4-4 shows the images of the wet granules produced using the twin screw extruder with a screw speed of 500 rpm using various liquid to solid ratio. Generally, the granules produced at L/S ratio 0.4 mainly consists of fine primary powder as there is insufficient

granulation liquid for wetting processes that initiate powder growth. As the L/S ratio was increased to 0.6, granules started to be formed. Larger granules will start exiting from the extruder when the L/S ratio is 0.8 and the fraction of the larger granules increases when the amount of granulation liquid used increases. When the L/S ratio was increased to 1.4 a small fraction of granules larger than 5 mm or lumps were formed. The powder seems to be over-wetted when L/S ratio reaches 1.6 and big wet lumps were formed instead of granules. If granulation liquid used exceeds L/S 1.6, the materials will come out from the extruder as paste or extrudates as shown in Figure 4-4.



Figure 4-4: Granules produced by TSE at 500 rpm using various liquid to solid ratio (dimension in cm)

For high shear mixer granulation, no granules were produced at L/S ratio 0.8 and below and the product is generally wet primary powder that remains un-granulated. By increasing the L/S ratio to 1.0, the high shear mixer will be able to make granules that give a uniform size. When more granulation liquid was used and L/S ratio is 1.2, larger granules were produced as more liquid will enhance wetting, nucleation and coalescence process. However, the powder will be over-wetted once the L/S ratio is higher than 1.2 as the granules will grow rapidly and this process is uncontrollable leading to the formation of big round pellets as shown in Figure 4-5.

When comparing the twin screw wet granulation and high shear granulation, it is shown in Figure 4-4 and Figure 4-5 the granules produced using high shear mixer are more uniform. However, the liquid operating range of high shear mixer is very narrow compared to the twin screw extruder.



Figure 4-5: Granules produced by HSM at 600 rpm using various liquid to solid ratio (dimension in cm)

The bar chart in Figure 4-6 shows the granule size fractions for various L/S ratios. In the present study, the granules with a size smaller than 125  $\mu\text{m}$  are considered as unwanted fines whilst granules larger than 1400  $\mu\text{m}$  are oversized products. It is shown that when the L/S ratio increases, the generation of unwanted fines decreases and reaches a negligible value when the L/S ratio is 1.4. HSM granulation relatively generates less unwanted fines and like TSE granulation the fraction of fines decreases as the L/S ratio increases.

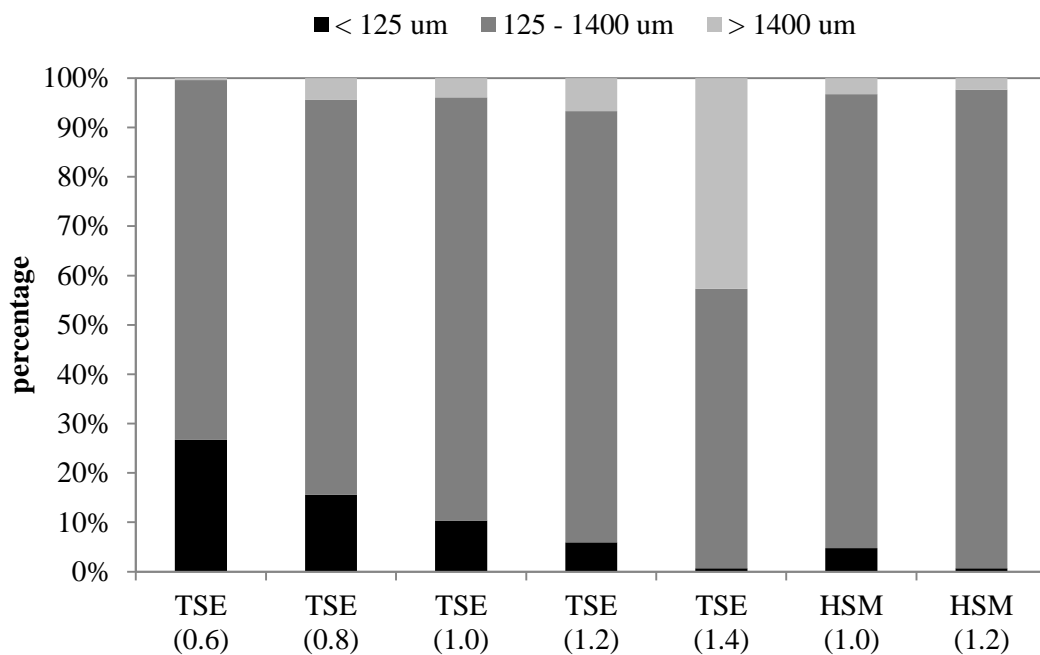


Figure 4-6: Unwanted fines and oversized granules produced by TSE and HSM at 500 rpm using different L/S ratio

Under conditions where the L/S ratio is low (0.6), due to the insufficient granulation liquid for wetting process, there is no oversize granules being generated for TSE granulation. The fraction of oversize granules then increases and has a relatively constant value of approximately 5 - 10% for L/S ratio between 0.8 and 1.2. When the L/S ratio is 1.4, the materials were slightly over-wetted and a huge fraction of the granules produced (40%) is considered oversize. Generally, granules produced by HSM have a higher fraction of

optimum size range between 125  $\mu\text{m}$  and 1400  $\mu\text{m}$  compare to TSE. However, TSE process remains robust as the fraction of granules with desirable size is considered high (more than 70%), except the processes with L/S ratio 0.6 and 1.4.

#### 4.4.1 Particle size distribution (PSD)

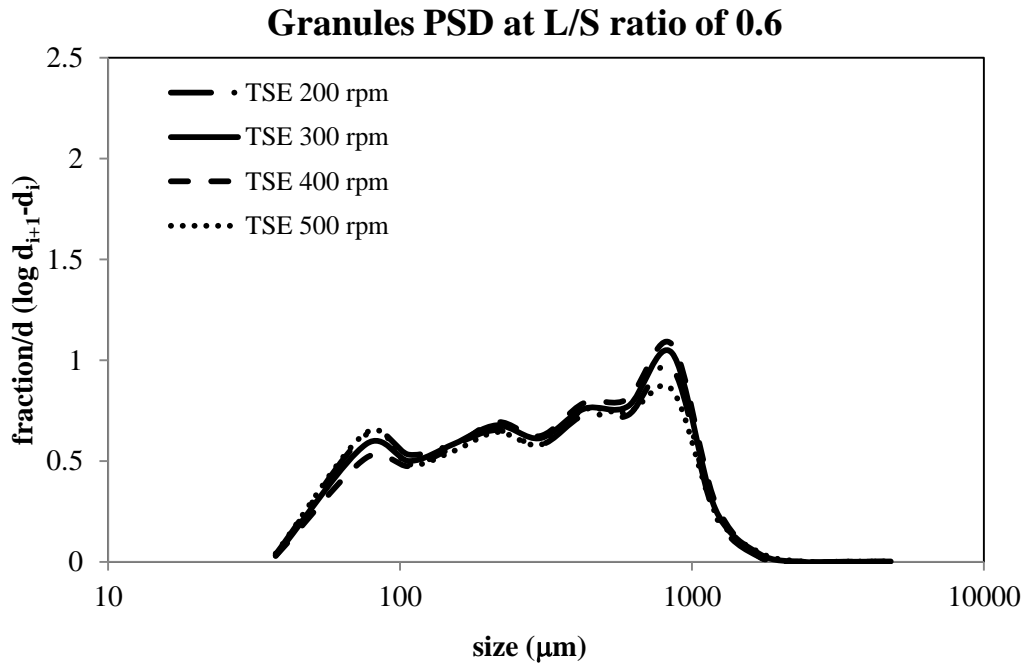


Figure 4-7: Particle size distribution of granules produced using L/S of 0.6 at different speed

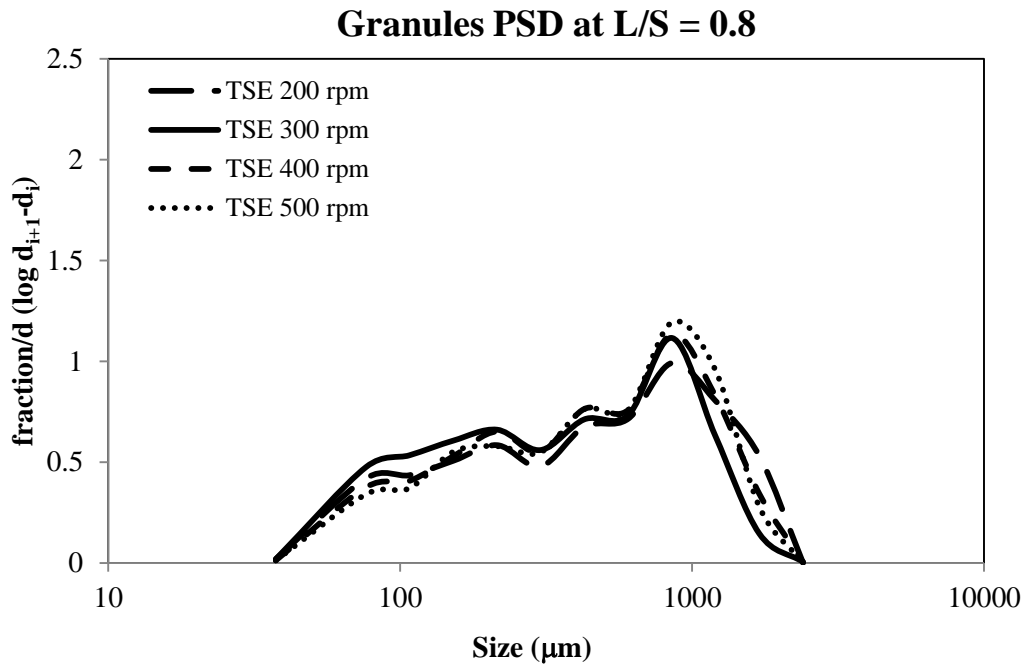


Figure 4-8: Particle size distribution of granules produced using L/S of 0.8 at different speed

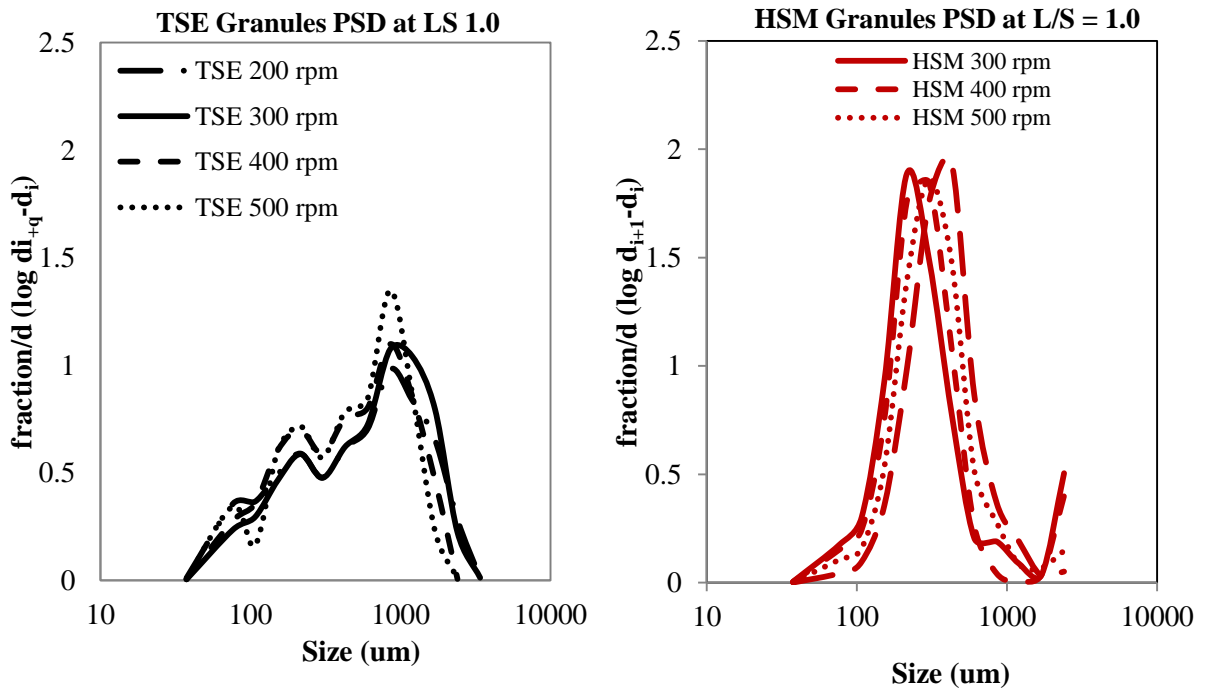


Figure 4-9: Particle size distribution of granules produced using L/S of 1.0 at different speed

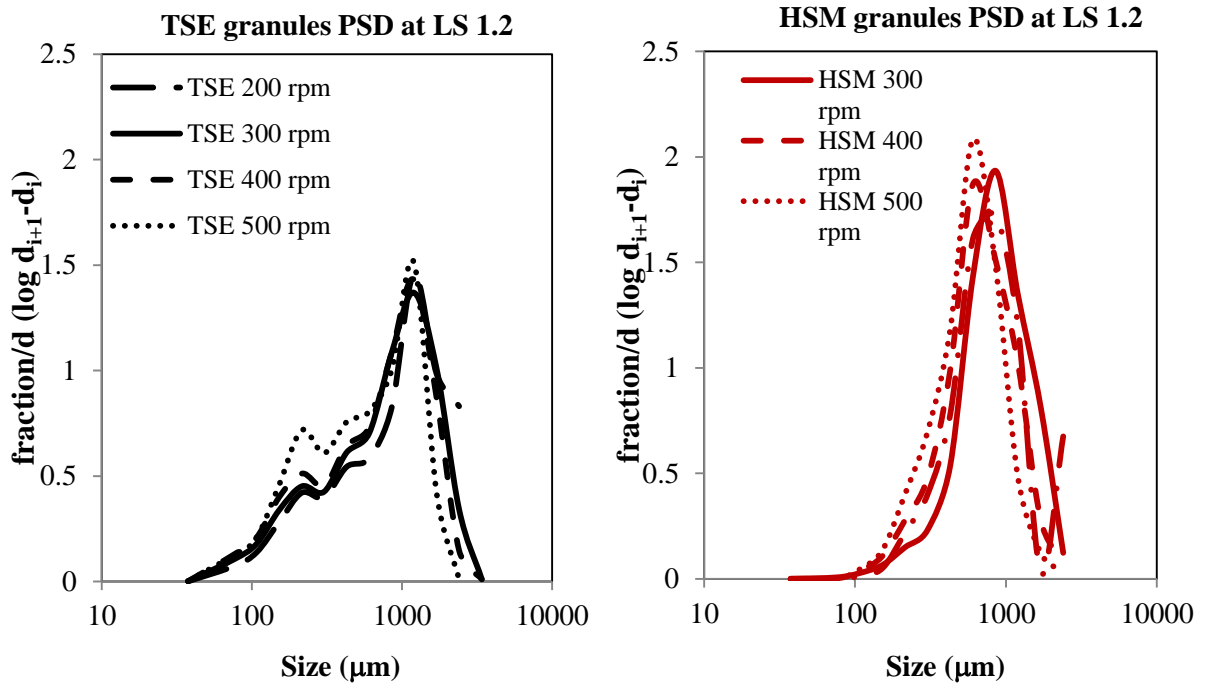


Figure 4-10: Particle size distribution of granules produced using L/S of 1.2 at different speed

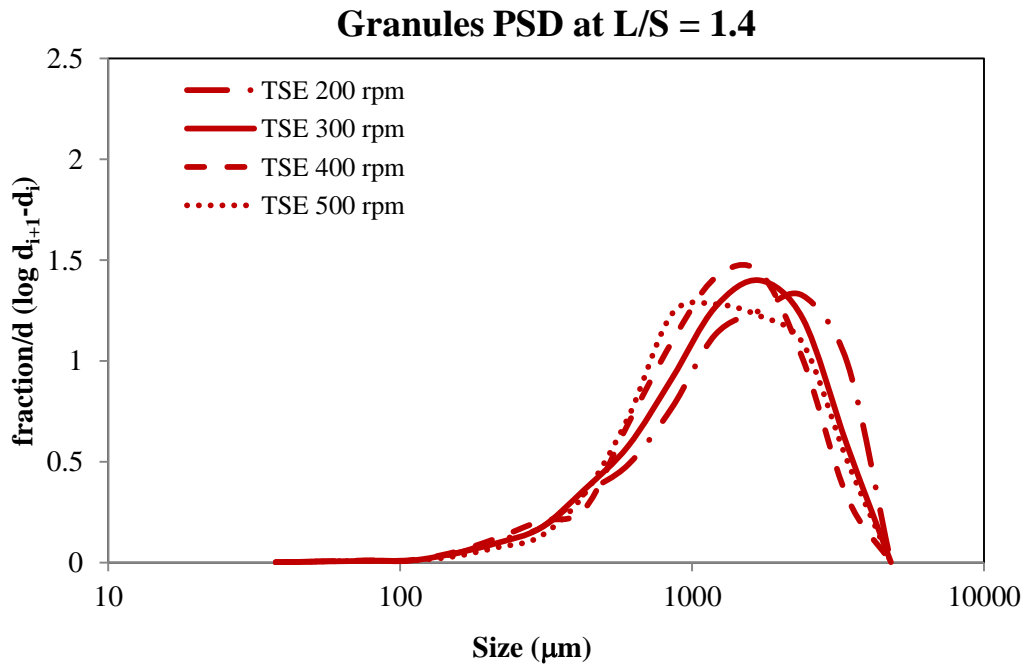


Figure 4-11: Particle size distribution of granules produced using L/S of 1.2 at different speed



Figure 4-7, Figure 4-8, Figure 4-9, Figure 4-10 and Figure 4-11 show the particle size distributions (PSD) of the granules produced by TSE and HSM with different speeds and L/S ratios. As discussed previously, HSM could not fabricate granules at an L/S ratio of 0.6 and 0.8 as the amount of granulation liquid used is too low. Nevertheless, the size distribution of the granules produced by HSM at L/S ratio of 1.0 and 1.2 is mono-modal (See Figure 4-9 and Figure 4-10). The presence of the tail in the HSM granules distribution curves is mainly due to the absence of a chopper in the system. A chopper normally provided in commercial HSM granulation system in order to break the huge granules formed so that a better granulation liquid distribution can be achieved. It is also shown that the size distribution curves moved towards the right when the amount of granulation liquid used increases. This indicates that the granules in the vessel will grow larger at higher L/S ratio.

For TSE granulation, the granules produced at a L/S ratio of 0.6 have a high fraction of fines and the size distribution is multi-modal. By increasing the L/S to 0.8, TSE produced a higher amount of large granules but the fines also remains significant. The size distributions of the granules become bi-modal when the L/S ratios are 1.0 and 1.2. Moreover, the generation of unwanted fines is less significant at these L/S ratios (Refer to Figure 4-6). At L/S ratio 1.4, negligible unwanted fines were produced and the granules give a mono-modal size distribution curve. The materials will be over-wetted beyond L/S ratio 1.4 to produced wet lumps.

By comparing both TSE and HSM size distribution curves, granules made by TSE have a wider distribution compared to HSM granules. The wider distribution of TSE granules could be due to poor granulation liquid distribution during the process. The multi-modal distribution shows that a fraction of the particle is not being wetted and generates fines whilst the oversize

granules indicate particles were over-wetted. Since a plunger metering pump was used in the present study, the granulation liquid was pumped in a pulsation mode into the barrel. The pulsation of the pump would cause the granulation liquid to be not distributed axially uniformly in the extruder during the process. In addition, the shape of the size distribution curves is independent of the screw speed or impeller speed used for both granulation techniques.

#### **4.4.2 Mean granule size**

Figure 4-12 shows the summary of the mean diameter of the granules produced using TSE. As expected, the granule  $d_{50}$  increases when the L/S ratio increases as more liquid will facilitate granule growth. However, at low L/S ratio, between 0.6 and 1.0, the changes in screw speed have no significant effect on the granules  $d_{50}$ . At a higher L/S ratio, between 1.2 and 1.4, the relationship between screw speed and  $d_{50}$  becomes more interesting as the mean granule size decreases when the screw speed increases. It is predicted that an increase in screw speed will decrease the filling degree along the twin screw leading to decrease in the packing of the materials inside the barrel. As the fill level decreases, the interactions of materials is expected to decrease with the consequence that the possibility of efficient material compaction and interlocking decreases. Therefore, it is believed that increases in screw speed and filling degree of the extruder will slightly diminish the granule growth. Besides this, it is also expected that an increase in screw speed will cause the breakage of larger granules to become more likely. The increases in screw speed will increase the shear rate giving a higher shear force that might be expected to break up the large agglomerates (Thompson and Sun 2010).

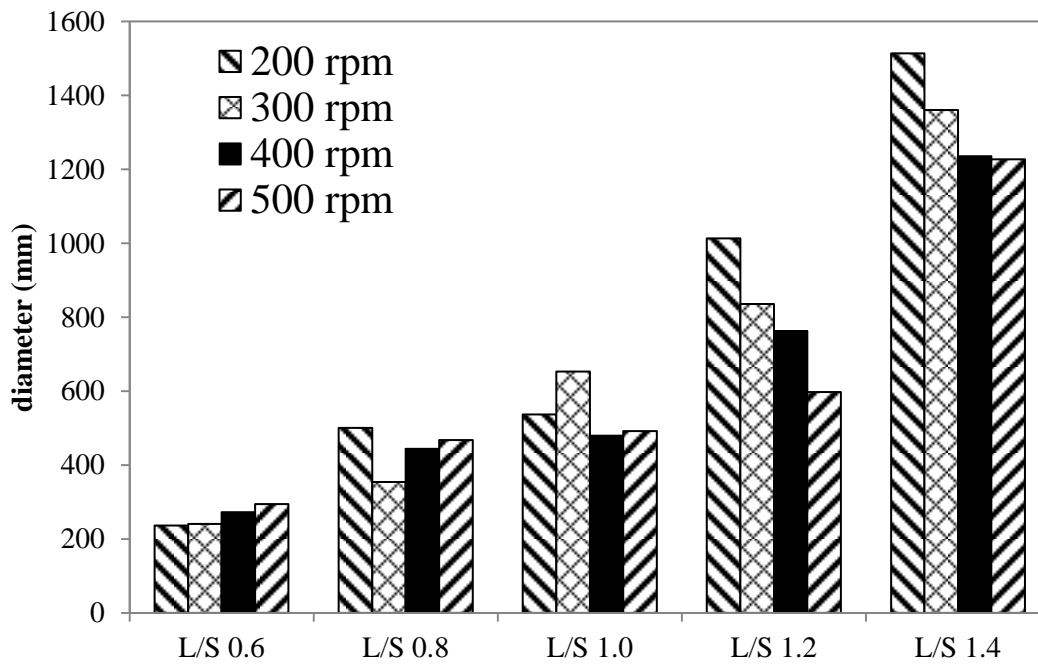


Figure 4-12: Mean diameter ( $d_{50}$ ) of granules produced using TSE

#### 4.4.3 Shape and morphology

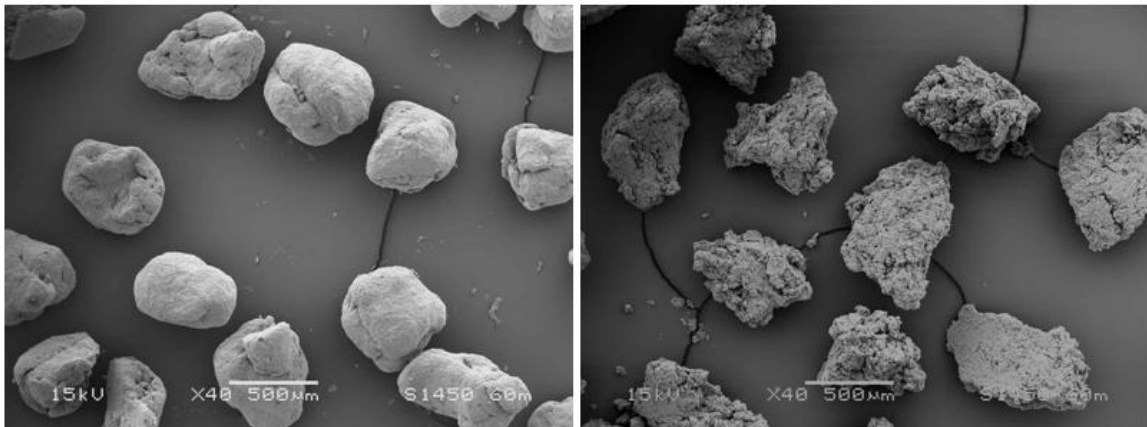


Figure 4-13: Image obtained from scanning electron microscopy High shear mixer (left), Twin screw extruder (right)

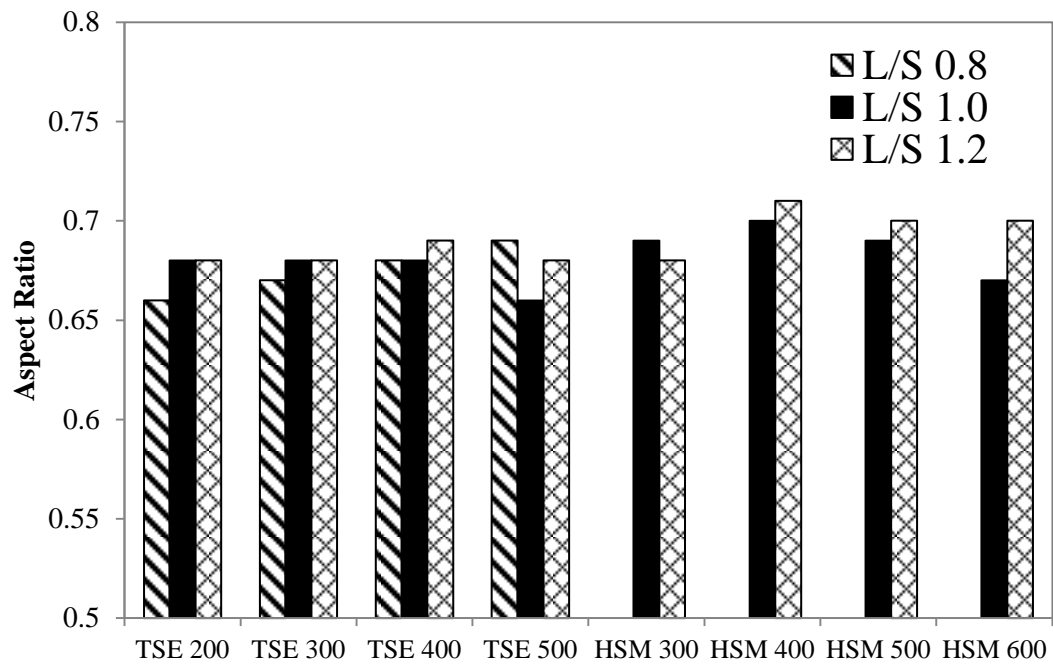


Figure 4-14: Aspect ratio of granules produced by TSE and HSM using various speed and L/S ratio

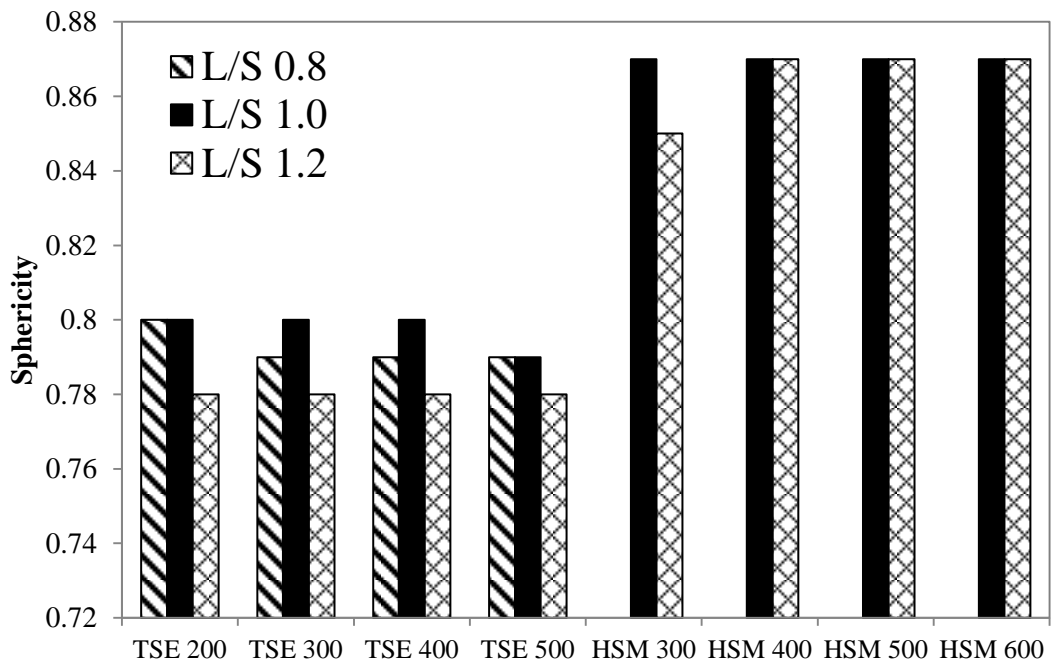


Figure 4-15: Sphericity of granules produced by TSE and HSM using various speed and L/S ratio

Figure 4-14 and Figure are the aspect ratio and the sphericity for the granules produced by TSE and HSM using different speed and L/S ratio. The aspect ratios of the granules produced by TSE and HSM have a similar value between 0.66 and 0.70. However, the granules produced by TSE have a lower sphericity compare to HSM granules and this indicates that TSE granules have a larger deviation from a sphere. The shape of the granules can be seen in the images obtained using SEM in Figure 4-13. The images also show that TSE granules have an irregular shape similar to flakes whilst HSM granules are round and uniform. Moreover, by observing the granule surface, it can be seen that the TSE granules are formed of loosely packed powder. These loosely packed granules were likely to be formed by a coalescence process after wetting and being compacted and deformed in the mixing zones. On the other hand, HSM granules appear to be denser with a smoother surface compared to the TSE granule due to lack of surface porosity. The granules produced by different L/S ratio and speed give similar shape and morphology described above.

#### 4.4.4 Internal structure of granules

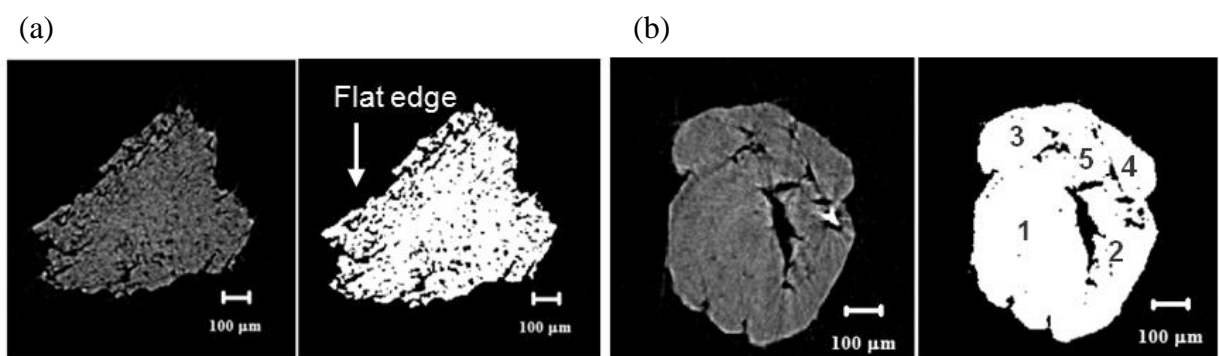


Figure 4-16: Raw Images and Binary Images of granules (centre slice) obtained from Micro X-Ray Tomography produced with liquid to solid ratio of 1.0: (a) Twin Screw Extruder 400 rpm ; (b) High Shear Mixer 450 rpm.

The numbers in last figure show the smaller individual granules that can be distinguished within the HSM granule.

Figure 4-16 are the images of granules (centre slice) obtained from micro X-Ray Tomography (XRCT). It is clear that the TSE granules are porous and consist of tiny pores spread uniformly throughout the granule. The TSE granules also have irregular shape and flat edges suggesting that the granules were being sliced by the intermeshing of the kneading blocks of the mixing zones. Nevertheless, this flat edge is not observed on all granules as the friction forces exist between barrel wall, conveying elements and neighbour particles giving a little spheronizing in the extruder.

The HSM granule looks similar to a sphere and is denser. However, the HSM granule has a few macro pores that appear to be interfaces between particles that have coalesced. Generally the figure shows that a large HSM granule is made up of deformed smaller granules which can be distinguished from each other (see Figure 4-16). As the particles came together and coalesce successfully, they are further deformed and compacted while they collide with neighbouring particles, the vessel wall or the impeller. This process will lead to the inner liquid and air from the interior being squeezed to the surface and then forming a liquid film surrounding the particle that may be followed by another successful coalescence giving granule growth. This process will be repeated until equilibrium is achieved between granule growth and breakage.

#### 4.4.5 Porosity of Granules

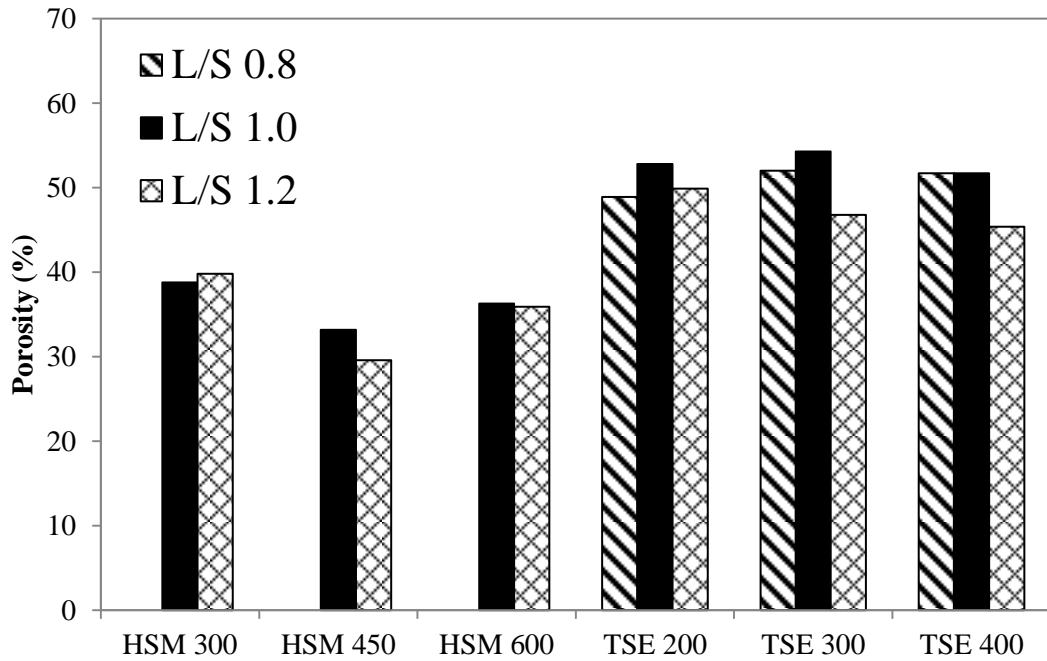


Figure 4-17: Porosity of granules measured by mercury porosimeter

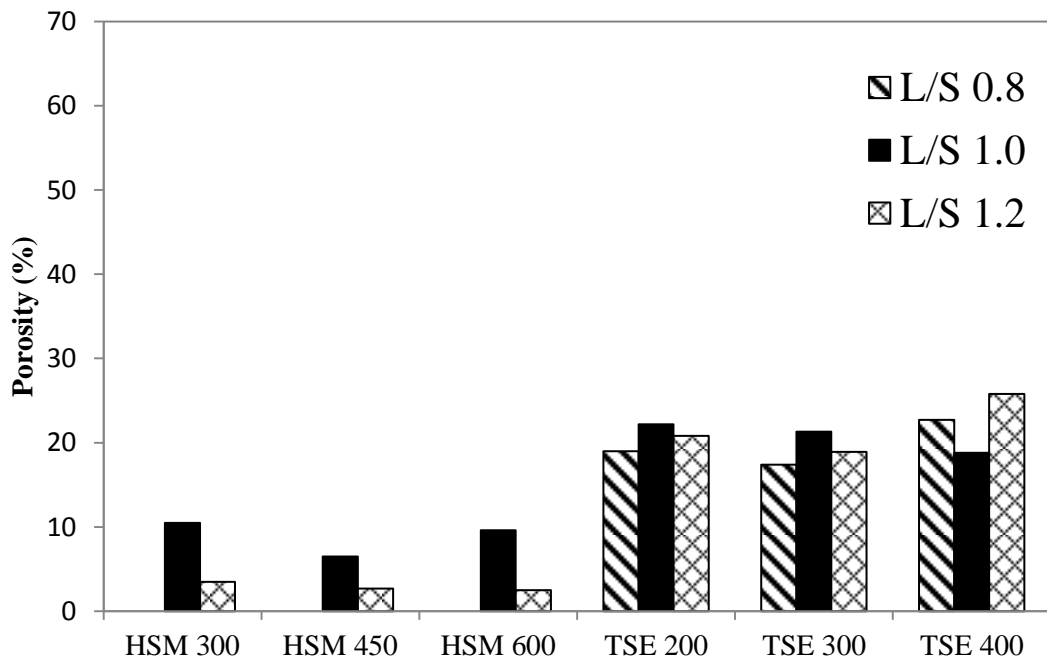


Figure 4-18: Porosity of granules measured by Micro X-Ray Tomography

The porosity of granules produced using TSE and HSM at selected L/S ratio and impeller or screw speed was measured in order to investigate the voidage differences of granules produced by both techniques. The porosity of both HSM and TSE granules do not change significantly when different amount of granulation liquid is used. The same observation was noted for TSE granules produced at different screw speeds. For HSM granulation, granules produced at 300 rpm have the highest porosity among the HSM granules. The granule porosity decreases when the impeller speed is increased to 450 rpm and decreases again when further increased to 600 rpm. The observation is in contradiction to the outcome of (Benali, Gerbaud et al. 2009) and (Rahmanian, Ghadiri et al. 2009). This has arisen because no binder is used in the granule formulation. Also, in the present study, the granulation liquid was added all at once during the pre-mixing stage and this is different to the previous studies by (Benali, Gerbaud et al. 2009; Rahmanian, Ghadiri et al. 2009) where the binder was added by spraying nozzle during the granulation. The dissimilarity of the granulation liquid addition method of the studies may influence the growth mechanism (Mangwandi, Adams et al. 2010) of the granules and hence the granule structure (Holm, Jungersen et al. 1983; Knight, Instone et al. 1998).

Moreover, the opposite findings may be also due to the limitations of both measurement techniques. The original reconstructed images obtained from XRCT had a relatively low signal-to-noise ratio, which resulted in an uncertainty of up to 10% in porosity calculation (Farber, Tardos et al. 2003). Besides this, the XRCT is unable to detect pores smaller than 2  $\mu\text{m}$  and due to this limitation, only intra-particle porosity was measured. On the other hand, Mercury Porosimetry is a high pressure process which allows mercury to be penetrated into nano-scale pores. However, the high pressure condition can cause deformation of the granule internal structure particularly of the weak TSE granules. Mercury porosimeter measures both



the intra- and inter-particle porosity which explains the observation of higher porosity values compared to the values measured by XRCT. The porosity results from mercury porosimeter is considered to be more representative as it measures porosity of bulk granules while X-Ray measures a single granule. Nevertheless both measurement techniques give a reasonable indication of the relative porosity of the granules prepared using both techniques. It is believed that the higher porosity of the TSE granules suggest that the material is relatively lightly compacted during the twin screw granulation process and the conventional consolidation stage exhibited in HSM granulation is absent in TSE process.

#### 4.4.6 Estimated granule fracture strength

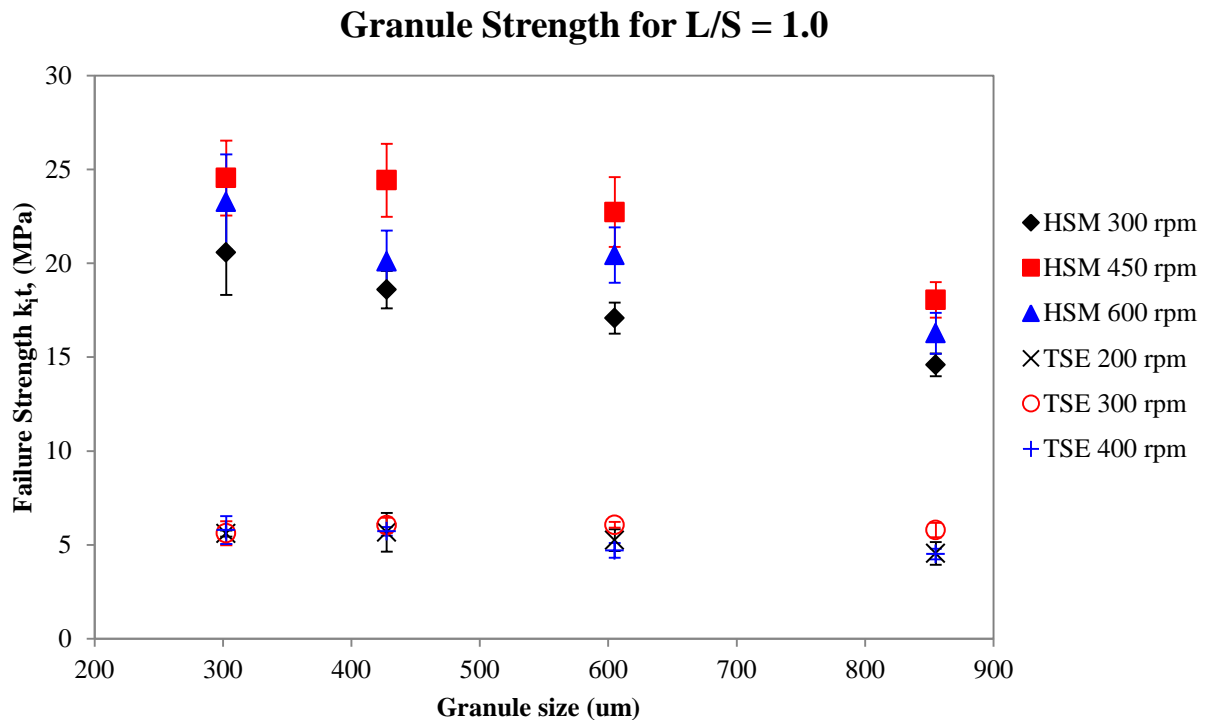


Figure 4-19: Estimated strength of granules produced using TSE and HSM at liquid to solid ratio of 1.0 for various impeller or screw speed

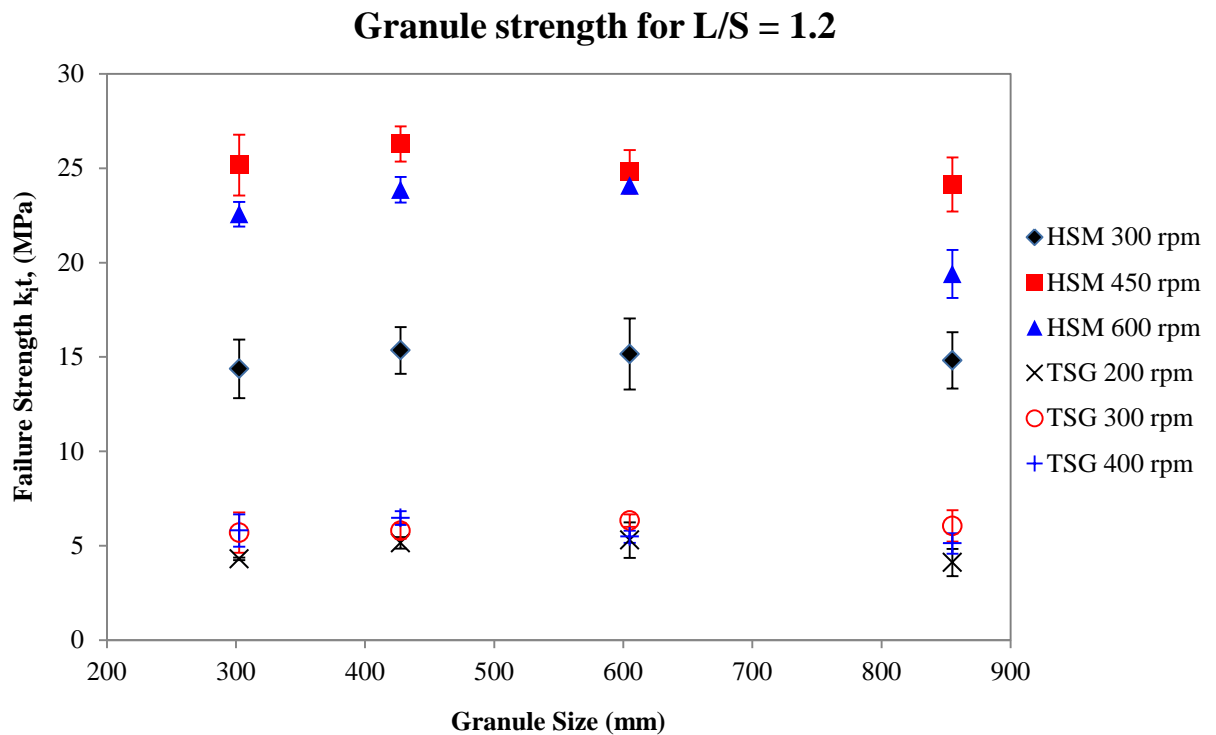


Figure 4-20: Estimated strength of granules produced using TSE and HSM at liquid to solid ratio of 1.0 for various impeller or screw speed

The strength of the granules produced using TSE and HSM at various process and formulation conditions was estimated using Adam's model and is shown in Figure 4-19 and Figure 4-20. It is shown that TSE granules have an estimated strength of 5MPa and this strength remains similar for different screw speed and L/S ratio. Moreover, this strength remains unchanged for different size classifications this indicates that the granules produced using TSE are consistent in mechanical property over the same population.

On the other hand, the denser HSM granules are stronger and the estimated strength is approximately 3 – 4 times higher than the TSE granules. Unlike the TSE granules, the strength of the HSM granules varies for different size classification especially the granules produced at a solid to liquid ratio of 1.0. As the granule size increases, the estimated granules strength decreases. Also, the strength of granules produced by HSM is affected by the

impeller speed. The granules produced at 300 rpm are generally weakest for both L/S ratios. When the impeller speed is increased to 450 rpm, the granule strength increases and decreases when the speed is further increases to 600 rpm. The effect of impeller speed on granule strength has a similar trend to that to the granule porosity as the strength of the granule is inversely proportional to the granule porosity (Benali, Gerbaud et al. 2009; Rahmanian, Ghadiri et al. 2009; Mangwandi, Adams et al. 2010). A plot of the granule strength against the porosity shows the granules strength decreases when the granule porosity increases (Figure 4-21).

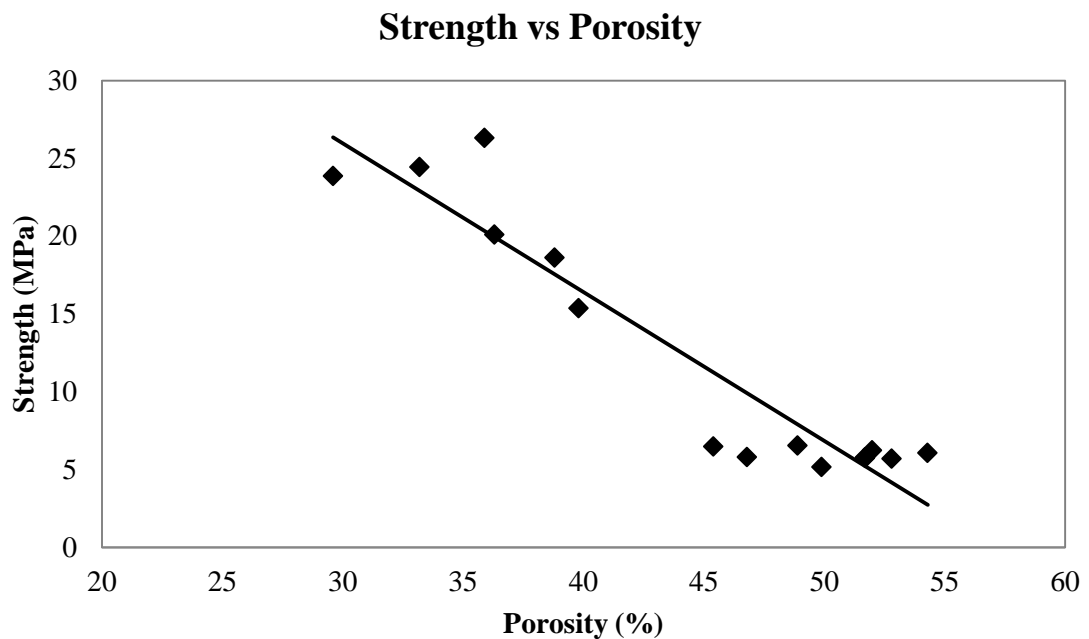


Figure 4-21: Relationship between granule porosity and strength

#### 4.4.7 Mechanisms of twin screw wet granulation

Wet granulation consists of processes such as wetting and nucleation, coalescence and consolidation, and breakage and attrition (Litster, Ennis et al. 2004). According to the results

obtained in previous sections, the mechanism of continuous wet granulation using TSE is different, as some of these processes appear to be absent in TSE granulation. It is shown that the granules produced by HSM are round and dense as the powder mixture experiences continuous impact of the granules with the impeller, vessel wall and neighbouring particles during the process. This is the stage defined as consolidation, which decides the density and final appearance of the granules (Iveson, Litster et al. 1996; Iveson, Wauters et al. 2001; Litster, Ennis et al. 2004; Darelius 2007).

In a TSE granulation process, liquid binder was added continuously into the barrel and the moving powder has undergone the immersion type wetting and forms an extrudate. This extrudate is then broken into smaller pieces due to the shearing force that exists during the process. The material was then transported by conveying elements into mixing zones where it was mixed, compacted and elongated by the kneading discs of the mixing zones. Furthermore, it is believed that the compacted powders will also be chopped by the 90° kneading blocks or the screws to form irregular and porous granules. The evidence for this is that some of the granules produced have flat edges. This is not observed in all granules because the friction between the granules and the stationary wall, the moving screws and neighbouring particles gives a spheronizing effect as the granules are conveyed along the barrel. This spheronization effect is not significant as the filling degree in the barrel is low especially in the conveying zones (Lee, Ingram et al. 2011). Moreover, in the Dhenge, Mirza et al. (2011) study, an experiment was carried by monitoring the flow of the granules using a high resolution camera through a transparent barrel, it was observed that most of the granules were moving forward individually and therefore the friction forces that existed to give the spheronization effect are very low.

Generally, TSE and HSM granulation show dissimilarity in the process mechanisms. However, they share the relation that the mean granules size is proportional to the L/S ratio. The screw speed also has an effect on the mean granule size at high L/S ratio. Like conventional process, it is believed that the granule growth in the TSE is related to Stokes deformation number,  $St_{def}$  and maximum granules pore saturation,  $S_{max}$  as discussed in Chapter 2. Nevertheless, there are uncertainties that exist, for example, in the TSE granulation, whether it is poor packing in low fill level in the barrel or breakage in high shear regions that decide the final granule size distribution. A similar granule growth regime map with HSM could be constructed for twin screw granulation as there is a close relation of granule  $d_{50}$  with the amount of liquid binder used which is related to  $S_{max}$ . More work is necessary to complete this study, for example, the modification on the  $St_{def}$  parameter is needed as twin screw granulation involves parameters like tip clearance, shear rate, screw configuration, filled level etc. that make the process more complicated.

#### 4.4.8 Effect of granule properties on tablet tensile strength

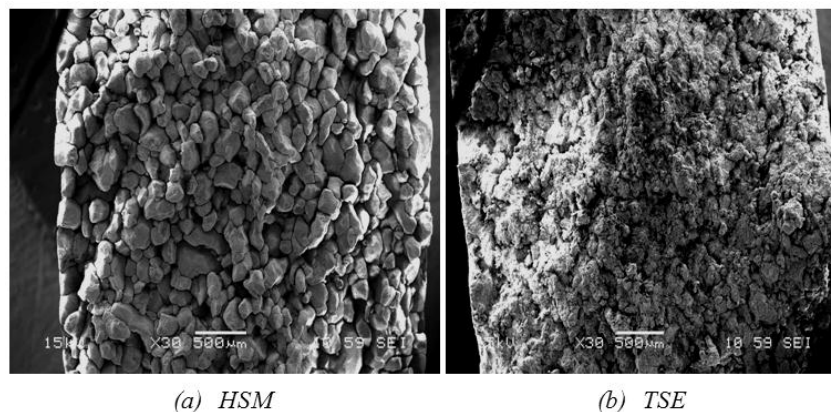


Figure 4-22: SEM images of fracture surface of the tablets

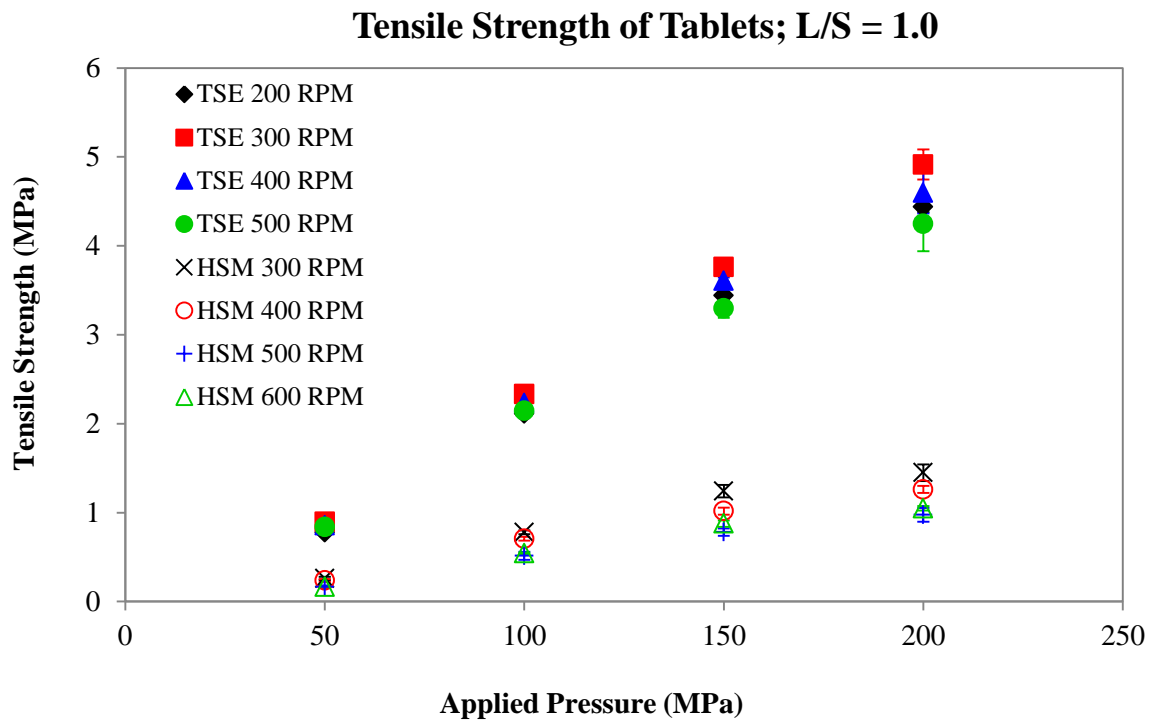


Figure 4-23: Tablet tensile strength produced using TSE and HSM granules produced at L/S = 1.0 (based on 5 tablets)

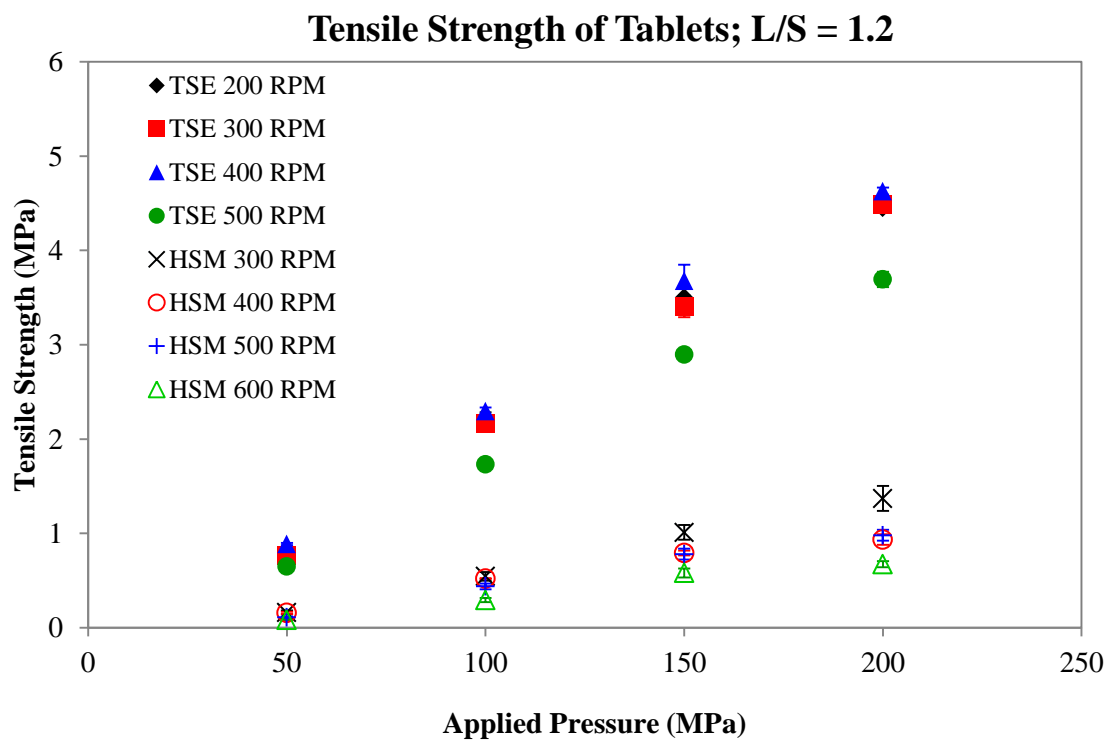


Figure 4-24: Tablet tensile strength produced using TSE and HSM granules produced at L/S = 1.2

The strength of tablets produced by both TSE and HSM granules is shown in Figure 4-23 and Figure 4-24. The strength of tablets produced at different L/S ratio and speed is similar. However, tablets produced from TSE granules are stronger than HSM tablets. Sun et al. stated that the friability of tablets is acceptable when the tablet tensile strength is higher than 2 MPa (Sun, Hou et al. 2009). Surprisingly, none of the tablets produced by HSM granules reach this critical value. It is likely that the material is over-granulated as it was granulated for 30 minutes in order to achieve equilibrium stage. The over-granulated process will lead to the formation of hard pellets that do not compact well during tablet production. The SEM images of the tablet fracture surface (Figure 4-22) shows that the TSE tablet is more amorphous because the weak and porous granules were fragmented during the compaction. Also, the irregular TSE granules tend to hook to each other giving strong inter-particle bonds during the tablet compaction. On the other hand, the strong and dense HSM granules experience rearrangement and deformation instead of fragmentation leading to some distinct particle boundaries. During the diametrical test, cracks will be initiated and propagate easily along these particle boundaries resulting in a low fracture force.

#### **4.5 CONCLUSION**

TSE has been shown to be a potential technique to operate wet granulation continuously. In the present study, it is shown that the overall mean size of HSM granules is larger when compared to TSE granules. Moreover, HSM produces granules with a mono-modal distribution and TSE produces granules with a multi-modal distribution. This multi-modal distribution exhibits in low L/S ratio and turns into bi-modal and mono-modal as the L/S ratio increases. TSE also produced more oversized granules and unwanted fines. This unwanted fines fraction decreases when the L/S ratio increases, giving granule with larger mean size. However, the fraction of desirable granule size is low when the L/S ration is smaller than 0.8

and higher than 1.2. In general, it is shown that the operating window for L/S ratio of TSE granulation is considered wide compare to HSM.

Images from SEM show that TSE granules are less spherical. Besides this the granules produced by TSE are formed with loosely packed materials whilst HSM granules have a smoother and denser surface. The internal porosity of TSE granules is also higher than that of HSM granules. Hence the strength of the TSE granules is lower compare to HSM granules. However, TSE granules have a uniform strength independent of the size classification and this strength is not affected by L/S ratio or screw speed.

By observing the differences in properties of TSE and HSM granules, it can be stated that the mechanism of these granulation processes are different. Wetting, nucleation and coalescence processes occur in TSE and HSM granulation. However the consolidation stage that determines the density of granule is believed to be absent in TSE. The powder in the TSE is likely to have immersion wetting to form extrudates. This extrudates are then mixed, compacted and elongated in the mixing zones. The extrudates will break into smaller pieces and form granules due to the shear force and kneading discs in the mixing zones. The breakage process in the granulation is still not well understood as limited information can be obtained from these experimental results. Finally, granules produced using TSE can be used to produce strong tablets even with a simple formulation showing the simplicity and flexibility of the technique. However, more work is needed to validate the mechanisms of TSE wet granulation and characterize the tablets produced to prove the suitability of TSE as granulation tool.



# CHAPTER 5 : THE STUDY OF CONTINUOUS TWIN SCREW GRANULATOR USING POSITRON EMISSION PARTICLE TRACKING (PEPT) TECHNIQUE

---

## SUMMARY

In this chapter Positron Emission Particle Tracking (PEPT) is utilised to track the trajectory of single particles through the mixing and conveying zones of a Twin Screw Granulator (TSG). A TSG consisting of conveying zones and mixing zones is used in this study. The mixing zones are arranged with kneading discs at an angle of  $30^\circ$ ,  $60^\circ$  or  $90^\circ$ . Experiments were carried out using different mixing configurations with various screw speeds and total mass flow rate. The PEPT data obtained was then used to obtain the residence time distribution (RTD) and the Peclet number in an attempt to gain some insight into the mixing of the process. The fill level of the granulator was also estimated to study the mechanism of granulation. As might be expected, it was shown that the residence time of the granulation process increases with decreasing screw speed; increasing powder feed rate or an increase in angle in the mixing zone. The fill level of the mixing zone in particular increases when the screw speed decreases or when powder feed rate increases. Furthermore, the fill level of the granulator will increase when the mixing zone configuration changes from  $30^\circ$  to  $90^\circ$ . It is shown that the granulator is never fully filled, even using  $90^\circ$  mixer elements implying limited compaction which may explain why the granules produced are porous compared to those from a high shear mixer. Interestingly the RTD analysis reveals that the extent of axial mixing in the mixing zone of the granulator does not change significantly for different

configurations and process conditions. There is evidence of a tail in the RTD which implies some material hold up and channelling.

## 5.1 INTRODUCTION

It is mentioned in previous chapters that many studies have been carried out to study the twin screw wet granulation technique. However most of them were investigating the effect of process conditions and process formulation on the granule properties and there is little work published to understand the mechanism inside the granulator. To date there has been little work has been done to visualise the flow and mixing in the twin screw granulator because of the difficulty in seeing through the barrel. One possible technique for observing the flow in opaque systems, widely used elsewhere, is positron emission particle tracking (PEPT). PEPT was invented and has been further developed at the University of Birmingham. It is a non-invasive imaging method derived from the medical technique of Positron Emission Tomography (PET) (Yang, Fryer et al. 2007). It can reveal in quantitative detail of the motion of a particle labelled with radioisotopes in a variety of process equipment (Bouwman, Henstra et al. 2005). PEPT involves radioactive tracer preparation where a particle is labelled with positron emitting radioactive isotope either through direct activation under the coverage of a 33 MeV  $^3\text{He}$  beam (Fan, Parker et al. 2006) or through ion exchange with radioactive water (Fan, Parker et al. 2006). This radioisotope which undergoes  $\beta^+$  decay emits a pair of ‘back-to-back’ gamma rays to be detected by a camera consisting of two position-sensitive detectors, each with an active area of  $500 \times 400 \text{ mm}^2$ , mounted on either side of the field of view (Yang, Fryer et al. 2007). The exact location of the tracer particle is then calculated using a triangulation and the speed can be determined by subsequent processing of the location data. The technique has now been developed to the point where it has the capability

to track tracer particles down to approximately 60  $\mu\text{m}$  in size, moving at up to 10 m/s, yielding locations to within  $\pm 1$  mm at frequencies better than 100 Hz (Seville, Ingram et al. 2009).

PEPT has been used to study a wide range of batch engineering processes. It has been used extensively in batch studies of particulate system notably: solid mixing in a V-mixer (Kuo, Knight et al. 2005), bubbling fluidised bed (Fairhurst, Barigou et al. 2001; Yee S 2006; Van de Velden, Baeyens et al. 2008; Chan, Seville et al. 2009; Chan, Brems et al. 2010) and rotating drum (Parker, Dijkstra et al. 1997; Ding, Seville et al. 2001). The technique is also popular in food apparatus (Cox, Bakalis et al. 2003; Bakalis, Cox et al. 2006; Mehauden, Cox et al. 2009) and multiphase systems (Barigou 2004; Pianko-Oprych, Nienow et al. 2009; Chiti, Bakalis et al. 2011). The PEPT system allows effective tracer tracking of up to three particles within a vessel at a time (Yang, Fryer et al. 2007) and it is very useful to determine velocity distributions, shear gradients, and occupancy plots of a system (Portillo, Vanarase et al. 2010).

Besides this, there has been also a few continuous processes being studied using PEPT. Laurent et al. (2005) highlighted that the possible use of PEPT to study the powder flow pattern in a continuous mixer. From then, Ingram et al. (2005) started to investigate the axial and radial dispersion in a rolling mode rotating drum using this technique (Ingram, Seville et al. 2005) and Portillo et al. (2010) examined the effect of impeller rotation rate, powder flow rate, and cohesion on powder flow behaviour in a continuous convective blender (Portillo, Vanarase et al. 2010).

## 5.2 OBJECTIVES

The aim of this study is to utilise PEPT to track a single particle tracer in a twin screw granulator and to visualise the flow motion of bulk materials through the conveying and mixing zones. The residence time distribution (RTD) of the process will also be obtained to get some insight into the performance of the mixing in the granulator. Moreover, the overall fill level of the granulator will then be calculated based on the powder feedrate and the residence time obtained. The residence time and fill level of different sections (conveying and mixing) in the twin screw granulator were also determined.

## 5.3 MATERIALS AND EXPERIMENTAL METHOD

### 5.3.1 Formulation of granules

The primary particles used in this experimental work consisted of  $\alpha$ -Lactose Monohydrate (Pharmatose 200 M, DMV-Fonterra, Netherlands) and Microcrystalline Cellulose (MCC Avicel PH101, FMC Biopolymer, Ireland) as excipients. Hydroxypropyl Cellulose (HPC M.W 100,000, Alfa Aesar, UK) was used as binder and Crosscarmelluose Sodium (Ac-Di-Sol SD-711 NF, USA) was added as a super disintegrant. Prior the granulation, 73.5 w/w% of Pharmatose, 20 w/w% of MCC, 5 w/w% of HPC and 1.5 w/w% of Ac-Di-Sol (J. Cartwright 2009) were premixed using a Pascal Lab Mixer for a period of 30 minutes to obtain a homogenous mixture. Distilled water, used as the granulating liquid was injected through the first liquid feed point (Figure 5-1).

### 5.3.2 Granulation Process

The granulation process was carried out using a 19 mm diameter Twin Screw Granulator which was designed and built in house by GEA Pharma System, UK. The barrel of the

granulator was modified to reduce the thickness of the construction materials in order to allow the application of PEPT. The screws of the granulator have a length to diameter ratio of 10: 1. The screws have 2 mixing zones which consist of six or seven kneading discs and were arranged at an angle of 30°, 60° or 90° as in Figure 5-1. The powder mixture was fed into the granulator using a screw feeder (K-Tron T20) whilst distilled water was pumped through the liquid injection point using a peristaltic pump. The temperature of the barrel was kept at 20 °C by circulating cool water through a jacket in the granulator.

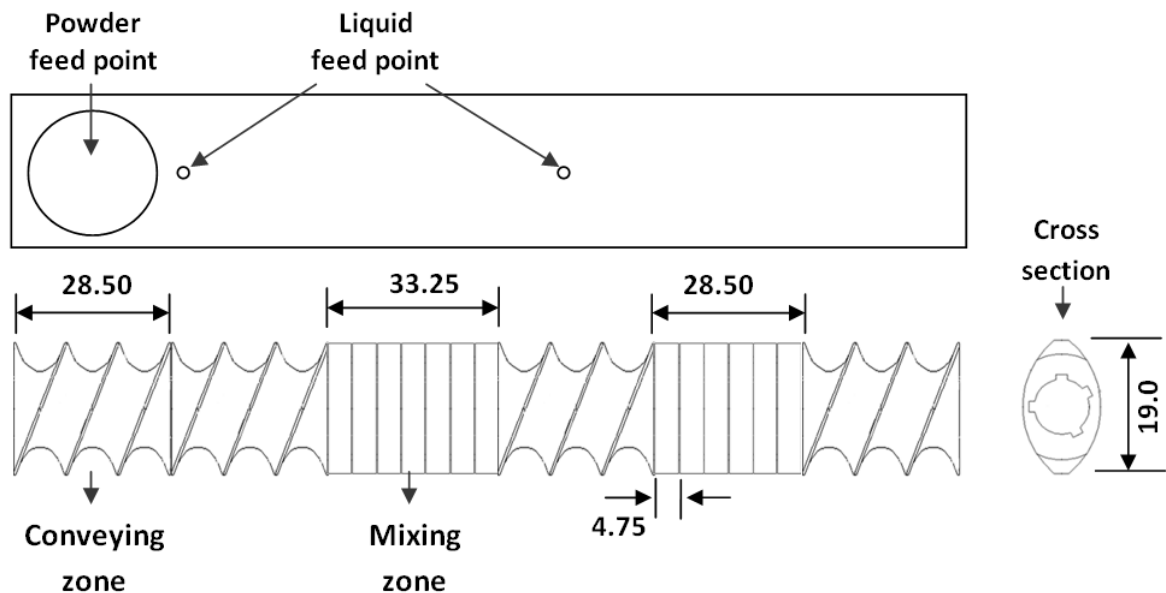


Figure 5-1: Schematic diagram of the granulator barrel and screw (dimensions are in mm)

In order to study the effects of process conditions on the system, experiments were carried out at different powder flow rates and screw speeds, whilst keeping one of the parameters constant. The liquid to solid ratio was kept constant at 0.35 for all the experiments. Figure 5-2 shows the matrix of all the experiments carried out in this study.

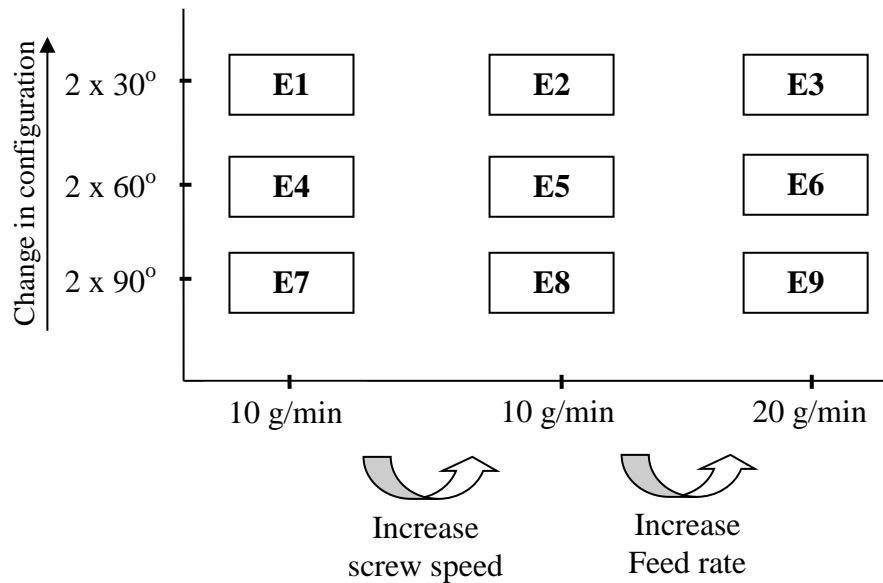


Figure 5-2: Experimental Matrix of PEPT for this study

### 5.3.3 Positron Emission Particle Tracking (PEPT)

PEPT, which allows a single radioactive label tracer to be tracked in three dimensions, is used for the first time to study the behaviour of a particle in a Twin Screw Granulator. To reflect the behaviour of interest, the tracer particle is required to be near identical to the bulk materials in the granulator (Fan, Parker et al. 2006). For the present study, a resin particle of 100  $\mu\text{m}$  diameter, with a density of  $1100 \text{ kg/m}^3$  was used to prepare the tracer. The resin particle is labelled using a radioisotope via an  $^{18}\text{F}$  ion exchange technique (Fan, Parker et al. 2006; Parker and Fan 2008). The activated tracer was then coated with a thin layer of super glue in order to prevent the dissolution of water soluble  $^{18}\text{F}$  in the water during the experiment. The  $^{18}\text{F}$  water used was produced from purified water by direct irradiation using a 35MeV  $^3\text{He}$  beam from the Birmingham Cyclotron. The radionuclide of the tracer ( $^{18}\text{F}$ ) is selected because it undergoes  $\beta^+$  decay which is accompanied by the release of a positron, ultimately resulting in the formation of two ‘back-to-back’ 511 keV  $\gamma$ -rays, which travel along the same line in opposite directions (Seville, Ingram et al. 2005; Saito, Ingram et al. 2009).

The  $\gamma$ -rays will penetrate the barrel construction material and will be detected by two highly sensitive detector cameras. A line can be constructed along which the tracer particle must lie as shown in Figure 5-3. The exact location of the tracer can then be determined by geometric triangulation using several dozen coincident pairs for each location. The detail of explanation of the PEPT can be found in references (Portillo, Vanarase et al. ; Parker, Broadbent et al. 1993; Parker, Hawkesworth et al. 1994; Fan, Parker et al. 2006; Fan, Parker et al. 2006)

For this study, the tracer particle was fed into the system through the powder injection port of the granulator once steady state operation was obtained. The tracer particle was then collected at the end of the granulator, separated and recycled back to the system as the next run. One strong tracer was recycled for an average of 20 times until the tracer particle became weak due to (a) the short half life of  $^{18}\text{F}$ ; (b) the tracer or the coating of the tracer fracturing due to the high shear stress condition or (c) the radioactivity dissolved slowly into the materials in the granulator. The experiments were repeated at least 100 times at each condition to obtain enough data points for residence time distribution calculations.

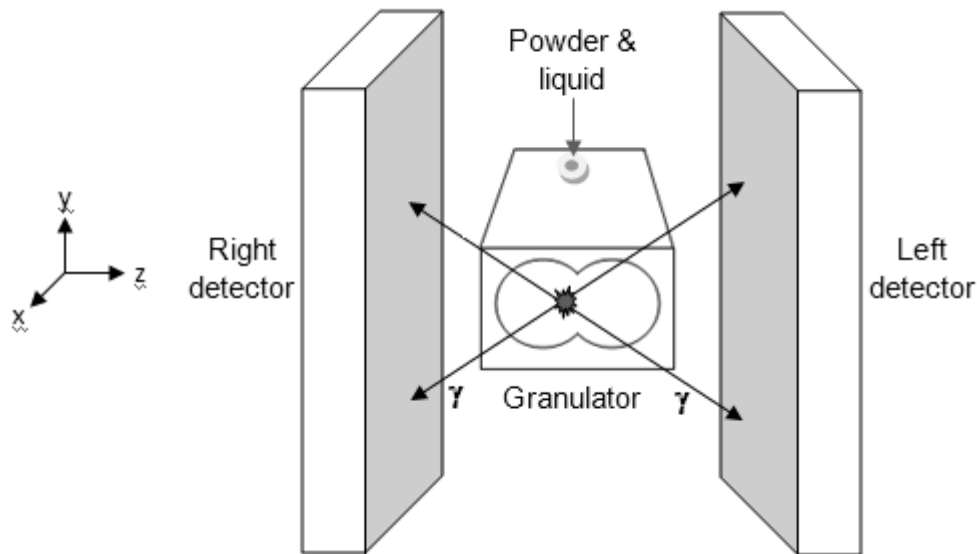


Figure 5-3: Experiment set up and location by triangulation of a particle in the granulator

### 5.3.4 PEPT Data Processing

To transform the raw PEPT data into particle tracer location, the location algorithm method previously developed by Parker et al. is used (Parker, Broadbent et al. 1993). The gamma ray pairs that are detected and recorded by the camera are first divided into subsets (slices) of sequential events. Each slice is used to generate a single location. In each slice, the coordinates of the tracer are located using an optimisation routine where events that lie furthest away from the initial estimated point are discarded as corrupted data. A new location is then calculated from these remaining events and this process is repeated until an optimum fraction,  $f_{opt}$ , of all the events listed in the subsets is kept. The processed data has the form of a list of spatial coordinates,  $x$ ,  $y$  and  $z$  in millimetre as well as the time in millisecond. In order to obtain a good quality of particle trajectory, the selection of parameters, number of events pairs per slices,  $N$ , and  $f_{opt}$  is important. Defining a general rule for these values that should be ascribed to these parameters is not straight forward as they depend on the radioactivity of the tracer, its absolute velocity and fluctuation characteristics, including the rate of change of



direction of the mean velocity of the tracer. The first choice of the value of these parameters can be decided by a trial and error approach. A previous study (Parker, Broadbent et al. 1993) showed that increased numbers of event per slice results in a more accurate reconstruction of tracer location.

In present study, the effect of data processing parameters on the co-ordinates of the tracer, raw data of a stationary tracer in the granulator is recorded and the relative standard deviation and location error were also quantified using different combinations of  $N$  and  $f_{opt}$ . Figure 5-4 shows that for a weak tracer particle, increasing the number of events per slice will result in the loss of some data points in the trajectory particularly in the  $y$  and  $z$  direction. On the other hand, Figure 5-5 shows that, low events per slice will lead to a noisier trajectory. Moreover, a low  $f_{opt}$  value will cut off most of the corrupted data leaving only a few events for the triangulation process that gives a less reliable location (e.g.  $N = 50$ ;  $f_{opt} = 0.05$ ; only 2.5 events left to calculate location). Therefore  $N = 150$  with a  $f_{opt}$  of 0.2 are considered as optimum parameters combination and are used to process the raw PEPT data.

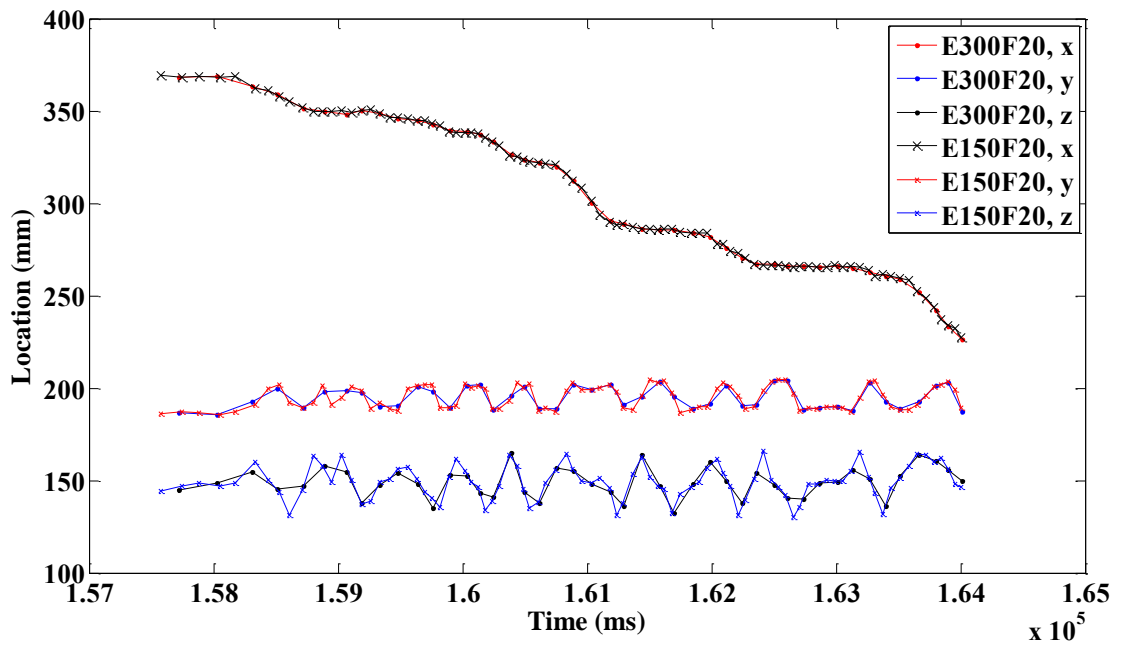


Figure 5-4: Trajectory with optimum and high number of events per slice of a weak tracer particle, E300F20 = 300 events per slice and  $F_{opt}$  of 20%

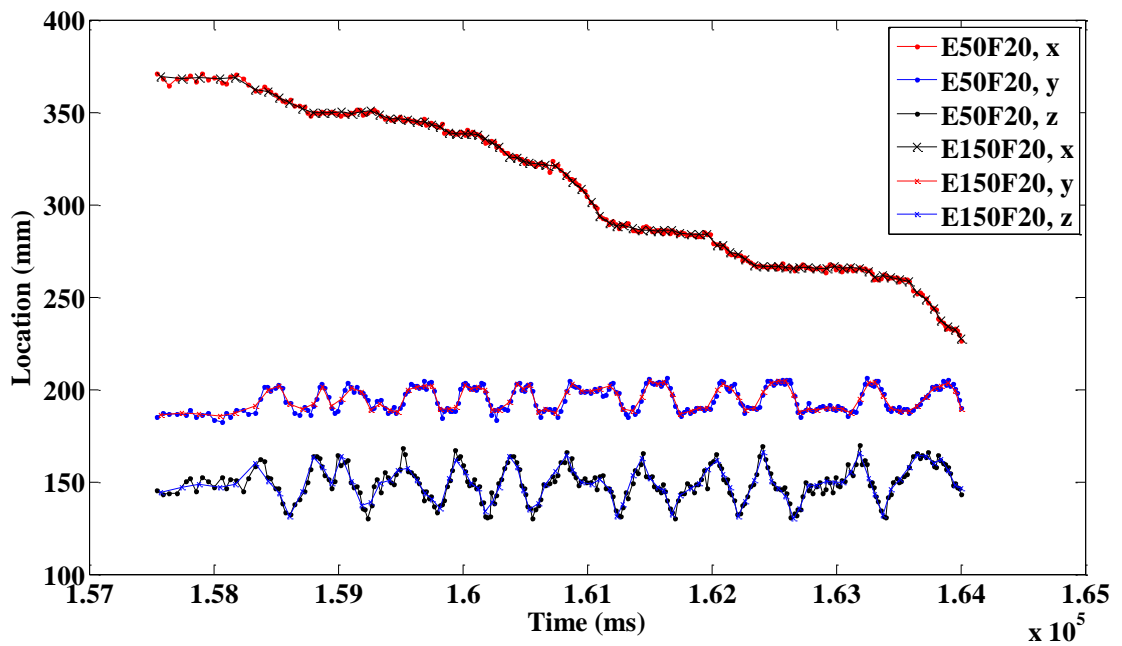


Figure 5-5: Trajectory with optimum and low number of events per slice of a weak tracer particle, E50F20 = 50 events per slice and  $F_{opt}$  of 20%

### 5.3.5 Residence Time Distribution

Conventionally, residence time distribution is obtained by injecting a pulse of dye tracer into the system and the residence time function is calculated using Eq 5-1 where  $c(t) dt$  is the concentration of the tracer at the outlet between  $t$  and  $t + dt$ . For this study, as the 100 passes of the tracer is discrete, Eq 5-1 is slightly modified to become a discrete function as shown in Eq 5-2 where  $a(t)$  is the number of passes with residence time between  $t$  and  $t + \delta t$ .

$$e(t) = \frac{c(t)}{\int_0^{\infty} c(t) dt} \quad \dots \text{Eq. 5-1}$$

$$e(t) = \frac{a(t) / \delta t}{\sum a(t)} \quad \dots \text{Eq. 5-2}$$

The mean residence time,  $t_m$  is then calculated from (Fogler 2006),

$$t_m = \frac{\int_0^{\infty} t \cdot e(t) dt}{\int_0^{\infty} e(t) dt} \quad \dots \text{Eq. 5-3}$$

The variance,  $\sigma^2$  is calculated by (Fogler 2006),

$$\sigma^2 = \frac{\int_0^{\infty} (t - t_m)^2 \cdot e(t) dt}{\int_0^{\infty} e(t) dt} \quad \dots \text{Eq. 5-4}$$

The shape of the residence time distribution curves was also observed by normalisation using the following equations

$$\text{normalised time, } \theta = \frac{t}{t_m} \quad \dots \text{Eq. 5-5}$$

and

$$e(\theta) = t_m \cdot e(t) \quad \dots \text{Eq. 5-6}$$

The axial mixing in the granulator can be characterised by calculating a dimensionless Peclet number,  $Pe$  as follows (Fogler 2006),

$$Pe = \frac{\text{Rate of transport by convection}}{\text{Rate of transport by diffusion or dispersion}} = \frac{UL}{D_{diff}} \quad \dots \text{Eq. 5-7}$$

Where  $U$  is velocity (m/s),  $L$  is the characteristic length (m) and  $D_{diff}$  is the diffusion or dispersion coefficient ( $s^{-1}$ ). By treating the boundary condition of the granulator as a closed/closed system with no dispersion or radial variation in concentration either upstream or downstream, the following equation can be derived (Fogler 2006), i.e. the material enters and stays in, and leaves and stays out.

$$\frac{\sigma^2}{t_m^2} = \frac{2}{Pe} - \frac{2}{Pe^2} (1 - e^{-Pe}) \quad \dots \text{Eq. 5-8}$$

Consequently, the  $t_m$  and  $\sigma^2$  can be obtained experimentally from the RTD data and the Peclet number can then be calculated using Eq 5-8 using numerical analysis. As  $\sigma^2$  approaches zero,  $Pe$  approaches infinity indicating that the extent of axial mixing is low. Plug flow occurs when  $\sigma^2 = 0$ .

### 5.3.6 Granulator Fill

It is reasonable to expect that the fill level will affect the degree of material compression or compaction in the granulator and therefore the level of occupancy of material in the granulator is estimated in this study. Since the flow rate of the process was kept constant during the experiment, the mass fill level in the granulator will be proportional to the length

of time the material spends in the granulator multiplied by the mass rate of material assuming steady state. If it is also assumed that the density of the material is uniform throughout the granulator, the mass fill level can be converted to volumetric fill level using Eq 5-10. The granulator was divided into several sections with the width of a single kneading disc and the residence time of each section was calculated to estimate the fill level. The fill level of each section is calculated as follows,

$$\text{Mass Fill Level} = \frac{\text{residence time of section} \times \text{mass flowrate}}{\text{section interval}} \frac{g}{\text{min}} \quad \dots \text{Eq. 5-9}$$

$$\text{Volumetric Fill Level} = \frac{\text{Mass fill level } mm^3}{\text{material density } mm} \quad \dots \text{Eq. 5-10}$$

$$\text{Overall Fill Fraction} = \frac{\text{Volume fill level } mm^3}{\text{Known free volume } mm^3} \quad \dots \text{Eq. 5-11}$$

## 5.4 RESULTS AND DISCUSSION

### 5.4.1 Single particle Trajectory

The location along the granulator (x), the upward and downward motion (y) and the left and right motion (z) of the particle tracer in the granulator were plotted against time as shown in Figure 5-6. For the tracer x-location, it is shown that the gradient of the curve in the mixing zones is less than that in the conveying zones. This is expected and it indicates that the axial velocity of the materials through the mixing zones is less than that through conveying zones. Besides this, when comparing different screw configuration, there is a decrease of the slope in the mixing zones when the kneading discs angle increases from 30° to 60° to 90°. This again is expected as the conveying capacity of the mixing zone decreases when kneading discs are arranged with a greater angle.

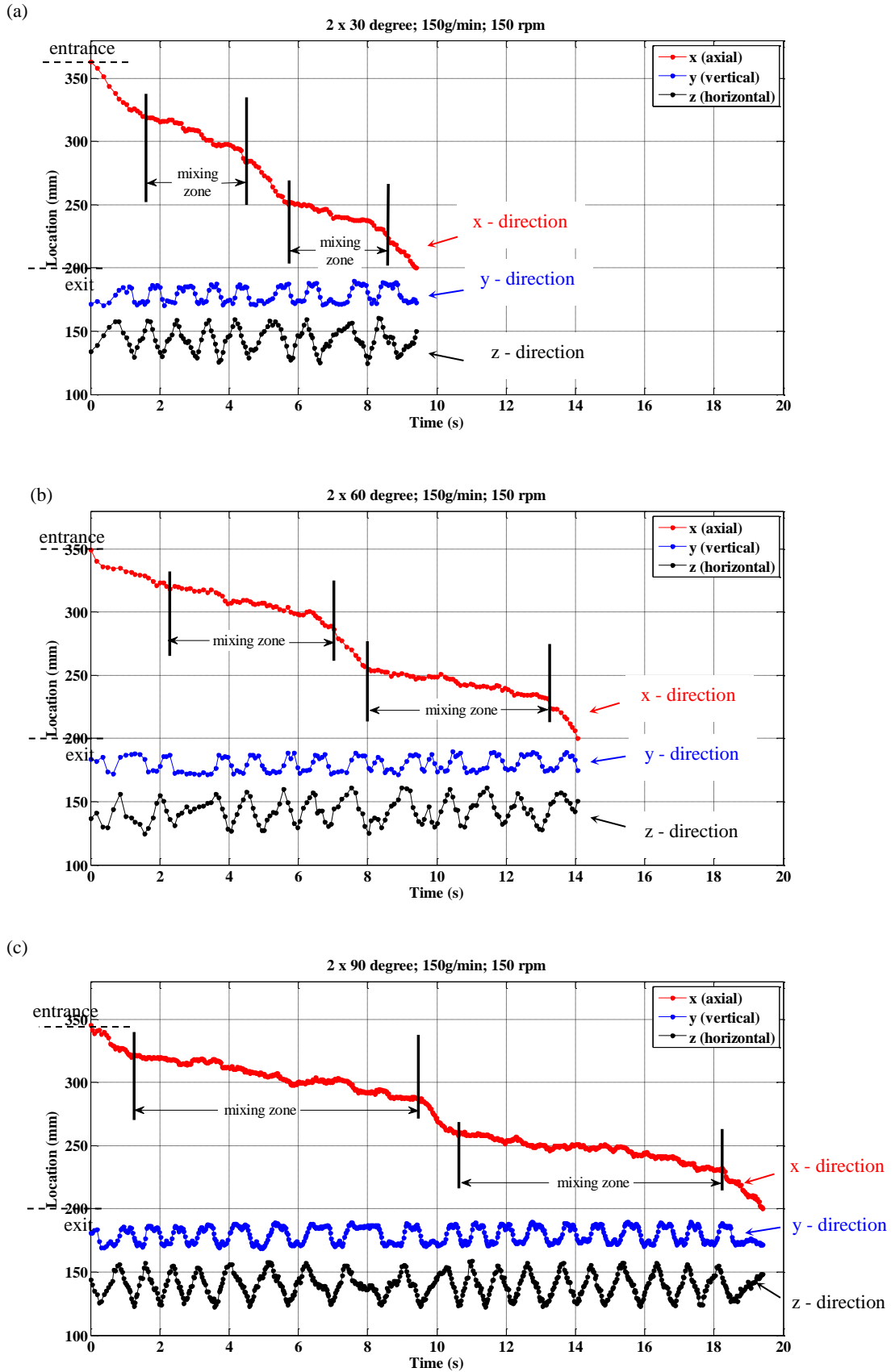


Figure 5-6: Single Particle Trajectory in X, Y and Z direction for (a)  $30^\circ$ ; (b)  $60^\circ$  and (c)  $90^\circ$  mixing zones

### 5.4.2 Single particle 2-D trajectory

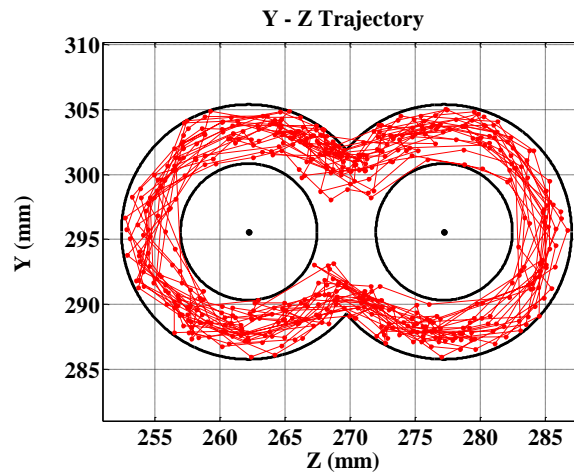


Figure 5-7: Track of a single particle tracer in Y-Z (cross section view) direction

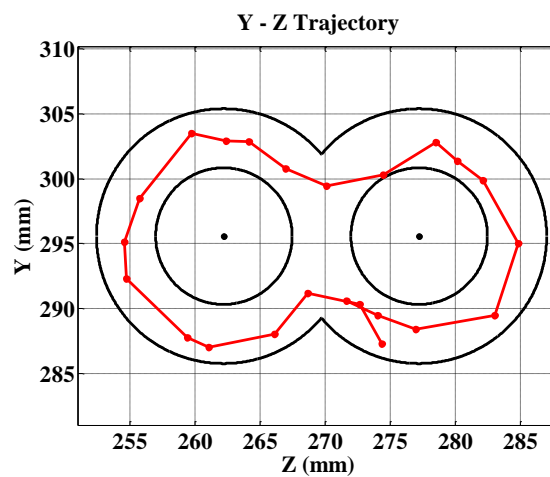


Figure 5-8: Example of particle tracer moving in shape of ' $\infty$ '

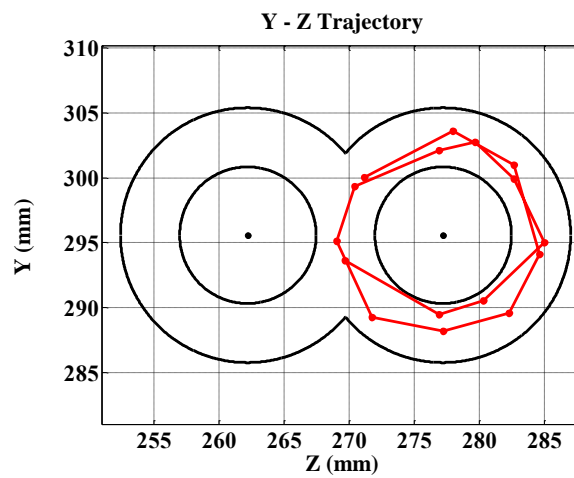


Figure 5-9: Example of particle tracer moving in a circle

Figure 5-7 shows the full 2-D trajectory of a single particle tracer viewing in the cross section direction. Generally there are two types of tracks that the particle tracer follows. The first type is shown in Figure 5-8 where the particle tracer is transferred from one screw to the other and moving in the shape of '∞'. Figure 5-9 shows the second type of track and the particle tracer remains in to only one screw and moves in a circle. This phenomenon occurs very occasionally and can also be found when the particle tracer is stuck to the surface of the screw. A particle tracer moving in a circle does not bring any disadvantages to the process as it is believed that it is relevant to the material mixing in the granulator. The higher number of the occasion materials moving in a circle, the better the mixing is believed can be achieved.

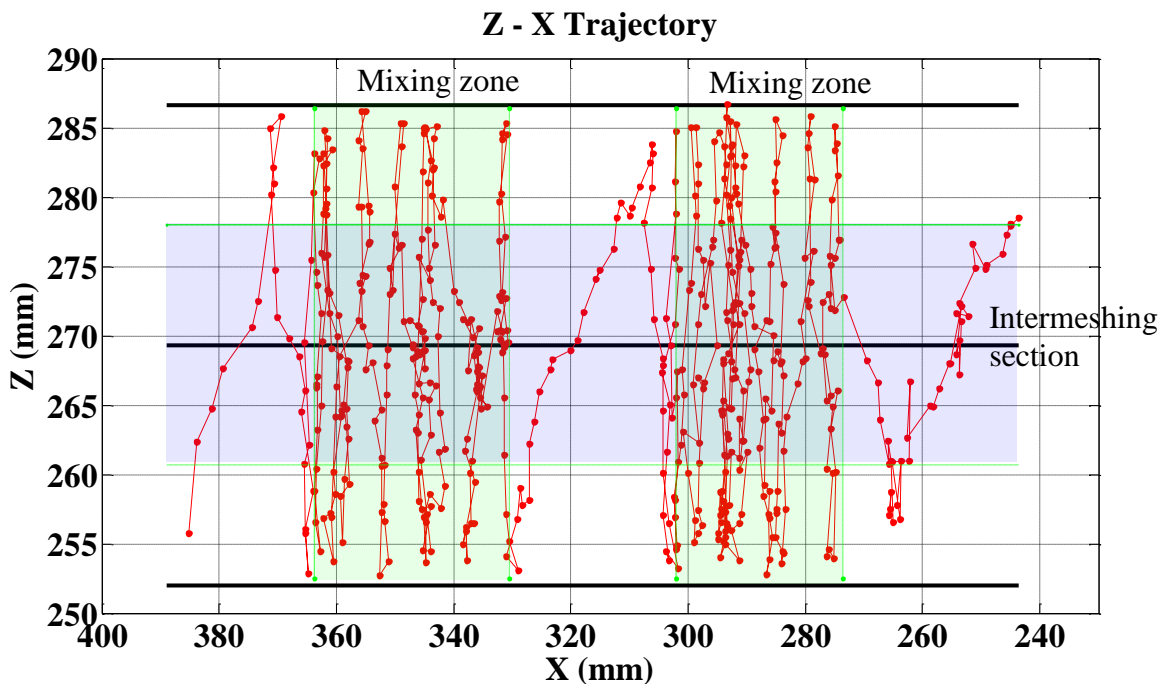


Figure 5-10: Track of single particle tracer in Z-X (plan view) direction



Figure 5-10 shows the plan view of the trajectory of the particle tracer in the granulator. It is shown that the material flows smoothly through the conveying zones and start to build up prior to entering the mixing zones and spend a longer time there. Also, the trajectory shows that the magnitude of flow in the x-direction is higher in the intermeshing section especially in the mixing zones. This explains that the materials are compressed and pushed forward or backward when they reach the intermeshing area. This phenomenon can be seen more clearly in the video file which is attached at the back of the thesis.

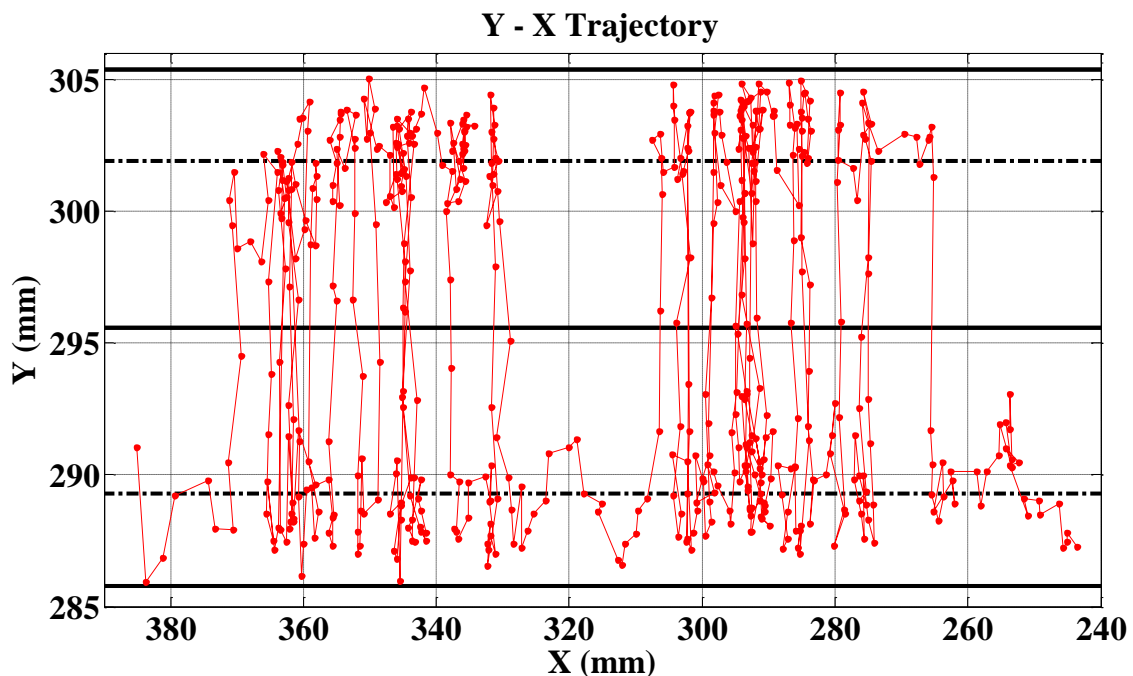


Figure 5-11: Track of single particle tracer in Y-X (side view) direction

The side view of the trajectory of particle tracer is shown in Figure 5-11. The particle tracer stays at the bottom of the granulator when it is in the conveying zones and moves upward and downward in the mixing zones. It is again shown that the materials have a higher magnitude of flow in x-direction in the intermeshing area. The details of the particle tracer trajectory in Z-Y, Z-X and Y-X direction can be found in the animation files attached at the back of the thesis.

### 5.4.3 Overall Residence Time Distribution

Figure 5-13 shows the residence time distribution (RTD) curves for various screw configurations at different process conditions. The change of the pattern of the RTDs at different process conditions is similar for all the screw geometries. For each screw configurations, the RTDs at low powder feedrate and low screw speed have a higher mean and a wider distribution. When there is an increase in screw speed, the RTDs move slightly to the left and become narrower. This is expected as increases in screw speed will increase the conveying rate and reduce the time the material spends in the granulator. Moreover, increases in the powder feedrate are shown to further decrease the mean residence time. The RTDs at high powder feedrate and screw speed are located furthest to the left and are the narrowest among those with the same screw configuration. As the powder feedrate increases, it is expected that there is more material pushing forward creating some extra conveying capacity in the granulator. The increase in the conveying rate explains the decrease in the time spent in the granulator when the powder feedrate increases.

When comparing the RTDs for different screw configuration for the same process conditions, it is shown that the RTDs move slightly to the right and become wider when the mixing angle changed from  $30^\circ$  to  $60^\circ$ . The mean residence time shows that the material spends an extra 3 to 4 seconds in the granulator. The increase in mean residence time is presumably due to the reduced conveying capacity of the  $60^\circ$  kneading elements compared to the  $30^\circ$  configuration. The RTDs for the screw configuration with  $90^\circ$  mixing zone have the widest distribution and are furthest on the right. A mixing zone with  $90^\circ$  kneading disk arrangement in principal gives no conveying capacity. Yet we observe that the materials will still flow through the granulator. Therefore, it is believed that the material flow through a  $90^\circ$  mixing zone is related to the powder feedrate and the gradient of fill degree along the

granulator. Hence, the residence time of the granulation process using 90° kneading blocks configuration is a lot higher than 30° and 60° configurations.

The mean residence time (MRT) of all 9 sets of experiments is summarized in Figure 5-12. The graph shows that the mean residence time increases when the mixing zone screw angle increases due to the decrease in conveying capacity. On the other hand, the mean residence time decreases when the screw speed and powder feedrate increases as explained above.

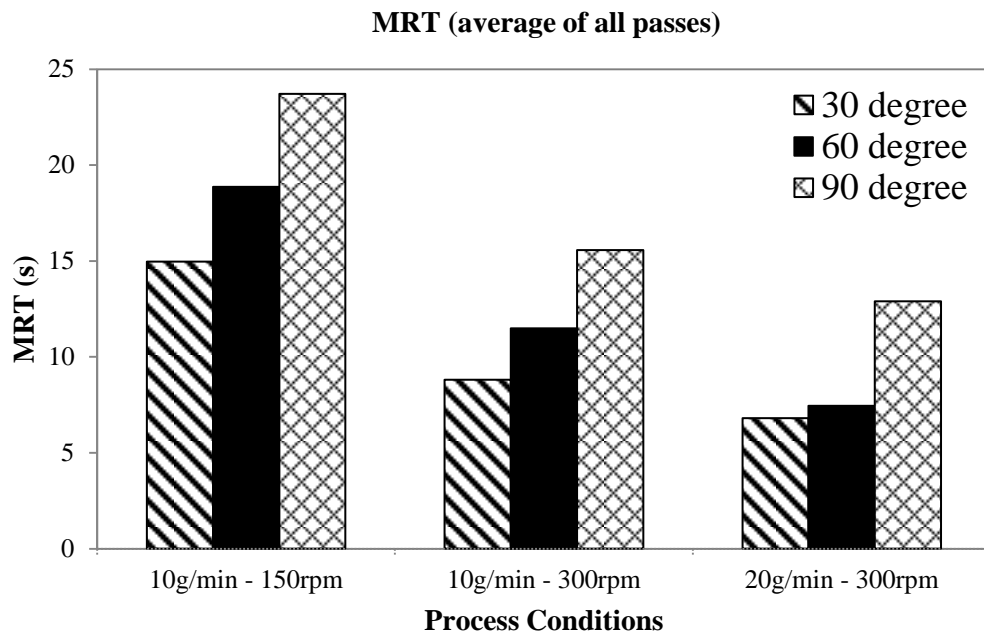
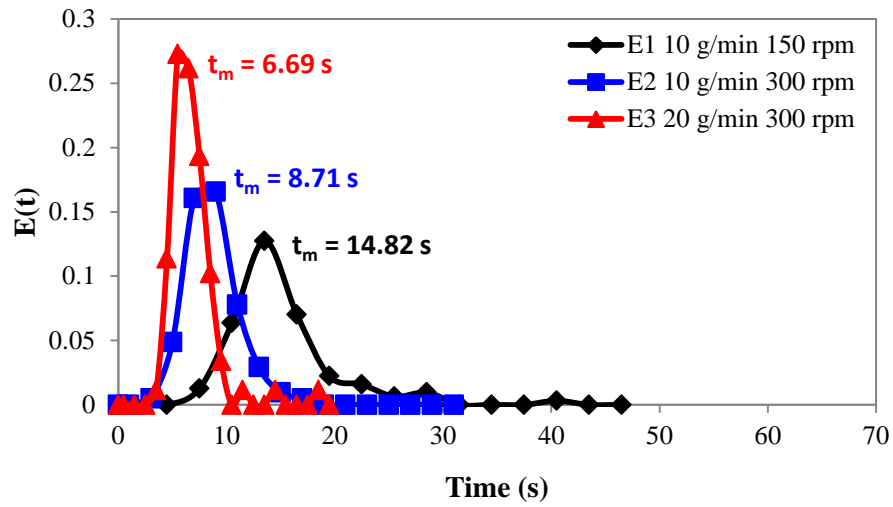
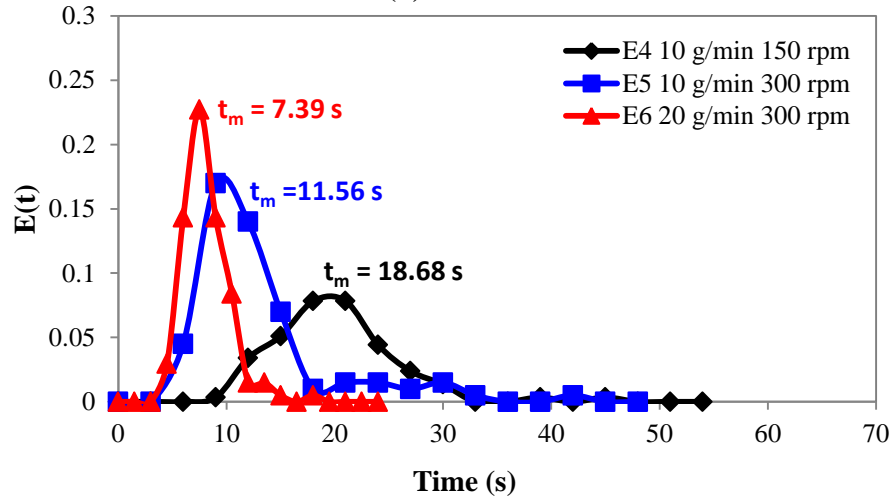


Figure 5-12: Mean Residence Time (MRT) for various screw configuration at different process conditions

(a) 30° RTD curves



(b) 60° RTD curves



(c) 90° RTD curves

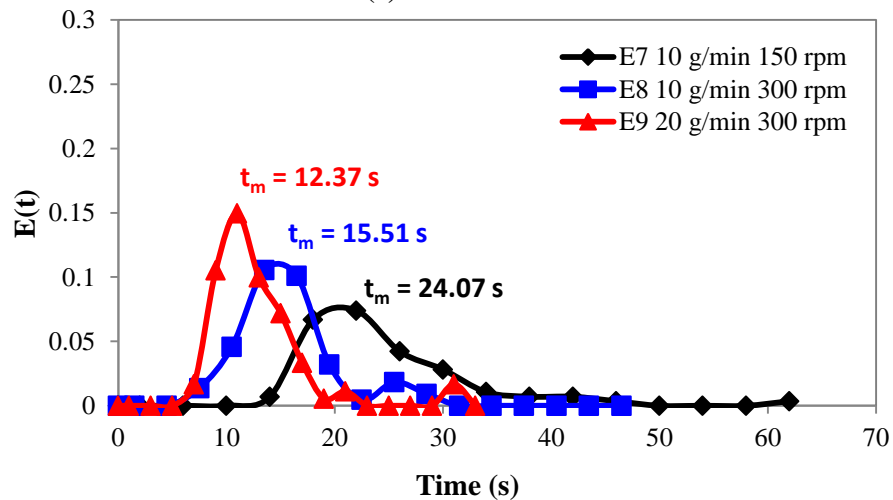


Figure 5-13: Residence Time Distribution curves at various process parameter (a) 30°, (b) 60° and (c) 90° mixing zones

<b>Fraction of <math>\theta &gt; 1.5</math></b>			
<b>Process conditions</b>	<b>30°</b>	<b>60°</b>	<b>90°</b>
<b>10 g/min; 150 rpm</b>	0.106	0.061	0.100
<b>10 g/min; 300 rpm</b>	0.087	0.015	0.097
<b>20 g/min; 300 rpm</b>	0.067	0.088	0.055

Table 5-1: Fraction of  $\theta > 1.5$  by assuming that particle is considered stuck either on screw or wall at this value

It is shown in Figure 5-13 that there is a tail in the RTDs of all the experiments. The presence of the tail in RTD curves is due in part to the particle tracer being occasionally stuck in the granulator during the experiments. Figure 5-14 shows that the situation when the particle stuck for approximately 1 second on the screw where there is no change in tracer's x-location (boxed area). The higher rotation frequency of the tracer's y-location and smaller amplitude of its z-location show that the particle tracer is stuck to one of the screws. The boxed areas in Figure 5-15 show a situation in which the tracer's y-location is generally constant while the x-location has a very small gradient. In this case, this indicates that the material was stuck on the wall and slipped very slowly forward in the x-direction due to the material flow. As the screws turn, they will shear the lodged material until this material escaped and follows the normal flow stream. From these examples, it can be assumed that materials will get stuck in the granulator and the tail is real i.e. the tail is not an artefact of the method with the evidence of the observation of residual material after a run. This also implies that the twin screw granulator is not absolutely self wiping and there is some clearance between the screws and the wall. However, more work is needed to validate this outcome by

repeating experiments in order to obtain more data for a more reliable residence time distribution.

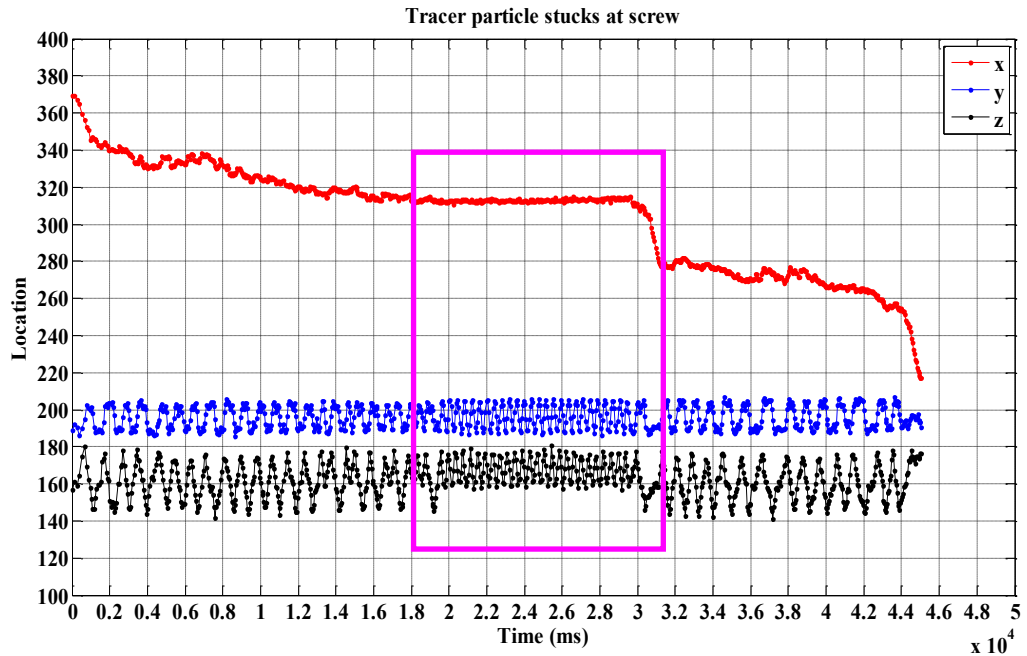


Figure 5-14: Situation when particle tracer gets stuck on the screw

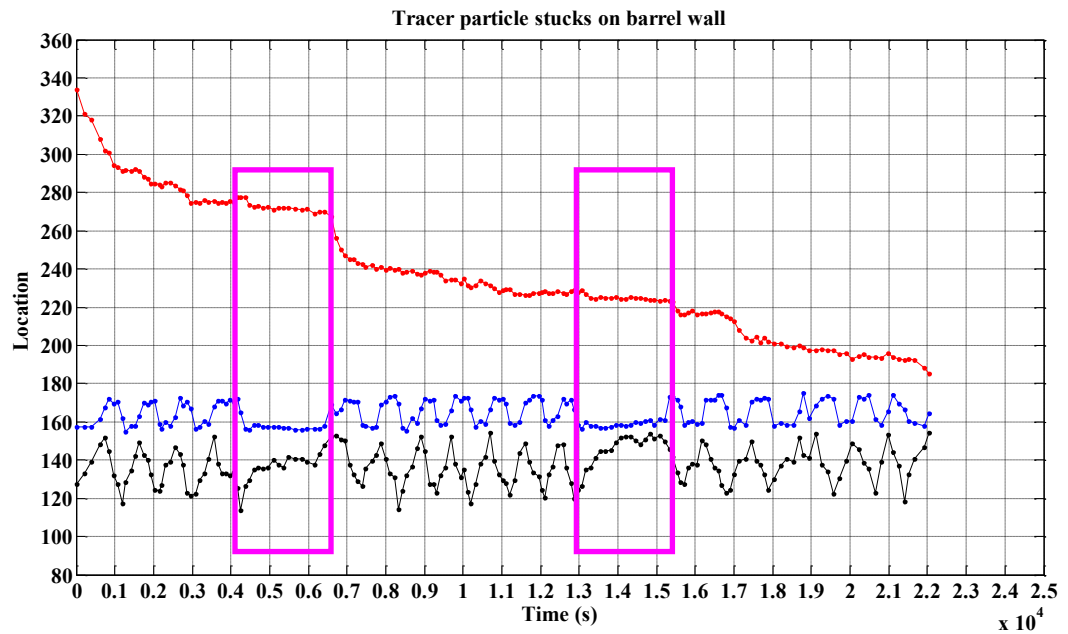


Figure 5-15: Situation when particle tracer gets stuck on the wall of granulator

### 5.4.4 Normalised Residence Time Distribution

Process conditions	Peclet Number (Pe)		
	30°	60°	90°
10 g/min; 150 rpm	19.96	19.19	21.26
10 g/min; 300 rpm	24.07	5.56	22.25
20 g/min; 300 rpm	24.92	24.06	22.09

Table 5-2: Peclet number for various process parameters and screw configuration

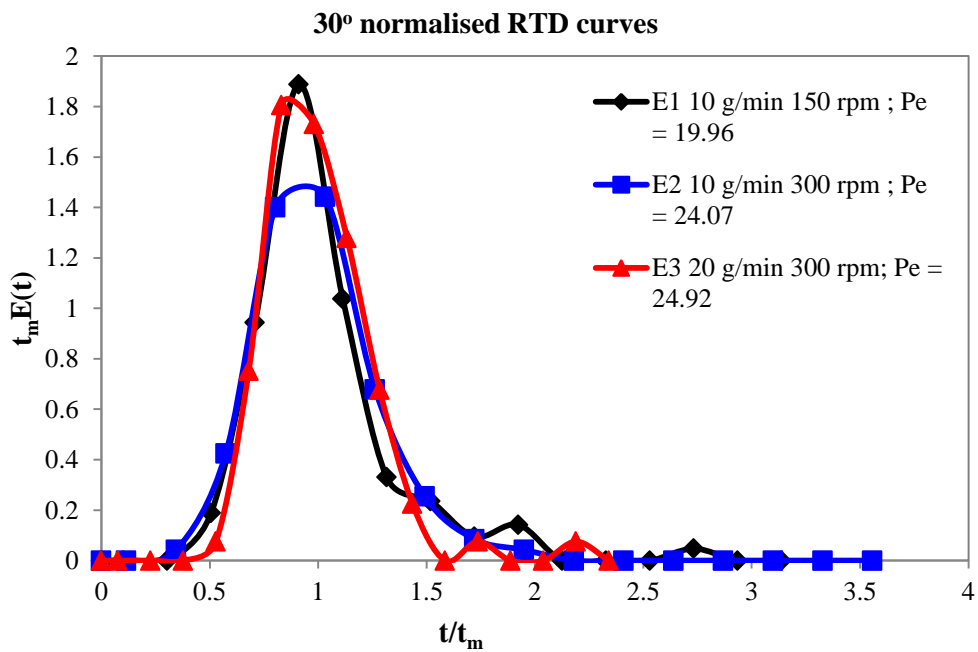


Figure 5-16: 30° mixing zones normalised RTD

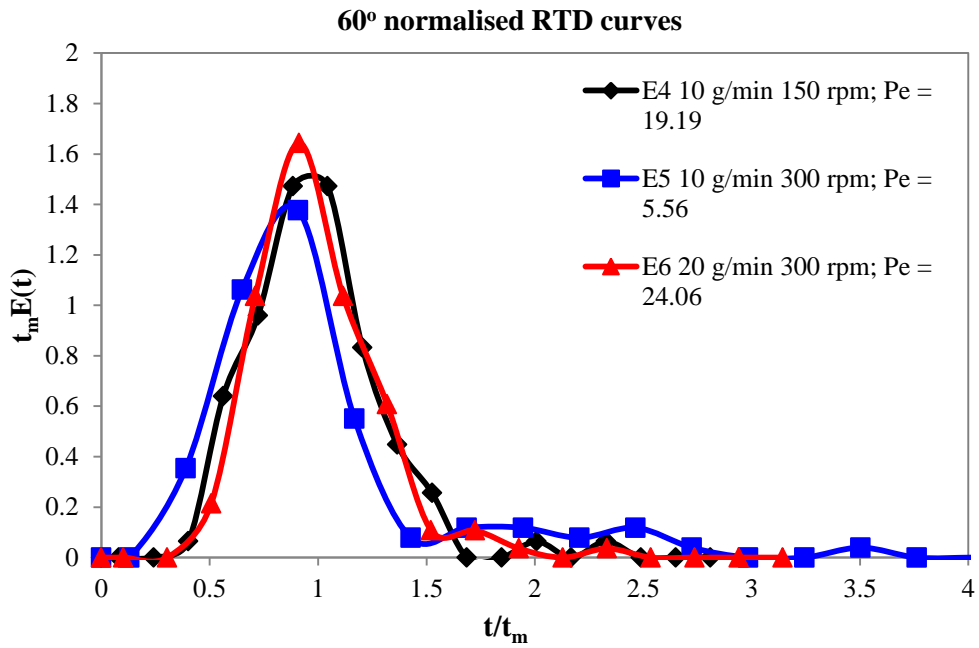


Figure 5-17: 60° mixing zones normalised RTD

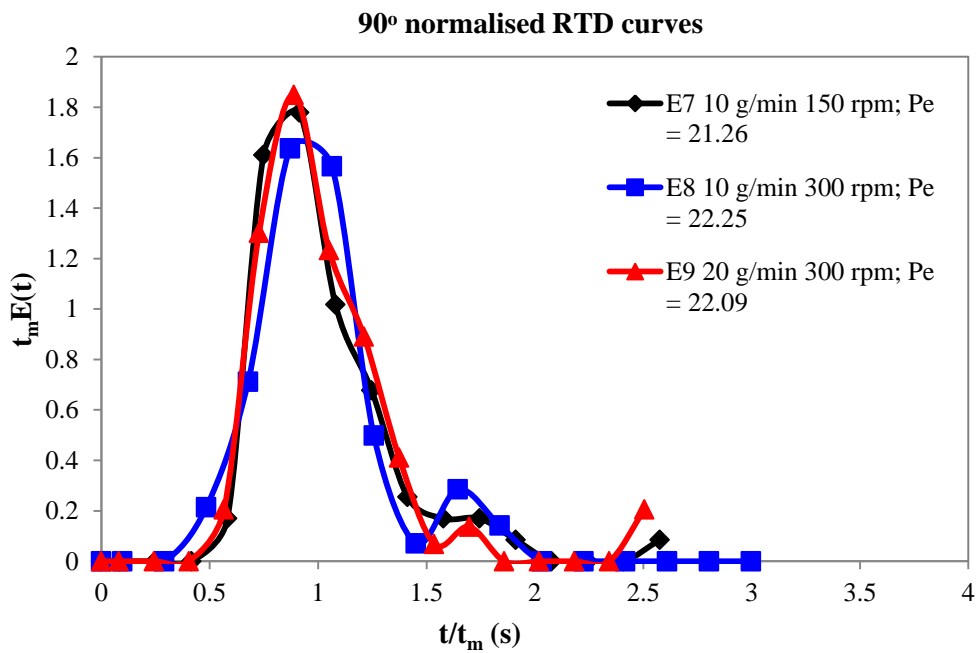


Figure 5-18: 90° mixing zones normalised RTD



In order to study the shape of the RTD and the extent of mixing, the Peclet number and normalised RTD were obtained using Eq 5.7. It was expected that both the Peclet number and shape of the normalised RTD would be different for various process parameters and particularly screw configuration. In the present study, however the shape of the normalised RTD which is shown in Figure 5-16, Figure 5-17 and Figure 5-18 is approximately identical for different powder feedrate and screw speed. The Peclet numbers calculated also give similar values approximately  $22 \pm 10\%$ . It is quite surprising perhaps that for different screw configurations the results show an approximately identical normalised RTD and Peclet number. Conclusion must be that the extent of axial mixing is similar regardless of the screw speed; powder feed rate and the screw configuration. The apparently anomalous observations of experiment E5 may be due to the particle getting stuck more regularly during the experiment either on the screw or the barrel of the granulator.

The use of Peclet number to study the extent of axial mixing in a twin screw extruder had also been previously studied by a few researchers. The results reported by Oberlehrer et. al. is in consistent to current results showing that the Peclet number is not significantly affected by screw configuration (Oberlehner, Cassagnau et al. 1994). Besides this, (Unlu and Faller 2002) measured the normalised RTD of a twin screw food extrusion process and reported that the material feedrate had no significant effect on the RTD spread which is identical to current study. However in the same study, the author also reported that the screw speed will alter the RTD spread (Unlu and Faller 2002). Gautam et. al. also did similar experiments on food extrusion and reported that the extend of the axial mixing in the twin screw extruder was affected by the screw types and screw geometries (Gautam and Choudhury 1999). The Peclet number has been well studied to represent the mixing in a series of continuous stir tank

reactors. However the use of Peclet number in twin screw extruder studies lead to inconsistent outcomes showing that further work is still needed to study the mixing in an extruder.

#### 5.4.5 Overall fill fraction of the TSE granulator

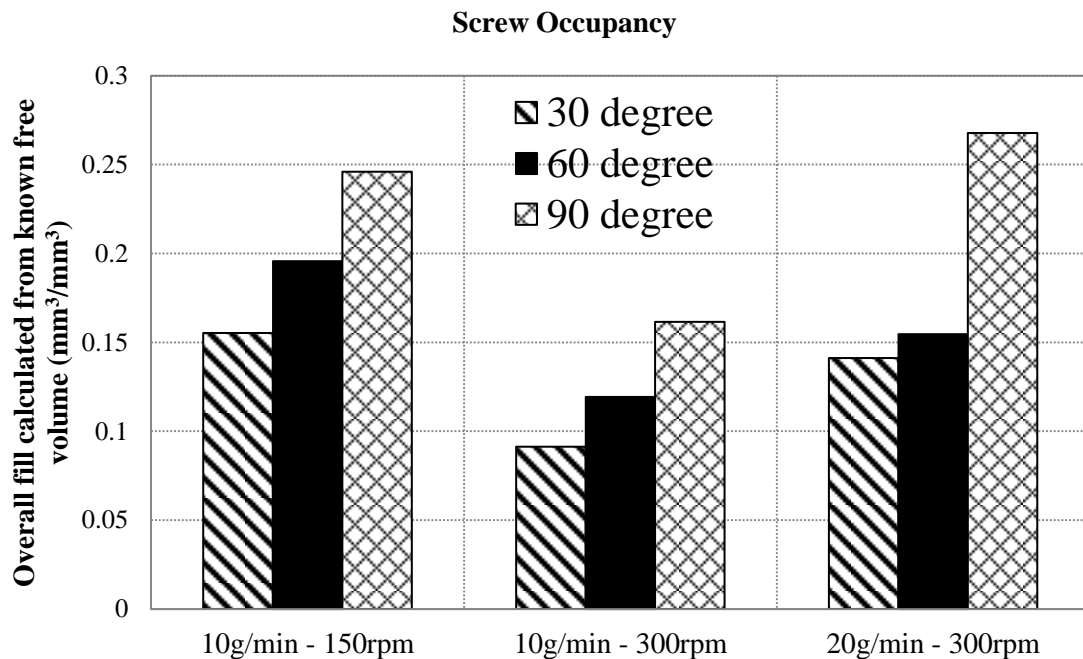


Figure 5-19: Overall occupancy of the granulator for various screw geometry at different process parameters

The overall fill fraction of the granulator was calculated using *Eq 5-11* based on the overall residence time and feedrate by assuming that the process was in steady state and the density of material in the granulator was constant throughout the barrel. It is assumed that the density of the material is similar to the material in the output stream with a value of  $0.39 \text{ gcm}^{-3}$ . As shown in Figure 5-19, due to the decreases in conveying capacity in the mixing zones, the overall fill fraction of the granulator increases when the kneading disc arrangement angle is increased from  $30^\circ$  to  $60^\circ$  and to  $90^\circ$ . This is because when the powder feedrate is kept constant, increases in screw speed will lead to a faster axial speed (pitch speed) that result in

less material is being caught by the pitch of the screw to give a lower fill level. On the other hand, when the powder feedrate increases, the overall fill fraction increases. Since the axial rotation of the screws is unchanged, the only way to convey materials that match the powder feedrate (to increase the flow rate) is to increase the fill of the screw pitches.

#### **5.4.6 Fill fraction along the TSE granulator**

One of the advantages in using PEPT techniques in this study is that it can magnify a small section of the granulator and study that particular area in detail.

Figure 5-20 shows an example of the residence time of a small section with a length equivalent to the width of a single kneading element (4.75 mm) along the granulator. Each column (along the x-axis) represents one element and the red circle in each column is a single pass residence time of that individual element. The mean residence time is obtained by taking the average value of the 100 residence times and is plotted in solid black circles. As can be seen the mixing zones have a higher residence time and wider distribution compare to the conveying zones.

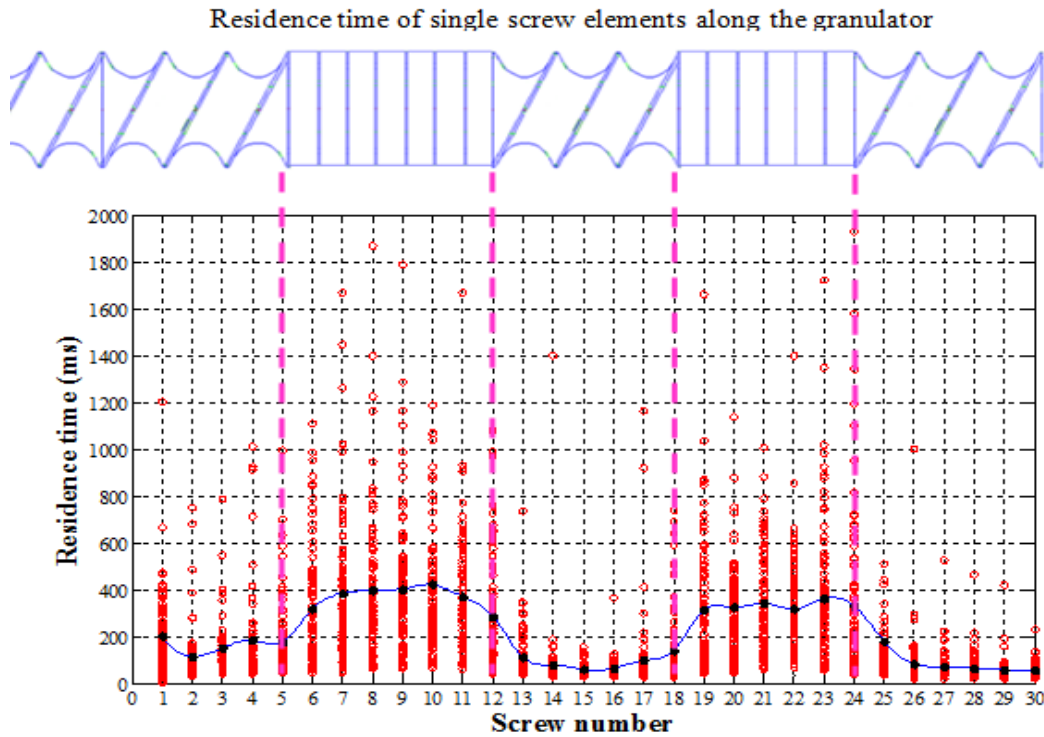


Figure 5-20: Calculated experiment data showing material occupancy of the granulator in different sections

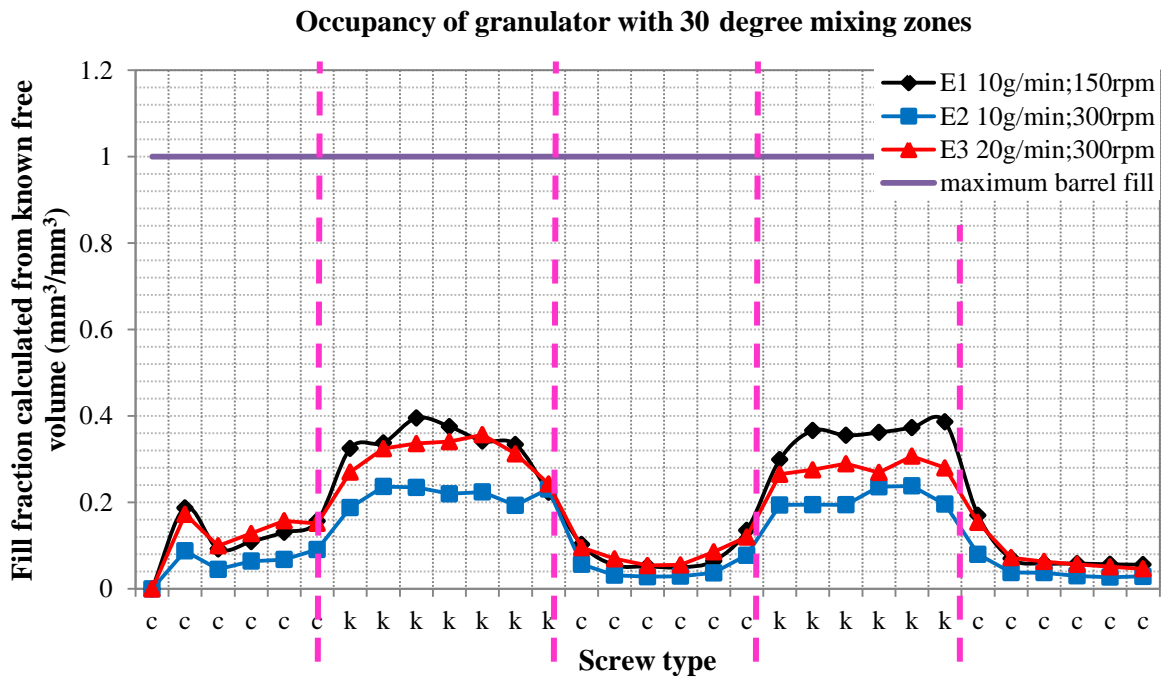


Figure 5-21: Occupancy of granulator with 30 degree mixing zones

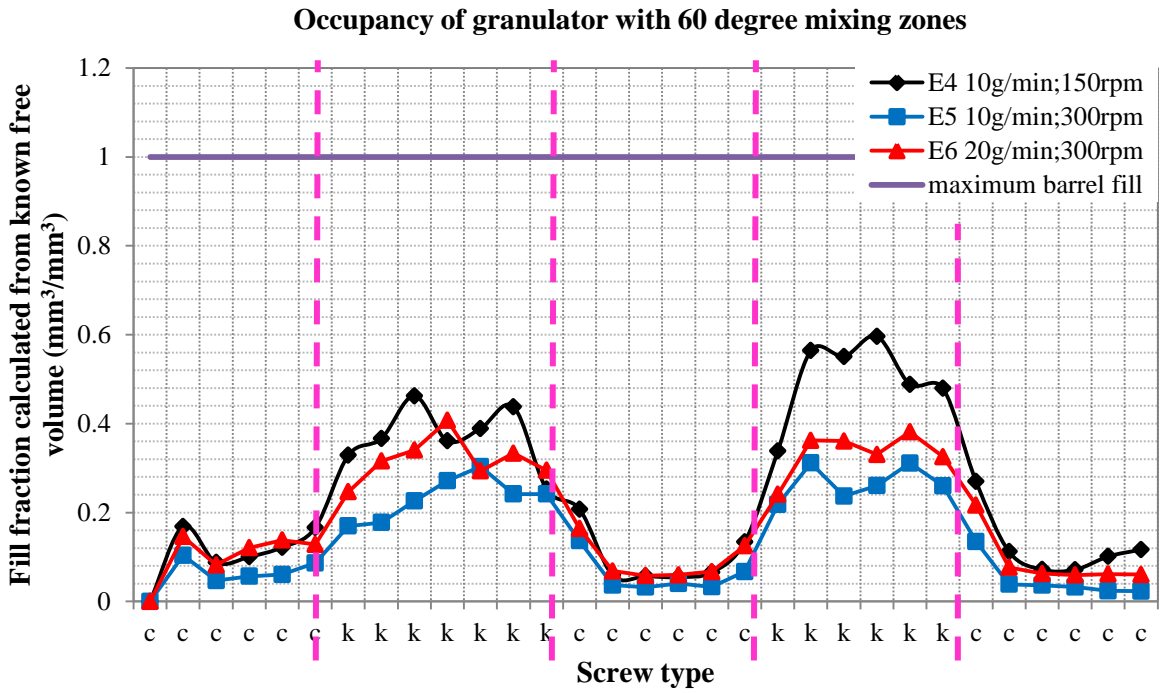


Figure 5-22: Occupancy of granulator with 60 degree mixing zones

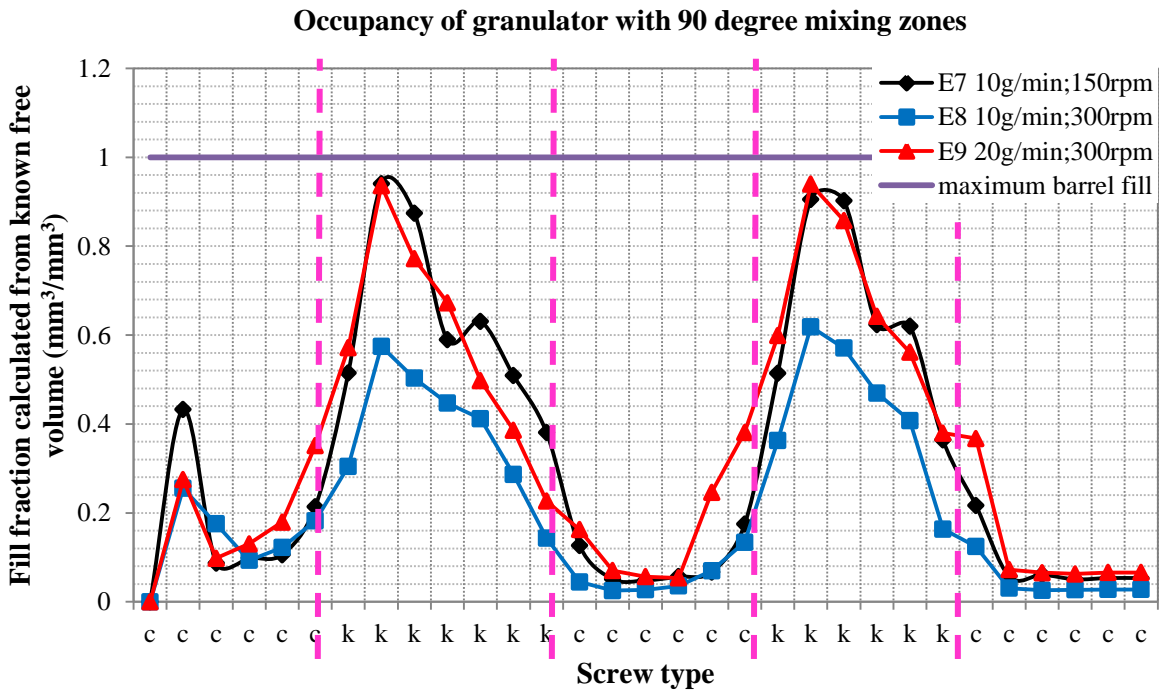


Figure 5-23: Occupancy of granulator with 90 degree mixing zones

Using the residence time calculated in Figure 5-20, the fill level through the granulator for various screw configurations at different screw speed and powder feedrate can be estimated and is shown in Figure 5-21, Figure 5-22 and Figure 5-23. As expected the fill level is high in the mixing zones compared to the conveying zones. For 30° screw configuration, the curves show that the fill level increases slowly and remains steady in the mixing zones. However, 60° screw configuration which has a slightly higher fill level is less steady through the mixing zones. As mentioned previously, a 90° mixing zone has no conveying capacity and therefore might be expected to be fully filled for any process conditions. However, the material flows forward in spite of the lack of conveying capacity. Curves in Figure 5-23 show that the material started to build up and reached a maximum in the second kneading block in the mixing zones creating a fill gradient. Note that the first kneading disc of the mixing zone is arranged 0° to the conveying element (completely open), it allows the material to flow easily into the first kneading disc. Therefore the first kneading disc of the mixing zone is essentially a continuation of the preceding conveying zone. The second kneading disc which is arranged 90° to the first kneading disc is completely closed and this is where the fill level peaks. Since there is no inherent conveying capacity in 90° mixing zone, it is believed that the material still flows through by a dispersive mechanism which is driven by the fill gradient in the mixing zone and the kneading action of the screws. Material in a highly filled level zone will flow into a less filled zone when the screws rotate and squeeze the material in the intermesh and this generates the conveying feature that flow the materials forward. As the powder feedrate increases, the gradient of the fill becomes larger giving a higher driving force to convey materials. This higher driving force will lead to an increase in the conveying capacity and therefore the residence time of the process is proportional to the powder feedrate. The material in 30° and 60° configurations can move forward when the fill level is constant

because the configurations are only partially closed and have conveying capacity by themselves.

When comparing the fill level in the mixing zones for different process conditions, the material occupancy in the granulator decreases when the screw speed increases. For 90° configurations, doubling the initial value of the screw speed and powder mass rate will lead to a similar occupancy to its initial value. This effect is not clearly shown in 30° and 60° configuration particularly in the second mixing zone. Unlike the 90° configuration, the fill level of 30° and 60° is considered low and flat, implying that the conveying capacity drives mainly from the screw elements and not the fill gradient. Also when the mixing zone angle increases the fill level of the granulator will increase. Thus we can conclude that the fill level in the granulator is directly proportional to the material input rate and fill degree and inversely proportional to the screw speed.

#### **5.4.7 Effect of fill level on granule properties**

Porosity and strength are two of the important properties that determine the quality of granule produced. High porosity means fast dissolving or disintegrating granules. Granules with high strength can prevent loss of material from granule breakage during transportation. Generally, the granule strength is inversely proportional to its porosity. The higher the porosity of a granule, the weaker the granule will be (Benali, Gerbaud et al. 2009; Rahmanian, Ghadiri et al. 2009; Mangwandi, Adams et al. 2010). Cartwright and co-workers reported that the strength of the granule increases when there is an increase in powder feedrate and decrease in screw speed. In the present study, it is shown that the fill level of the granulator is proportional to the powder feedrate and inversely proportional to the screw speed. Therefore, it is believed that the porosity of the granule decreases when the occupancy level of the

granulator increases. As the fill level becomes higher, the compaction force increases and more material interlocking occurs producing stronger granules. Also, a 90° mixing zone which has no conveying capacity is never fully filled in this study. Since the material is transported by dispersive mechanisms driven by fill gradient, a fully filled 90° mixing zone means there is no fill gradient and in consequence will cause blockage in the granulator as material could not flow. Moreover, the variation of fill level for various process conditions also indicates the granulator is not fully filled. Mathematically, the free volume per unit length of the granulator is  $0.289 \text{ cm}^3 \text{ mm}^{-1}$ . The maximum mass fill level of  $0.10 \text{ g mm}^{-1}$  would imply a density of  $0.35 \text{ g cm}^{-3}$  if fully filled: this seems very low. The partially filled mixing zone may also signify that material in the granulator was not highly compacted and therefore explains why the extruder produces granules with high porosity and low fracture force compare to those produced by High Shear Mixer (Lee, Ingram et al. 2010). However, more work is needed to further validate these findings for example to determine the work done per unit mass of both techniques and to determine the density of materials along the extruder to establish the fill level of the granulator.

## 5.5 CONCLUSION

PEPT has been shown to be very useful in visualisation of particle motion in a twin screw granulator. The real time trajectory of the particle can be visualised and measured accurately using this technique. The mean residence time of the process decreases when there is an increase in screw speed and material throughput. However the shape of the distribution curves remains similar for various screw geometry and process conditions. It is believed that the extent of axial mixing is similar for different screw geometry. The fill level in the granulator is proportional to powder feedrate and inversely proportional to screw speed. It was also observed that in the material is conveyed through a 90° mixing zone by a dispersion



mechanism driven by the granulator fill gradient. In addition to that, the 30° and 60° mixing configurations can transport material even when there is no fill gradient as they have conveying capacity. For the screw geometry and process conditions studied here the granulator is never fully filled and due to the partially filled condition, the granulator is predicted not to exert a high compaction force which results in weak and porous granules. Future work is needed to validate these findings. In subsequent chapters a model will be fitted to the empirical fill level and the variance reduction ratio will be employed to study the performance of mixing of the granulator.

# **CHAPTER 6 : MODELLING OF RESIDENCE TIME DISTRIBUTION TO INVESTIGATE SOLID MIXING**

---

## **SUMMARY**

In this Chapter, residence time distributions (RTD) of a twin screw granulator were obtained using Positron Emission Particle Tracking (PEPT) for different process conditions and screw configurations as presented in Chapter 5. The RTDs were then modelled using a Tanks-In-Series (T-I-S) model which included a plug flow fraction to fit curves to the experimental data. The variance reduction ratio (VRR) was then introduced to describe the extent of axial mixing and to investigate the ability of the continuous granulator to remove inconsistencies in the ingredients being fed in or fluctuations in the feed rate. The granulator was also divided into several zones and RTDs were obtained for these zones in order to observe the changes of VRR along the granulator.

It was found that the simulation curve of the T-I-S model can fit the experimental RTDs reasonably well. However when a plug flow fraction was considered in the T-I-S model, the simulation curve fits the experimental data better, particularly the initial portion of the curve and describes the overall RTD more accurately. The same observation was noted when these models were used to fit the RTDs of different sections of the granulator.

The parameters, number of tanks ( $n$ ) and plug flow fraction ( $p$ ) were also considered in the present study to obtain some insight into the behaviour of the granulator. The  $n$  calculated from the model with a plug flow fraction is similar for different zones of the granulator and might demonstrate that the extent of axial mixing is independent of the screw geometry. The

plug flow fraction ranges from 0.1 to 0.5 but the value shows no clear relation to the screw geometry or process conditions.

For the VRR analysis, it shows that for a given disturbance frequency, the VRR depends on the RTD and the mean residence time to the period of the fluctuation. In general the fluctuations could be removed when the period of these fluctuations is of the order of the magnitude of the mean residence time or less.

### **6.1 1. INTRODUCTION**

Powder mixing is an important operation and is widely used in the pharmaceutical industry in order to obtain a homogenous product mixture. A traditional batch process is among the most popular techniques to use to obtain desired powder mixtures. However, continuous mixing has been studied in recent years as an efficient alternative technique in high throughput manufacturing (Marikh, Berthiaux et al. 2006). The influences of the operating conditions and geometric design on mixing performance were the main focus of many studies. Modelling of a continuous mixing process has also received significant attention through the application of residence time distribution (RTD) theory (Gao, Muzzio et al. 2011; Gao, Vanarase et al. 2011). Studies have also been carried out using RTD to characterise solid mixing for optimising processes such as rotary drum (Abouzeid, Fuerstenau et al. 1980) and convective mixer (Marikh, Berthiaux et al. 2005; Berthiaux, Marikh et al. 2008; Marikh, Berthiaux et al. 2008; Gao, Vanarase et al. 2011). Besides this, several RTD models were introduced to characterise the experimental RTD curves of different operations, for example, models that link to plug flow reactors and continuous stirred tank reactors with delay and dead volumes (Yeh and Jaw 1999; Ziegler and Aguilar 2003; Kumar, Ganjyal et al. 2008; Gao, Vanarase et al. 2011). Moreover, the degree of mixing was analysed by a few

researchers using the variance reduction ratio through powder density spectrum analysis (Weinekötter and Reh 1995; Ghaderi 2003). The studies on continuous blending of powder were then summarised and reviewed by Pernenkil and Cooney to trace the underlying theory and practice of continuous powder blending providing a foundation for its development (Pernenkil and Cooney 2006).

Positron Emission Particle Tracking (PEPT) was utilised in this study to obtain the RTD of a twin screw granulator and the details of the experiment programme carried out can be seen in Chapter 5. The experimental RTD curves were then modelled using a Tank-In-Series model as well as a model which included the plug flow fraction. The variance reduction ratio was then obtained using the modelled RTD to study the efficiency of the mixing for various process conditions and screw geometries. The granulator was also divided into several sections in order to obtain the residence time distribution of different zones to observe the change in variance reduction along the granulator. In addition, a RTD model and sinusoidal signal were simulated to investigate the influences of the frequency of the signal on the variances reduction ratio achievable by a system.

## **6.2 MATERIALS AND EXPERIMENTAL METHOD**

The materials used and the granulation process were similar to that used in the PEPT study (See Chapter 5). Briefly, a premixed powder mixture with 73.5 %w/w of  $\alpha$ -Lactose Monohydrate, 20 %w/w of Microcrystalline Cellulose, 5 %w/w of hydroxypropyl Cellulose and 1.5 %w/w of croscarmellose sodium was continuously fed using a screw feeder into the twin screw granulator which was running at steady speed. After the screw barrel was filled by the powder mixture (ie powder was being discharged at a steady rate), granulation liquid (distilled water) was injected into the barrel with a peristaltic pump. The granulation process

was run for 15 minutes before a fresh radioactive tracer was introduced into the granulator through the feeding zone. After passing through the granulator, the radioactive tracer which is embedded in a granule was recovered from the outlet stream and recycled back into the granulator as a new pass. The residence time distribution was then obtained from the 100 pass experiment for various process conditions and screw geometries using Eq 5-1 in Chapter 5.

## 6.3 RESULTS AND DISCUSSION

### 6.3.1 Modelling of residence time distribution

RTD is the fundamental theory which can characterise mixing in a reactor. The concept was used extensively after Prof. P.V. Danckwerts expressed the importance of RTD by defining most of the distributions of interests (Danckwerts 1953; Fogler 2006). The RTD is normally determined by pulse injection of an inert tracer into a steady state system and by measuring the concentration of the tracer in the effluent stream as a function of time,  $C(t)$ . The quantitative spread of time that different tracers spend in the system is then expressed as residence time distribution function,  $e(t)$ . The detailed theories of residence time distribution including residence time function, variances and Peclet number were discussed in Chapter 5.

In order to precisely predict the mixing of the granulator, a smooth RTD curve is desirable and therefore modelling of RTD is required. For a non-ideal reactor, the models used for RTD modelling generally consists of combinations of plug flow, continuous stirred tank and dead space in the configuration to closely represent the flow pattern of a reactor. In the present study, two models were chosen to model the RTD of the twin screw granulator: the Tank-In-Series (T-I-S) model (Levenspiel 1972) without and with a plug flow fraction (Kumar, Ganjyal et al. 2008).

The number of tanks,  $N$ , was estimated using the least sum of squares error (sse). The sum of error between the estimated value and the empirical data was calculated for the  $N$  value ranging from 0 – 50 and the parameter that give the least sum error are selected for the modelling. The coefficient of determination was then calculated using Eq 6-1 in order to see how close the models fit the experimental data (Everitt 2002). The model mean residence time was also calculated using Eq 5-3 – 5-7 to compare with the empirical values. The above procedure was calculated using programming software, MATLAB (The Mathworks Inc., Natick, MA, USA).

$$\text{Coefficient of determination, } R^2 = 1 - \frac{SS_{\text{error}}}{SS_{\text{total}}} \quad \dots \text{Eq. 6-1}$$

Where  $SS_{\text{error}}$  is the residual sum of square and  $SS_{\text{total}}$  is the total sum of squares as expressed in Eq 6-2 and Eq 6-3.

$$SS_{\text{error}} = \sum_i [f(x_i) - g(x_i)]^2 \quad \dots \text{Eq. 6-2}$$

$$SS_{\text{total}} = \sum_i [f(x_i) - \overline{f(\mathbf{x})}]^2 \quad \dots \text{Eq. 6-3}$$

Where  $f(x_i)$  is the data obtained from experiment;  $g(x_i)$  is the data estimated from models and  $\overline{f(\mathbf{x})}$  is the average value of empirical data.

### 6.3.2 Parameters estimated using Tank-in-series (T-I-S) models

The T-I-S model is described as a process consisting of a series of equal size well mixed reactors. It can be used to describe the axial mixing of the bulk material stream under a non-ideal mixing condition. The degree of mixing is represented by the number of well mixed

tanks. The flow is considered in perfect (axial) mixing condition when the number of tanks-in-series is unity and there is no mixing when the number of stirred tanks reaches infinity. The mathematical equation of the T-I-S model is expressed as in Eq 6-4 (Levenspiel 1972),

$$e(\theta) = \frac{n(n\theta)^{n-1}}{(n-1)!} \exp(-n\theta) \quad \dots \text{Eq. 6-4}$$

Where  $n$  is the number of tanks and  $\theta = t/t_m$ ,  $t$  is time and  $t_m$  is mean residence time.

Table 6-1: Parameters estimated using T-I-S Model

Experiment number	Process Conditions			Experimental	T-I-S Model		
	Screw config	Feed rate (g/min)	Screw speed (rpm)	MRT	MRT	n	R <sup>2</sup>
E1	30	10	150	15.46	15.46	17	0.87
E2		10	300	8.74	8.74	14	0.93
E3		20	300	6.76	6.76	19	0.94
E4	60	10	150	19.94	19.94	12	0.89
E5		10	300	11.27	11.27	5	0.85
E6		20	300	7.45	7.44	14	0.94
E7	90	10	150	24.90	24.80	13	0.81
E8		10	300	15.57	15.57	15	0.82
E9		20	300	12.59	12.59	18	0.91

The parameters estimated using the least sum square error by fitting the TIS model to the experimental RTD is shown in Table 6-1. For most of the screw configurations and process conditions, the coefficient of determination,  $R^2$ , is considered high ( $R^2 > 0.80$ ), and indicates that the model fits the empirical data well (See Figure 6-1). Besides this, the mean residence time estimated using the model matches the empirical values.

The  $n$  was found to have a high value, ranging from 12 to 19. The exceptionally low  $n$  for experiment E5 is possibly due to the fact that the particle became stuck more frequently than

other experiments and which gave rise to a much larger tail in the RTD that result in more apparent axial mixing. It was reported that  $n$  indicates the degree of mixing (Kumar, Ganjyal et al. 2008). The closer the  $n$  value to unity, the higher the degree of mixing, and vice-versa. The parameter  $n$  might be considered high in present study indicating that axial mixing in the twin screw granulator less than ideal. In other words, the high number of tanks might suggest that the material in the twin screw granulator has plug flow behaviour and is not desirable for mixing.



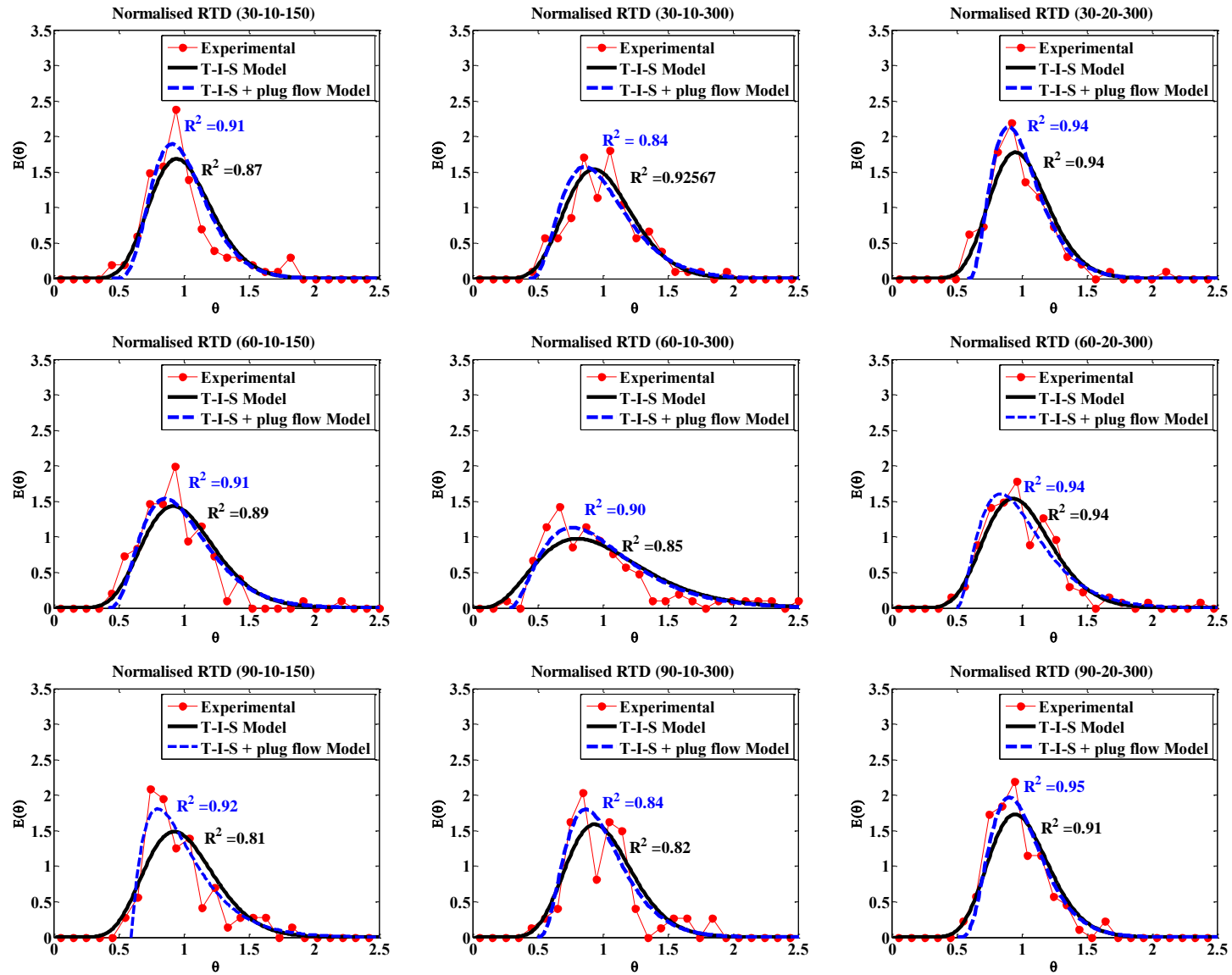


Figure 6-1: Predicted RTD by Tank-In-Series and Complete model; (30-10-150 means geometry = 30°; feedrate = 10 g/min; screw speed = 150 rpm)

### 6.3.3 T-I-S with plug flow model

The T-I-S model with a plug flow model was developed by modifying the Tank-In-Series model to include the plug flow fraction in the reactor (Levenspiel 1972). The comparison of the T-I-S model with and without a plug flow fraction can be used to investigate qualitatively the deviations of the twin screw granulator from the ideals of plug and mixed flow which in this case are used to identify the existence of a plug flow regime. This regime is not desirable in continuous processing as the existence of plug flow indicates poor axial mixing in the granulator. Figure 6-2 shows a schematic diagram of a plug flow fraction in a series of continuous stirred tank reactors. The model can be described by Eq 6-5 – 6-7.

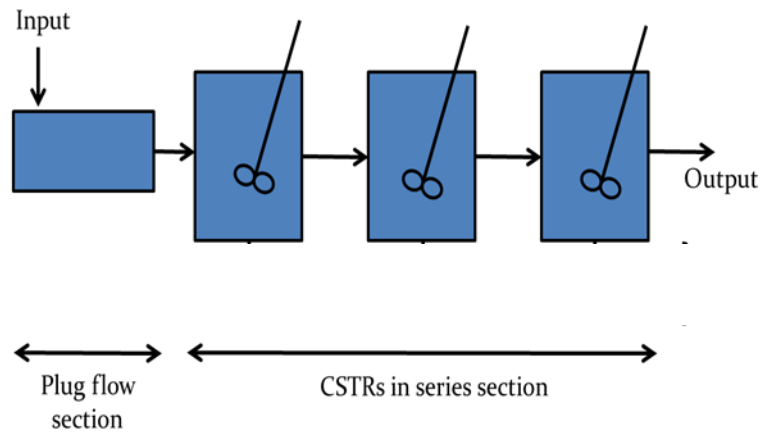


Figure 6-2: schematic diagram of plug flow fraction in a series of continuous stirred tank reactors having a dead volume fraction

$$e(\theta) = \frac{b[b(\theta - p)]^{n-1}}{(n-1)!} \exp[-b(\theta - p)] \quad \dots \text{Eq. 6-5}$$

Where

$$b = \frac{n}{(1-p)} \quad \dots \text{Eq. 6-6}$$

$$p = \frac{t_{\min}}{t_m} \quad \dots \text{Eq. 6-7}$$

Where  $p$  is the plug flow fraction,  $n$  is the number of tanks and  $t_{\min}$  is the smallest residence from the 100 passes and  $t_m$  is the mean residence time.

Table 6-2: Parameters estimated using T-I-S model with a plug flow fraction

Process Condition			Experimental	T-I-S Model with plug flow			
Screw config	Feed rate (g/min)	Screw speed (rpm)	MRT	MRT	n	p	R <sup>2</sup>
30	10	150	15.46	15.46	6	0.44	0.91
	10	300	8.74	8.84	4	0.43	0.84
	20	300	6.76	6.78	4	0.58	0.94
60	10	150	19.94	19.92	4	0.42	0.91
	10	300	11.27	11.26	3	0.48	0.90
	20	300	7.45	7.45	3	0.49	0.94
90	10	150	24.90	23.72	2	0.59	0.92
	10	300	15.57	15.56	4	0.49	0.84
	20	300	12.59	12.59	5	0.50	0.95

By introducing a plug flow,  $p$ , into the T-I-S model, the  $R^2$  values of some of the experiments increase slightly. The mean residence time estimated using this model generally matches the experimental values. The parameters estimated for the modelling are recorded in Table 6-2. The  $n$  values are small compared to the T-I-S model without a plug flow fraction and range from 2 – 6. The plug flow fraction,  $p$ , of this study ranged from 0.42 to 0.59. The plug flow in the twin screw granulator might be expected to be originated from the conveying elements as negligible mixing is expected there (Kumar, Ganjyal et al. 2008). So, by removing the plug flow driven by the conveying zones, the mixing zones of the granulator are expected to be able to achieve a high degree of mixing as highlighted by (Kumar, Ganjyal et al. 2008). In order to study the contribution of the conveying sections in plug flow regime of

the granulator, the granulator is divided into different sections and the residence time distribution of each section was calculated and modelled using T-I-S model with and without a plug flow fraction.

### 6.3.4 Residence time distribution of the granulator sections

Table 6-3: Prediction of the parameters of T-I-S model of the conveying and mixing zones (S1 = section 1; C = conveying zone; M = mixing zone)

Process Condition			N					R <sup>2</sup>				
Screw config	Feed rate (g/min)	Screw speed (rpm)	S1	S2	S3	S4	S5	S1	S2	S3	S4	S5
			C	M	C	M	C	C	M	C	M	C
30	10	150	5	6	5	10	3	0.80	0.85	0.78	0.93	0.70
	10	300	5	8	3	5	4	0.79	0.88	0.65	0.72	0.72
	20	300	4	11	6	9	4	0.73	0.88	0.71	0.92	0.66
60	10	150	7	5	3	5	2	0.88	0.86	0.63	0.87	0.69
	10	300	3	4	2	3	2	0.70	0.85	0.57	0.75	0.42
	20	300	5	6	4	7	3	0.75	0.88	0.75	0.89	0.80
90	10	150	7	11	7	7	4	0.88	0.80	0.86	0.84	0.56
	10	300	4	7	4	8	3	0.84	0.90	0.61	0.78	0.62
	20	300	3	9	3	6	4	0.80	0.88	0.79	0.82	0.57

Table 6-4: Total residence time and number of tanks estimated from the summation of granulator sections

Process Conditions			Residence Time (s)		Number of Tanks (n)		
Screw config	Feed rate (g/min)	Screw speed (rpm)	Overall	Sum of sections	Overall	Sum of all sections	Sum of mixing zone
			30	10	150	15.46	14.93
10	300	8.74		8.51	14	25	13
20	300	6.76		6.62	19	24	20
60	10	150	19.94	19.13	12	22	10
	10	300	11.27	11.10	5	14	7
	20	300	7.45	7.23	14	25	13
90	10	150	24.90	24.73	13	36	18
	10	300	15.57	15.37	15	26	15
	20	300	12.59	12.10	18	25	15

The granulator in the present study consists of 3 conveying zones and 2 mixing zones which consist of 6 or 7 kneading discs (See Figure 5-1). Each section has been simulated by T-I-S model and the number of tanks representing each section and the summation of residence times were recorded in Table 6-3 and Table 6-4. In general, the conveying zones

have an  $n$  value lower than the mixing zones for all the process conditions. The summation of the residence time of all the sections in the granulator is underestimated but not by much from the overall calculation. This might be mainly due to experimental error arising from the limitation of PEPT. Also, if the residence time of each apparent tank in each section was the same, it would expect each to contribute the same and be additive. However, the summation of the number of tanks of each section does not match the value when the complete granulator was modelled as a single unit. On the other hand, the summation of the  $n$  value for the mixing zones only is close to the overall value. This might suggest that the modelling of the overall granulator is dominated by the mixing zones because these have larger residence time than the conveying zone. The larger  $n$  value in the mixing zones also suggests that the degree of mixing in the mixing zones is not as good as the conveying zones which are contrary to the literature. This might be due to the experimental error as the figures suggest that the fit to the conveying zone is not so good.

In order to investigate if the plug flow regime exists in each type of screw element, the sections of the granulator were also modelled using the T-I-S model with a plug flow fraction and the  $n$  and  $p$  value are recorded in Table 6-5. Like the overall granulator residence time distribution, the model with a plug flow fraction more comprehensively describes the residence time distribution of smaller sections and fits the entire experimental data better. The  $n$  determined by the complete model has a similar value for both conveying and mixing zones and ranges from 2 to 5. The  $p$  value estimated using this model suggests that the plug flow is attributable not only to conveying zones as all the screw elements have a plug flow fraction ranging from 0.10 - 0.45. Also, the similarity of  $n$  value of different screw elements and geometries might again suggest that the degree of axial mixing of these screw elements and geometries remain unchanged. This observation is in concurrence with the results previously

suggested in Chapter 5 where degree of mixing was investigated using the shape and Peclet number of residence time distributions.

Table 6-5: Prediction of the parameters of complete model of the conveying and mixing zones (S1 = section 1; C = conveying zone; M = mixing zone)

Process Condition			N					p					R <sup>2</sup>				
Screw config	Feed rate (g/min)	Screw speed (rpm)	S1	S2	S3	S4	S5	S1	S2	S3	S4	S5	S1	S2	S3	S4	S5
			C	M	C	M	C	C	M	C	M	C	C	M	C	M	C
<b>30</b>	<b>10</b>	<b>150</b>	2	3	5	5	3	0.33	0.36	0.10	0.27	0.09	0.90	0.87	0.78	0.94	0.71
	<b>10</b>	<b>300</b>	3	4	2	3	3	0.34	0.25	0.35	0.22	0.24	0.87	0.85	0.78	0.65	0.75
	<b>20</b>	<b>300</b>	2	3	2	4	2	0.28	0.42	0.45	0.37	0.40	0.85	0.86	0.84	0.90	0.80
<b>60</b>	<b>10</b>	<b>150</b>	3	2	2	2	2	0.32	0.36	0.35	0.30	0.21	0.91	0.81	0.73	0.88	0.73
	<b>10</b>	<b>300</b>	2	2	2	2	2	0.30	0.28	0.06	0.22	0.04	0.84	0.77	0.61	0.80	0.45
	<b>20</b>	<b>300</b>	3	3	4	3	2	0.33	0.28	0.12	0.29	0.34	0.86	0.90	0.83	0.88	0.84
<b>90</b>	<b>10</b>	<b>150</b>	2	5	4	2	2	0.44	0.40	0.25	0.41	0.27	0.91	0.85	0.82	0.82	0.65
	<b>10</b>	<b>300</b>	2	3	4	2	3	0.31	0.33	0.07	0.44	0.09	0.87	0.88	0.63	0.84	0.62
	<b>20</b>	<b>300</b>	2	3	2	3	5	0.26	0.44	0.22	0.33	0.05	0.84	0.84	0.83	0.83	0.56

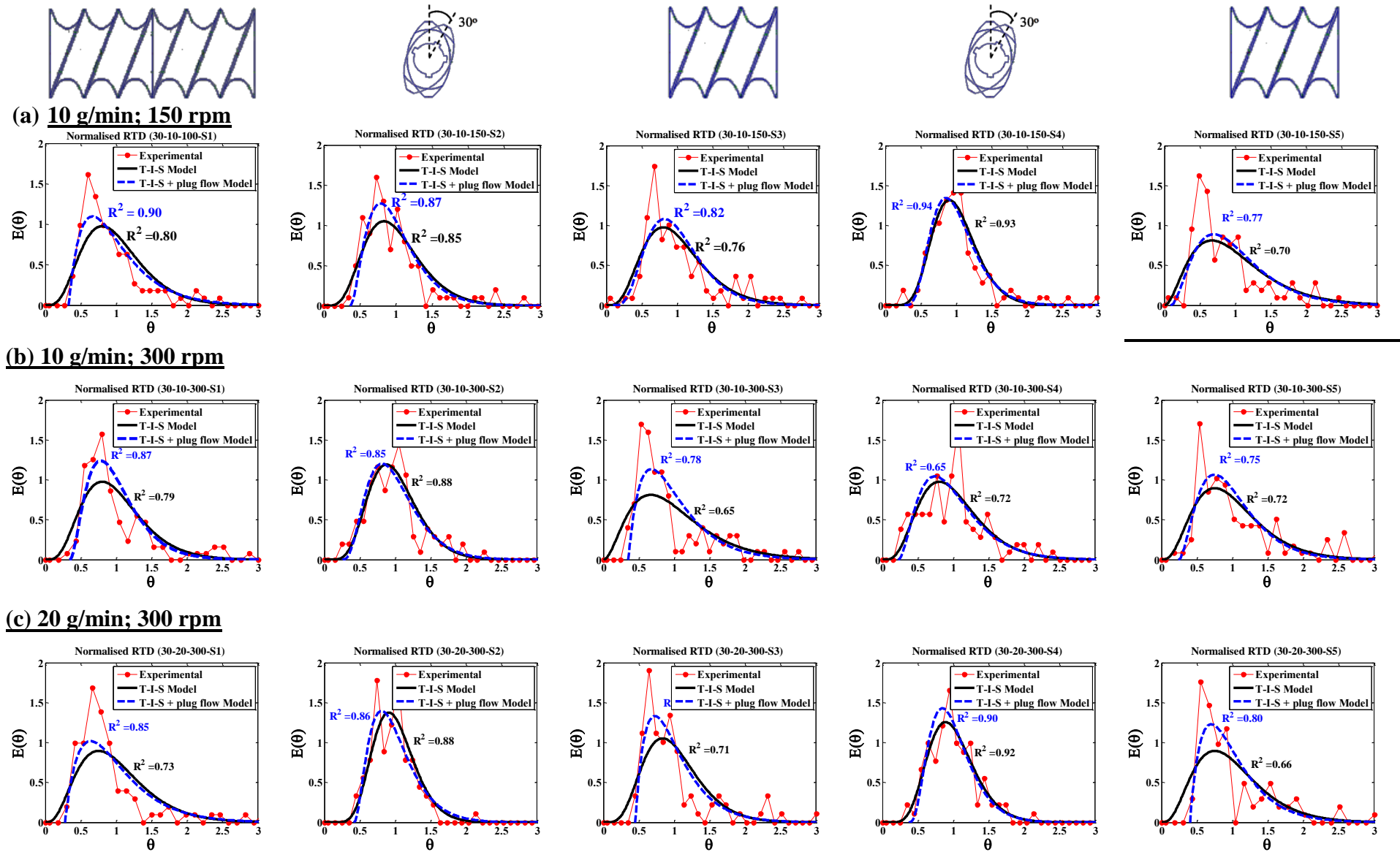


Figure 6-3: T-I-S model and complete model for section RTD for 30° mixing zone



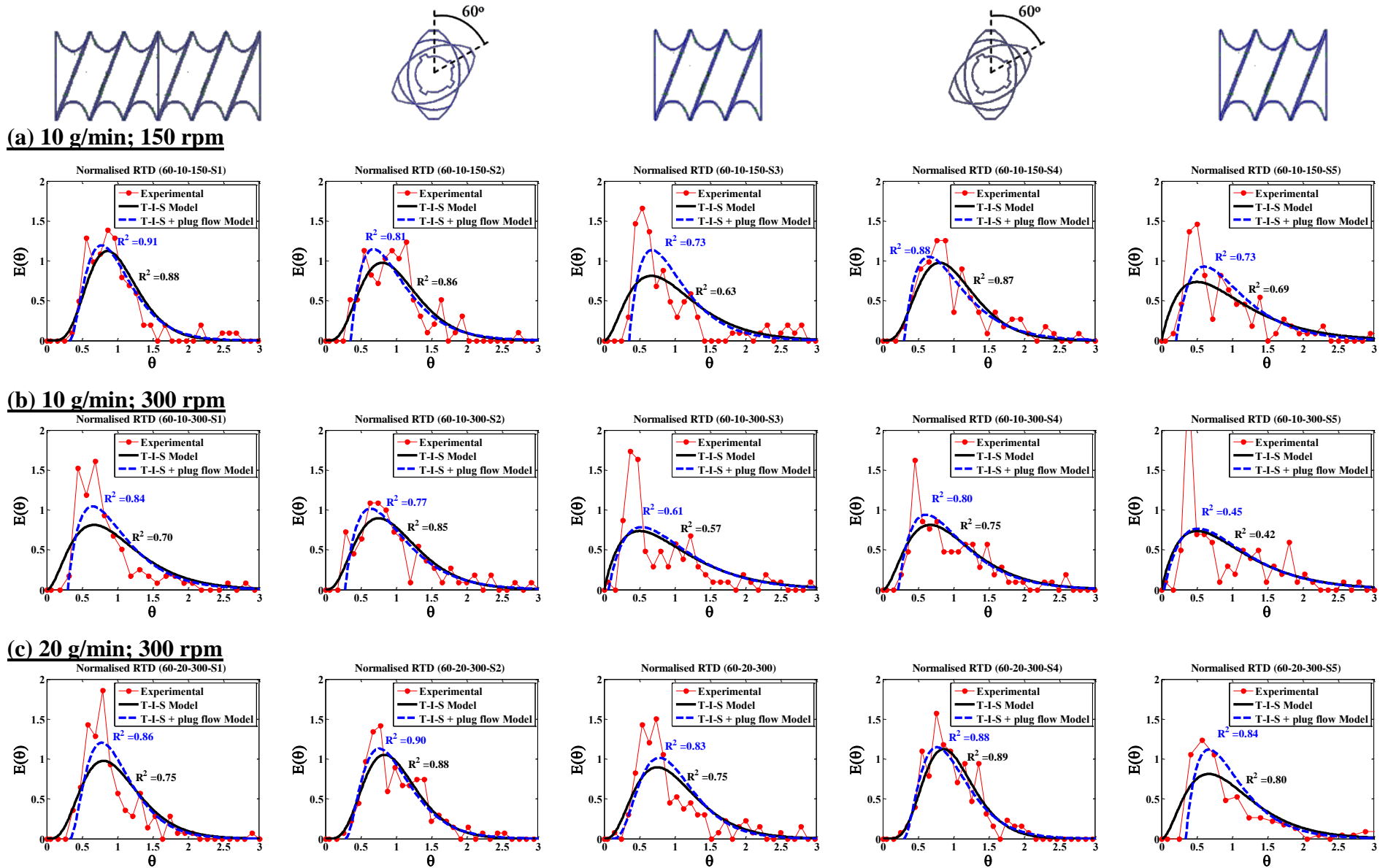


Figure 6-4: T-I-S model and complete model for section RTD for 60° mixing zone

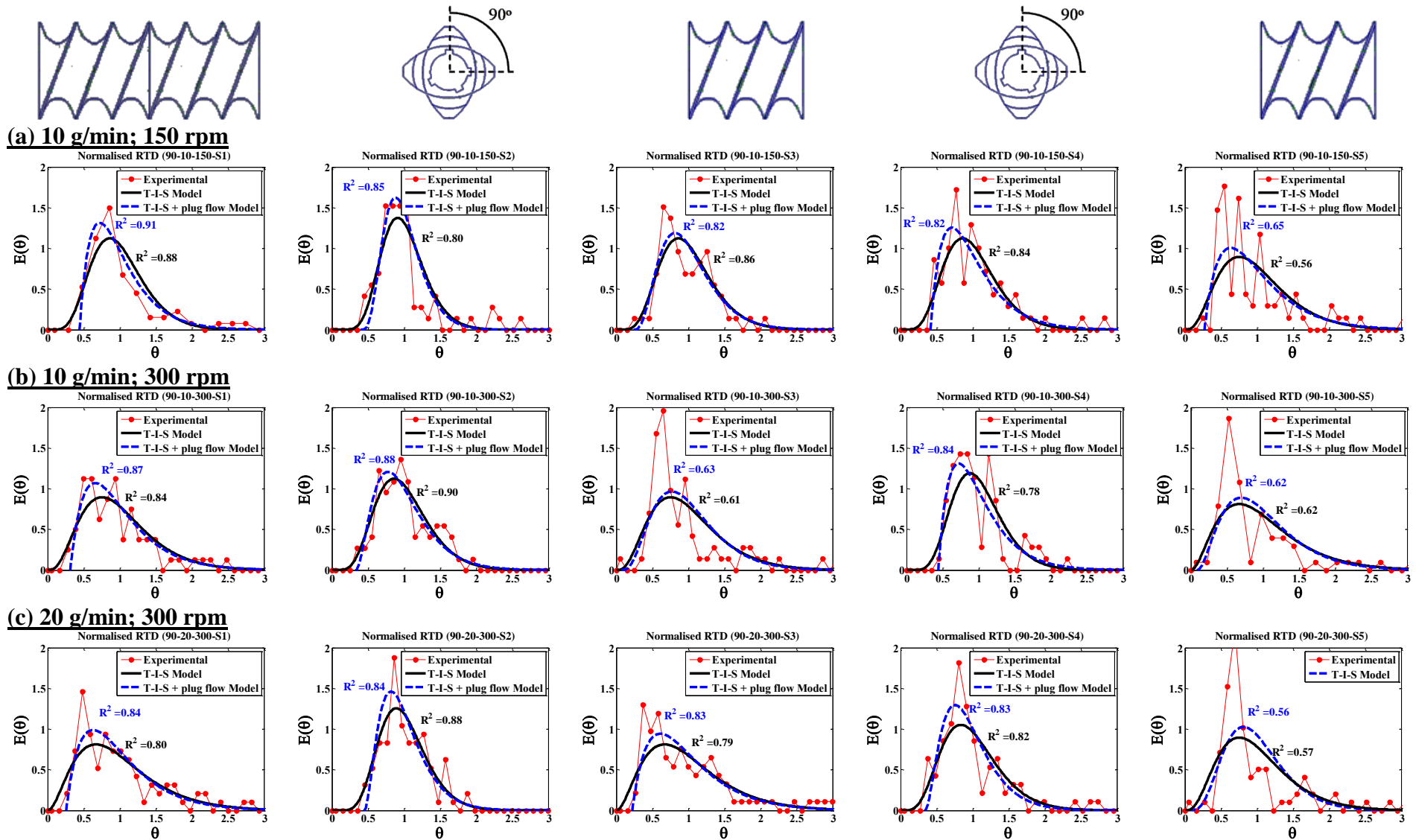


Figure 6-5: T-I-S model and complete model for section RTD for 90° mixing zone

### 6.3.5 Variance reduction ratio for axial mixing in continuous processing

In a continuous mixer, the quality of a mix can be described using the variance of the feed and the products leaving the mixer (Weinekötter and Gericke 2000). Besides the quality of a continuously produced mix, it is also of great interest to know to what extent by axial mixing a continuous mixer can remove inconsistencies in the ingredients being fed or fluctuations in the feedrate (Weinekötter and Gericke 2000). Danckwerts first introduced the term variance reduction ratio (VRR) to describe the extent of solid axial mixing (Danckwerts 1953). The VRR is defined as the ratio of the variance of the input stream,  $\sigma_{in}^2$ , to the variance of the output stream,  $\sigma_{out}^2$ .

$$\mathbf{VRR} = \frac{\sigma_{in}^2}{\sigma_{out}^2} \quad \dots \text{Eq. 6-8}$$

Thus the variance reduction ratio is a comparison of the mix quality at the system inlet and outlet and thereby describes the efficiency of a continuous mixer (Weinekötter and Gericke 2000). Generally VRR describes the quality of mixing by determining the ability of a system to remove the inconsistency or fluctuation in the feeding. In order to investigate the influence of feedrate variability to the output variance, the active ingredient was fed as a minor side stream in terms of feedrate. It is assumed that the bulk feed is in steady state while the side stream fluctuates and the variance of the VRR is therefore determined by the variance of the active ingredient in the feed and the amount it is smoothed by the granulator. The feeder fluctuation is obtained by measuring the feedrate of the feeder using a weighing scale that records the weight as a function of time. The powder was fed continuously onto a balance for about 30 minutes and the temporal feedrate of the feeder was then calculated based on the rate of change of the cumulative weight.

The fluctuation of the outlet stream can be estimated using the Danckwerts convolution integral (Danckwerts 1953),

$$c_{\text{out}}(t) = \int_0^{\infty} c_{\text{in}}(t - \theta) e(\theta) d\theta \quad \dots \text{Eq. 6-9}$$

Where  $E(\theta)$  is the effect of RTD to spread the variability in feed concentration. It is assumed that the variability in the inlet stream does not significantly alter the flow of the materials through the granulator and there is a perfect mixing in the cross section. The prediction of the fluctuation of the outlet stream was studied previously by other researchers and it was validated that the empirical outlet stream oscillations match the predicted value using Danckwert's equation (Danckwerts 1953). A more detailed and complex relationship can be found in the following research articles (Williams and Rahman 1972; Williams and Rahman 1972; Williams and Richardson 1982; Williams and Richardson 1983; Danckwerts 1995; Weinekötter and Gericke 2000; Gao, Muzzio et al. 2011; Gao, Vanarase et al. 2011).

Eq 6-9 shows that the output stream fluctuation and the VRR depend on the period of the input stream relative to the system residence time distribution. Therefore, in this section, the influence of the frequency (1/period) of the input stream on the VRR was explored. The residence time distribution was simulated using the Tank-in-Series model with various numbers of tanks and the ability of the system to remove sinusoidal signal was determined.

Figure 6-6 is the model residence time distribution of 21 tanks in series. When a sinusoidal input stream with a period double the mean residence time (Figure 6-7) was passed through the system, the system is not able to dampen the oscillation resulting in the output stream having a similar pattern and amplitude to the input stream. When the sinusoidal input has a period equal to mean residence time (Figure 6-8), the magnitude of the noise is reduced. The

pattern of the output stream remains similar to the input stream and the fluctuation remains significant. However, when the input stream is with the period half the mean residence time (Figure 6-9) the oscillation of the stream is well damped and the output stream was smooth and with a much lower amplitude. An input stream which consists of both low and high frequency signal was also studied using the similar system and the outcome shows that only the high frequency signal is removed by the system whilst the low frequency signal remains in the stream (see Figure 6-10).

### 6.3.6 Influences of input stream fluctuation frequency on variance reduction ratio

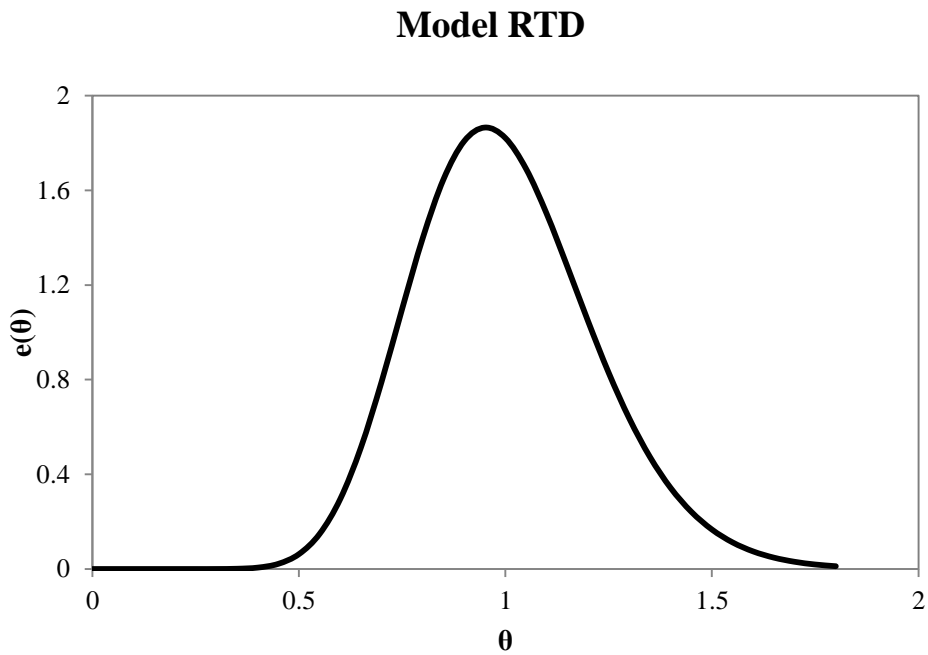


Figure 6-6: Model residence time distribution using 21 Tank-In-Series

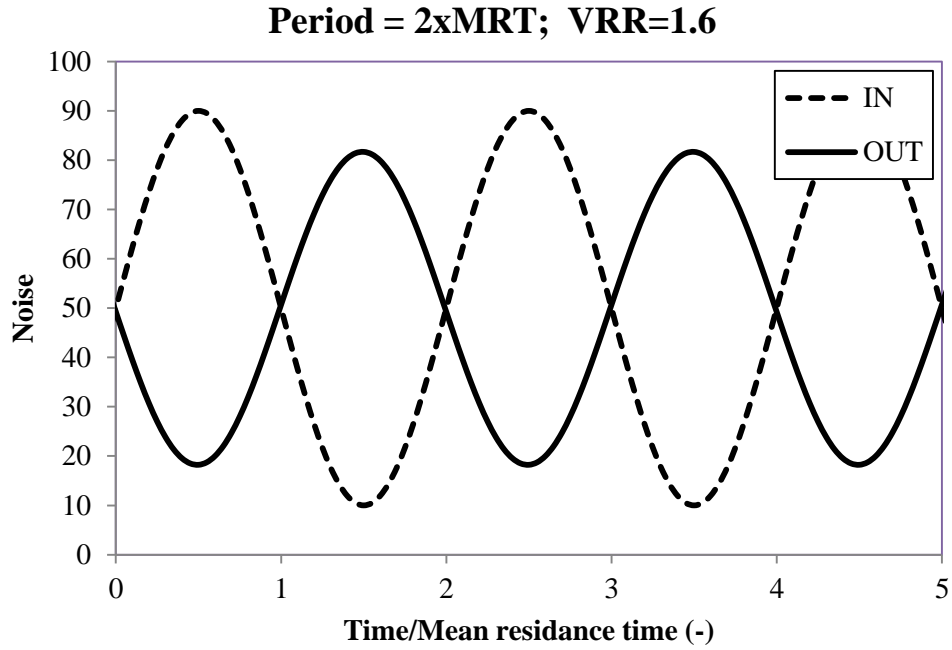


Figure 6-7: Variance reduction ratio achieved by system with RTD in Figure 6-6 with the period of noise is twice the mean residence time

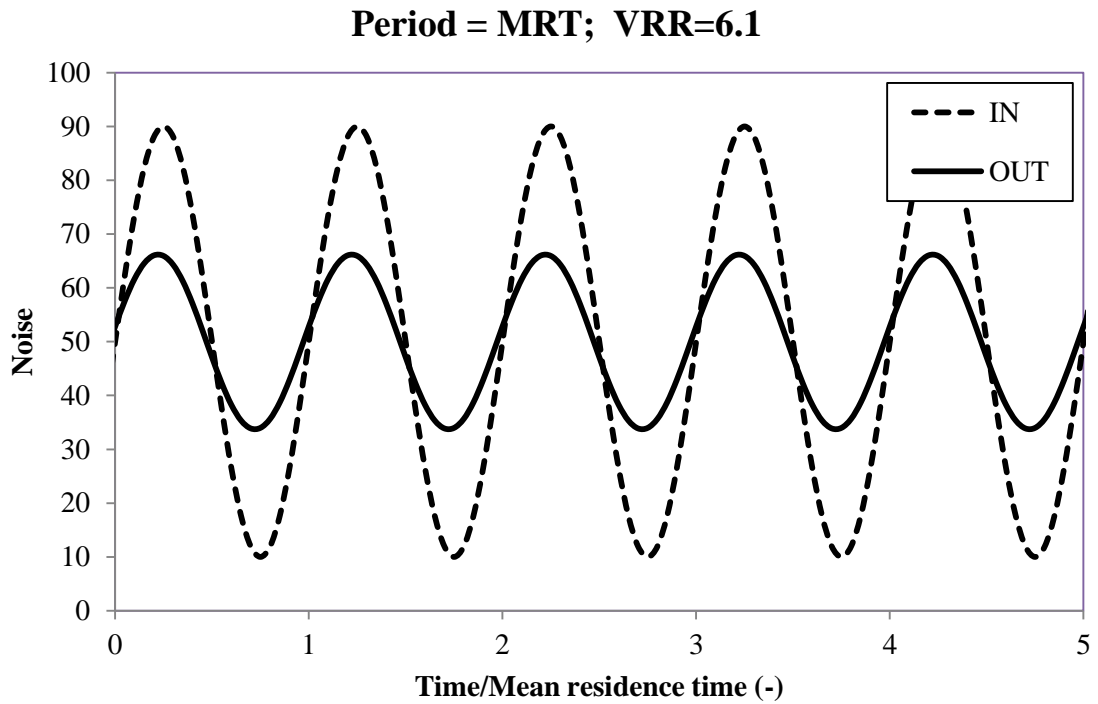


Figure 6-8: Variance reduction ratio achieved by system with RTD in Figure 6-6 with the period of noise is equal to the mean residence time

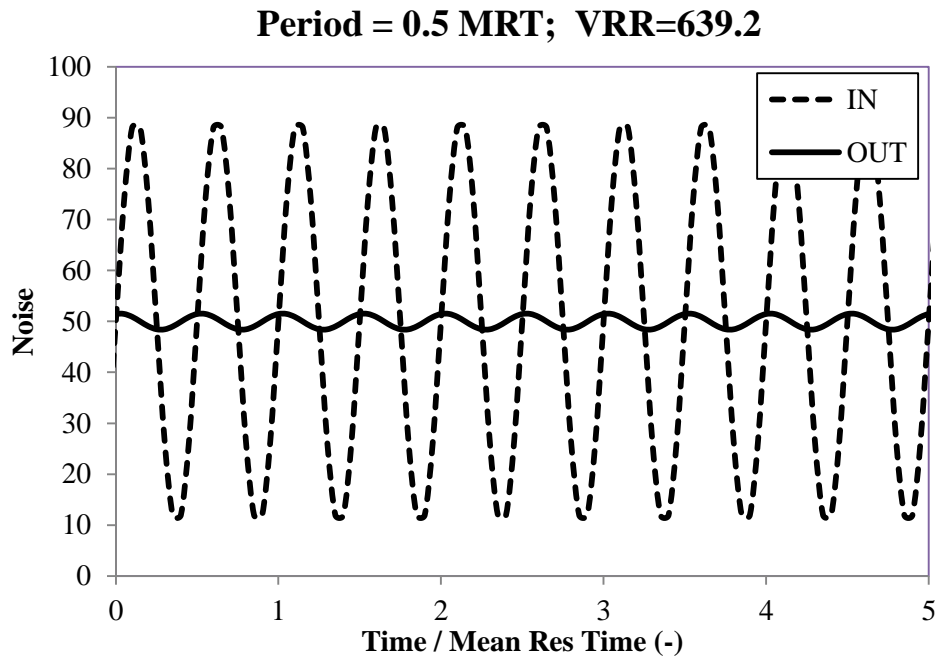


Figure 6-9: Variance reduction ratio achieved by system with RTD in Figure 6-6 with the period of noise is half of the mean residence time

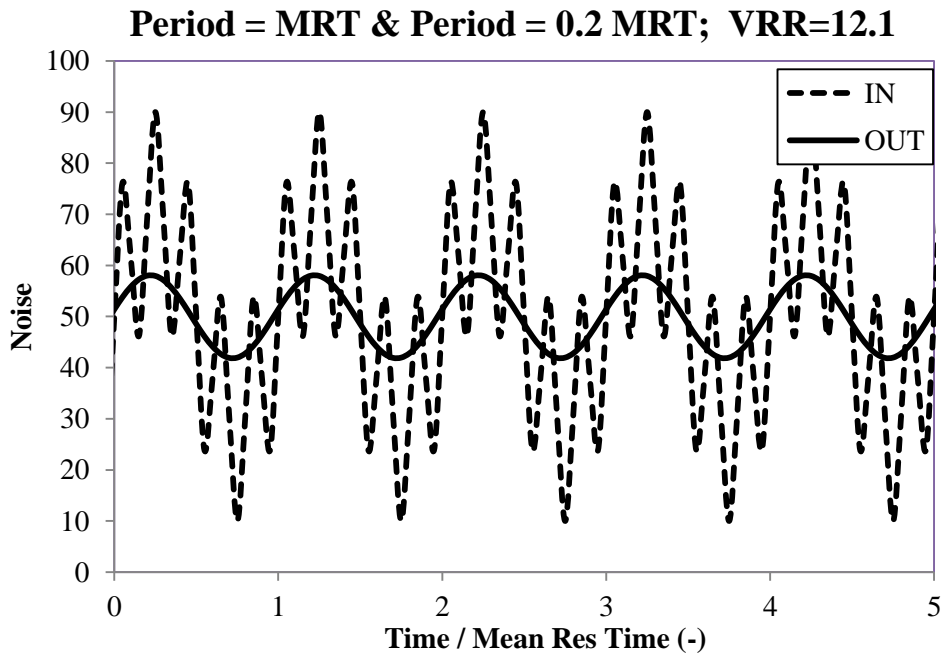


Figure 6-10: Variance reduction ratio achieved by system with RTD in Figure 6-6 with both low and high frequency noise

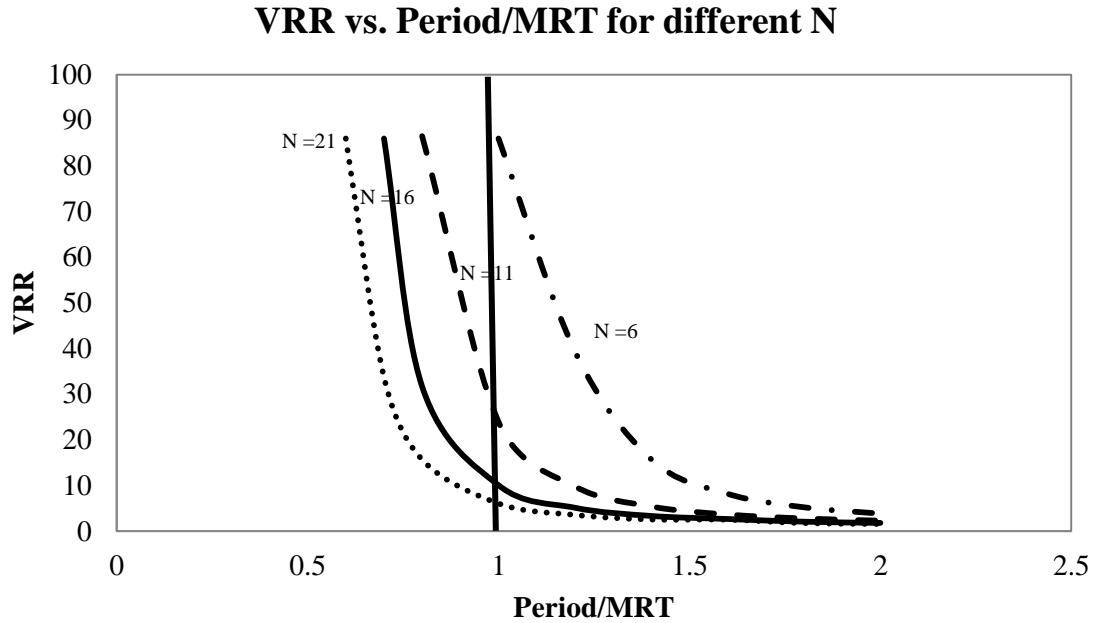


Figure 6-11: Effects of input signal frequency on VRR for different N

Figure 6-11 is the plot showing the relationship of VRR to the ratio of noise period to the mean residence time (period/MRT) for various RTDs (modelled as tanks in series). It is clearly shown that the VRR decreases exponentially with the period/MRT. In general, a system is expected to be able to achieve a high VRR if the input stream has a period smaller than the mean residence time. Also, the plots show that a system with fewer reactors is able to achieve high VRR even when the input stream frequency is low. This is because a system with low N is closer to an ideal mixer and an increase in N indicates that a system is more plug flow like. Therefore, the ability of a system to damp the input fluctuations to achieve a high VRR is strongly determined by the ratio of the feed fluctuation cycle to the mean residence time of the system.

### 6.3.7 Variance Reduction Ratio achievable by the granulator

Figure 6-12 (a) – (e) shows the mass flowrate fluctuation of the input stream and the stream along the twin screw granulation running at 300 rpm with powder feedrate of 10 g/min. It is shown that the fluctuation of the input stream remains significant and the variance



reduction achievable after the first conveying section is low at 3.21 (see Table 6-6). The fluctuation is then dampened dramatically after the first mixing zone and the variance of the stream is reduced by a factor of 10. The variance reduction ratio increases slightly after another conveying zone, and reaches a value of 73.85 in second mixing zone before coming out the granulator at a total value of 74.34. As highlighted previously, the capacity of a granulator to dampen the input fluctuation is sensitive to the ratio of input stream period to the mean residence time. The fluctuation of the stream is smoothed out barely in the conveying zones because the residence times in these sections are short. On the other hand, the mixing zones of the granulator have higher residence times, therefore the reduction of the stream variance is more prominent. It is also noticeable that the damping of the stream fluctuation after the first mixing zone becomes less significant. This is not surprising because as highlighted previously, the granulator ability to dampen the fluctuation is determined by the ratio of the fluctuation period to the mean residence time. Since the first mixing zone removed the short period fluctuations, the remaining long period noise will hardly be dampened by the remaining sections as the period is approximately equal to the mean residence time. The variance reduction ratios achievable by different process conditions are summarised in Table 6-6.

Table 6-6: Variance reduction ratio achievable by the granulator for various conditions

Process Condition			Cumulative Variance Reduction Ratio				
Screw config	Feed rate (g/min)	Screw speed (rpm)	Section 1 Conveying	Section 2 Mixing	Section 3 Conveying	Section 4 Mixing	Section 5 Conveying
30°	10	150	2.29	46.79	66.13	90.33	92.28
	10	300	3.21	34.92	39.75	73.85	74.34
	20	300	3.08	13.69	14.95	22.22	28.54
60°	10	150	1.33	69.78	70.08	115.53	119.89
	10	300	2.49	44.35	68.54	88.22	102.21
	20	300	5.00	16.79	18.83	41.55	53.51
90°	10	150	1.32	89.21	94.49	128.08	128.62
	10	300	1.82	71.57	72.45	95.20	100.46
	20	300	1.99	35.91	54.93	78.57	83.64

As shown in Table 6-6, the variance reduction ratios achievable in the conveying zone are always lower than the mixing zones of the granulator as the residence time is short for any process conditions. It is also observed in Table 6-6 that the final variance reduction ratio achieved by the granulator decreases when the screw speed and powder feedrate increases. This is because the mean residence time decreases when there is an increase in screw speed and powder feedrate. An increase in the granulator screw speed will lead to a higher axial speed (pitch speed) and therefore increase the conveying rate that reduces the time the materials spent in the granulator. Moreover, a higher powder feedrate will result in a greater gradient in the granulator causing more materials pushing forward creating some extra conveying capacity. The increase in transport rate then shortens the mean residence time causing the granulator's ability to dampen the feeder fluctuations to decrease. On the other hand, an increase in the angle of arrangement of the mixing zones will decrease the conveying capacity, generating more material hold up and therefore giving a higher mean residence time with a broader distribution. This will decrease the ratio of the period of input stream to the mean residence time and therefore increase the capacity of the granulator to dampen input fluctuations.

#### **6.4 CONCLUSION**

Residence time distribution of a twin screw granulator can be modelled using the continuous tanks in series model. The model however describes the tail portion of the curve but the initial portion of the curve does not fit the experimental RTD curve. With modifications of the T-I-S model to include the plug flow fraction, it improves the prediction of the RTD curve and describes the overall experimental data better.

The parameter obtained from the T-I-S model shows that the granulator can be modelled as 5 – 19 continuous stirred tank reactors and this indicates that it is partially plug flow. With

plug flow component included, the granulator was described as a 2 - 5 continuous stirred tanks with a plug flow fraction of approximate 50%. These parameters obtained by both models do not change significantly for different screw configurations and this indicates that the extent of axial mixing of the granulator is similar for different screw configurations.

The T-I-S model with and without plug flow fraction were also used to predict the RTD of the conveying and mixing zones of the granulator. Parameters predicted by the T-I-S model show that the conveying zones of the granulator were modelled as low number of tanks. On the other hand, the prediction using the model with a plug flow fraction indicates that the degree of axial missing of both the conveying and mixing zones is similar and it is in agreement with the previous findings using Peclet number (see Chapter 5).

VRR is another approach used to characterise the axial mixing in the twin screw granulator and it measures the ability to remove the inconsistency in the feeding. VRR is strongly influenced by the ratio of the feed fluctuation cycle to the mean residence time of a system. The VRR achievable in the conveying zone is lower than the mixing zones of the granulator. Generally all the process conditions and the screw configurations used in the present study manage to smear the feed fluctuation to give high VRR. Generally low feedrate, low screw speed and mixing zones arranged in higher angle can smooth the input fluctuation more efficiently.

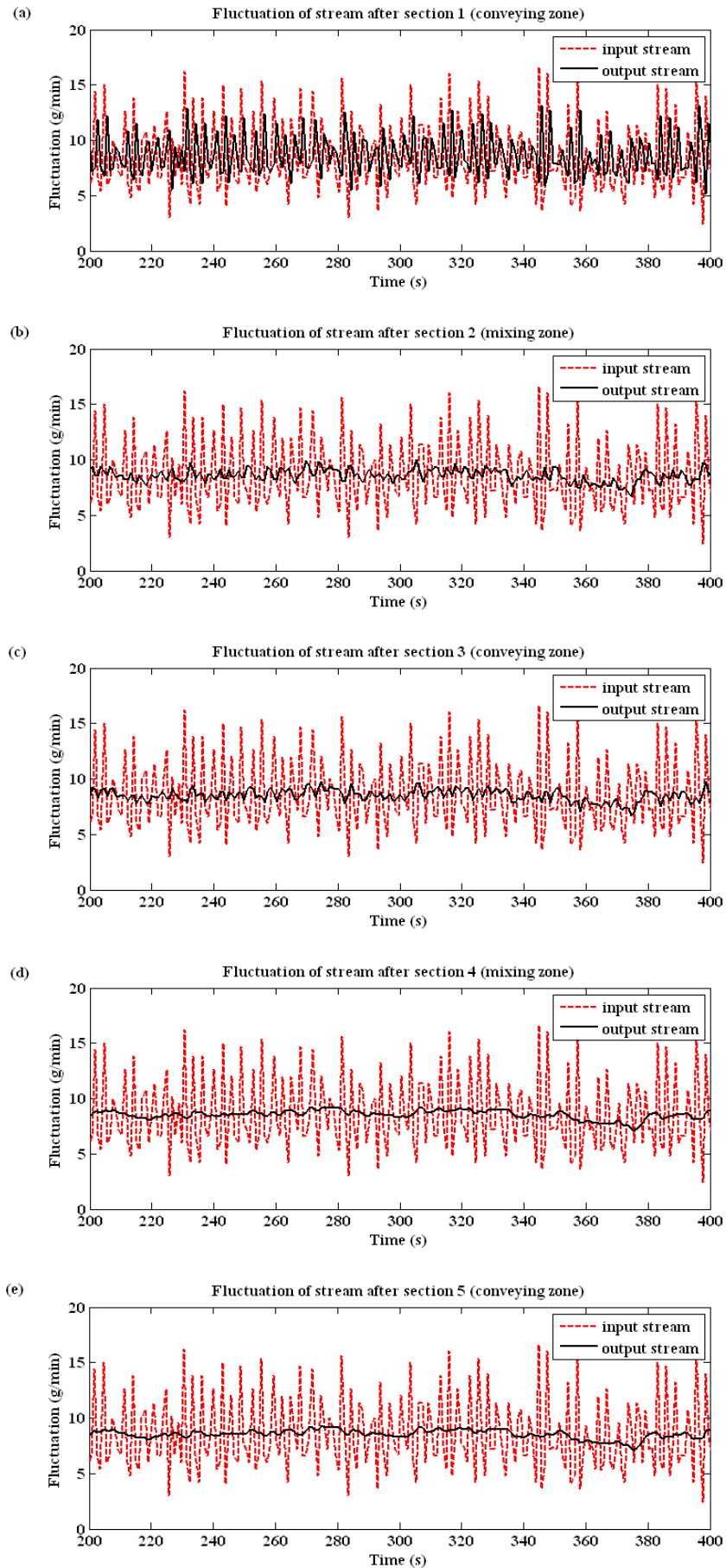


Figure 6-12: Mass flowrate fluctuation along the granulator. (30° mixing zone; 10 g/min; 300 rpm)

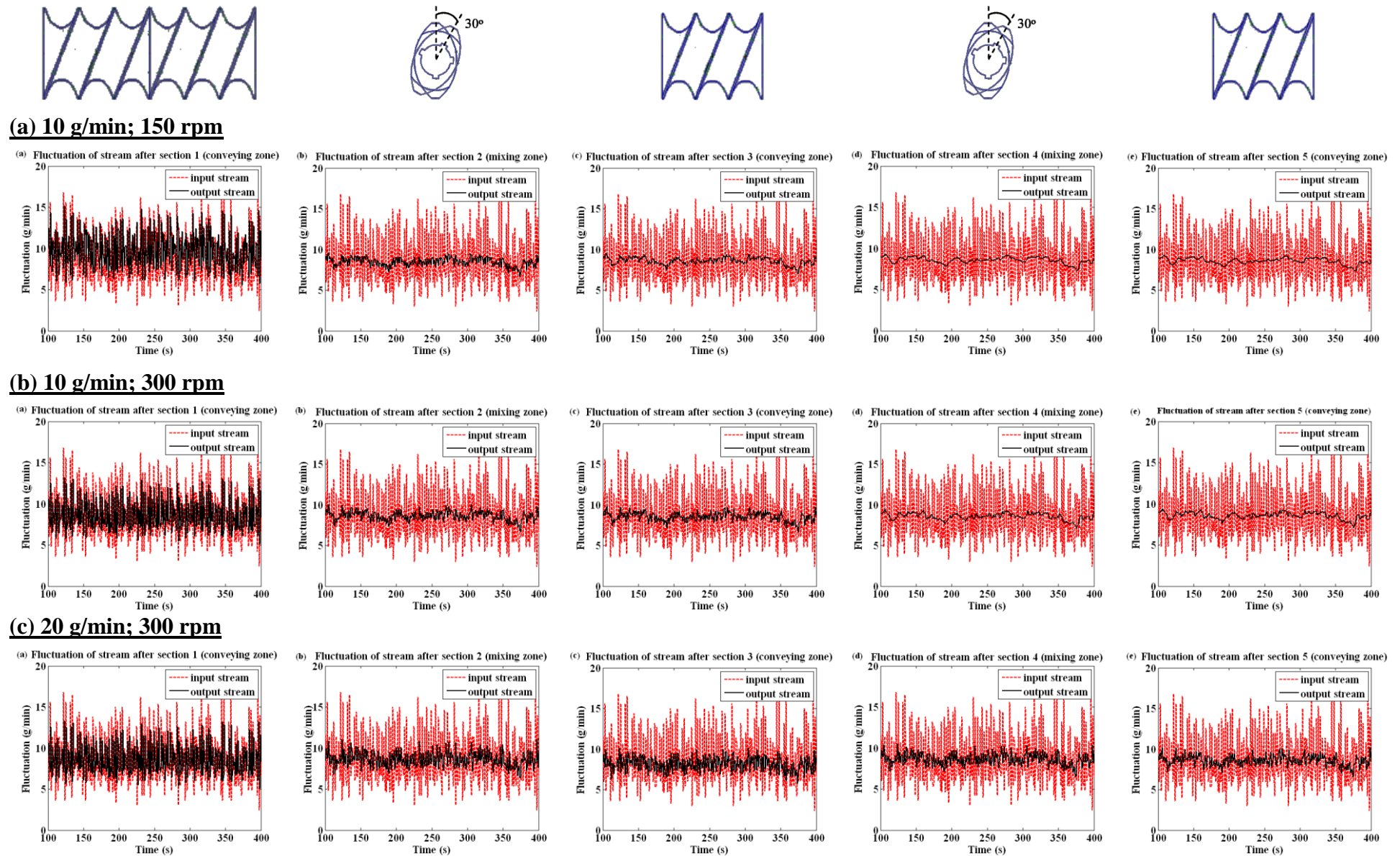
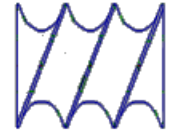
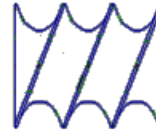
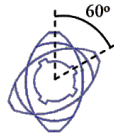
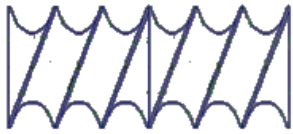
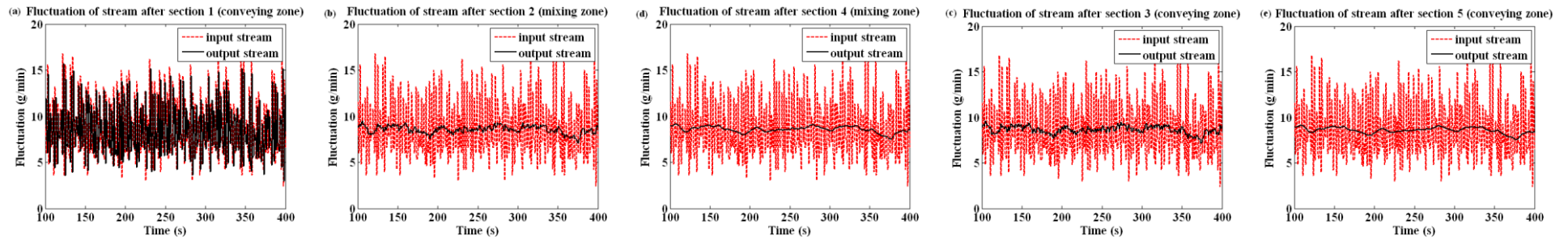


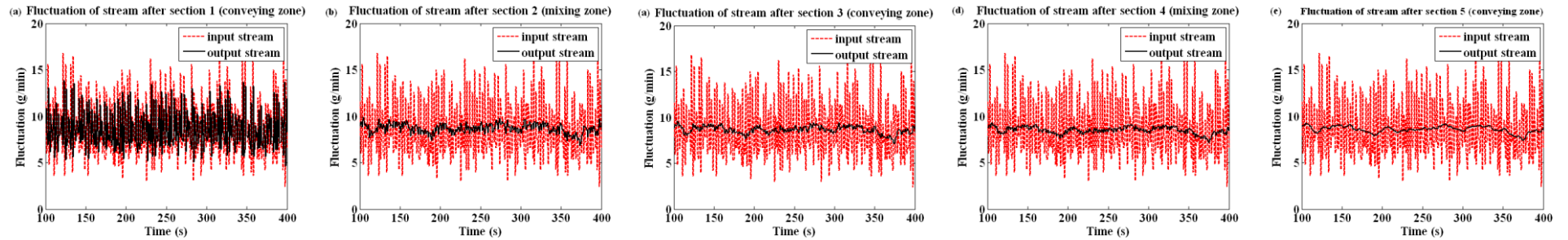
Figure 6-13: Mass flow rate fluctuation of input stream and along the granulator with screw geometry 30°



**(a) 10 g/min; 150 rpm**



**(b) 10 g/min; 300 rpm**



**(c) 20 g/min; 300 rpm**

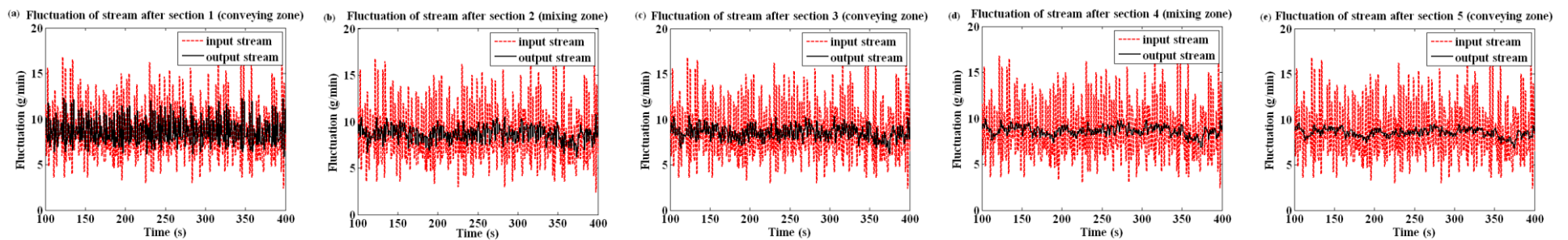


Figure 6-14: Mass flow rate fluctuation of input stream and along the granulator with screw geometry  $60^\circ$

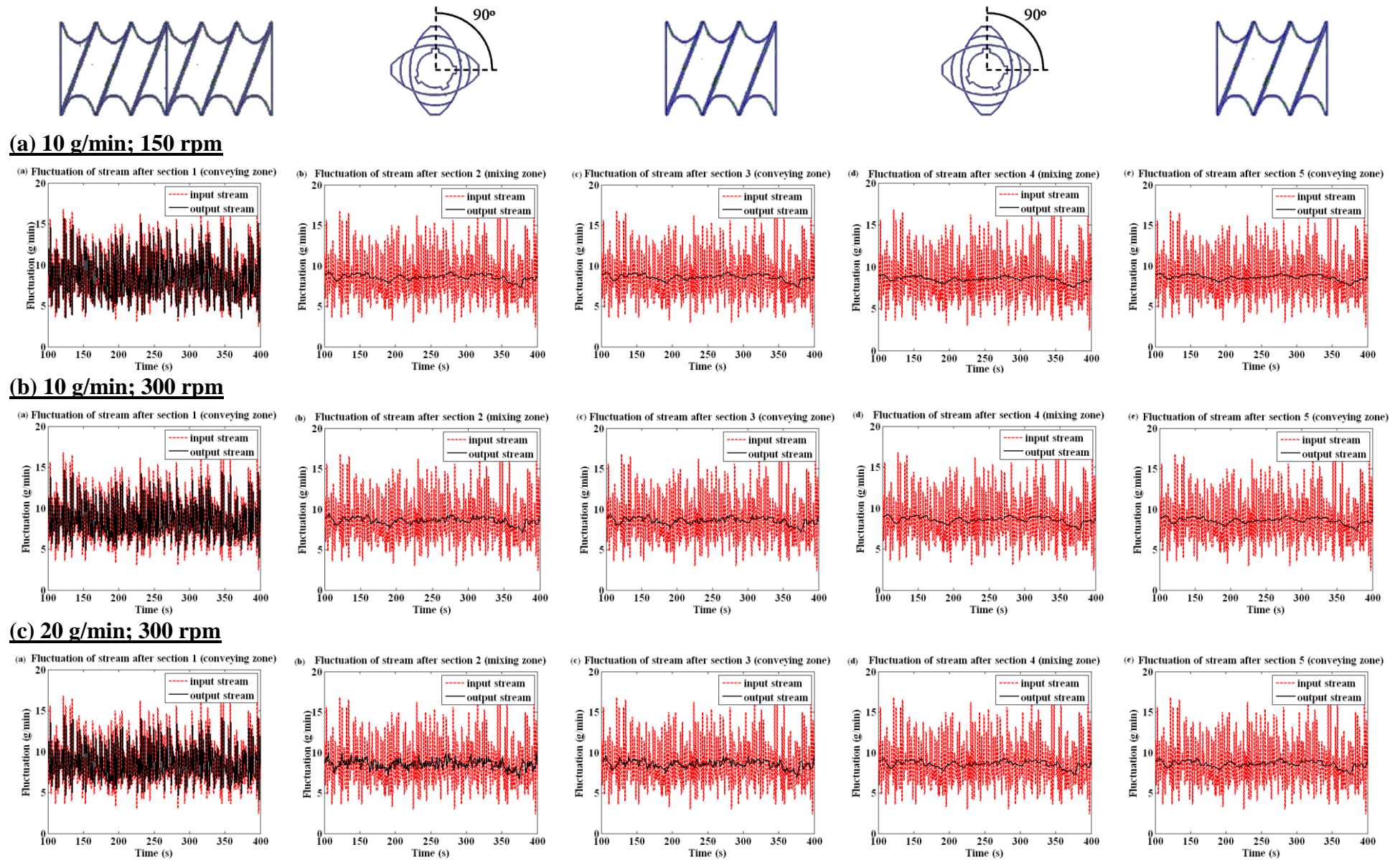


Figure 6-15: Mass flow rate fluctuation of input stream and along the granulator with screw geometry  $90^\circ$

## **CHAPTER 7 : THE EFFECT OF SCREW SPEED AND SCREW CONFIGURATION ON GRANULE AND TABLET QUALITY**

---

### **SUMMARY**

In this chapter, a widely studied formulation was used to make granules using the twin screw granulator. The equipment used and the experimental procedures were similar to that explained in Chapter 5. Different mixing configurations and screw speeds were used in order to study influences on granule properties which included Particle Size Distribution (PSD), shape and morphology, strength and packing coefficient. Caffeine was used as the model drug (API) in this study and the quality of tablets made from different types granules was also investigated which included tablet tensile strength and the dissolution profile. The caffeine content was mapped using Raman Spectroscopy to observe and predict the homogeneity of API distribution in the tablet matrix.

The results obtained show that the granules produced over a range of process conditions have a mono-modal distribution. The fraction of fines generated during the granulation process is low, < 5%. The mean granule diameter decreases when the screw speed increases but only up to 400 rpm and increases slightly at 500 rpm. The 30° mixing configuration produced the smallest granules followed by 90° mixing configuration and 60° mixing configuration produced the largest granules. The granule strength, which was estimated using Adam's uniaxial compaction equation, shows that 30° and 90° granules have similar strength while 60° granules have a lower strength and higher porosity but the difference is not statistically significant. The packing coefficient was similar for all granules produced over a



range of process conditions. The packing coefficient is < 25 % which indicates that all the granules have good/free flowing behaviour.

For the tablets produced using different types of granules, the tensile strength obtained from diametrical compression generally has a similar value. All the tablets have a fast dissolution time. However, the mean dissolution time has a complicated relation with the various process conditions that remained unclear. The caffeine in the tablets was seen to be dispersed homogeneously by observing the distribution on the tablet surfaces. This implies that the granulator could be used as mixer and that pre-mixing of powder mixtures is unnecessary.

It was concluded that the twin screw granulator is an efficient tool to run wet granulation continuously as the granules and tablets produced have acceptable quality. Besides this, Raman Spectroscopy is a promising tool for studying the homogeneity of API distribution and the technique might also be used for quality control purpose during granulation.

## **7.1 INTRODUCTION**

In previous chapters, the operating mechanism of twin screw wet granulation was studied by comparing the properties of the pure MCC granules with those produced using the high shear mixer. The reason for pure MCC being used was to simplify the system in order to understand the granule structure easily. However, the properties of the pure MCC granules could not represent those of granules produced commercially as formulation of commercial granules involves other materials such as binders, disintegrants and lubricants.

According to Table 2-1 in chapter 2, the characterisation of granule properties is more popular in twin screw granulation research compared to tablet properties. (Keleb, Vermeire et al. 2001) first evaluated the porosity, friability, tensile strength and disintegration time of

tablets produced from cold extrusion. The same author then evaluated the same properties of tablets produced from lactose granules made from twin screw extrusion in the following year (Keleb, Vermeire et al. 2002). (Van Melkebeke, Vervaet et al. 2008) then repeated Keleb et al. (2001) research and characterised the tablet properties produced using different screw configurations. The tensile strength of the tablets was also studied by other research groups (Djuric and Kleinebudde 2008; Djuric, Van Melkebeke et al. 2009; Djuric and Kleinebudde 2010). The summary of these work can be found in Table 2-1, Table 2-2, Table 2-3 and Table 2-4 in Chapter 2.

In the present study, granules were produced using a formulation which includes excipients, binder and disintegrant using a twin screw granulator. The quality of intermediate product was investigated by evaluation of the granule properties. The quality of the final product which is the tablets was also evaluated in this study.

## **7.2 OBJECTIVES**

The aim of this study is to investigate the quality of the granules and tablets produced using a twin screw granulator. Various screw speeds and mixing configurations were used in this study to investigate how these parameters affect the properties of intermediate products and final products. Raman Spectroscopy was also utilised in this study to examine the suitability of the tool to detect API and its distribution in a tablet.

## **7.3 MATERIALS AND EXPERIMENTAL METHOD**

### **7.3.1 Formulation of granules**

The primary particles used in this experimental work consisted of  $\alpha$ -Lactose Monohydrate (Pharmatose 200 M, DMV-Fonterra, Netherlands) and Microcrystalline Cellulose (MCC

Avicel PH101, FMC Biopolymer, Ireland) as excipients. Hydroxypropyl Cellulose (HPC M.W 100,000, Alfa Aesar, UK) was used as binder and Crosscarmelluose Sodium (Ac-Di-Sol SD-711 NF, USA) was added as a super disintegrant. For dissolution experiments, caffeine (Sigma, UK) was used as the model active ingredient. The powder mixture was prepared according to the formulation given in Table 7-1. Distilled water was used as the granulation liquid for the experiments and magnesium stearate (Sigma, UK) was used to lubricate the die for tablet compaction.

Table 7-1: Formulation of granules (J. Cartwright 2009)

<b>Ingredient</b>	<b>Normal experiments (%w/w)</b>
Pharmatose	73.5
Microcrystalline Cellulose	20.0
Hydroxypropyl Cellulose	5.0
Croscarmellose sodium	1.5
Caffeine <sup>1, 2, 3</sup>	10 % w/w of powder mixture

<sup>1</sup> no caffeine was used for general purpose of experiments

<sup>2</sup> 10 % w/w of caffeine was premixed with the powder mixture for dissolution experiments

<sup>3</sup> 10 % w/w of caffeine was fed into the granulator as second stream using a screw feeder

### 7.3.2 Granulation Process

The granulation process was run using the 19 mm diameter Twin Screw Granulator which was used in Chapter 5 for the PEPT study. The granulator was designed and built in house by GEA Pharma Systems, UK. The screws of the granulator have a length to diameter ratio of 10:1. The screws have conveying zones and 2 mixing zones which consist of six or seven kneading discs that can be arranged in various configurations. The powder mixture was fed into the granulator using a screw feeder (K-Tron T20) whilst granulation liquid was pumped

through the liquid injection point using a peristaltic pump. Before each experiment, powder and granulation liquid feedrates were determined by repeatedly weighing the amount of powder and liquid delivered for a period of 5 minutes. The temperature of the barrel was kept constant at 25 °C by circulating cool water through the jacket in the granulator.

Prior to the granulation, the powder mixture was prepared according to the formulation in Table 7-1 by means of premixing them in a Pascal Lab Mixer for a period of 30 minutes to obtain a homogenous mixture. The granules were collected 10 minutes after the process started in order to allow the system to reach steady state. The collected granules were then oven dried at 50 °C for 24 hours before the properties were evaluated.

In order to study the effects of process conditions on the quality of granules and tablets produced, experiments were carried out using different screw geometries and screw speeds. Based on the preliminary experiments, powder was introduced at 20g/min and the liquid to solid ratio was set and kept constant at 0.35 for all the experiments. Figure 7-1 shows the matrix of all the experiments carried out in this study.

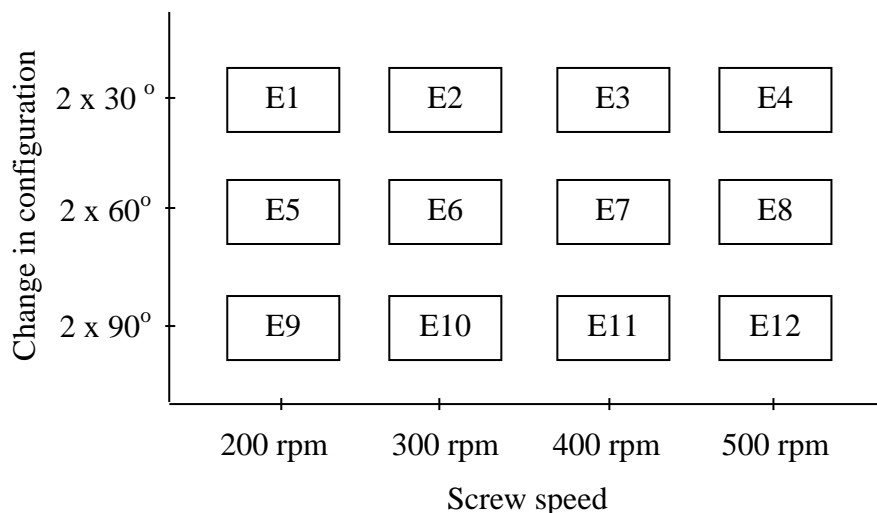


Figure 7-1: Experiments matrix

### **7.3.3 Tablet preparation**

In this study, two types of tablets were produced. The first type of tablet was prepared for the dissolution test to study the model drug release. 10 % w/w of caffeine (of total weight of powder mixture based on the formulation shown in Table 7-1) was blended into the powder mixture in the Pascal mixer prior to the granulation process. The powder mixture with caffeine was then fed using the screw feeder into the granulator.

The second type of tablet was prepared for the purpose to map and observe the distribution of the active ingredient within the tablet matrix using a Confocal Raman Microscopy. The formulation of the granules remains the same as Table 7-1 but the 10% caffeine was fed as a second stream. The caffeine was fed using a screw feeder into the granulator whilst the excipient mixture was fed using a vibratory feeder.

Tablets were then made from granules produced in order to investigate the quality of the final products. 500 mg of dry granules were manually fed into a 13 mm die (Specac, Kent, UK) and the powder bed was then compressed using a Universal Testing Machine (Zwick, Germany) to a maximum pressure of 100 MPa. The crosshead speed was set constant at 1 mm/s and the compaction process was carried out without addition of any lubricant to the granules. However, the die was pre-lubricated by pressing magnesium stearate before each compaction.

### **7.3.4 Granule characterisation**

#### ***7.3.4.1 Particle size distribution (PSD)***

The granule size distribution was determined as discussed in Chapter 4 where approximately 100 - 200g of the granules were sieved at 1mm amplitude for 10 minutes using

a shaker (Retsch, AS 200, Germany) through a series of sieves with aperture size of 63, 90, 125, 180, 250, 355, 500, 710, 1000 and 1400  $\mu\text{m}$  (ISO standard, every 3rd sieve of root 40 series). The weight of granules retained on each sieve was measured and particle size distribution curves were plotted. In this study we defined the fraction of granules smaller than 125  $\mu\text{m}$  as fines, assumed to comprise un-granulated material.

#### ***7.3.4.2 Shape and morphology***

The shape of the granule was measured in terms of sphericity and was determined using Sympatec Image Analysis (QICPIC) by dispersing the granules under gravity through high speed cameras. The definition and the equation of sphericity can be found in section 4.3.5.2 in Chapter 4. A Scanning Electron Microscopy, (SEM, JOEL 6060) was also used to observe the surface morphology of the granules.

#### ***7.3.4.3 Confined uni-axial bulk compression***

The granule strength was measured by compressing granules using a piston in a rigid cylinder using single ended compression with a moving top punch (uniaxial bulk confined compression) (Adams, Mullier et al. 1994). 500 mg of dry granule with size classification of 710 – 1000  $\mu\text{m}$  was filled into a 13 mm stainless steel die (Specac, UK) and tapped to remove any large packing irregularities. The powder bed was then compressed using a Universal Testing Machine (Zwick, Germany) with real time data logging and analysis at a speed of 3.5 mm/min to an upper pressure limit of 100 MPa. The test was repeated 5 times in order to obtain reliable results. The fracture strength was then calculated using Adam's equation by non-linear regression of the data to Eq 4.3 which can be found in Chapter 4.

#### 7.3.4.4 Determination of packing coefficient

During the compaction, the particles will arrange under the low uniaxial pressure before any fragmentation or plastic deformation. The entrapped air will be evacuated slowly until the powder bed reaches a maximum packed structure where the relative movement of the particles is impossible without particle deformation. Packing coefficient,  $C_t$ , was introduced by (Gabaude, Gautier et al. 2001) to estimate the flow properties of granular materials. It is defined as the ability of granular materials to rearrange under low pressure and was expressed in the following equation (Gabaude, Gautier et al. 2001),

$$C_t = \frac{h_o - h_i}{h_o} \times 100\% \quad \dots \text{Eq. 7-1}$$

Where  $h_o$  is the initial bed height and  $h_i$  the bed height at a certain pressure. In order to determine bed height where the powder bed is completely packed, a plot of the incremental packing coefficient  $\Delta C_t$ , versus the applied pressure is needed (Figure 7-2). As shown in the figure, the slope change is insignificant and negligible after 0.5 MPa for any material which suggests the powder bed is completely packed at this pressure. Therefore, only packing and slippage are assumed to occur until the pressure reaches 0.5 MPa. The packing coefficient was then calculated using the bed height at 0.5 MPa and the materials can be classified into 3 types of behaviour according to the  $C_t$  value which is shown in Table 7-2.

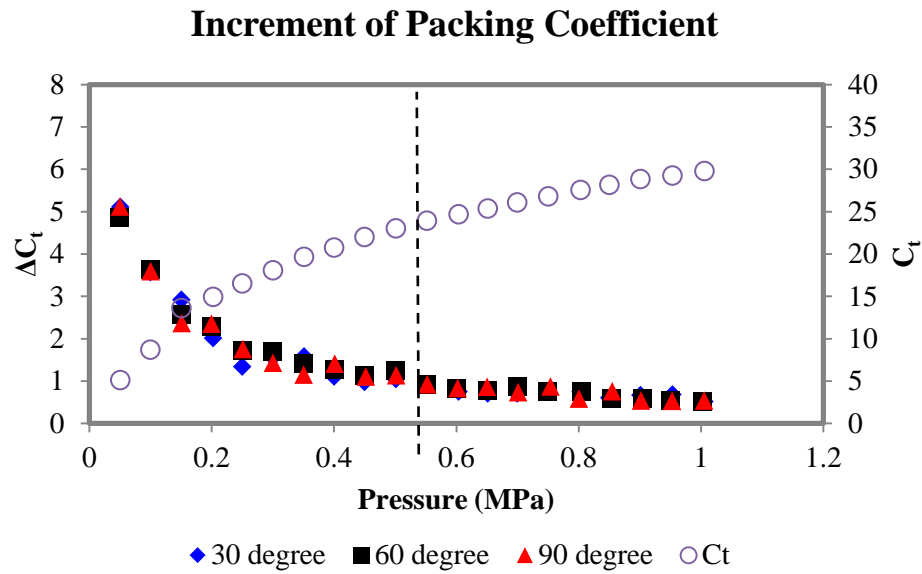


Figure 7-2: Evolution of incremental packing coefficient value corresponding to the applied pressure

Table 7-2: Behaviour of particles for different  $C_t$  classification (Gabaude, Gautier et al. 2001; Chantraine, Viana et al. 2007; Mangwandi, Adams et al. 2010)

$C_t$	Type of behaviour
< 25 %	Tendency to close pack under load; good ability to rearrange under low pressure
25 % – 30 %	intermediate behaviour
> 30 %	High resistance to pack; poor ability to rearrange under low pressure

Besides this, the packing coefficient is representative of the material flow properties evaluated using a shear cell measurement. Gabaude, Gautier et al. (2001) study shows that material with packing coefficient < 25 % has an easy or free flowing property and when this packing coefficient increases, the materials will gradually become poor in flowability. Therefore, it is possible to predict at an early stage the flow properties of a material using the packing coefficient and a value lower than 25 % is considered easy to handle.



### **7.3.5 Tablet characterisation**

#### ***7.3.5.1 Tensile strength***

The diametrical compression test was performed to measure the tablet tensile strength in the present study and the test was performed immediately after the tablets were made. A universal testing machine (Zwick, Germany) with a 5kN load cell was used to perform the test to measure the maximum diametrical crushing force accurately. Together with the measured thickness and diameter, the tablet tensile strength is related to the load at fracture proposed by (Fell and Newton 1970) and the equation was explained previously and can be found as Eq 4.4 in Chapter 4.

#### ***7.3.5.2 Dissolution rate***

The dissolution of the caffeine tablets was conducted using a dissolution apparatus (Varian 705 DS, Agilent Technologies, USA) following the paddles method (USP/Ph. Eur, method II) with 900 ml of distilled water as dissolution medium. The temperature of the dissolution medium was kept constant at  $37 \pm 0.5$  °C and the rotational speed of the paddles was set at 100 rpm (USP XXIII). 2 ml of sample was withdrawn at time intervals of 5, 10, 15, 20, 25, 30, 45 and 60 minutes using a pipette. The concentration of the caffeine was then measured using a UV spectrometer (Jasco V-530 UV/VIS spectrophotometer, USA) at wavelength 273 nm in a silica cuvette (UV quartz, Hellma, Germany).

#### ***7.3.5.3 Active ingredient distribution***

Confocal raman microspectroscopy (WITEC alpha, Laser length 785 nm, Germany) was used in the present study to observe the distribution of caffeine on the tablet surface. The surface to be scanned was made as smooth as possible using fine sand paper (ISO/FEPA Grit

P220) to avoid spectra intensity differences within the sample as the intensity is sensitive to the probe distance. The tablet surface was uniformly divided across the width into 200 lines and along each line, the spectra of 200 points was obtained. In other words, the distribution of caffeine was obtained by point to point mapping mode with a step size of 65  $\mu\text{m}$  in both vertical and horizontal directions (= 40000 points per map).

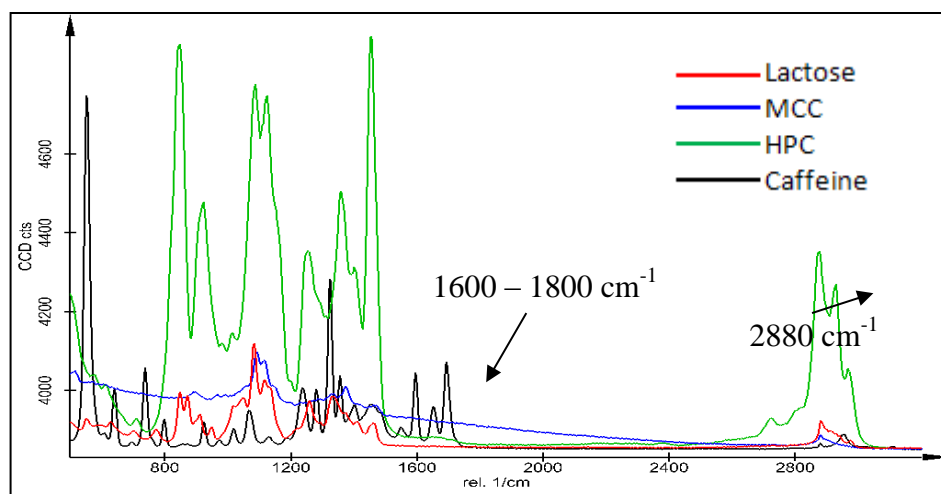


Figure 7-3: Raman spectra of lactose, MCC, HPC and caffeine

The Raman spectra of lactose, MCC, HPC and caffeine are shown in Figure 7-3. The caffeine spectrum shows a finger print peaks at band  $1600\text{ cm}^{-1}$  to  $1800\text{ cm}^{-1}$ . In order to detect caffeine in the tablets, a chemical map must be constructed from the peak area characteristic to caffeine and therefore, the  $1700\text{ cm}^{-1}$  band was used. On the other hand, the excipients map was constructed at the  $2880\text{ cm}^{-1}$  band. A successful detection of a component will show a bright spot in the map constructed that can be found in Figure 7-19 to Figure 7-21.

## 7.4 RESULTS AND DISCUSSIONS

### 7.4.1 Granule Particle Size Distribution (PSD)

Figure 7-4, Figure 7-5 and Figure 7-6 are the particle size distribution curves of granules produced using 30°, 60° and 90° mixing zone configurations with different screw speeds. Generally the PSD curves of the granules are mono-modal in shape and these mono-modal shape PSD curves remain similar when the granules were produced using different screw speed and different screw geometries.

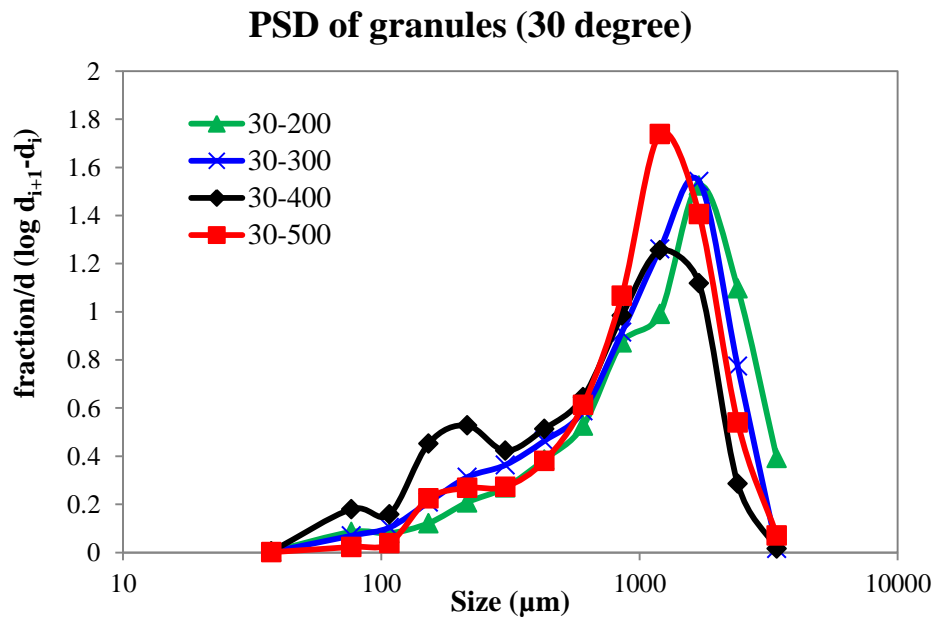


Figure 7-4: PSD of granules produced using 30 degree mixing zones

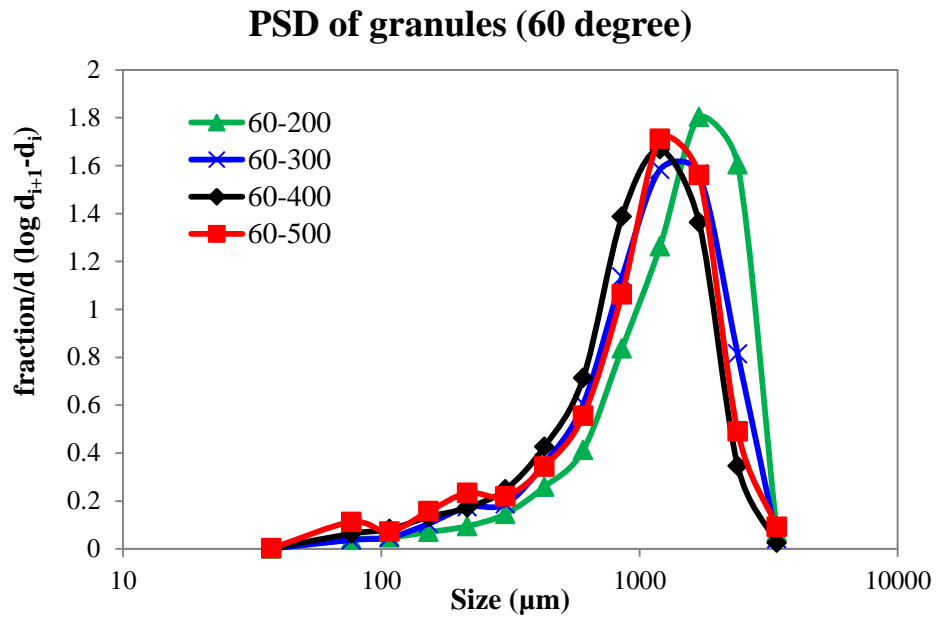


Figure 7-5: PSD of granules produced using 60 degree mixing zones

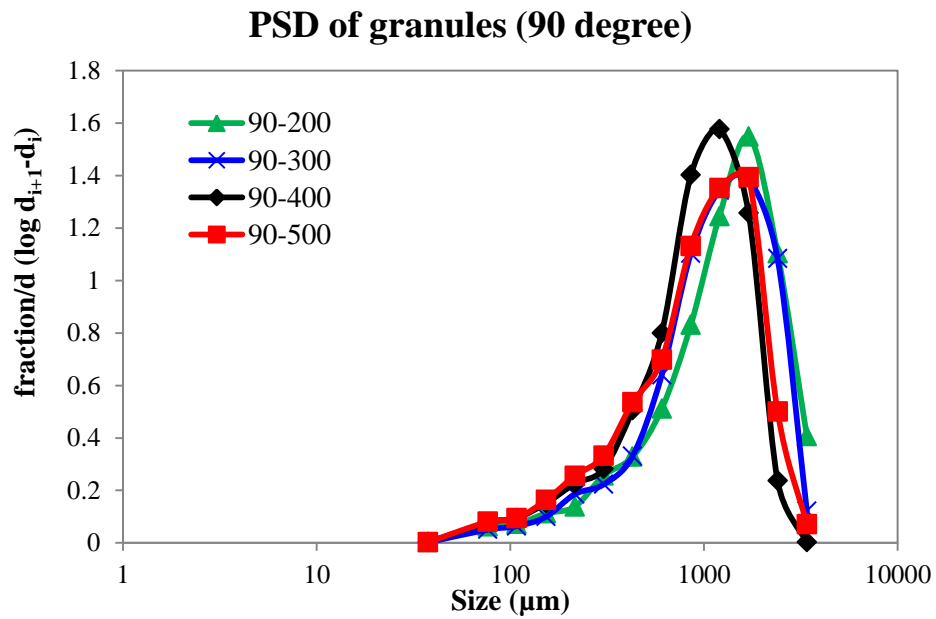


Figure 7-6: PSD of granules produced using 90 degree mixing zones

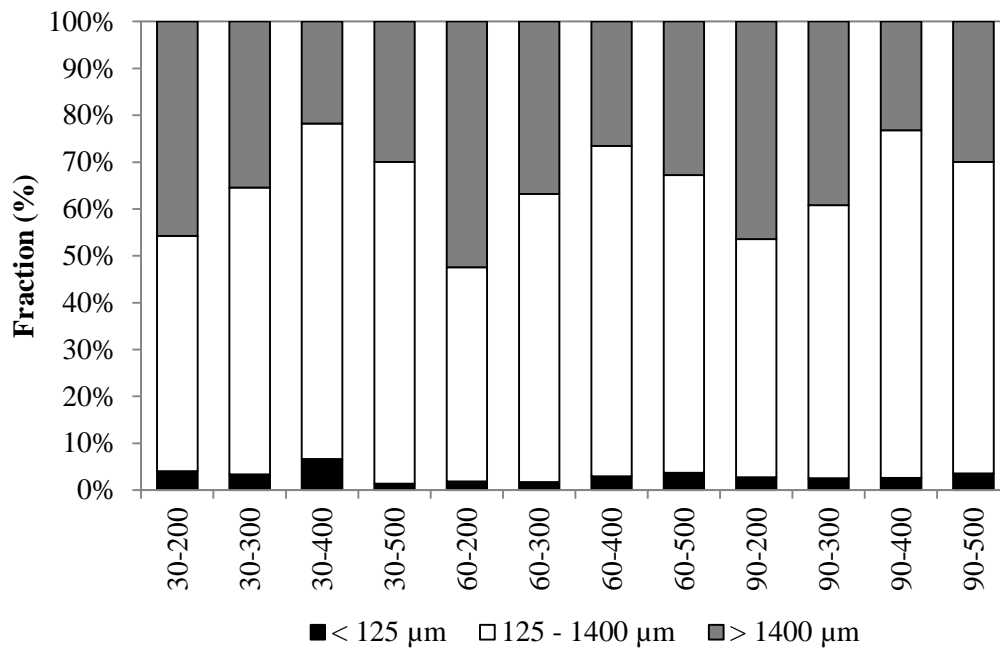


Figure 7-7: Fines (<125 μm), yield (125 – 1400 μm) and oversize (>1400 μm) of granules produced using various screw speed and screw configuration (30-200 = 30 degree mixing zones with 200 rpm screw speed)

The fraction of fines (<125 μm), yield (125 – 1400 μm) and oversize (>1400 μm) of the granules produced are shown in Figure 7-7. The results show that the granulator only produces a small fraction of fines, generally lower than 5 % w/w of the total granules produced under the various conditions. However, there is a larger amount of oversized granules being produced. These oversized granules then determine the granule yield values. The more oversized granules produced the lower the granule yield, yet this can be solved by having a milling process after the granulator. The granule yield values are ranging from 45.7 % for granules produced using 60° degree mixing configuration at 200 rpm and up to 73.5 % for 90° configuration at 400 rpm. Besides this, the influence of screw speed on the yield fractions of the granules has a similar relation for different mixing zone configurations. The granule yield value increases with increasing screw speed and reaches a maximum value when screw speed is 400 rpm. The value will then decrease slightly at 500 rpm.

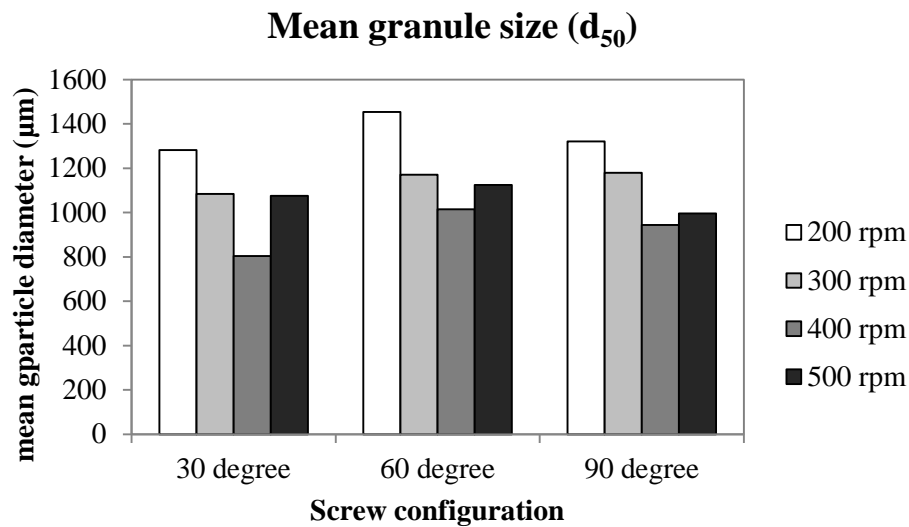


Figure 7-8: Mean diameter ( $d_{50}$ ) of granules produced with different screw speed and screw configuration

The mean granule diameter,  $d_{50}$  was also calculated and is shown in Figure 7-8. The effect of screw speed on mean size of the granules has an opposite trend to the yield fraction. The  $d_{50}$  decreases when the screw speed increases and has a minimum value when the screws rotate at 400 rpm. The granule size then increases slightly thereafter. When comparing the mean diameter of granules in terms of screw geometry, the granules produced using 30° mixing configurations have the smallest size followed by 90° and then 60° configurations. The influence of screw geometry on granule size is less significant compared to screw speed.

The small fraction of fines indicates that there is sufficient granulation liquid for the formulation during granulation process. Besides this, it is also believed that the granulation liquid was homogeneously dispersed within the powder bed which then results in monomodal granule size distribution being produced for all screw speeds and geometries.

The granules produced using 60° mixing configurations generally have a larger size. This might be because the advance angle of this configuration offers more bypass possibility for the materials around the lobes avoiding being sheared by the kneading discs (Thiele, Ghebre-

Selassie et al. 2003; Djuric 2008). On the other hand, 30° mixing configurations, as described by Thiele, Ghebre-Selassie et al. (2003), has a more dispersive character and less bypass possibility due to smaller advance angle. Besides this, as highlighted previously (Chapter 5), the more dispersive 30° mixing zones have a lower fill level compared to 60° configurations. The lower filled barrel might be expected to have lower compaction force that could reduce the possibility of efficient material interlocking and therefore generating smaller granules. 90° mixing configuration has no conveying character and is considered close to distributive type of mixer. The lack of conveying means there is a high hold up that might improve efficient coalescence of the materials in the mixing zone. At the same time, higher hold up might also create a higher shear stress regime that could cause granule breakage. This possibly explains why the 90° configuration produces larger granules than those generated by 30° configuration but smaller than that generated by 60° configuration. Note that the influence of the screw configurations on mean granule size is not significant especially for the low filling granulator estimated in Chapter 5 (Thompson and Sun 2010).

The mean granule size is more strongly affected by the screw speed and follows a decreasing trend when the screw speed increases. As discussed in Chapter 4 and 5, increasing screw speed will decrease the fill level of the granulator and slightly diminish the granule growth. Moreover, increasing the screw speed increases the shear rate and the higher shear force is expected to break up large agglomerates more easily (Thompson and Sun 2010). Beyond the screw speed of 400 rpm, the mean granule size increases slightly. Since binder is considered in the granule formulation, a possible explanation is that the high kinetic energy that exhibited due to high screw speed is enough to encourage re-coalescence of the smaller particles into larger granules particularly in the conveying zones. Nevertheless more work is

needed to validate the above finding such as recycling the wet granules into a conveying only granulator and study if the kinetic energy will cause breakage or agglomeration.

#### 7.4.2 Granule Shape and Morphology

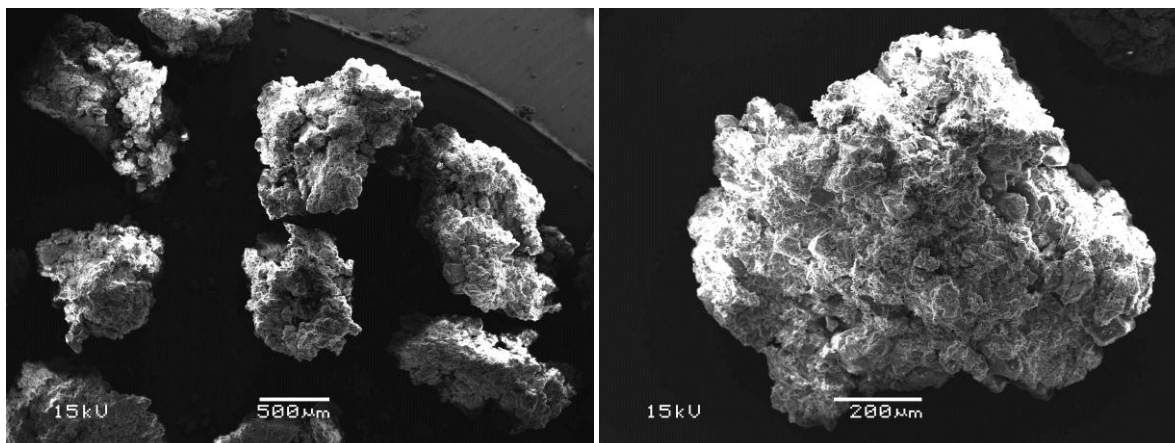


Figure 7-9: SEM images of granules at different magnification

Figure 7-9 presents images of granules obtained using Scanning Electron Microscopy (SEM, JOEL 6060, Oxford Instrument, UK). Like pure MCC granules, these granules produced from the more representative formulation using the granulator have irregular shape. The granule surface is porous and the granules appear to be formed from loosely packed smaller particles. Also, the granules are not spherical, have rough surfaces and some of the granules seem to be elongated. The shape and surface morphology remain similar for granules produced using different screw speed and mixing configuration.

The shape of the granules which can be described using aspect ratio was measured over a wide range of granule sizes and is shown in Figure 7-10. As expected the small particles have lower aspect ratio as they are mainly primary particles (MCC is in needle shape, HPC is in flake shape, Croscamellose sodium is rod shaped and lactose is irregular crystal shaped). As the granule size increases the aspect ratio increases to 0.7 and stays constant between the sizes



ranging from 100 – 500  $\mu\text{m}$ . The aspect ratio value then follows a decreasing trend with the granule size that there is more elongation. The higher aspect ratio value for the granules ranging from 100 – 500  $\mu\text{m}$  may imply that those granules were being coalesced, elongated, broken and spheronised during the manufacture. The low aspect ratio value for larger granules on the other hand indicates that these granules were coalesced and exposed to a greater elongation without experiencing breakage process because of the screw rotation and the nature of the clearances in the granulator.

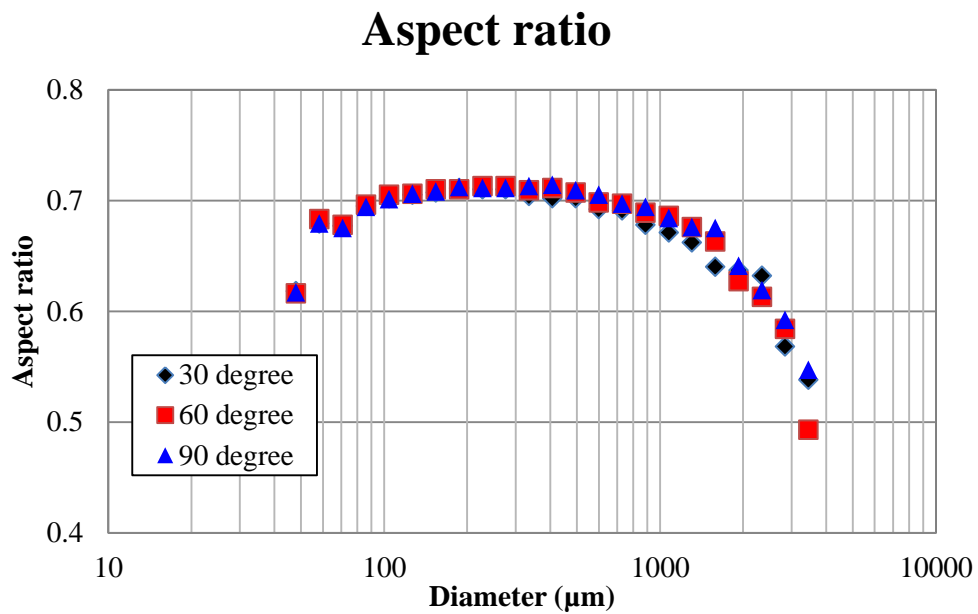


Figure 7-10: Aspect ratio of granules produced using 30°, 60° and 90° screw configuration

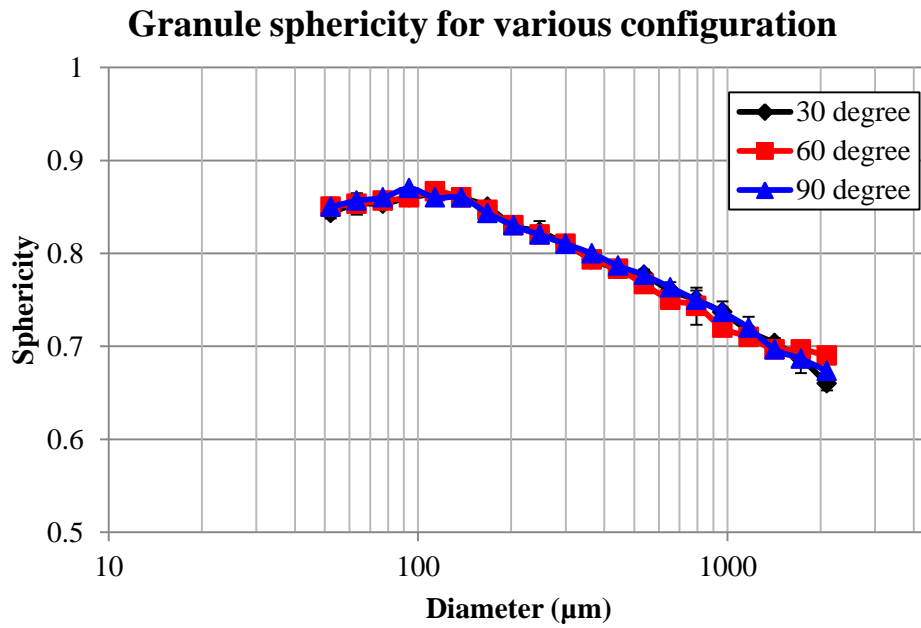


Figure 7-11: Sphericity for various size classifications of granules produced using different screw configuration

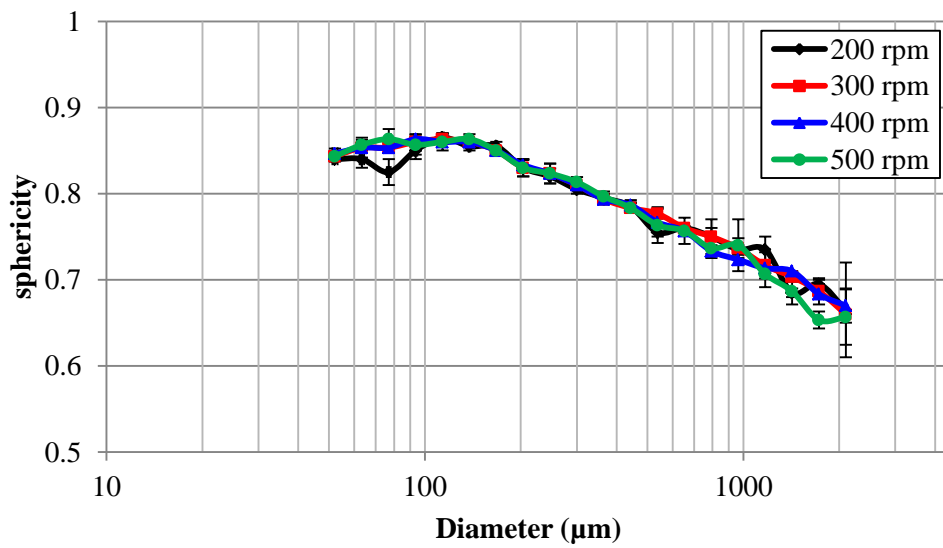


Figure 7-12: Sphericity for various size classifications of granules produced using different screw speed

Figure 7-11 and Figure 7-12 show the sphericity of granules against different size classification (from 50 μm up to 2000 μm) produced using different process conditions.

Generally the granules produced using different screw speed and mixing configurations have a similar sphericity and it is inversely proportional to the granule size. The particles smaller than 150  $\mu\text{m}$  are more spherical and have a sphericity value of approximately 0.85. As the particle size increases, the sphericity value starts to decrease and reaches a minimum value of approximately 0.65 for the granules larger than 2 mm. As discussed previously, the granules were formed from loosely packed particles because of the partially filled barrel that results in low compaction force in granulator. The partially filled barrel also leads to limited spheronization effect (Dhenge, Fyles et al. 2010) and therefore the granules produced are less spherical and have a rough surface.

Since the granulation liquid was added continuously during the granulation process, the materials will be subject to immersion type of wetting to form extrudates. The smaller size granules are expected to be formed from the breakage when the extrudates were being sheared in the granulator. Therefore this might explain lower sphericity and aspect ratio when the granule size is larger.

### 7.4.3 Granule Strength and Packing Coefficient

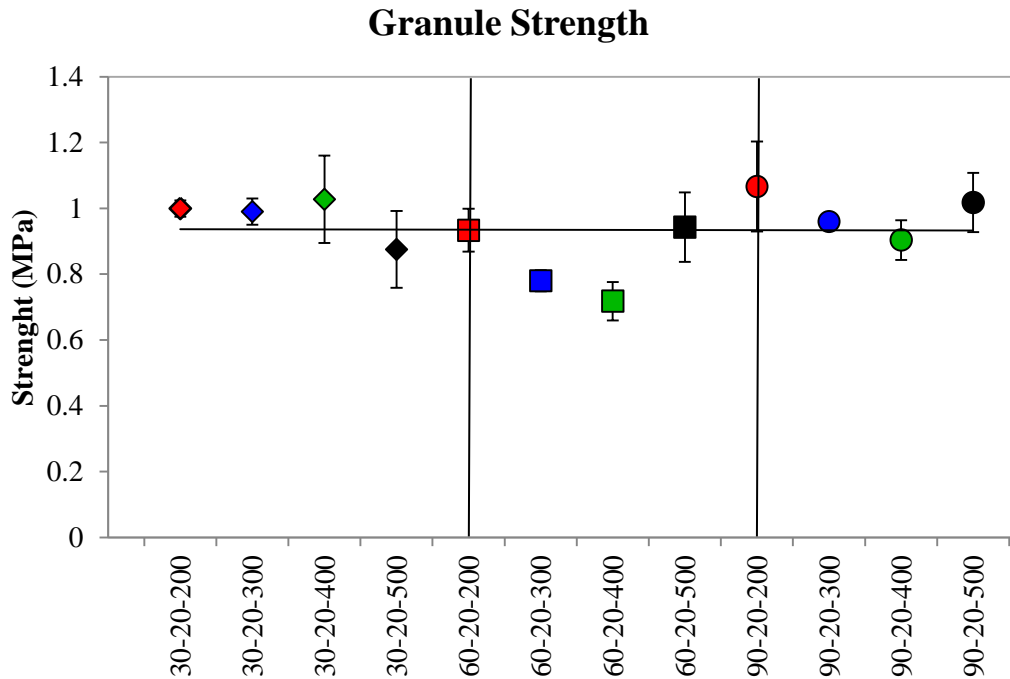


Figure 7-13: Estimated fracture strength of granules produced using various screw speed and screw configuration

The strength of the granules estimated using Adams' equation is shown in Figure 7-13. Statistically, the results obtained show that there is no significant difference between the fracture strength of the granules. Since the granule strength is inversely proportional to the granule porosity (Figure 4-21), the granules produced using different process conditions are expected to have similar porosity. The finding is dissimilar from the results reported in (Djuric and Kleinebudde 2008) study. There it was reported that materials in the 90° mixing configuration were more kneaded and gave granules with the lowest porosity due to the non-conveying character. The granules produced by 60° mixing configuration have highest porosity and the one produced by 30° has intermediate value. This might be due to the 60° advance angle which offers more bypass possibility in comparison to the 30°, which has a more dispersive character and fewer bypasses.

Table 7-3: Packing coefficient of granules

configuration	Packing Coefficients, $C_t$ (%)			
	200 rpm	300 rpm	400 rpm	500 rpm
30 degree	21.65 ± 0.50	21.86 ± 0.37	21.42 ± 0.92	22.62 ± 1.03
60 degree	22.63 ± 0.53	24.02 ± 0.55	24.62 ± 0.82	22.16 ± 0.83
90 degree	21.01 ± 0.84	21.78 ± 0.24	22.29 ± 0.58	21.00 ± 0.54

Similar to the granule strength, the packing coefficients (shown in Table 7-3) of the granules produced using different process conditions have similar value ranging from 21.0 – 24.6 %. The granules can be classified as having good packing behaviour since the  $C_t < 25\%$  and would be expected to have easy flowing properties (Gabaude, Gautier et al. 2001). The packing coefficients were found to be uniform because the granules produced using different process conditions consistently have irregular shape (Mangwandi, Adams et al. 2010). Packing coefficient is good parameter to predict the flowability at the beginning stage of a study but application of the shear cell tester is needed to validate the above findings.

#### 7.4.4 Tablet Tensile Strength

The tensile strength of the tablets compacted using different types of granule is shown in Figure 7-14. 5 tablets were tested and the data was statically tested (student t-test) and result shows that the tablets produced using different types of granule have similar tensile strength except the one produced by 30° mixing configuration with 400 rpm screw speed. Tablet tensile strength could be affected by many factors. It was reported that tablet strength is proportional to the tablet porosity of the tablets (Djuric 2008) and also, it could be influenced by the size distribution of the particles that are used to produce the tablet (Riepma, Vromans et al. 1993). Since the compression force to make tablets is high, the difference in tablet

porosity is expected to be insignificant as shown in Figure 7-15 (Selkirk and Ganderton 1970) and therefore the tablet strength is expected to remain similar. The exceptional high tensile strength of the tablets produced by 30° mixing configuration at 400 rpm is possibly due to the broader particle size distribution of the granules (See Figure 7-7). Generally, the higher amount of fines generated during the granulation process could result in the production of stronger tablet (Riepma, Vromans et al. 1993).

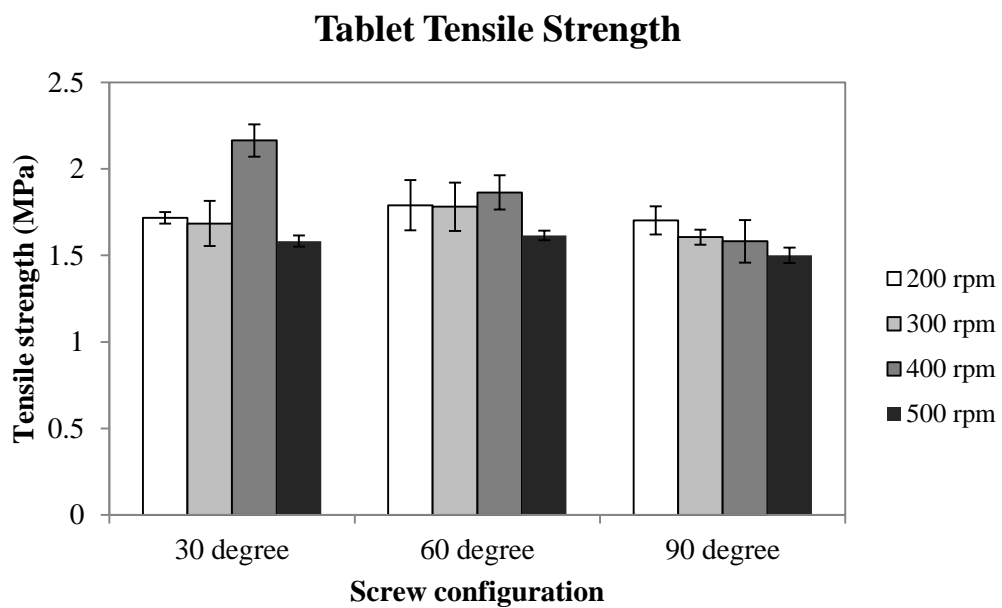


Figure 7-14: Tablet tensile strength for various screw speeds and configurations (error bars are 95% confidence interval)

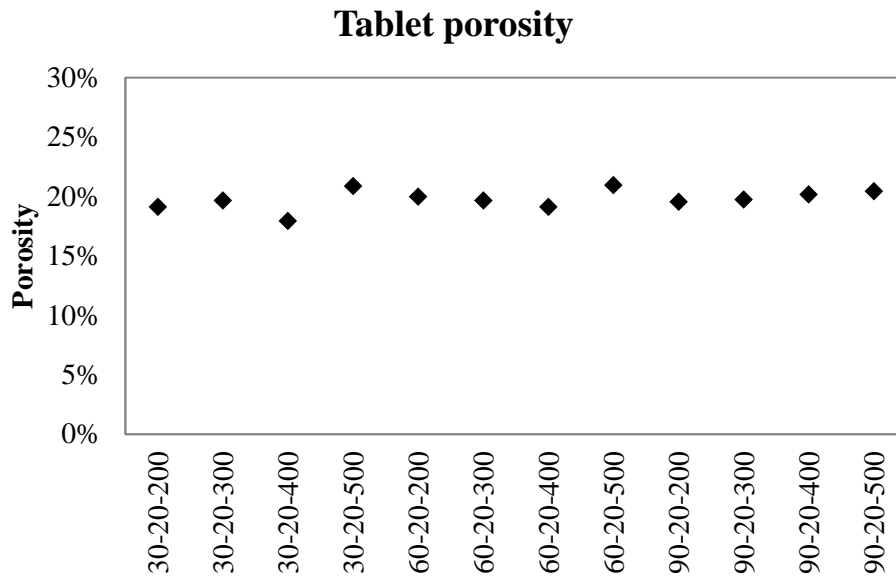


Figure 7-15: Porosity of tablets produced using a range of process conditions

#### 7.4.5 Caffeine Dissolution Rate

In order to characterise the dissolution profile, the Weibull distribution (Langenbucher 1976; Dévay, Mayer et al. 2006) function was applied to model the dissolution of caffeine from tablets in the following form,

$$Y = 1 - \exp\left(-\left(\frac{t - t_0}{\tau_d}\right)^\beta\right) \quad \dots \text{Eq. 7-2}$$

Where  $Y$  is the fraction of the active ingredient dissolved at time  $t$ ,  $\beta$  is the curve shape factor,  $t_0$  is the lag time of dissolution and  $\tau_d$  is the mean dissolution time when 63.2% of active ingredient has been dissolved. It is assumed that on exposure to the solvent the caffeine dissolves immediately without any time delay, so  $t_0 = 0$ .  $\tau_d$  and  $\beta$  is calculated by non linear regression of the data to Eq. 7-2. The fit of the Weibull model to the experimental data is shown in Figure 7-16 and the mean dissolution time of the tablets is shown in Figure 7-17.

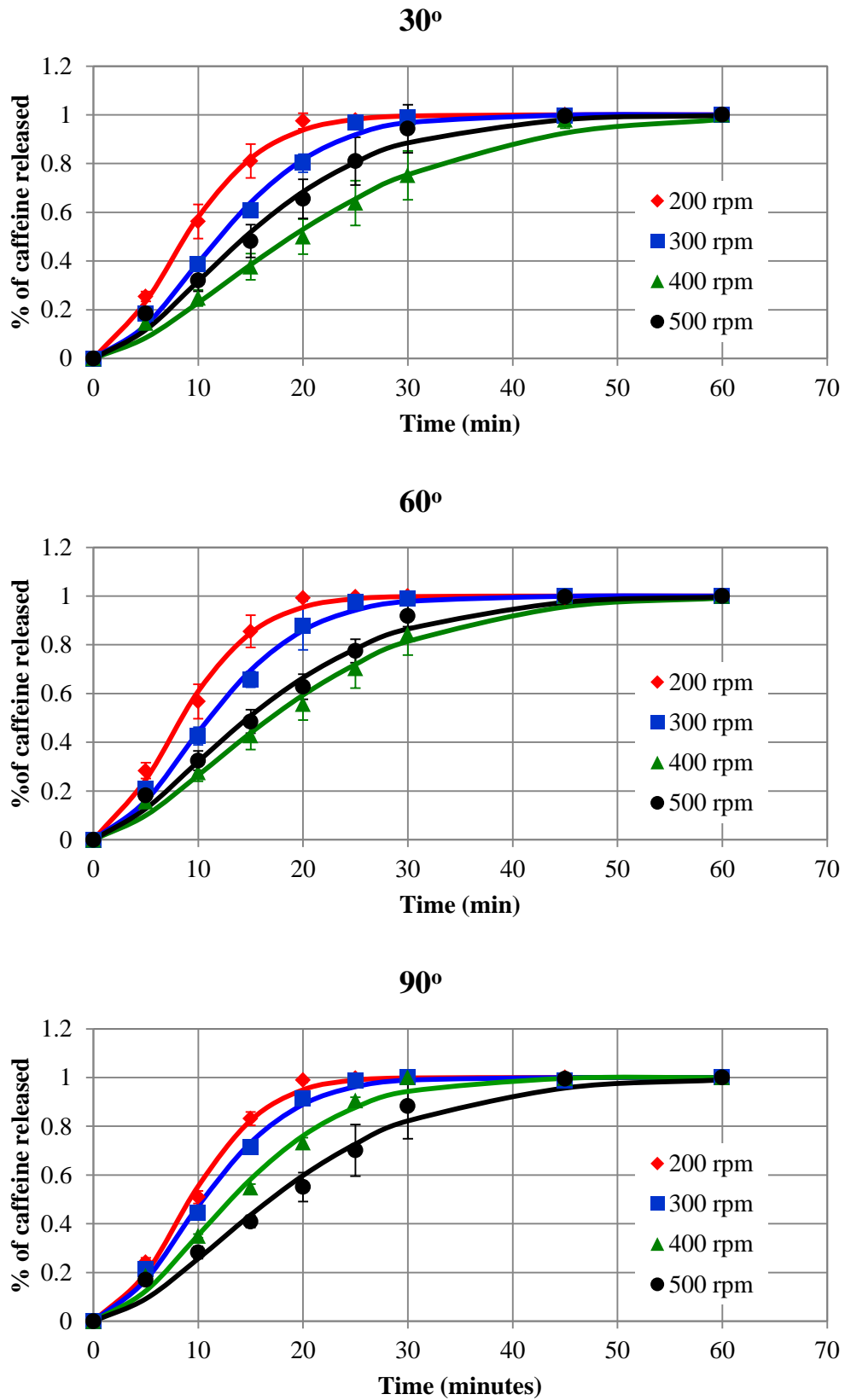


Figure 7-16: Weibull's Dissolution curves of tablets made using granules produced using different types of process conditions (solid line is Weibull's model; experimental points are the average of 5 tablets dissolution)



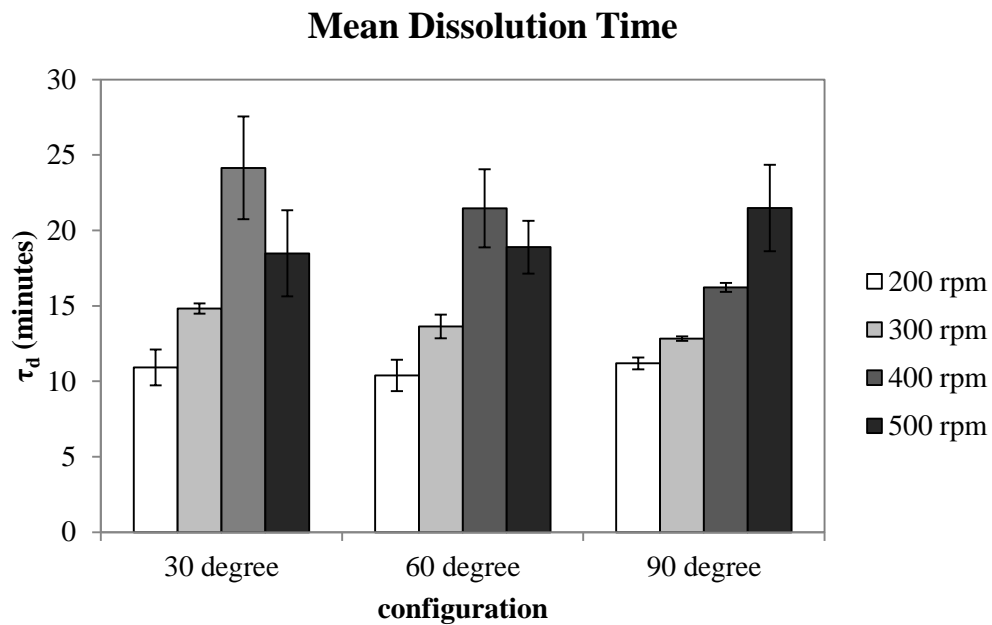
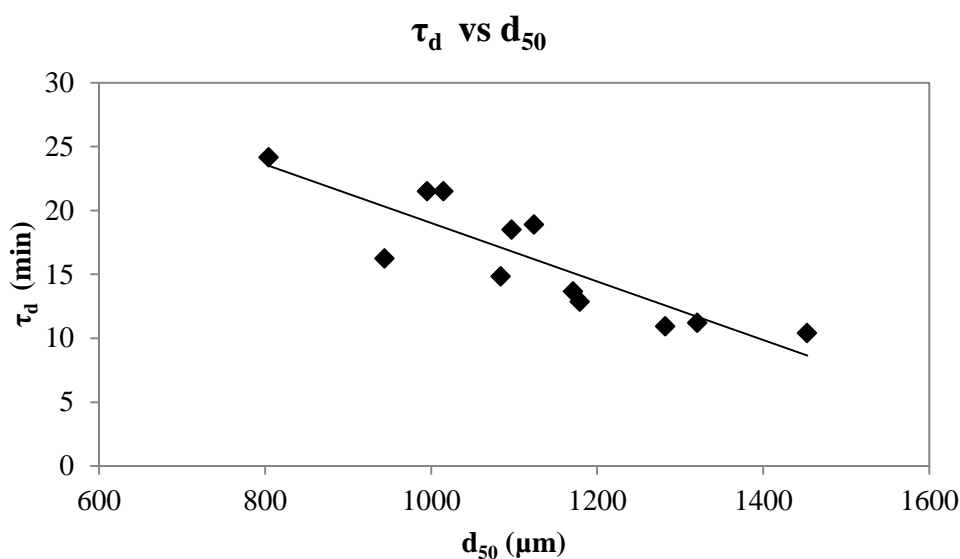


Figure 7-17: Mean dissolution time of caffeine tablets for various screw speed and screw configuration

The tablets produced using different types of granules are considered to give fast dissolution as the mean dissolution times are lower than 30 minutes. There is little or no significant change in mean dissolution time for granules produced using different mixing configurations. However, the mean dissolution times become complicated for different screw speeds. For 30° and 60° mixing configurations, the mean dissolution time increases when the screw speed increases and reaches a maximum value at 400 rpm. The mean dissolution time then decreases slightly when screw speed was increased to 500 rpm. On the other hand, the tablets made using granules produced by 90° mixing configuration have mean dissolution times that are continuously increasing with the screw speeds. The relation between the mean dissolution times and the screw speed is not well understood in current study. However, plot of  $\tau_d$  against  $d_{50}$  shows that the dissolution might be related to the mean granules size and there is an increase in  $\tau_d$  when the  $d_{50}$  decreases. This might indicate that the dissolution rate of the tablets is controlled by the tablet disintegration rate since the porosity of the tablets is

similar for all the tablets. Hypothetically, the larger the granules, the faster the tablet disintegration as the surface area for granule interlocking decreases during tablet formation. More work will be needed for further investigation to obtain a better understanding of the mechanism of tablet dissolution for example to determine the disintegration time of the tablets.



7-18: Plot of  $\tau_d$  against mean granule size

#### 7.4.6 Caffeine Distribution in Tablet

Confocal Raman Spectroscopy is becoming popular in the pharmaceutical industry and gaining wide acceptance for characterisation of solid dosage forms. (Vasanthavada, Wang et al. 2011) and (Haefele and Paulus 2011) recently concluded that Confocal Raman Spectroscopy is beneficial in the analysis of drug products which includes the substances visual appearance, content uniformity, chemical identity and physical state. The distribution and the composition of a substance in a product can also be revealed using this technique at very low concentration and pixel resolution.

In this study, the distribution of model drug was obtained and Figure 7-19 (a) & (c), Figure 7-20 (a) & (c) and Figure 7-21 (a) & (c) show the caffeine mapping of tablets (both surfaces) using Confocal Raman Spectroscopy. The bright spots in these figures represent the positive detection of caffeine on the tablet surfaces and the integration over the range of the strongest caffeine band at around  $1700\text{ cm}^{-1}$  (see Figure 7-3) demonstrates the homogenous distribution of this compound in the tablets produced using different types of mixing configurations. The mapping of excipients (Figure 7-19 (b) & (d), Figure 7-20 (b) & (d) and Figure 7-21 (b) & (d)) also shows that the caffeine was well dispersed within the tablets as black spots present at the same location in caffeine maps when the chemical maps were constructed from peak areas with  $2880\text{ cm}^{-1}$  band.

The uniform distribution of caffeine in the tablets indicates the capability of the twin screw granulator to achieve good mixing during the granulation. Thus, the granulator would also serve as a continuous mixer device and the pre-mixing stage could be replaced by introducing a couple of feed ports in the granulator. Besides this, the results shown also emphasize that Raman Spectroscopy is a promising tool for studying the homogeneity of API distribution within a tablet matrix. The technique can also be used for quality control purpose during granulation process and it requires only simple sample preparation.

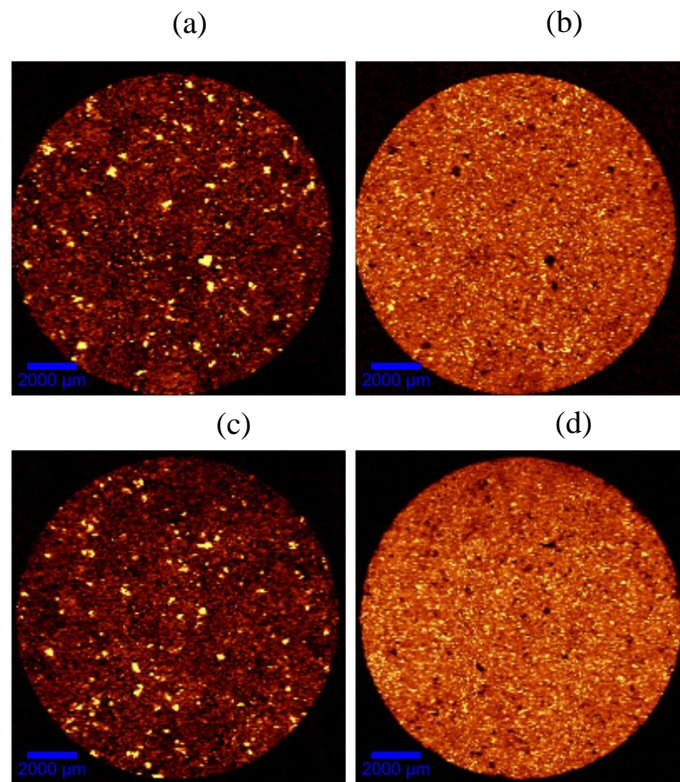


Figure 7-19: Raman mapping of caffeine (a & c) and excipients (b & d) of tablet made using granules produced by 30° mixing configuration

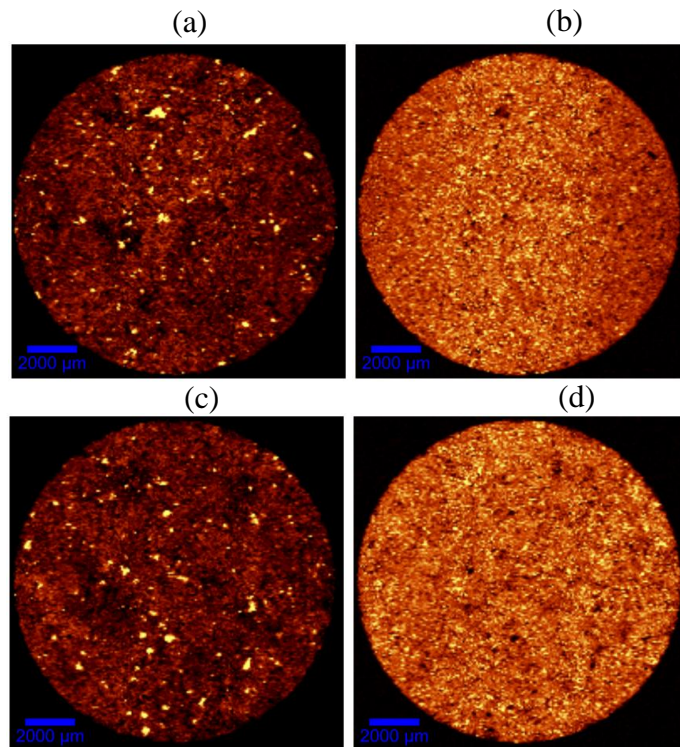


Figure 7-20: Raman mapping of caffeine (a & c) and excipients (b & d) of tablet made using granules produced by 60° mixing configuration

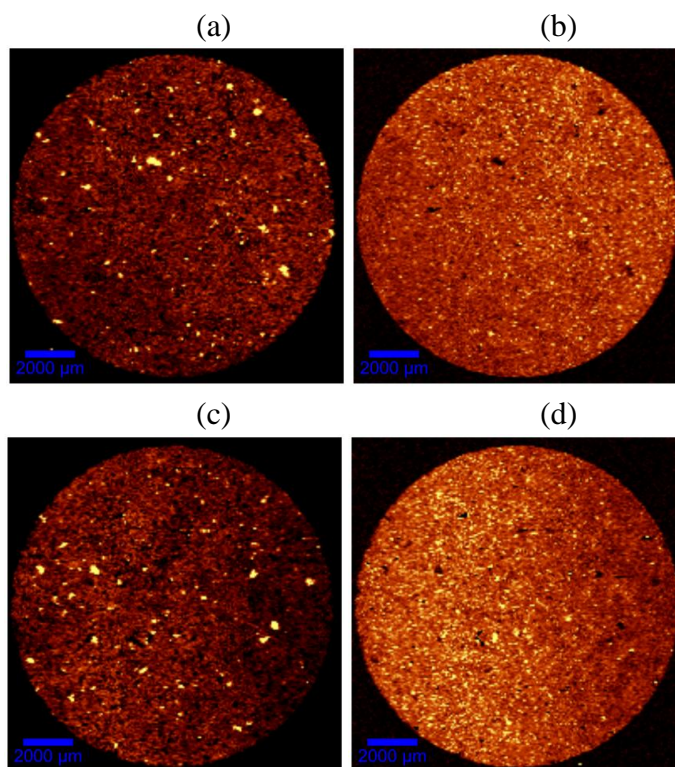


Figure 7-21: Raman mapping of caffeine (a & c) and excipients (b & d) of tablet made using granules produced by 90° mixing configuration

## CONCLUSION

Granules and tablets with well studied formulation were made using a twin screw granulator. The quality of the granules and tablets were examined by characterisation of the product properties. The influence of the granulator screw speed and mixing configuration on the intermediate and final products were also examined in the present study.

The study shows that the granules produced using different screw speeds and mixing configurations have mono-modal size distribution. The unwanted fines generation is low for all the process conditions suggesting sufficient granulation liquid was used. The mean granule diameter decreases when the screw speed increases but only up to 400 rpm. For different mixing configuration, the mean granule diameter has the following trend,  $60^\circ > 90^\circ > 30^\circ$ . The

30° configuration produced smallest granules as it has a more dispersive character and less bypass possibility due to smaller advance angle. The 60° mixing configuration has higher fill level and offers more bypass possibility for the materials and therefore generates larger granules. On the other hand, 90° mixing configuration which has more materials hold up and is possibly a distributive type of mixer and gives more kneading and chopping actions, resulting the production of intermediate size granules. Generally the shape of all the granules is random and irregular. The granule surface is porous and was made up by loosely packed particles. Besides this, there is insignificant change in granule fracture strength for different process conditions. The granules also have similar packing coefficient value and it is < 25% which indicates good/ free flowing flow ability.

The tensile strength of the tablets produced by different process conditions has similar values between 1 to 2 MPa. The mean dissolution time obtained using Weibull's distribution shows that there is a complicated and unclear relationship between dissolution rate and screw speed. However, the dissolution rate of the tablets is considered fast as all tablets can dissolve within 30 minutes. The dissolution rate of the tablets decreases with the mean granule size which might indicate that the dissolution of the tablets is controlled by the disintegration of the tablets. Beside this, the distribution of caffeine was examined using Confocal Raman Spectroscopy and it was found that the active ingredient was homogeneously dispersed on the surface of the tablets and highly possible within the tablet matrix.

Finally a twin screw granulator is a promising tool for continuous wet granulation to produce acceptable quality of granules and tablets in the pharmaceutical industry. Moreover, homogenous distribution of active ingredients within the tablet matrix indicates that the granulator can be used as a continuous mixer and therefore the pre-mixing of powder can be

eliminated. Confocal Raman Spectroscopy is also a useful inspection tool for quality control purpose during granulation process as it can examine the API distribution readily with minimum sample preparation.

## CHAPTER 8 : OVERALL CONCLUSION AND FUTURE WORK

---

### 8.1 OVERALL CONCLUSION

The twin screw wet granulation process which allows continuous processing to give consistent quality products was studied in terms of the process mechanisms including the flow behaviour and the mixing performance. A preliminary study was carried out to compare the properties of the granules produced by a twin screw extruder (TSE) with those from a high shear mixer(HSM). It was shown that TSE produces porous granules with multi-modal size distribution and it generates oversized product and unwanted fines. HSM on the other hand produces denser granules with mono-modal distribution. The dissimilarity of the granules produced using both techniques are mainly because of the difference in process conditions. The dense HSM granules are due to the higher residence time in HSM granulation and could potentially lead to over granulation that results in poor compactibility. Nevertheless the observations in this study give a reasonable indication of the differences in process mechanisms occurring in TSE and HSM.

It is believed that the mechanisms of twin screw wet granulation are different from conventional granulation methods due to the absence of a consolidation stage. The images from XRCT show that the internal structure of granules produced by the twin screw extruder consists of tiny pores distributed uniformly across the structure whilst the granules produced from the high shear mixer are made up by smaller deformed particles due to collision and coalescence and have a smoother and denser surface through the consolidation process. The proposed process mechanisms for the twin screw wet granulator used in the current study involve an immersion type of nucleation to form paste-like extrudates that will be broken into



smaller pieces travelling through the conveying zone, followed by coalescence, compaction and elongation in the mixing zones and then breakage of the oversize granules in conveying zones to form irregular and porous products. Spheronisation processes also exist during the granulation process but it is not significant as the fill level in granulator is not high.

The real time trajectory of the particle can be visualised and measured accurately in a twin screw granulator by tracing a radioactive particle in the twin screw granulator using a Positron Emission Particle Tracking technique. PEPT revealed that the material in the twin screw granulator will flow quickly through the conveying zone and slow down before entering the mixing zones. Generally, the material will stay longer in the mixing zone when the kneading discs are arranged at a higher angle as it loses the conveying capacity. The material flow stream is not only driven by the conveying feature of a screw but also the degree of granulator filling level. In the 90° mixing zone which does not have conveying capacity, material is believed to be conveyed by a dispersion mechanism driven by the granulator fill gradient. When viewing from the granulator's cross section direction, the material mainly flows in the shape of '∞' and occasionally in a circle.

Due to the existence of a clearance between the screw and barrel, a thin layer of material will be formed during the granulation process. Particles may fall into this region as well as escape from the layer because of the shear force induced when the screws rotate and when materials flow. It is believed that particles escaping from and falling into the layer are in equilibrium when the granulation process reaches a steady state.

Besides the flow, mean residence time was also obtained from PEPT. The mean residence time is dependent on the kneading disc arrangement angle and is inversely proportional to the screw speed and feedrate. The shapes of the residence time distributions however are similar

for different process conditions and screw geometries which suggest that the extent of axial mixing in granulator does not change. On the other hand, the overall fill level of the granulator which was calculated based on the mean residence time is proportional to the powder feedrate and the kneading disc arrangement angle and is inversely proportional to the screw speed. It is also postulated that the granulator is never fully filled.

Residence time distribution of the twin screw granulator could be modelled using a Tanks-in-Series model. However, the model does not describe the front part of the RTD curve. By including a plug flow fraction, the prediction of the RTD improves as the prediction more closely matches the overall experimental data. The model shows that the twin screw granulator could be described by 2 – 5 tanks in series with a small fraction of plug flow. This plug flow was initially attributed to the conveying zone but a later study of the model with plug flow to model the RTD of the conveying and kneading sections shows that the plug flow may exist in all the geometries. The parameters,  $n$  and  $p$  generally do not change significantly for different process parameters, screw types and screw configurations. This again may imply that the extent of axial mixing of the granulator remains similar for various screw geometries and process conditions.

Variance reduction ratio which measures the ability to remove inconsistencies in feeding was also used to study the mixing performance of the twin screw granulator. VRR is strongly influenced by the ratio of the feed fluctuation cycle period to the mean residence time of a system. In general, the granulator manages to remove the fluctuations of the input stream very well as the VRR achievable is high. The entire high frequency signal was efficiently removed leaving the signal with period close to the mean residence time. Low feedrate, low screw

speed and mixing zones arranged in higher angle can smooth the input fluctuation more efficiently due to higher mean residence time.

The quality of the granules produced using a common placebo formulation by the twin screw granulator is acceptable. With a suitable formulation, the granules produced will have a mono-modal distribution. The shape of the granules produced is generally random and irregular. The surface of the granules is porous and made up of loosely packed particles. The granules produced by the granulator seem to be free flowing as the packing coefficient is < 25%.

The tablets produced using the granules from the twin screw granulator also gave acceptable quality. The tablets give reasonable tensile strength and the model drug in the tablet formulation was fully released within 30 minutes. Under Confocal Raman Spectroscopy, it was also observed that the active ingredient was uniformly distributed on the surface of the tablets which might also indicate that it is homogeneously dispersed within the tablets matrix.

Twin screw wet granulation can potentially bring significant advantages in continuous pharmaceutical wet granulation. Unlike batch wise process, twin screw wet granulation is a continuous process which does not have batch to batch variation. The process can be run in a controlled continuous mode with the potential application of Process Analytical Tools and it is highly complementary to Quality by Design (QbD). The present study is a major step forward to understand the twin screw wet granulation process which follows the QbD concepts that emphasize the quality should be built into the products through the understanding of the product and process. The findings of the work have provided an insight

of the mechanism of process as well as the mixing performance, which is a great use for the further research to enhance the understanding of granulation process.

## **8.2 FUTURE WORK**

It was suggested that the quality of the PEPT data could be improved; this would help describe the process more accurately. More work should be conducted to validate the data that shows the existence of a dead volume fraction in the granulator. The use of statistics to find the number of particles that would give sufficient confidence is needed. The work should also be extended to include a full experimental matrix in order to complete the present study. Another approach that can also be used to study the twin screw granulator is Positron Emission Tomography which allows the observation of the liquid phase. A quantity of radioactive water can be injected into the granulator in order to observe the spread of the liquid in different sections. Also the use of frequency response analysis could be used to help the understanding of mixing effects. For example the use of Fourier Transforms to analyse the changes of frequency in the input and output streams.

Other attempts can also be done to further understand the mechanism of twin screw wet granulation for example a nucleation only granulation where the screws consist of only conveying screws. This configuration will allow the study of nucleation process as well as effects of conveying zone and the kinetic energy on the breakage of nuclides. Multiple granulation liquid injection points can also be used to promote the liquid distribution of the process so that the products are more uniform. Besides this, recycling the granules back into the granulator could also improve granule uniformity as larger granules are expected to be broken and smaller granules are expected to further coalesce. Many different types of screw geometries can also be explored for example combing elements, reverse flow elements,

some sophisticated elements with both conveying and kneading properties etc. can be used for optimising the granulation process.

## APPENDIX: PUBLISHED WORK

---

### Journal publication (attached at the back of the thesis)

Lee, K. T., A. Ingram, et al. "Comparison of granule properties produced using Twin Screw Extruder and High Shear Mixer: A step towards understanding the mechanism of twin screw wet granulation." *Powder Technology*

Lee, K. T., A. Ingram, et al. "Twin screw wet granulation: The study of a continuous twin screw granulator using Positron Emission Particle Tracking (PEPT) technique." *European Journal of Pharmaceutics and Biopharmaceutics*

### Conference publication

Lee, K. T., A. Ingram, et al. (2010). "Continuous Granulation of Pharmaceutical Powder using a Twin Screw Extruder." World Congress on Particle Technology 6, Nuremberg, Germany.

Lee, K. T., A. Ingram, et al. (2011). "Mechanisms of continuous granulation of pharmaceutical powder using a twin screw compounder." 5th International Granulation Workshop, Lausanne 20th - 23rd June.

---

## REFERENCES

---

- Abberger, T., A. Seo, et al. (2002). "The effect of droplet size and powder particle size on the mechanisms of nucleation and growth in fluid bed melt agglomeration." International Journal of Pharmaceutics **249**(1-2): 185-197.
- Abouzeid, A. Z. M., D. W. Fuerstenau, et al. (1980). "Transport behaviour of particulate solids in rotary drums - scale-up of residence time distribution using the axial-dispersion model." Powder Technology **27**(2): 241-250.
- Adams, M. J. and R. McKeown (1996). "Micromechanical analyses of the pressure-volume relationships for powders under confined uniaxial compression." Powder Technology **88**(2): 155-163.
- Adams, M. J., M. A. Mullier, et al. (1994). "Agglomerate strength measurement using a uniaxial confined compression test." Powder Technology **78**(1): 5-13.
- Aulton, M. E. (2007). Aulton's Pharmaceutics: The Design And Manufacture of Medicines, Elsevier Limited, Oxford.
- Bacher, C., P. M. Olsen, et al. (2008). "Compressibility and compactibility of granules produced by wet and dry granulation." International Journal of Pharmaceutics **358**(1-2): 69-74.
- Bakalis, S., P. W. Cox, et al. (2006). "Development and use of positron emitting particle tracking (PEPT) for velocity measurements in viscous fluids in pilot scale equipment." Chemical Engineering Science **61**(6): 1864-1877.
- Bakalis, S. and M. V. Karwe (1999). "Measuring of Velocity Distributions in the Nip Region of a Co-Rotating Twin-Screw Extruder." Food and Bioproducts Processing **77**(3): 205-212.
- Bakalis, S. and M. V. Karwe (2002). "Velocity distributions and volume flow rates in the nip and translational regions of a co-rotating, self-wiping, twin-screw extruder." Journal of Food Engineering **51**(4): 273-282.
- Barigou, M. (2004). "Particle Tracking in Opaque Mixing Systems: An Overview of the Capabilities of PET and PEPT." Chemical Engineering Research and Design **82**(9): 1258-1267.

- Benali, M., V. Gerbaud, et al. (2009). "Effect of operating conditions and physico-chemical properties on the wet granulation kinetics in high shear mixer." Powder Technology **190**(1-2): 160-169.
- Berthiaux, H., K. Marikh, et al. (2008). "Continuous mixing of powder mixtures with pharmaceutical process constraints." Chemical Engineering and Processing **47**(12): 2315-2322.
- Booy, M. L. (1980). "Isothermal flow of viscous liquids in corotating twin screw devices." Polymer Engineering & Science **20**(18): 1220-1228.
- Bouwman, A. M. (2005). Form, formation, and deformation: the influence of material properties and process conditions on the shape of granules produced by high shear granulation.
- Bouwman, A. M., M. J. Henstra, et al. (2005). "The effect of the amount of binder liquid on the granulation mechanisms and structure of microcrystalline cellulose granules prepared by high shear granulation." International Journal of Pharmaceutics **290**(1-2): 129-136.
- Carneiro, O. S., G. Caldeira, et al. (1999). "Flow patterns in twin-screw extruders." Journal of Materials Processing Technology **93**: 309-315.
- Chan, C. W., A. Brems, et al. (2010). "PEPT study of particle motion for different riser exit geometries." Particuology **8**(6): 623-630.
- Chan, C. W., J. Seville, et al. (2009). "Particle motion in the CFB riser with special emphasis on PEPT-imaging of the bottom section." Powder Technology **196**(3): 318-325.
- Chantraine, F., M. Viana, et al. (2007). "From compressibility to structural investigation of sodium dodecyl sulphate — Part 2: A singular behavior under pressure." Powder Technology **177**(1): 41-50.
- Chiti, F., S. Bakalis, et al. (2011). "Using positron emission particle tracking (PEPT) to study the turbulent flow in a baffled vessel agitated by a Rushton turbine: Improving data treatment and validation." Chemical Engineering Research and Design(0).
- Cox, P. W., S. Bakalis, et al. (2003). "Visualisation of three-dimensional flows in rotating cans using positron emission particle tracking (PEPT)." Journal of Food Engineering **60**(3): 229-240.



- Danckwerts, P. V. (1953). "Continuous flow systems: Distribution of residence times." Chemical Engineering Science **2**(1): 1-13.
- Danckwerts, P. V. (1995). "Continuous flow systems. Distribution of residence times: P. V. Danckwerts, Chem. Engng Sci. 2: 1–13, 1953." Chemical Engineering Science **50**(24): 3855.
- Darelius, A. (2007). Fluid dynamics and granular growth in high shear wet granulation : experiments and mechanistic modelling. Doktorsavhandlingar vid Chalmers tekniska högskola, 0346-718X ; ny ser., nr. 2588. Göteborg, Chalmers University of Technology
- Chalmers tekniska högskola: 1 v. (various pagings).
- Dévy, A., K. Mayer, et al. (2006). "Investigation on drug dissolution and particle characteristics of pellets related to manufacturing process variables of high-shear granulation." Journal of Biochemical and Biophysical Methods **69**(1-2): 197-205.
- Dhenge, R. M., J. J. Cartwright, et al. (2011). "Twin screw wet granulation: Effect of powder feed rate." Advanced Powder Technology **22**(2): 162-166.
- Dhenge, R. M., R. S. Fyles, et al. (2010). "Twin screw wet granulation: Granule properties." Chemical Engineering Journal **164**(2-3): 322-329.
- Ding, Y. L., J. P. K. Seville, et al. (2001). "Solids motion in rolling mode rotating drums operated at low to medium rotational speeds." Chemical Engineering Science **56**(5): 1769-1780.
- Djuric, D. (2008). Continuous Granulation with a Twin-Screw Extruder, Cuvillier Verlag.
- Djuric, D. and P. Kleinebudde (2008). "Impact of Screw Elements on Continuous Granulation With a Twin-Screw Extruder." Journal of Pharmaceutical Sciences **97**(11): 4934-4942.
- Djuric, D. and P. Kleinebudde (2010). "Continuous granulation with a twin-screw extruder: Impact of material throughput." Pharmaceutical Development and Technology **15**(5): 518-525.
- Djuric, D., B. Van Melkebeke, et al. (2009). "Comparison of two twin-screw extruders for continuous granulation." European Journal of Pharmaceutics and Biopharmaceutics **71**(1): 155-160.

- 
- El Hagrasy, A. S. and J. D. Lister (2011). "Twin screw wet granulation: Influence of formulation parameters." 5th International Granulation Workshop, Lausanne 20th - 23rd.
- Everitt, B. (2002). The Cambridge dictionary of statistics, Cambridge University Press.
- Fairhurst, P. G., M. Barigou, et al. (2001). "Using positron emission particle tracking (PEPT) to study nearly neutrally buoyant particles in high solid fraction pipe flow." International Journal of Multiphase Flow **27**(11): 1881-1901.
- Fan, X., D. J. Parker, et al. (2006). "Enhancing <sup>18</sup>F uptake in a single particle for positron emission particle tracking through modification of solid surface chemistry." Nuclear Instruments and Methods in Physics Research Section A: Accelerators, Spectrometers, Detectors and Associated Equipment **558**(2): 542-546.
- Fan, X., D. J. Parker, et al. (2006). "Labelling a single particle for positron emission particle tracking using direct activation and ion-exchange techniques." Nuclear Instruments and Methods in Physics Research Section A: Accelerators, Spectrometers, Detectors and Associated Equipment **562**(1): 345-350.
- Farber, L., G. Tardos, et al. (2003). "Use of X-ray tomography to study the porosity and morphology of granules." Powder Technology **132**(1): 57-63.
- FDA, F. a. D. A. (2003). "Final report on pharmaceutical cGMPs for the 21st century—A risk-based approach. (Last Updated: 08/17/2009 )."
- Fell, J. T. and J. M. Newton (1970). "Determination of tablet strength by the diametral-compression test." Journal of Pharmaceutical Sciences **59**(5): 688-691.
- Fitzpatrick, S., J. F. McCabe, et al. (2002). "Effect of moisture on polyvinylpyrrolidone in accelerated stability testing." International Journal of Pharmaceutics **246**(1-2): 143-151.
- Fogler, H. S. (2006). Elements of chemical reaction engineering, Prentice Hall PTR.
- Fogler, H. S. (2006). Elements of chemical reaction engineering. Upper Saddle River, N.J., Pearson Education International.

- Freitag, F. and P. Kleinebudde (2003). "How do roll compaction/dry granulation affect the tableting behaviour of inorganic materials? Comparison of four magnesium carbonates." European Journal of Pharmaceutical Sciences **19**(4): 281-289.
- Gabaude, C. M. D., J. C. Gautier, et al. (2001). "Validation of a new pertinent packing coefficient to estimate flow properties of pharmaceutical powders at a very early development stage, by comparison with mercury intrusion and classical flowability methods." Journal of Materials Science **36**(7): 1763-1773.
- Gamlen, M. J. and C. Eardley (1986). "Continuous Extrusion Using a Raker Perkins MP50 (Multipurpose) Extruder." Drug Development and Industrial Pharmacy **12**(11-13): 1701-1713.
- Gao, J., G. C. Walsh, et al. (1999). "Residence-time distribution model for twin-screw extruders." AIChE Journal **45**(12): 2541-2549.
- Gao, Y., F. Muzzio, et al. (2011). "Characterization of Feeder Effects on Continuous Solid Mixing Using Fourier Series Analysis." Aiche Journal **57**(5): 1144-1153.
- Gao, Y., A. Vanarase, et al. (2011). "Characterizing continuous powder mixing using residence time distribution." Chemical Engineering Science **66**(3): 417-425.
- Gasner, G. E., D. Bigio, et al. (1999). "A new approach to analyzing residence time and mixing in a co-rotating twin screw extruder." Polymer Engineering & Science **39**(2): 286-298.
- Gautam, A. and G. S. Choudhury (1999). "Screw configuration effects on residence time distribution and mixing in twin-screw extruders during extrusion of rice flour." Journal of Food Process Engineering **22**(4): 263-285.
- Ghaderi, A. (2003). "On Characterization of Continuous Mixing of Particulate Materials." Particulate Science and Technology **21**(3): 271-282.
- Haefele, T. and K. Paulus (2011). Confocal Raman Microscopy in Pharmaceutical Development
- Confocal Raman Microscopy. T. Dieing, O. Hollricher and J. Toporski, Springer Berlin / Heidelberg. **158**: 165-202.
- Hamed, E., D. Moe, et al. (2005). Handbook of pharmaceutical granulation technology - Chapter 4: Binders and Solvents, Taylor & Francis.

- Hapgood, K. P., S. M. Iveson, et al. (2007). Granulation - Chapter 20: Granulation Rate Processes, Elsevier Science.
- Hapgood, K. P., J. D. Litster, et al. (2002). "Drop Penetration into Porous Powder Beds." Journal of Colloid and Interface Science **253**(2): 353-366.
- Hapgood, K. P., J. D. Litster, et al. (2003). "Nucleation regime map for liquid bound granules." Aiche Journal **49**(2): 350-361.
- Holm, P., O. Jungersen, et al. (1983). "Granulation in high speed mixers 1. Effects of process variables during kneading." Pharmazeutische Industrie **45**(8): 806-811.
- Hussain, M. S. H., P. York, et al. (1992). "Effect of commercial and high purity magnesium stearates on in-vitro dissolution of paracetamol DC tablets." International Journal of Pharmaceutics **78**(1-3): 203-207.
- Ingram, A., J. P. K. Seville, et al. (2005). "Axial and radial dispersion in rolling mode rotating drums." Powder Technology **158**(1-3): 76-91.
- Iveson, S. M., J. A. Beathe, et al. (2002). "The dynamic strength of partially saturated powder compacts: the effect of liquid properties." Powder Technology **127**(2): 149-161.
- Iveson, S. M. and J. D. Litster (1998). "Growth regime map for liquid-bound granules." Aiche Journal **44**(7): 1510-1518.
- Iveson, S. M., J. D. Litster, et al. (1996). "Fundamental studies of granule consolidation Part 1: Effects of binder content and binder viscosity." Powder Technology **88**(1): 15-20.
- Iveson, S. M., P. A. L. Wauters, et al. (2001). "Growth regime map for liquid-bound granules: further development and experimental validation." Powder Technology **117**(1-2): 83-97.
- J. Cartwright, D. D., R Dhenge, R. Fyles, M. J. Hounslow, A. D. Salman (2009). "Twin Screw Extrusion: Granule Properties." 8th International Symposium on Agglomeration and 3rd International Granulation Workshop, Sheffield, UK.
- Kato, Y., M. Ohkuma, et al. (2005). "Evaluation of the flowability of surface-modified preparations by the measurement of the inter-particle adhesive force." Journal of Drug Delivery Science and Technology **15**(3): 217-221.

- Keleb, E. I., A. Vermeire, et al. (2001). "Cold extrusion as a continuous single-step granulation and tableting process." European Journal of Pharmaceutics and Biopharmaceutics **52**(3): 359-368.
- Keleb, E. I., A. Vermeire, et al. (2002). "Continuous twin screw extrusion for the wet granulation of lactose." International Journal of Pharmaceutics **239**(1-2): 69-80.
- Keleb, E. I., A. Vermeire, et al. (2004). "Single-step granulation/tableting of different grades of lactose: a comparison with high shear granulation and compression." European Journal of Pharmaceutics and Biopharmaceutics **58**(1): 77-82.
- Keleb, E. I., A. Vermeire, et al. (2004). "Twin screw granulation as a simple and efficient tool for continuous wet granulation." International Journal of Pharmaceutics **273**(1-2): 183-194.
- Kiekens, F., R. Zelko, et al. (2000). "Effect of the Storage Conditions on the Tensile Strength of Tablets in Relation to the Enthalpy Relaxation of the Binder." Pharmaceutical Research **17**(4): 490-493.
- Knight, P. C., T. Instone, et al. (1998). "An investigation into the kinetics of liquid distribution and growth in high shear mixer agglomeration." Powder Technology **97**(3): 246-257.
- Knight, P. C., J. P. K. Seville, et al. (2001). "Prediction of impeller torque in high shear powder mixers." Chemical Engineering Science **56**(15): 4457-4471.
- Kumar, A., G. M. Ganjyal, et al. (2008). "Modeling residence time distribution in a twin-screw extruder as a series of ideal steady-state flow reactors." Journal of Food Engineering **84**(3): 441-448.
- Kuo, H. P., P. C. Knight, et al. (2005). "Solids circulation and axial dispersion of cohesionless particles in a V-mixer." Powder Technology **152**(1-3): 133-140.
- Langenbacher, F. (1976). "Parametric representation of dissolution-rate curves by the RRSBW distribution." Pharmazeutische Industrie **38**: 472-477.
- Lee, K. T., A. Ingram, et al. (2010). "Continuous Granulation of Pharmaceutical Powder using a Twin Screw Extruder." World Congress on Particle Technology 6, Nuremberg, Germany.

- Lee, K. T., A. Ingram, et al. (2011). "Mechanisms of continuous granulation of pharmaceutical powder using a twin screw compounder." 5th International Granulation Workshop, Lausanne 20th - 23rd June.
- Levenspiel, O. (1972). Chemical reaction engineering. 2nd ed, New York, London: Wiley.
- Lindberg, N.-O., M. Myrenas, et al. (1988). "Extrusion of An Effervescent Granulation with a Twin Screw Extruder, Baker Perkins MPF 50D. Determination of Mean Residence Time." Drug Development and Industrial Pharmacy **14**(5): 649-655.
- Lindberg, N.-O., C. Tufvesson, et al. (1987). "Extrusion of an Effervescent Granulation with a Twin Screw Extruder, Baker Perkins MPF 50 D." Drug Development and Industrial Pharmacy **13**(9-11): 1891-1913.
- Litster, J., B. Ennis, et al. (2004). The science and engineering of granulation processes, Kluwer Academic Publishers.
- Litster, J., B. Ennis, et al. (2004). The science and engineering of granulation processes. Dordrecht ; London, Kluwer Academic.
- Litster, J. D. (2003). "Scaleup of wet granulation processes: science not art." Powder Technology **130**(1-3): 35-40.
- Liu, L. X., I. Marziano, et al. (2008). "Effect of particle properties on the flowability of ibuprofen powders." International Journal of Pharmaceutics **362**(1-2): 109-117.
- Mangwandi, C., M. J. Adams, et al. (2010). "Effect of impeller speed on mechanical and dissolution properties of high-shear granules." Chemical Engineering Journal **164**(2-3): 305-315.
- Marikh, K., H. Berthiaux, et al. (2008). "Influence of stirrer type on mixture homogeneity in continuous powder mixing: A model case and a pharmaceutical case." Chemical Engineering Research & Design **86**(9A): 1027-1037.
- Marikh, K., H. Berthiaux, et al. (2005). "Experimental study of the stirring conditions taking place in a pilot plant continuous mixer of particulate solids." Powder Technology **157**(1-3): 138-143.

- Marikh, K., H. Berthiaux, et al. (2006). "Flow analysis and Markov chain modelling to quantify the agitation effect in a continuous powder mixer." Chemical Engineering Research & Design **84**(A11): 1059-1074.
- Mehauden, K., P. W. Cox, et al. (2009). "The flow of liquid foods in an agitated vessel using PEPT: Implications for the use of TTI to assess thermal treatment." Innovative Food Science & Emerging Technologies **10**(4): 643-654.
- Mehta, K. A., M. S. Kislalioglu, et al. (2000). "Effect of formulation and process variables on porosity parameters and release rates from a multi unit erosion matrix of a poorly soluble drug." Journal of Controlled Release **63**(1-2): 201-211.
- Miller, R. W. and D. M. Parikh (2005). Chapter 6: Roller Compaction Technology. Handbook of pharmaceutical granulation technology Taylor & Francis.
- Oberlehner, J., P. Cassagnau, et al. (1994). "Local residence time distribution in a twin screw extruder." Chemical Engineering Science **49**(23): 3897-3907.
- Parikh, D. M. (2005). Handbook of pharmaceutical granulation technology. Boca Raton ; London, Taylor & Francis.
- Parker, D. J., C. J. Broadbent, et al. (1993). "Positron emission particle tracking - a technique for studying flow within engineering equipment." Nuclear Instruments and Methods in Physics Research Section A: Accelerators, Spectrometers, Detectors and Associated Equipment **326**(3): 592-607.
- Parker, D. J., A. E. Dijkstra, et al. (1997). "Positron emission particle tracking studies of spherical particle motion in rotating drums." Chemical Engineering Science **52**(13): 2011-2022.
- Parker, D. J. and X. Fan (2008). "Positron emission particle tracking--Application and labelling techniques." Particuology **6**(1): 16-23.
- Parker, D. J., M. R. Hawkesworth, et al. (1994). "Industrial positron-based imaging: Principles and applications." Nuclear Instruments and Methods in Physics Research Section A: Accelerators, Spectrometers, Detectors and Associated Equipment **348**(2-3): 583-592.
- Pernenkil, L. and C. L. Cooney (2006). "A review on the continuous blending of powders." Chemical Engineering Science **61**(2): 720-742.

- 
- Perry, R. H., D. W. Green, et al. (1998). Perry's Chemical Engineers' Handbook, McGraw-Hill.
- Pianko-Oprych, P., A. W. Nienow, et al. (2009). "Positron emission particle tracking (PEPT) compared to particle image velocimetry (PIV) for studying the flow generated by a pitched-blade turbine in single phase and multi-phase systems." Chemical Engineering Science **64**(23): 4955-4968.
- Portillo, P. M., A. U. Vanarase, et al. "Investigation of the effect of impeller rotation rate, powder flow rate, and cohesion on powder flow behavior in a continuous blender using PEPT." Chemical Engineering Science **65**(21): 5658-5668.
- Portillo, P. M., A. U. Vanarase, et al. (2010). "Investigation of the effect of impeller rotation rate, powder flow rate, and cohesion on powder flow behavior in a continuous blender using PEPT." Chemical Engineering Science **65**(21): 5658-5668.
- Puaux, J. P., G. Bozga, et al. (2000). "Residence time distribution in a corotating twin-screw extruder." Chemical Engineering Science **55**(9): 1641-1651.
- Rahmanian, N., M. Ghadiri, et al. (2009). "Characterisation of granule structure and strength made in a high shear granulator." Powder Technology **192**(2): 184-194.
- Richard, P., M. Nicodemi, et al. (2005). "Slow relaxation and compaction of granular systems." Nature Materials **4**(2): 121-128.
- Riepma, K. A., H. Vromans, et al. (1993). "The effect of dry granulation on the consolidation and compaction of crystalline lactose." International Journal of Pharmaceutics **97**(1-3): 29-38.
- Rowe, R. C., P. J. Sheskey, et al. (2009). Handbook of pharmaceutical excipients, Pharmaceutical Press.
- Saito, Y., A. Ingram, et al. (2009). "Visualization of Powder Mixing in a High Shear Mixer using Positron Emission Particle Tracking." Journal of Visualization **12**(4): 291-292.
- Salman, A. D., M. J. Hounslow, et al. (2007). Granulation, Elsevier Science.
- Santomaso, A., P. Lazzaro, et al. (2003). "Powder flowability and density ratios: the impact of granules packing." Chemical Engineering Science **58**(13): 2857-2874.



- Schmidt, C. and P. Kleinebudde (1998). "Comparison between a twin-screw extruder and a rotary ring die press. Part II: influence of process variables." European Journal of Pharmaceutics and Biopharmaceutics **45**(2): 173-179.
- Schmidt, C., H. Lindner, et al. (1997). "Comparison between a twin-screw extruder and a rotary ring die press. I. Influence of formulation variables." European Journal of Pharmaceutics and Biopharmaceutics **44**(2): 169-176.
- Selkirk, A. B. and D. Ganderton (1970). "The influence of wet and dry granulation methods on the pore structure of lactose tablets." Journal of Pharmacy and Pharmacology **22**(S1): 86S-94S.
- Selkirk, A. B. and D. Ganderton (1970). "An investigation of the pore structure of tablets of sucrose and lactose by mercury porosimetry." Journal of Pharmacy and Pharmacology **22**(S1): 79S-85S.
- Seville, J. P. K., A. Ingram, et al. (2009). Chapter 4 Positron Emission Imaging in Chemical Engineering. Advances in Chemical Engineering. L. Jinghai, Academic Press. **Volume 37**: 149-178.
- Seville, J. P. K., A. Ingram, et al. (2005). "Probing processes using positrons." Chemical Engineering Research & Design **83**(A7): 788-793.
- Shearer, G. and C. Tzoganakis (2000). "The effects of kneading block design and operating conditions on distributive mixing in twin screw extruders." Polymer Engineering & Science **40**(5): 1095-1106.
- Shearer, G. and C. Tzoganakis (2001). "Distributive mixing profiles for co-rotating twin-screw extruders." Advances in Polymer Technology **20**(3): 169-190.
- Staniforth, J. and M. E. Aulton (2002). Pharmaceutics: the science of dosage form design - Powder flow. pg 197-210, Churchill Livingstone.
- Sun, C. C., H. Hou, et al. (2009). "Development of a high drug load tablet formulation based on assessment of powder manufacturability: Moving towards quality by design." Journal of Pharmaceutical Sciences **98**(1): 239-247.
- Swarbrick, J. (2007). Encyclopedia of pharmaceutical technology, Informa Healthcare.

- Tardos, G. I., M. I. Khan, et al. (1997). "Critical parameters and limiting conditions in binder granulation of fine powders." Powder Technology **94**(3): 245-258.
- Thiele, W., I. Ghebre-Selassie, et al. (2003). Pharmaceutical Extrusion Technology, Marcel Dekker Incorporated.
- Thiele, W., I. Ghebre-Selassie, et al. (2003). Pharmaceutical Extrusion Technology: Twin screw extrusion and screw design, Marcel Dekker Incorporated.
- Thompson, M. R. and J. Sun (2010). "Wet Granulation in a Twin-Screw Extruder: Implications of Screw Design." Journal of Pharmaceutical Sciences **99**(4): 2090-2103.
- Tu, W.-D., A. Ingram, et al. (2009). "Exploring the regime map for high-shear mixer granulation." Chemical Engineering Journal **145**(3): 505-513.
- Tunón, Å., J. Gråsjö, et al. (2003). "Effect of intragranular porosity on compression behaviour of and drug release from reservoir pellets." European Journal of Pharmaceutical Sciences **19**(5): 333-344.
- Unlu, E. and J. F. Faller (2002). "RTD in twin-screw food extrusion." Journal of Food Engineering **53**(2): 115-131.
- Vainio, T. P., A. Harlin, et al. (1995). "Screw optimization of a co-rotating twin-screw extruder for a binary immiscible blend." Polymer Engineering & Science **35**(3): 225-232.
- Van de Velden, M., J. Baeyens, et al. (2008). "The solids flow in the riser of a Circulating Fluidised Bed (CFB) viewed by Positron Emission Particle Tracking (PEPT)." Powder Technology **183**(2): 290-296.
- Van Melkebeke, B., B. Vermeulen, et al. (2006). "Melt granulation using a twin-screw extruder: A case study." International Journal of Pharmaceutics **326**(1-2): 89-93.
- Van Melkebeke, B., C. Vervaet, et al. (2008). "Validation of a continuous granulation process using a twin-screw extruder." International Journal of Pharmaceutics **356**(1-2): 224-230.
- van Zuilichem, D. J., E. Kuiper, et al. (1999). "Mixing effects of constituting elements of mixing screws in single and twin screw extruders." Powder Technology **106**(3): 147-159.

- Vasanthavada, M., Y. Wang, et al. (2011). "Application of melt granulation technology using twin-screw extruder in development of high-dose modified-release tablet formulation." Journal of Pharmaceutical Sciences **100**(5): 1923-1934.
- Vervaet, C. and J. P. Remon (2005). "Continuous granulation in the pharmaceutical industry." Chemical Engineering Science **60**(14): 3949-3957.
- Vonk, P., C. P. F. Guillaume, et al. (1997). "Growth mechanisms of high-shear pelletisation." International Journal of Pharmaceutics **157**(1): 93-102.
- Weinekötter, R. and H. Gericke (2000). Mixing of solids, Kluwer Academic Publishers.
- Weinekötter, R. and L. Reh (1995). "Continuous Mixing of Fine Particles." Particle & Particle Systems Characterization **12**(1): 46-53.
- Weiner, M. L. and L. A. Kotkoskie (2000). Excipient toxicity and safety, M. Dekker.
- White, J. L. (1991). Twin Screw Extrusion: Technology and Principles, Hanser Gardner Pubns.
- Williams, J. C. and M. A. Rahman (1972). "Prediction of the performance of continuous mixers for particulate solids using residence time distributions Part I. Theoretical." Powder Technology **5**(2): 87-92.
- Williams, J. C. and M. A. Rahman (1972). "Prediction of the performance of continuous mixers for particulate solids using residence time distributions: Part II. Experimental." Powder Technology **5**(5): 307-316.
- Williams, J. C. and R. Richardson (1982). "The continuous mixing of segregation particles." Powder Technology **33**(1): 5-16.
- Williams, J. C. and R. Richardson (1983). "The continuous mixing of segregating particles." Powder Technology **33**(1): 5-16.
- Wu, C.-Y., S. M. Best, et al. (2006). "Predicting the tensile strength of compacted multi-component mixtures of pharmaceutical powders." Pharmaceutical Research **23**(8): 1898-1905.

- Wu, C. Y., B. C. Hancock, et al. (2008). "Numerical and experimental investigation of capping mechanisms during pharmaceutical tablet compaction." *Powder Technology* **181**(2): 121-129.
- Wu, C. Y., O. M. Ruddy, et al. (2005). "Modelling the mechanical behaviour of pharmaceutical powders during compaction." *Powder Technology* **152**(1-3): 107-117.
- Yang, Z., P. J. Fryer, et al. (2007). "An improved algorithm for tracking multiple, freely moving particles in a Positron Emission Particle Tracking system." *Nuclear Instruments and Methods in Physics Research Section A: Accelerators, Spectrometers, Detectors and Associated Equipment* **577**(3): 585-594.
- Yee S, W. (2006). "Particle motion in relatively thin fluidised bed models." *Chemical Engineering Science* **61**(18): 6234-6238.
- Yeh, A.-I. and Y.-M. Jaw (1999). "Predicting residence time distributions in a single screw extruder from operating conditions." *Journal of Food Engineering* **39**(1): 81-89.
- Yerramilli, L. and M. V. Karwe (2004). "Velocity Distributions and Mixing in the Translational Region of a Kneading Section in a Co-rotating Twin-screw Extruder." *Food and Bioproducts Processing* **82**(1): 5-12.
- Yu, L. (2008). "Pharmaceutical Quality by Design: Product and Process Development, Understanding, and Control." *Pharmaceutical Research* **25**(4): 781-791.
- Ziegler, G. R. and C. A. Aguilar (2003). "Residence time distribution in a co-rotating, twin-screw continuous mixer by the step change method." *Journal of Food Engineering* **59**(2-3): 161-167.